Summer 8-15-2015

Intraurban Spatiotemporal Variability of Ambient Air Pollutants across Metropolitan St. Louis

Li Du
Washington University in St. Louis

WASHINGTON UNIVERSITY IN ST. LOUIS

School of Engineering and Applied Science

Department of Energy, Environmental and Chemical Engineering

Dissertation Examination Committee:
Jay Turner, Chair
Pratim Biswas
Benjamin de Foy
Aaron Hipp
Rudolf Husar
Brent Williams

Intraurban Spatiotemporal Variability of Ambient Air Pollutants across Metropolitan St. Louis

by

Li Du

A dissertation presented to the
Graduate School of Arts and Sciences
of Washington University in
partial fulfillment of the
requirements for the degree
of Doctor of Philosophy

August 2015
St. Louis, Missouri

Table of Contents

List of Figures

List of Tables

Acknowledgments

Above all, I would like to express my deepest gratitude to my advisor, Dr. Jay Turner, for his excellent guidance, patience and for being willing to make me part of his team. This work would not have been possible without his continuing support and encouragement. His dedication to research, a keen sense of integrity and commitment to highest standards have inspired me and will continue to motivate me in every aspect of my life.

I also wish to thank Drs. Pratim Biswas, Benjamin de Foy, Aaron Hipp, Rudolf Husar and Brent Williams for serving on my committee and providing guidance throughout this process. Specifically, I would like to acknowledge Dr. Rudolf Husar with whom I worked on multiple related projects, for supporting my learning in atmospheric science.

I would like to extend my gratitude to my friends and department staff for the encouragement, great joy and help along the way. Specifically, my prior and current colleagues of the Turner Lab: Neil Feinberg, Kelsey Haddad, Chris Peng and Dr. Varun Yadav have been supporting me and made this journey a memorable experience.

I would also like to thank my parents in China who always encourage me with their best wishes.

Finally, this work is dedicated to my wife, Jiewei Wu. She was always there cheering me up and inspired me every day to face the challenges and the unknown.

Li Du

Washington University in St. Louis

August 2015

ABSTRACT OF THE DISSERTATION

Intraurban Spatiotemporal Variability of Ambient Air Pollutants across Metropolitan St. Louis

By

Li Du

Doctor of Philosophy in Energy, Environmental & Chemical Engineering

Washington University in St. Louis, 2015

Professor Jay R. Turner, Chair

Ambient air monitoring networks have been established in the United States since the 1970s to comply with the Clean Air Act. The monitoring networks are primarily used to determine compliance but also provide substantive support to air quality management and air quality research including studies on health effects of air pollutants. The Roxana Air Quality Study (RAQS) was conducted at the fenceline of a petroleum refinery in Roxana, Illinois. In addition to providing insights into air pollutant impacts from the refinery, these measurements increased the St. Louis area monitoring network density for gaseous air toxics and fine particulate matter ($PM_{2.5}$) speciation and thus provided an opportunity to examine intraurban spatiotemporal variability for these air quality parameters.

This dissertation focused on exploring and assessing aspects of ambient air pollutant spatiotemporal variability in the St. Louis area from three progressively expanded spatial scales using a suite of methods and metrics. RAQS data were used to characterize air quality conditions in the immediate vicinity of the petroleum refinery. For example, $PM_{2.5}$ lanthanoids were used to track impacts from refinery fluidized bed catalytic cracker emissions. RAQS air toxics data were interpreted by comparing to network data from the Blair Street station in the

City of St. Louis which is a National Air Toxics Trends Station. Species were classified as being spatially homogeneous (similar between sites) or heterogeneous (different between sites) and in the latter case these differences were interpreted using surface winds data. For $PM_{2.5}$ species, there were five concurrently operating sites in the St. Louis area - including the site in Roxana - which are either formally part of the national Chemical Speciation Network (CSN) or rigorously follow the CSN sampling and analytical protocols. This unusually large number of speciation sites for a region the size of St. Louis motivated a detailed examination of these data. Intraurban spatiotemporal variability for certain species was evaluated in the context of measurement error. For example, for species otherwise considered homogeneous, differential impacts from local point sources at different locations could be identified after comparing the observed day-to-day variations to those contributed by measurement error. In addition, source apportionment modeling was conducted using single- and multi-site datasets to assign measured $PM_{2.5}$ mass to emission source categories. A suite of approaches were used to aid in the selection of an appropriate number of factors including metrics recently added to the US EPA Positive Matrix Factorization (EPA PMF) modeling software and the sensitivity of modeling results to perturbations on the measurement uncertainties.

Chapter 1 : Introduction

1.1. Introduction

1.1.1. Air Pollutant Spatial Variability

An understanding of air pollutant spatial variability is important for effective air quality management and to support health effects studies. In the latter case, many epidemiological studies have indicated adverse health effects, including mortality and morbidity, from exposure to ambient particulate matter (PM) and air toxic compounds (Dockery et al., 1993; Pope et al., 1995; Woodruff et al., 1998; Zanobetti et al., 2003). Early ambient PM epidemiological studies focused on ambient PM mass concentration and used data from a single monitoring site (typically called the "central" site) to represent population exposures over relatively large study areas (Pope et al., 2002; Roosli et al., 2001; Zanobetti et al., 2003) while other studies simply averaged the concentrations monitored at multiple sites over the study area to estimate human exposure (Burnett et al., 2001). These approaches assumed the ambient PM mass was homogeneously distributed across the study area (or at least nearly so). In some cases this approach appears justified because the pollutant of interest is nearly homogeneous or at least well correlated (Burton et al., 1996; Pope et al., 2002). However, in other cases the spatial variability can be relatively large and lead to potential misclassification of exposure levels based on the homogenous distribution assumption (Ito et al., 2004; Pinto et al., 2004; Zhu et al., 2002). Therefore, considerable effort has focused on developing more sophisticated approaches to estimating exposures including, but not limited to, developing a better understanding of the spatial variability of the pollutants of concern.

There are several factors that could influence spatial variability of PM on urban and finer spatial scales. Pinto et al. (2004) has grouped the factors into six categories:

- local sources of primary PM (i.e. PM emitted directly from emission sources);
- transient emission events that differentially impact some sites more than others;
- differences in the behavior of semi-volatile components;
- topographical barriers separating sites;
- meteorological phenomena; and
- measurement error.

Spatial variability is usually driven by factors from one or more of these categories. A variety of metrics have been developed to characterize spatiotemporal variability. Table 1-1 lists the most commonly used metrics and their advantages and disadvantages. The metrics listed in this table can be classified into two categories. The first category includes descriptive statistics such as the Pearson correlation coefficient, coefficient of variance, coefficient of divergence and absolute concentration difference. The second category includes tools such as the conditional probability function (CPF) and non-parametric wind regression (NWR) which characterize the wind direction dependence of pollutant concentrations. Applying these latter tools to several monitoring sites within the area can lead to the identification of emission source zones and spatial variability can be inferred. Based on a survey of numerous previous studies (Houthuijs et al., 2001; Pakbin et al., 2010; Wang et al., 2011; Wilson and Suh, 1997), it is clear that PM spatial homogeneity and heterogeneity are typically investigated using several metrics because each metric captures only some aspects of spatial variability and may not necessarily be adequate to characterize its full scope. However, the spatial variability introduced by

measurement error has been inadequately characterized. Measurement error may have significant confounding effects on some of the metrics and lead to potential misinterpretation of spatial variability (Haddad, 2015). Thus, considerable effort needs to be taken in advancing the understanding of spatial variability when using commonly applied statistical metrics in the presence of measurement error.

Spatiotemporal variability is commonly assessed using monitoring data collected at receptor sites. The generalized source-receptor relationship is $C(x,t) = D(x,t)E(t)$ where C

Table 1-1. Metrics to characterize intraurban spatial variability.

Metric	Description	Advantages	Disadvantages
Pearson correlation coefficient	A measure of correlation between two variables with the value from -1 to +1. Values close to 0 indicate lower correlation.	Tracks temporal variation between two datasets.	Not representative for spatial variability. Only tracks the correlation for site pairs.
Coefficient of Divergence	Quantifies concentration difference between two sites. Values are bounded by 0 and 1 with 0 representing perfect homogeneity.	Accounts for spatial variability.	Only available for the analysis for site pairs. Does not track temporal variability
Coefficient of variation	Quantifies the variation compared to the mean. Larger values indicate larger variation.	Tracks spatial variability. Can be applied to multiple sites across a region.	Does not track temporal variability.
Absolute concentration difference	Calculated as the concentration difference measured at two locations.	Simple and direct measure metric of characterizing spatial variability.	Usually requires time averaging and may lose some of the temporal information. Only available for site pairs.
Conditional probability function	Estimates the probability that the frequency of high contributions from sources in given wind direction exceeds a predetermined threshold value.	Determines the bearing of potential pollution sources.	Threshold value of probability needs be predetermined. Time-resolution of pollutant monitoring and wind data should match.
Non-parametric wind regression	Quantifies the relation between pollutant concentration and wind direction without making any assumption of the data or functional dependence between the variables.	Determines the bearing of potential pollution sources. Independent of any assumption regarding the concentration distribution of pollutants.	Selection of smoothing factor needs to be carefully examined. Sensitive to concentration outliers.

is the concentration at the receptor, *D* is the dispersion and *E* is the source emission rate. Concentrations observed at a receptor are modulated by variations in both the emission source strength and dispersion characteristics. Emission rate fluctuations lead to temporal variability while changes in dispersion (which depend on emission source characteristics such as stack height, meteorological conditions, and atmospheric processes) influence both spatial and temporal variability. For example, a short-term decrease in pollutant concentration at a receptor might arise from a transient in the source emission rate, an increase in dispersion because of changes in wind speed or mixing height, or a wind shift that decreases or even eliminates the impact of the source at the receptor. In the first two cases the decrease would be observed throughout the domain whereas in the latter case the impact is simply shifted from one location to another location. This space-time coupling must be appreciated when interpreting receptor data to assess spatial and temporal variability. Furthermore, the space-time coupling is affected by averaging time and typically longer averaging times lead to more homogeneous spatial patterns because the fluctuations are, at least to some extent, averaged out. Saturation monitoring with passive samplers has been used to assess spatial variability but typically requires long sample collection times which suppresses spatiotemporal variability. The emergence of low-cost sensors with high time resolution provides an opportunity to assess spatiotemporal variability at shorter time scales for some pollutants. However, at this time routine monitoring network data typically forms the basis for assessing spatiotemporal variability.

1.1.2. Ambient Air Quality Monitoring

National Ambient Air Quality Standards (NAAQS) were established by the Clean Air Act Amendments of 1970 for the control of wide-spread pollutants that are considered to be harmful to human health and public welfare. The US Environmental Protection Agency (EPA) set NAAQS for six pollutants including carbon monoxide, airborne lead, nitrogen dioxide, ozone, particulate matter and sulfur dioxide, which are commonly referred to as "criteria pollutants". Monitoring plans for these pollutants were implemented to comply with the Clean Air Act. Areas are designated as being in or out of compliance "attainment" based on monitored concentrations relative to the NAAQS. The Clean Air Act also requires states to submit plans, known as State Implementation Plans (SIPs), to attain the NAAQS when out of compliance and to maintain compliance after meeting the NAAQS. Among the six criteria pollutants, particulate matter and ozone are the most wide-spread health threats (US EPA, 2015b).

Ambient PM is a complex mixture of solid particles and liquid droplets of varying size. The 1971 NAAQS regulated PM using Total Suspended Particles (TSP) size indicator which is more oriented to the measurement of primary emission sources. The earliest practice of TSP monitoring was usually by local agencies as a result of the complaints concerning visual pollution. State and Local Air Monitoring Stations (SLAMS) and National Air Monitoring Stations (NAMS), a subset of SLAMS, were then implemented because of the needs for uniformity in monitor siting and data comparability (US EPA, 1989). In 1987 EPA changed the PM NAAQS indicator from TSP to PM_{10} which are particles with aerodynamic diameters less than 10μm and could be inhaled and deposited in the respiratory system. Corresponding adjustments were also made to the monitoring

plans for the SLAMS and NAMS. During the time period that followed pioneering studies on PM health effects of particulate matter indicated that fine PM ($PM_{2.5}$) had more serious health impacts to human health with evidence showing the association between exposure to $PM_{2.5}$ and increased mortality (Dockery et al., 1993; Pope et al., 1995). In 1997 the US EPA added a PM NAAQS indicator for $PM_{2.5}$ because of its severe health effects. In the following years, routine monitoring of $PM_{2.5}$ was implemented in nationwide air monitoring networks.

With the understanding of airborne particles being a complex mixture of chemical components, more recent studies have progressed to examine the linkage between specific PM components and mortality as well as morbidity (Aschner et al., 2005; Bollati et al., 2010; Ito et al., 2006; Ito et al., 2011; Ostro et al., 2007; Peng et al., 2009). In order to support air quality management towards NAAQS compliance and inform health related studies, the Chemical Speciation Network (CSN) was implemented in 1999 to provide insights into the chemical composition of $PM_{2.5}$ primarily in urban areas. The Health Effects Institute (HEI) funded the National Particle Components Toxicity (NPACT) initiative which included two large-scale studies, with both epidemiology and toxicology substudies, specifically focusing on the effects of PM components. These and a few other recent studies (Bell et al., 2009; Peng et al., 2009) have used data from the nationwide CSN. Currently 195 CSN sites are in operation with 53 Speciation Trends Network sites (STN) which is a subset of the CSN designated by US EPA for assessing long term trends. 24 hour integrated samples are collected on a 1-in-3 day or 1-in-6 day schedule and $PM_{2.5}$ gravimetric mass, water soluble ions, elements, and carbon fractions are reported for each site. Details of the samplers and analytical protocols were described

in prior reports and publications (Birch and Cary, 1996; Chow et al., 1993; Solomon et al., 2014; Solomon et al., 2000). Another speciation network is the Interagency Monitoring of Protected Visual Environments (IMPROVE) network that was established for the protection of visual environments such as national parks with a focus on regional haze. Therefore, most of the sites are located in the non-urbanized areas. $PM_{2.5}$ mass, elemental components, water soluble ions, elements, carbon fractions and PM_{10} mass are reported at IMPROVE sites.

The 1990 Clean Air Act Amendments designated a list of 188 toxic chemicals, including select VOCs and carbonyl compounds, as hazardous air pollutants (HAPs). To comply with the statute, US EPA initiated the National Air Toxics Trends Station (NATTS) Program in 2003. This network was developed to fulfill the need for long-term ambient air toxics monitoring data acquired using consistent measurement approaches and to provide information about the trends in HAPs concentrations. The current NATTS network includes 27 sites across the United States with 20 urban sites and 7 rural sites. Typically over 100 pollutants are monitored at each location including volatile organic compounds (VOCs), carbonyl compounds, PM_{10} metals, hexavalent chromium and polycyclic aromatic hydrocarbons (PAHs) even though the state/local agencies are only required to report 19 of high priority compounds. The sampling protocols are designed for each pollutant class and the temporal resolution is typically 24 hour integrated sampling on a 1-in-6 day schedule (US EPA, 2015a).

Currently there are five $PM_{2.5}$ long-term routine speciation sites in the St. Louis region which is an unusually large number of sites for a metropolitan area of its size. Three of these sites are formally part of the CSN network while two sites, including one at

Roxana, IL operated by the Turner group at Washington University, rigorously follow the CSN protocols. One site out of these sites is also formally part of the NATTS network and the Roxana site reports VOCs and carbonyls using the NATTS sampling and analytical protocols.

1.1.3. Roxana Air Quality Study

The Roxana Air Quality Study (RAQS) is funded by ConocoPhillips Company (former Wood River Refinery operator) in response to a settlement agreement with American Bottom Conservancy, the Sierra Club, the Environment Integrity Project, and the Natural Resources Defense Council. The study is being conducted in the Village of Roxana, IL located 25km northeast of the City of St. Louis, MO, central business district. The monitoring site (38°50′54.20″ N, 90° 04′ 35.50″ W) is at the fenceline of a petroleum refinery and next to a residential neighborhood. Datasets for $PM_{2.5}$ speciation, gaseous air toxics as well as other gaseous pollutants are collected with different temporal resolution and coverage. Measurements were phased in starting summer 2001 and the sampling is scheduled to end in July 2015.

1-in-6 day 24-hour integrated $PM_{2.5}$ mass and speciation data collection started July 14th 2011 and follows the CSN sampling protocols. The sampler used is a Met One Spiral Ambient Speciation Sampler (SASS; Met One Instrument Inc., Grants Pass, OR) with five sampling channels. Sampling flow rates for three of the five channels were actively controlled by mass flow controllers. The remaining two channels were equipped with critical orifices for passive flow control. Filters for $PM_{2.5}$ sampling were enclosed in metal canisters. Each of them has a cyclone with a cut point of 2.5 μm. Starting in July 2012, two filters collected from channels with active flow control were sent to RTI

International – the US EPA CSN contract laboratory – with a Nylon filter analyzed for major ions and a PTFE filter analyzed for gravimetric mass and for elemental mass by X-ray Fluorescence (XRF). The remaining three 47 mm PTFE filters (MTL, Minneapolis, MN) from each sampling event were archived for in-house analyses. These Teflon filters were weighed prior to and after the sampling event to assure the comparability between filters collected from different channels. 1-in-6 day 24-hour integrated air toxics gas data collection started June 8th 2012 and follows the NATTS sampling and analysis protocols. Samples collected in passivated stainless steel canisters and DNPH (2,4-dinitrophenylhydrazine) cartridges are sent to the Eastern Research Group (ERG) – a USEPA contract laboratory – and analyzed for 71 VOCs including 13 carbonyls by US EPA Compendium Methods TO-15 and TO-11A, respectively. Other RAQS measurements include continuous H_2S/SO_2 and meteorological parameters at 5 minute time resolution.

1.2. Motivation for this Dissertation Research

Petroleum refinery fenceline monitoring provides an opportunity to evaluate the contribution of a complex industrial facility to local air quality. Petroleum refinery operations have been associated with a variety of volatile organic compound (VOC) emission from transport, processing and storage of gases and liquids. Recent studies have drawn attention to PM emissions from fluidized catalytic cracking (FCC) units. For example, Kulkarni et al. (2007) reported that on days with FCC emissions upsets a Houston refinery could account for as high as 37% of ambient $PM_{2.5}$ mass measured at a nearby ambient monitoring site. RAQS presents an opportunity to track VOC and FCC-related emissions over several years.

Intraurban variability metrics need to be scrutinized. In spite of the growing number of epidemiological studies that realize exposure misclassification can result from the assumption of spatial homogeneity, the strengths and limitations of several key metrics for the characterization of spatiotemporal variability remained inadequately discussed. For example, measurement error can distort the interpretation of variability metrics and this effect appears to vary depending on different species (Haddad, 2015).

The St. Louis area has an unusually large $PM_{2.5}$ speciation monitoring network. The availability of a five-site $PM_{2.5}$ speciation dataset for the St. Louis region provides an opportunity to examine spatial variability in PM components. Air toxics data can be compared and contrasted across two of these sites.

1.3. Thesis Objectives and Structure

This dissertation research seeks to address certain aspects of spatial variability characterization by capitalizing on the St. Louis area air toxics and $PM_{2.5}$ speciation networks including RAQS measurements. The author was responsible for all day-to-day RAQS operations including field sampling, equipment maintenance QA/QC, in-house laboratory analysis and data analysis.

The main body of this dissertation is structured in a hierarchical manner starting with sample collection and data analysis for a site at the fenceline of a single facility, to data analysis across an urban scale network. For the case of air toxics compounds the RAQS measurements are compared and contrasted with air toxics monitoring at a site in the City of St. Louis. For the case of $PM_{2.5}$ speciation the RAQS measurements are the newest addition to a network of five sites in the St. Louis area, with measurements at some sites

dating back to 2000. Broadly, the objectives are to develop/evaluate/implement data analysis methodologies to better characterize local source impacts and spatial variability. The goal was not a comprehensive assessment of spatiotemporal variability in the St. Louis area but rather an examination of various approaches such as the strengths and limitations of source apportionment modeling using contemporary CSN datasets.

The first objective of this dissertation was to analyze RAQS $PM_{2.5}$ samples using inductively coupled plasma mass spectrometry (ICP-MS) to complement the XRF data from the US EPA contract laboratory analysis. Sample digestion and analysis protocols were optimized for lanthanoid elements, selenium, and lead isotopes. Protocols were implemented that work within the constraints of in-house analytical instrumentation. Chapter 2 presents a tracking of impacts from emissions by the refinery fluidized catalytic cracking unit using lanthanoid elements. Previous work by other researchers failed to effectively utilize surface winds data to interpret observed impacts whereas our work uses surface winds data to place the observed impacts in context. Chapter 2 has been accepted for publication in *Science of the Total Environment*. Chapter 3 presents an analytical method for analyzing $PM_{2.5}$ selenium at the low mass loadings that would be expected in contemporary samples from the CSN. A method borrowed from the analysis of aquatic samples was used to increase the analytical sensitivity for selenium. Chapter 4 focuses on the optimization of an analytical method for semi-quantitative analysis of lead isotope ratios in ambient PM. A limited number of RAQS $PM_{2.5}$ samples were analyzed with the results placed in context using Pb isotope ratios reported from previous studies. The optimized analytical method was subsequently used by Stephen Feinberg in his study of lead emissions from piston engine aircraft.

The second objective was to examine the RAQS air toxics data. Chapter 5 explores the spatial variability of air toxics compounds by comparing and contrasting RAQS data with routine measurements conducted in the City of St. Louis. Emphasis is placed on quantifying contributions from refinery operations and surface winds data were used to refine the interpretation of refinery impacts.

The third objective was to advance the application and interpretation of commonly used metrics to characterize spatiotemporal variability. Chapter 6 presents a discussion of select issues starting with sensitivity of the Pearson correlation coefficient to extreme values. Next, the work of Haddad (2015) to characterize CSN precision from collocated data is expanded to examine implications from the concentration dependence of precision. Finally, it is demonstrated that there can be cases where standard comparison metrics might lead to the conclusion that species concentrations across two sites are homogeneous (and therefore local sources are inconsequential), yet the differences cannot be explained by measurement error. A detailed examination of these data reveals impacts from local sources and this provides further evidence for using measurement error as a context for assessing intersite differences.

The fourth objective, summarized in Chapter 7, was to examine opportunities and challenges to assessing spatiotemporal variability from source apportionment modeling results. The five CSN sites in the St. Louis area were modeled using Positive Matrix Factorization (PMF). $PM_{2.5}$ mass in this area is dominated by regional sources with contributions from local sources that vary by site. A given source might have different factor loadings across the single-site analyses which can confound spatiotemporal variability estimates. A multi-site analysis ensures the same source profile is used

across the sites and might help to stabilize the results for regional sources but may cause issues when quantifying impacts from local sources that have differential impacts on the sites. Modelling uncertainty estimation, which is far less studied in many previous source apportionment studies, is also systematically evaluated using the tools incorporated into the newest version of publicly available EPA PMF model.

Finally, the two appendices summarize preliminary and tangential work. Appendix A presents preliminary results from a collaboration with Yuyang Peng to automate Potential Source Contribution Function (PSCF) analyses. Appendix B briefly summarizes certain aspects of an analysis conducted for Dr. Mario Castro and Leonard Bacharier, Washington University School of Medicine, to estimate exposure to air pollutants in support of an asthma inception study.

1.4. References

Aschner, M., Erikson, K.M., Dorman, D.C., 2005. Manganese dosimetry: Species differences and implications for neurotoxicity. Crit. Rev. Toxicol. 35, 1-32.

Bell, M.L., Ebisu, K., Peng, R.D., Samet, J.M., Dominici, F., 2009. Hospital Admissions and Chemical Composition of Fine Particle Air Pollution. American Journal of Respiratory and Critical Care Medicine 179, 1115-1120.

Birch, M.E., Cary, R.A., 1996. Elemental carbon-based method for monitoring occupational exposures to particulate diesel exhaust. Aerosol Science and Technology 25, 221-241.

Bollati, V., Marinelli, B., Apostoli, P., Bonzini, M., Nordio, F., Hoxha, M., Pegoraro, V., Motta, V., Tarantini, L., Cantone, L., Schwartz, J., Bertazzi, P.A., Baccarelli, A., 2010. Exposure to Metal-Rich Particulate Matter Modifies the Expression of Candidate MicroRNAs in Peripheral Blood Leukocytes. Environmental Health Perspectives 118, 763-768.

Burnett, R., Ma, R.J., Jerrett, M., Goldberg, M.S., Cakmak, S., Pope, C.A., Krewski, D., 2001. The spatial association between community air pollution and mortality: A new method of analyzing correlated geographic cohort data. Environmental Health Perspectives 109, 375-380.

Burton, R.M., Suh, H.H., Koutrakis, P., 1996. Spatial variation in particulate concentrations within metropolitan Philadelphia. Environmental Science & Technology 30, 400-407.

Chow, J.C., Watson, J.G., Pritchett, L.C., Pierson, W.R., Frazier, C.A., Purcell, R.G., 1993. The dri thermal/optical reflectance carbon analysis system: description, evaluation and applications in U.S. Air quality studies. Atmospheric Environment Part A, General Topics 27, 1185-1201.

Dockery, D.W., Pope III, C.A., Xu, X., Spengler, J.D., Ware, J.H., Fay, M.E., Ferris Jr, B.G., Speizer, F.E., 1993. An association between air pollution and mortality in six U.S. cities. N. Engl. J. Med. 329, 1753-1759.

Haddad, K., 2015. An assessment of air pollution databases to inform their use in epidemiological studies, Department of Energy, Environmental and Chemical Engineering. Washington University in St. Louis.

Houthuijs, D., Breugelmans, O., Hoek, G., Vaskovi, E., Mihalikova, E., Pastuszka, J.S., Jirik, V., Sachelarescu, S., Lolova, D., Meliefste, K., Uzunova, E., Marinescu, C., Volf, J., de Leeuw, F., van de Wiel, H., Fletcher, T., Lebret, E., Brunekreef, B., 2001. PM10 and PM2.5 concentrations in Central and Eastern Europe: results from the Cesar study. Atmospheric Environment 35, 2757-2771.

Ito, K., Christensen, W.F., Eatough, D.J., Henry, R.C., Kim, E., Laden, F., Lall, R., Larson, T.V., Neas, L., Hopke, P.K., Thurston, G.D., 2006. PM source apportionment and health effects: 2. An investigation of intermethod variability in associations between source-apportioned fine particle mass and daily mortality in Washington, DC. Journal of Exposure Science and Environmental Epidemiology 16, 300-310.

Ito, K., Mathes, R., Ross, Z., Nádas, A., Thurston, G., Matte, T., 2011. Fine particulate matter constituents associated with cardiovascular hospitalizations and mortality in New York City. Environmental Health Perspectives 119, 467-473.

Ito, K., Xue, N., Thurston, G., 2004. Spatial variation of PM2.5 chemical species and source-apportioned mass concentrations in New York City. Atmospheric Environment 38, 5269-5282.

Kulkarni, P., Chellam, S., Fraser, M.P., 2007. Tracking petroleum refinery emission events using lanthanum and lanthanides as elemental markers for $PM_{2.5}$. Environmental Science & Technology 41, 6748-6754.

Ostro, B., Feng, W.-Y., Broadwin, R., Green, S., Lipsett, M., 2007. The effects of components of fine particulate air pollution on mortality in California: Results from CALFINE. Environmental Health Perspectives 115, 13-19.

Pakbin, P., Hudda, N., Cheung, K.L., Moore, K.F., Sioutas, C., 2010. Spatial and Temporal Variability of Coarse (PM(10-2.5)) Particulate Matter Concentrations in the Los Angeles Area. Aerosol Science and Technology 44, 514-525.

Peng, R.D., Bell, M.L., Geyh, A.S., McDermott, A., Zeger, S.L., Samet, J.M., Dominici, F., 2009. Emergency Admissions for Cardiovascular and Respiratory Diseases and the Chemical Composition of Fine Particle Air Pollution. Environmental Health Perspectives 117, 957-963.

Pinto, J.P., Lefohn, A.S., Shadwick, D.S., 2004. Spatial variability of PM2.5 in urban areas in the United States. Journal of the Air & Waste Management Association 54, 440-449.

Pope III, C.A., Burnett, R.T., Thun, M.J., Calle, E.E., Krewski, D., Ito, K., Thurston, G.D., 2002. Lung cancer, cardiopulmonary mortality, and long-term exposure to fine particulate air pollution. Jama-Journal of the American Medical Association 287, 1132-1141.

Pope III, C.A., Thun, M.J., Namboodiri, M.M., Dockery, D.W., Evans, J.S., Speizer, F.E., Heath Jr, C.W., 1995. Particulate air pollution as a predictor of mortality in a prospective study of U.S. Adults. American Journal of Respiratory and Critical Care Medicine 151, 669-674.

Roosli, M., Theis, G., Kunzli, N., Staehelin, J., Mathys, P., Oglesby, L., Camenzind, M., Braun-Fahrlander, C., 2001. Temporal and spatial variation of the chemical composition of PM10 at urban and rural sites in the Basel area, Switzerland. Atmospheric Environment 35, 3701-3713.

Solomon, P.A., Crumpler, D., Flanagan, J.B., Jayanty, R.K., Rickman, E.E., McDade, C.E., 2014. U.S. national PM2.5 Chemical Speciation Monitoring Networks-CSN and IMPROVE: description of networks. Journal of the Air & Waste Management Association (1995) 64, 1410-1438.

Solomon, P.A., Mitchell, W., Tolocka, M., Norris, G.A., Gemmill, D., Wiener, R., Vanderpool, R., Murdoch, R., Natarajan, S., Hardison, E., 2000. Evaluation of $PM_{2.5}$ chemical speciation samplers for use in the EPA National $PM_{2.5}$ Chemical Speciation Network. EPA-454/R-01-005. Office of Air Quality Planning and Standards, US Environmental Protection Agency, Research Triange Park, NC.

United States Environmental Protection Agency, 1989. PM_{10} monitoring task force report.

United States Environmental Protection Agency, 2015a. National Air Toxics Trends Station work plan template.

United States Environmental Protection Agency, 2015b. What are the six common air pollutants.

Wang, G., Hopke, P.K., Turner, J.R., 2011. Using highly time resolved fine particulate compositions to find particle sources in St. Louis, MO. Atmospheric Pollution Research 2, 12.

Wilson, W.E., Suh, H.H., 1997. Fine particles and coarse particles: Concentration relationships relevant to epidemiologic studies. Journal of the Air & Waste Management Association 47, 1238-1249.

Zanobetti, A., Schwartz, J., Samoli, E., Gryparis, A., Touloumi, G., Peacock, J., Anderson, R.H., Le Tertre, A., Bobros, J., Celko, M., Goren, A., Forsberg, B., Michelozzi, P., Rabczenko, D., Hoyos, S.P., Wichmann, H.E., Katsouyanni, K., 2003. The temporal pattern of respiratory and heart disease mortality in response to air pollution. Environmental Health Perspectives 111, 1188-1193.

Zhu, Y.F., Hinds, W.C., Kim, S., Shen, S., Sioutas, C., 2002. Study of ultrafine particles near a major highway with heavy-duty diesel traffic. Atmospheric Environment 36, 4323-4335.

Chapter 2 : Using $PM_{2.5}$ Lanthanoid Elements and Nonparametric Wind Regression to Track Petroleum Refinery FCC Emissions

This chapter has been published in Science of the Total Environment (L. Du and J. Turner, volume 529, pages 65-71 (2015).

2.1. Abstract

A long term air quality study is being conducted in Roxana, Illinois, USA, at the fenceline of a petroleum refinery. Measurements include 1-in-6 day 24-hour integrated ambient fine particulate matter ($PM_{2.5}$) speciation following the Chemical Speciation Network (CSN) sampling and analysis protocols. Lanthanoid elements, some of which are tracers of fluidized-bed catalytic cracker (FCC) emissions, are also measured by inductively coupled plasma – mass spectrometry (ICP-MS) after extraction from $PM_{2.5}$ using hot block-assisted acid digestion. Lanthanoid recoveries of 80-90% were obtained for two ambient particulate matter standard reference materials (NIST SRM 1648a and 2783). Ambient $PM_{2.5}$ La patterns could be explained by a two-source model representing resuspended soil and FCC emissions with enhanced La/Ce ratios when impacted by the refinery. Nonparametric wind regression demonstrates that when the monitoring station was upwind of the refinery the mean La/Ce ratio is consistent with soil and when the monitoring station is downwind of the refinery the mean ratio is more than four times higher for bearings that corresponds to maximum impacts. Source apportionment modeling using EPA UNMIX and EPA PMF could not reliably apportion $PM_{2.5}$ mass to the FCC emissions. However, the weight of evidence is that such contributions are small with no large episodes observed for the 164 samples analyzed.

This study demonstrates the applicability of a hot block-assisted digestion protocol for the extraction of lanthanoid elements as well as insights obtained from long-term monitoring data including wind direction-based analyses.

2.2. Introduction

Petroleum refinery operations have historically been associated with emission of a variety of volatile organic compounds (VOCs) from transport, processing and storage of gases and liquids, whereas their contribution to ambient particulate matter (PM) has been less studied. However, studies by Chellam and coworkers (Bozlaker et al., 2013; Kulkarni et al., 2007a; Kulkarni et al., 2006; Kulkarni et al., 2007b; Kulkarni et al., 2007c) and Moreno et al. (2008a) have drawn attention to particulate matter (PM) primary emissions from petroleum refinery fluidized-bed catalytic cracking (FCC) units which are used to crack the heavy, long-chain molecules in crude oil feedstock into lighter, shorter-chain products. While lanthanoid element concentrations in the atmosphere are typically dominated by emissions from natural sources such as resuspended crustal material, anthropogenic processes including but not limited to motor vehicle emissions, ceramic industries and refinery operations can be significant contributors (Bozlaker et al., 2013; Kitto et al., 1992; Kulkarni et al., 2006; Moreno et al., 2008b). Particulate matter emitted from the FCC unit is mainly comprised of zeolite catalyst material enriched in crustal elements such as Al and Si as well as lanthanoid elements with a notable enhancement in lanthanum; thus, La/Ce ratios and La/Sm/Ce ratios have been used to identify ambient PM samples with FCC emissions impacts with supporting evidence provided by source apportionment modeling (Bozlaker et al., 2013; Kulkarni et al., 2007a; Kulkarni et al.,

2006) or air mass classifications derived from air mass back trajectories (Moreno et al., 2008a).

Chellam and coworkers have focused on measurements in the greater Houston, Texas (USA) area. In a one month study with 114 short-term (3 or 6 hour) PM_{10} samples they concluded that 70% of samples were negligibly impacted by FCC emissions (Bozlaker et al., 2013). Kulkarni et al. (2006; 2007b) apportioned 1-2% of the ambient fine PM ($PM_{2.5}$) to refinery operations during days without FCC emission episodes for twenty-five 24-hour samples collected over a nominally three month period. In contrast, contributions as high as 37% of ambient $PM_{2.5}$ mass were estimated for emission episode days including one event estimated to have released about 57 kg of $PM_{2.5}$ over two days in 2005 and another event that released about 45 tons of catalyst because of a break in the FCC unit cyclone of the FCC in 2006 (Kulkarni et al., 2007b). The role of transient emissions events and their reporting was further examined by Bozlaker et al. (2013).

Moreno et al. (2008a) conducted a 14-month sampling campaign that collected 110 PM_{10} samples and 111 $PM_{2.5}$ samples at a monitoring station located about 3-4 km from the FCC unit at a petroleum refinery in Puertollano, Spain. Air mass back trajectories were used to classify each sampling day as crustal North African, crustal non-North African, local, regional and oceanic advective scenarios. Scenarios presumed to be dominated by local influences exhibited the highest La enrichment compared to Ce and Sm. Three days were deemed “lanthanum anomaly days” with particularly high La enrichment and in each case the prevailing winds were from the direction of the petroleum refinery.

The aforementioned studies demonstrate the utility of using lanthanoid elements to track FCC unit emissions impacts. Ambient PM samples, especially from routine monitoring networks, are commonly analyzed for elemental composition by x-ray fluorescence (XRF) but for the air volumes sampled the trace to ultra-trace level lanthanoid concentrations are typically well below detection limits. Instrumental neutron activation analysis (INAA) and inductively coupled plasma-mass spectrometry (ICP-MS) have been widely accepted as accurate methods to quantify ambient PM lanthanoid elements (Kowalczyk et al., 1982; Olmez and Gordon, 1985). ICP-MS has become the preferred method because of its easy accessibility, relatively low cost, and less stringent requirement for laboratory infrastructures. High temperature, high pressure acid digestion is often used to extract a wide range of elements from ambient PM samples (Kotchenruther, 2013; Kulkarni et al., 2007a; Kulkarni et al., 2007c; Moreno et al., 2008a; Wu et al., 1996) and microwave-assisted acid digestion is commonly used when the focus is on lanthanoid elements (Celo et al., 2012; Kulkarni et al., 2006; Moreno et al., 2008a).

In this study, ambient $PM_{2.5}$ data were already available for many elements from the routine XRF analysis and we sought a low-cost, high-throughput method to analyze lanthanoids in these samples. The prevailing microwave digestion systems usually provide a digestion environment with temperature of about 200°C and pressure of about 200 psig (Danadurai et al., 2011; Kulkarni et al., 2007a; Kulkarni et al., 2007c; Wu et al., 1996). In contrast, we evaluated the capability of extracting lanthanoid elements using hot plate-assisted digestion which is conducted at moderately high temperature (90°C in our case) and atmospheric pressure. Ambient $PM_{2.5}$ filter samples collected over a three-

year period at the fenceline of a petroleum refinery were analyzed for lanthanoid elements to track FCC emissions. Nonparametric wind regression was used to determine the La concentrations and La/Ce ratios when the sampling site was upwind and downwind of the FCC unit.

2.3. Methods

2.3.1. Ambient $PM_{2.5}$ Sampling

Ambient $PM_{2.5}$ samples were collected during the Roxana Air Quality Study (RAQS). The Village of Roxana, Illinois (USA), is 25 km northeast of the City of St. Louis, MO, central business district and the monitoring site (38°50′54.20″ N, 90°04′35.50″ W) is at the fenceline of a petroleum refinery and next to a residential neighborhood (Figure 2-1). Measurements include: continuous H_2S, SO_2, and meteorological parameters; 1-in-6 day 24-hour integrated volatile organic compounds and carbonyls by USEPA Methods TO-15 and TO-11A, respectively; and 1-in-6 day 24-hour integrated $PM_{2.5}$ mass and speciation following the Chemical Speciation Network (CSN) sampling and analysis protocols. For the period of interest (July 14th 2011 – June 28th 2014), 178 valid sampling events were conducted (out of 181 events attempted) with ambient $PM_{2.5}$ collected onto 47mm PTFE filters (MTL, Minneapolis, MN) using the Met One Spiral Ambient Speciation Sampler (SASS; Met One Instruments Inc., Grants Pass, OR) operating with flow rate of 6.7 LPM. The SASS has five sampling channels.

Starting in July 2012, two filters were sent to RTI – the USEPA CSN contract laboratory – with a Nylon filter analyzed for major ions and a PTFE filter analyzed for gravimetric mass and for elemental mass by XRF. The remaining three filters from each sampling

event were archived in a freezer with one filter used for lanthanoids analysis and a second filter sometimes analyzed to determine collocated precision.

Figure 2-1. Roxana (IL) air monitoring station and the adjacent petroleum refinery. The thick black line is the refinery boundary for the main operations; refinery satellite operations areas are not marked. Map source: ESRI (2015).

2.3.2. Soil Samples

Three soil samples were collected from the area within 3 km of the monitoring station to obtain the lanthanoids profile of local crustal material. To minimize contamination from FCC emissions deposition, the soil collection sites were intentionally selected to be away from the prevailing wind directions for FCC emissions impacts and the samples were taken from 5 cm below the surface. The collected soil samples were stored in jars and kept frozen in the laboratory until analysis. Prior to digestion the soil samples were homogenized, resuspended and deposited onto filter media. Before the resuspension

procedure, soil samples were first dried in a heated oven at 65^{o}C for 24 hours and grounded using a porcelain pestle and mortar set. The grounded and homogenized soil samples were resuspended in a custom-made resuspension chamber based on designs from related studies (Carvacho et al., 2004; Chow et al., 1994; Martuzevicius et al., 2011) and the particles less 2.5 μm were collected on 47mm PTFE filters which are identical to the filter media used in the routine ambient sampling. Each soil sample was resuspended and sampled three times. The soil samples deposited on the filters were subsequently stored in a refrigerator until further analysis.

2.3.3. Hot Acid Digestion

A two-stage HNO_3-HF-HBO_3 protocol for the extraction of elements in silicon-containing solid materials was first explored and demonstrated by Wu et al (1996). Recent studies have adopted and customized this protocol for the analysis of ambient particulate matter as well as FCC catalysts (Danadurai et al., 2011; Kulkarni et al., 2007a; Kulkarni et al., 2007c). While these previous studies used microwave-assisted digestion, in this study a hot plate digestion system (ModBlock^{TM}, CPI International, Santa Rosa, CA) was used with a specific focus on quantifying the light lanthanoids rather than a broader range of elements. The aforementioned previous studies provided the framework to optimize the Wu et al. (1996) protocol for this application.

Digestion efficiencies for the target lanthanoids were evaluated as recoveries using two standard reference materials (SRMs) purchased from the National Institute of Standard and Technology (NIST). SRM 1648a was collected as total suspended particulate (TSP) from St. Louis, MO and provided as a homogenized powder whereas SRM 2783 was $PM_{2.5}$ from Baltimore, MD that was homogenized, resuspended, and collected onto

polycarbonate filter media. The filter-deposited SRM is substantially more expensive per unit analysis than the bulk powder SRM and thus the acid matrix was optimized using SRM 1648a and then validated using SRM 2783.

Two-stage digestions were conducted in Capitol Vials (Fisher Scientific, Pittsburgh, PA) which are compatible with the ModBlock^{TM} system. For the ambient PM samples the filter deposit area was cut from the PTFE support ring to avoid contamination form the adhesive used to attach the support ring to the membrane filter. A combination of concentrated (69 ~70%) nitric acid (Trace metal analysis, J.T. Baker, Center Valley, PA) and concentrated (47 ~ 51%) hydrofluoric acid (Suprapur Grade, BDH, UK) was used in the first stage to extract the elements. In the second stage, 5% (m/v) boric acid (J.T. Baker, Center Valley, PA) solution was added to the acid matrix to complex the excess HF to protect the ICP-MS and to dissolve the insoluble metal fluoride that formed in the digestion process (Kulkarni et al., 2007c). In each stage the samples were digested for 2 hours at 90^{o}C and atmospheric pressure. After the digestion process, the sample solutions were diluted with DI water to a final HNO_3 concentration of 5% (v/v) and filtered using Acrodisc (Pall Corporation, Port Washington, NY) syringe filters before ICP-MS analysis.

The effect of filter wettability on extraction efficiency was tested using a subset of collocated samples. For each pair, one sample was handled as described above while 100 μL ethanol was added to the other sample. Extraction efficiencies in the presence and absence of ethanol were statistically indistinguishable (95% C.L.) and thus ethanol was not included in the final protocol.

2.3.4. Elemental Analysis by ICP-MS

An ICP-MS instrument (Elan DRC II, Perkin Elmer, Norwalk, CT) operated in standard mode was used for the elemental analysis. Before each analysis batch, the ICP settings were optimized following the standard protocol using a Smart Tune solution (Perkin Elmer) (Danadurai et al., 2011). The ICP-MS instrument was then calibrated with multi-element calibration standards made from a multi-element stock standard solution consisting of 18 elements (CPI International, Santa Rosa, CA) and a stock standard solution with 15 lanthanoid elements (Perkin Elmer, Norwalk, CT). A digested acid matrix matched blank solution with composition identical to the sample acid matrices (5% HNO_3, 0.025% HF and 0.25% H_3BO_3) was used to make the calibration standards. Isobaric and spectral interferences were suppressed by applying the correction equations suggested by the instrument data analysis software. Additional quality assurance measures included reagent blanks and method blanks (clean filters) that were processed with each batch of digested samples as well as a spiked reagent blank (with calibration standards) and check standards that ran every ten samples. ^{115}In has been used as the internal standard for the measurement of lanthanoid elements by ICP-MS in related studies (Kulkarni et al., 2007a; Kulkarni et al., 2006; Kulkarni et al., 2007b; Kulkarni et al., 2007c). However, there is evidence for In in the $PM_{2.5}$ samples collected at Roxana and this could potentially interfere with the stability of the internal standard signal intensity. Thus, in this study 20 ppb ^{103}Rh was used for light lanthanoid elements (La, Ce, Pr) and 20 ppb ^{187}Re was used for the heavy lanthanoid elements (Nd, Sm, Eu, Gd, Tb, Dy, Ho, Er, Tm, Yb, Lu). Pm was not quantified because of the lack of stable isotopes.

Fourteen of the 178 ambient $PM_{2.5}$ sampling events analyzed for lanthanoids were invalidated – four samples because of contamination and ten samples because of poor reanalysis precision or poor collocated sample precision. None of the invalidated samples had anomalously high La concentrations. The remaining 164 samples were used in the data analysis.

2.3.5. Method Detection Limit

Method Detection Limits (MDLs) were evaluated according to the method recommended by the US Environmental Protection Agency (USEPA, 2005). In this study, the MDL for each element was calculated as 3.143 times the standard deviation of the analysis of seven replicate digested acid matrix matched blank solutions spiked with the lowest concentrations used to calibrate the ICP-MS instrument.

2.3.6. Nonparametric Wind Regression (NWR)

Nonparametric wind regression was introduced by Henry et al. (2002) as a type of pollution rose that does not require *a priori* binning of the data into discrete wind direction sectors. A Gaussian kernel is used in conjunction with a user-defined smoothing parameter to generate a smooth curve relating the expected (mean) concentration to wind direction. NWR was initially implemented on hourly concentration data and hourly winds data but has also been used on 24-hour integrated concentration data and hourly winds data. The latter approach can lead to smearing across wind directions yet often generates interpretable results including good agreement with the conditional probability function (CPF) approach to locate the bearings of emission sources (Kim and Hopke, 2004).

In this study, NWR was conducted on 24-hour integrated concentration data using hourly surface winds data. Hours with calm winds (operationally defined as wind speeds less than 0.5 m/s) were excluded from the analysis. Confidence intervals were generated by bootstrapping the dataset; no blocking was needed because the 1-in-6 day concentration values for the parameters of interest were not serially correlated. Analyses were conducted using two independent surface winds datasets. One dataset was hourly 10m winds collected at the Roxana monitoring station where the PM samples were collected. Nearby trees immediately southwest of the site potentially pose an obstruction to airflow and thus the analyses were also conducted using 10m surface winds from the Automated Surface Observing System (ASOS) at Lambert St. Louis International Airport which is located ~30 km west-southwest of the site. The winds data were generally in good agreement with Lambert data having modest higher wind speeds and also southerly wind directions more evenly distributed across the southeast-to-southwest range; the latter pattern is consistent with the Mississippi River Valley channeling of airflow at Roxana as well as the possible influence of the aforementioned obstructions.

2.4. Results and Discussion

2.4.1. Digestion and Analysis Protocol Optimization

The influence of acid matrix on lanthanoids recoveries from SRM 1648a was evaluated by fixing the HNO_3 volume and systematically varying the HF and HBO_3 volumes. H_2O_2 has been used as an oxidant in similar studies with high organic matter content in the samples (Wu et al., 1996). Thus, each acid matrix was tested with and without H_2O_2 addition. Recoveries did not increase with H_2O_2 addition and the oxidant was not included in the optimized protocol. An acid matrix of 5 mL HNO_3, 150 µL HF and 1.5

mL H_3BO_3 was deemed optimal for the recovery of lanthanoids from 10 mg of the SRM with H_3BO_3 in stoichiometric excess of HF for complete complexation of excess HF. The optimized digestion protocol was validated using SRM 2783. Table 2-1 summarizes the measured concentrations and recoveries of certified and reference lanthanoids in the SRMs. Recoveries in the range 80-90% were obtained for all cases. Acceptable recoveries (80 – 120%) were also observed for certain other non-lanthanoid elements. However, they are beyond the scope of this study and thus are not discussed.

The acid volumes for digesting ambient PM deposited on filter media were proportionally scaled down to 15 μL HF and 150 μL H_3BO_3 because of the lower PM loading yet to ensure stoichiometric excess relative to the siliceous materials. HNO_3 was kept at 3 mL instead of its proportionally lower volume to ensure adequate liquid for the full submergence of the filter media.

Table 2-1. Recoveries of SRM 1648a (n=5) and SRM 2783 (n=4) by ICP-MS after optimized digestion. Uncertainties are represented by the standard deviation of the replicates. All NIST concentrations are certified values except La and Sm in SRM 1648a which are reference values.

Element	NIST concentration (mg/kg)	This study (mg/kg)	Recovery (%)
SRM 1648a			
La	39 ± 3	31.7 ± 1	81 ± 7
Ce	54.6 ± 2.2	45.4 ± 1	83 ± 5
Sm	4.3 ± 0.3	3.8 ± 0.1	89 ± 6
SRM 2783			
Ce	23.4 ± 3.5	19.5 ± 1.2	83 ± 13
Sm	2.04 ± 0.15	1.62 ± 0.07	80 ± 7

2.4.2. Lanthanoids in Ambient $PM_{2.5}$ and Soil Samples

Figure 2-2 shows the concentration distributions of lanthanoid elements observed in the Roxana ambient $PM_{2.5}$ samples. MDL values are shown as thick horizontal lines and

concentration values below the MDL were retained as reported. There are two key features to these distributions. First, the concentration values are higher for the light lanthanoids compared to the heavy lanthanoids. Second, lanthanoids with odd atomic numbers are typically less abundant than their even-numbered neighbors as shown by the alternating high-low patterns in Figure 2-2; this pattern is consistent with lanthanoid abundances in crustal material (Moreno et al., 2008a). An exception to this pattern is lanthanum (atomic number 57) which has a concentration distribution similar to its even-numbered neighbor, cerium (atomic number 58). The high La/Ce ratio is consistent with impacts from anthropogenic sources. Kulkarni et al. (2006) and Moreno et al. (2008a) observed elevated La/Ce ratios in ambient PM samples collected in areas where the La enrichment was attributed to the catalyst used in petroleum refinery FCC units. Other studies have identified lanthanoids with La to Ce ratio of 0.2-0.8 to be primarily from the resuspension of local dust and possibly motor vehicle emissions (Huang et al., 1994; Taylor and McLennan, 1985).

For most of the heavy lanthanoids, over 50% of the data were below their respective MDL yet the geochemical pattern of the lanthanoids was well maintained. 40 CFR 136 (USEPA, 2005) defines MDL as "the minimum concentration of a substance that can be measured and reported with 99% confidence that the analyte concentration is greater than zero and is determined from analysis of a sample in a given matrix containing the analyte". In other words, this MDL provides a criterion for identifying data with a very high confidence (99%) of being detected. Data values below MDL may be still trusted to a lower level of confidence and indicative information can be exacted from these data. In this case, the geochemical pattern of the odd-numbered heavy lanthanides being less

abundant than their even-numbered neighbors is preserved even when most of the data are below the MDL values.

Lanthanoid profiles for the nine soil analyses (three resuspension replicates for each of three soil samples) are provided in Table 2-2 of the Supplementary Material. La/Ce ratios were statistically indistinguishable (95% C.L.) across these data and thus were pooled to yield a mean La/Ce ratio ($\pm 1\sigma$) of 0.519 ± 0.041. To place this ratio in context, geochemical and mineralogical data for soils were obtained from the United States Geological Survey database (USGS, 2014) which includes 47 elements measured in

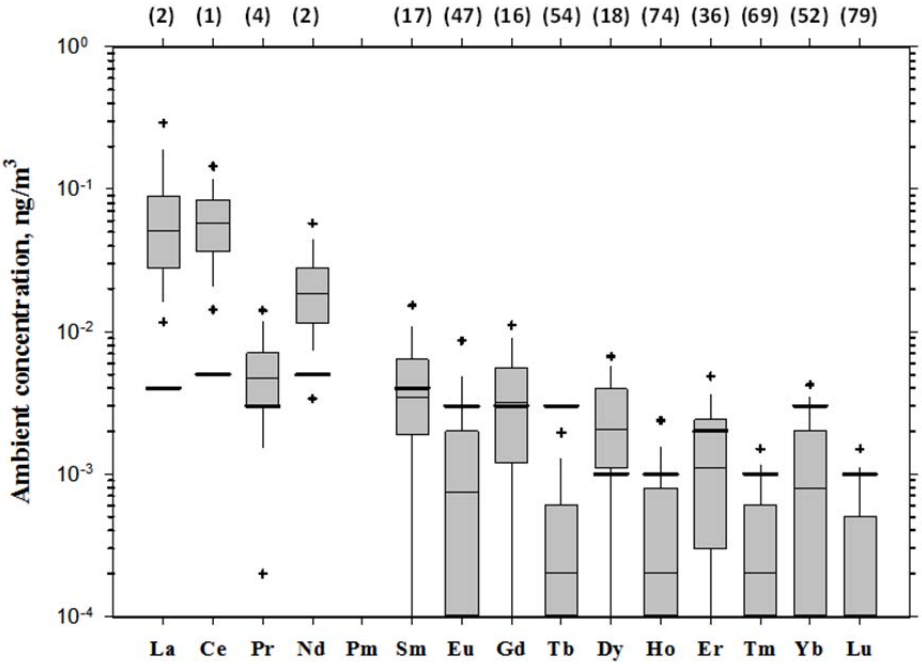

Figure 2-2. Concentration distributions of ambient $PM_{2.5}$ lanthanoid elements for samples collected from July 2011 through July 2014 (N=164). The boxes are 25th and 75th percentiles, whiskers are 10th and 90th percentiles, and crosses are 5th and 95th percentiles. The interior thin solid lines are the medians and the thick horizontal lines are the MDL estimates. The numbers of non-detects are denoted in parentheses.

various soil horizons. For the "Top 5 cm" soil horizon and including all locations in the conterminous US, the mean La/Ce ratio ($\pm 1\sigma$) was 0.504 ± 0.051 (N=4836). A regional soil profile was developed using a Geographical Information System (ArcGIS) to identify the samples collected within 200 km of Roxana and in this case the mean La/Ce ratio ($\pm 1\sigma$) was 0.507 ± 0.049 (N=79). Both regional and nationwide soil profiles agree well with the in-house analysis of soil samples collected at Roxana.

2.4.3. Evidence for FCC Emissions Impacts

As previously mentioned, La/Ce ratios and La/Sm/Ce ratios have been used to identify ambient PM samples with FCC emissions impacts. In this study more than 50% of Sm values were below the MDL and thus the analysis focuses on La/Ce ratios. Figure 2-3 shows a scattergram of La concentration on Ce concentration. $PM_{2.5}$ Ce ranged from 0.005 to 0.28 ng/m^3 whereas $PM_{2.5}$ La spanned a wider range from 0.003 to 0.91 ng/m^3. The local soil La/Ce ratio (solid line in Figure 2-3) is a lower edge for the ambient data and soil is likely the dominant source of La and Ce for samples near this edge. About 50% of the samples exhibited an La/Ce ratio in the range from 0.2 to 0.8 which has been attributed to soil resuspension and motor vehicle emissions (Kulkarni et al., 2007a). In contrast, the other 50% of the sampling days exhibited higher La/Ce ratios which suggest impacts from additional emission sources.

The source(s) of excess La was examined using surface winds data. Figure 2-4 shows expected concentrations as a function of wind direction from NWR analysis on the 3-year dataset of La, and Ce, and La/Ce. (Figure 2-6 in the Supplementary Materials shows these profiles with bootstrapped confidence intervals.) For Roxana winds (solid curves), the La expected concentrations profile exhibits a maximum of ~0.3 ng/m^3 at ~ 125^{o}N

whereas for Ce there is no dominant wind direction for maximum impacts. The La/Ce data were conditioned to include only those days with both La and Ce concentrations larger than 3×MDL to suppress the influence of large uncertainties in the ratio at low concentrations. The La/Ce NWR profile is quite similar to the La profile because the Ce NWR profile lacks strong features. Both La and La/Ce NWR profiles have a maximum for winds from the southeast which is consistent with the main unit

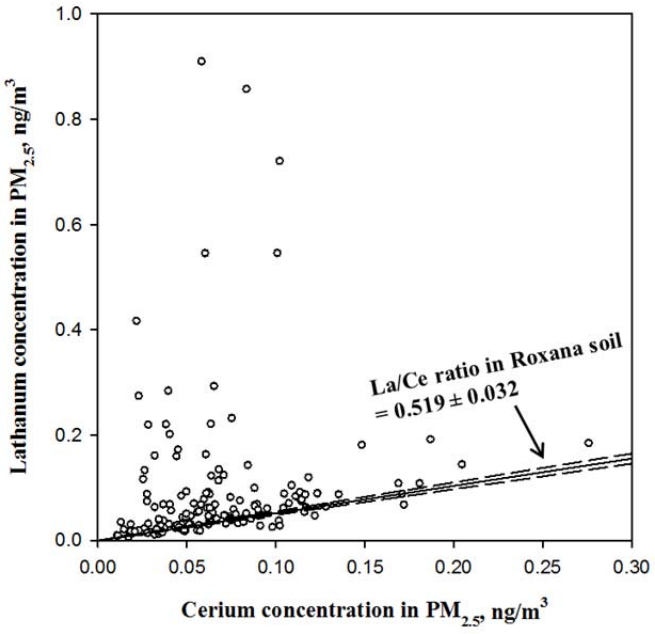

Figure 2-3. La and Ce in the ambient $PM_{2.5}$ samples. The solid line is the La/Ce mean ratio (± 95% C.L.) in Roxana soil samples.

operations area of the refinery. The maximum is sharper for Roxana winds than for Lambert winds (dashed curves) because of the relatively lower frequency of southeast winds in the Roxana data which makes the expected value more sensitive to extreme values. Both winds datasets do demonstrate elevated La and La/Ce for winds from the southeast. Figure 2-8 in the Supplementary Material shows Figure 2-4c as a Cartesian

plot. The expected La/Ce ratio has maximum of 3-4 (depending on winds dataset) for winds from the southeast and is typically in the range 0.8-1.0 from winds from other directions which place the monitoring station upwind of the refinery. These values are lower and upper bounds for mean FCC and soil impacts, respectively, because the NWR analysis is performed using 24-hour integrated PM data and hourly winds and thus there is smearing of impacts across the wind directions observed on a given day.

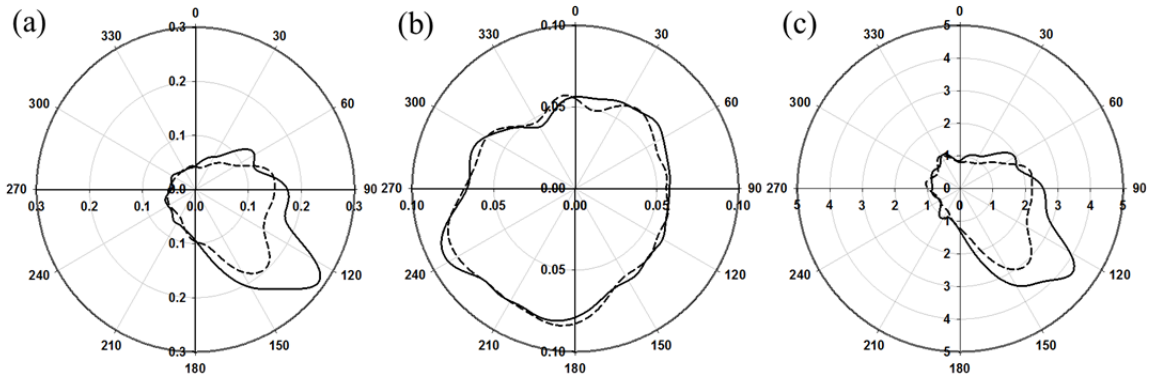

Figure 2-4. Nonparametric wind regression expected values for ambient $PM_{2.5}$ La (a), Ce (b), and the La/Ce ratio (c) using Roxana winds (solid curves) and Lambert winds (dashed curves). Expected values in panels (a) and (b) have units of ng/m^3.

High La concentrations in Figure 2-3 correspond to relatively high FCC impacts but not necessarily days with anomalously high emissions because impacts at the monitoring station are a function of both emissions and dispersion characteristics. Figure 2-5 shows the distributions of La, Ce, and La/Ce stratified by the frequency of hourly winds from the southeast quadrant over the 24 hour sampling period. (Figure 2-8 in the Supplementary Materials shows these figures using Lambert St. Louis International Airport winds.) Median La concentrations, which are

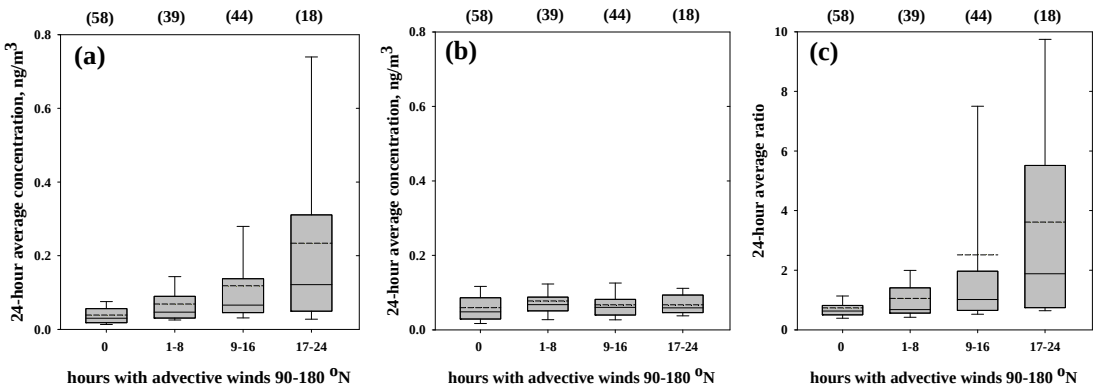

Figure 2-5. Distributions for 24-hour integrated ambient $PM_{2.5}$ La (a), Ce (b), and the La/Ce ratio (c) after stratifying the data by the number of hours with advective winds (speeds > 0.5 m/s) from the southeast quadrant using Roxana winds. Interior solid lines are medians and dashed lines are arithmetic means. The numbers of samples in each distribution are denoted in parenthesis.

24-hour integrated values, monotonically increase with increasing hours of southeasterly winds (Figure 2-5a). For both La and La/Ce there are statistically significant differences in the medians (Kruskal Wallis test, 95% C.L.) and Dunn's test reveals the nearest neighbor medians (e.g. comparing the medians for 9-16 hours to 17-24 hours) are statistically indistinguishable (family error rate of 95% C.L.) but the remaining comparisons are statistically different (e.g., medians for 0 and 1-8 hours compared to 17-24 hours).

In addition, the enrichment of La and Ce in $PM_{2.5}$ relative to local soil was quantified by the enrichment factor (EF) suggested by (Kulkarni et al., 2006) using Gd as the reference element. Enrichment factors for La and Ce were both close to unity which is consistent with resuspended soil being the dominant contributor of these elements to ambient $PM_{2.5}$.

2.4.4. Source Apportionment Modeling

Source apportionment modeling was conducted as described in Section 2.8.3 of the Supplementary Material. A combined dataset was prepared using the CSN data (gravimetric mass, elements by XRF, ions, and elemental/organic carbon) and the ICP-MS data (lanthanoids and select other elements). Modeling with EPA UNMIX (Version 6.0) generated a feasible four factor solution including one factor that explained about 80% of the La mass. The average source contribution estimate for this factor was 0.6 $\mu g/m^3$ which represents about 5% of the $PM_{2.5}$ mass. However, there was substantial nitrate, sulfate and organic carbon loaded onto this factor and it is likely an admixture of FCC emissions and ubiquitous secondary aerosol and thus overestimates the FCC emissions contribution. Modeling with EPA PMF (Version 5.0) resulted in an eight factor solution including one factor that explained about 60% of the La mass. The average source contribution estimate for this factor was 1.2 $\mu g/m^3$ which represents about 11% of the $PM_{2.5}$ mass. Like the UNMIX result, this factor was loaded with nitrate, sulfate and organic carbon and thus likely overestimates the FCC emissions contribution. Previous studies attempted to address the problem of ubiquitous PM species loading onto the point source factors by excluding such species from the modeling (Bozlaker et al., 2013; Buzcu et al., 2003; Kulkarni et al., 2006). However, as discussed in the Supplementary Material, it is not clear how to appropriately adjust the $PM_{2.5}$ mass in such cases and thus it was not further pursued. The relatively small dataset (98 sample days with complete data) and the limited number of lanthanoids included in the modeling have may contribute to the poor ability to model FCC emissions impacts for this dataset. For each sample we examined the $PM_{2.5}$ mass and species that should account for most of the

FCC emissions mass (i.e. Al, Si) but did not observe consistent patterns for enrichment on high La days. This suggests that the FCC contributions to $PM_{2.5}$ mass are relatively low.

2.5. Summary

Lanthanoid elements in ambient fine particulate matter were quantified by ICP-MS using a relatively less aggressive digestion protocol compared to microwave-assisted digestion. Good recoveries from standard reference materials were obtained for those lanthanoids with certified or reference values reported. While this digestion protocol is perhaps inferior to microwave-assisted digestion when a large suite of elements is to be analyzed, it is suitable for a subset of elements including the light lanthanoids.

In general, $PM_{2.5}$ lanthanoid concentrations measured at the Roxana station are dominated by contributions from crustal material. La/Ce ratios for a three year time series of 1-in-6 day data does suggest a two-source model with local crustal material and FCC emissions as the major contributors to La. Nonparametric wind regression analysis provided supporting evidence for FCC impacts occurring when winds placed the monitoring station downwind of the refinery core unit operations. Impacts were modulated by the persistence of winds from the refinery during the 24-hour sampling period. There is no evidence of non-routine, episodic emissions from the FCC in this dataset. However, episodic emissions would not be detected if they occur when the monitoring station is upwind of the FCC or if the event is of sufficiently low magnitude and short duration that the impact is damped out in the 24-hour average. A network of high time resolution measurements at monitoring stations along the facility perimeter

would be needed to provide comprehensive surveillance. Source apportionment modeling could not reliably estimate FCC contributions to ambient $PM_{2.5}$ and the weight of evidence is that the FCC unit is at most a minor contributor to ambient $PM_{2.5}$ mass concentrations for routine emissions as was observed throughout this study.

2.6. Acknowledgements

The Roxana Air Quality Study is funded by ConocoPhillips in response to a settlement agreement with American Bottom Conservancy, the Sierra Club, the Environmental Integrity Project, and the Natural Resources Defense Council. None of these five entities have formally reviewed or approved this manuscript and their approval or endorsement should not be inferred.

2.7. References

Bozlaker, A., Buzcu-Güven, B., Fraser, M.P., Chellam, S., 2013. Insights into PM_{10} sources in Houston, Texas: Role of petroleum refineries in enriching lanthanoid metals during episodic emission events. Atmospheric Environment 69, 109-117.

Buzcu, B., Fraser, M.P., Kulkarni, P., Chellam, S., 2003. Source identification and apportionment of fine particulate matter in Houston, TX, using positive matrix factorization. Environmental Engineering Science 20, 533-545.

Carvacho, O.F., Ashbaugh, L.L., Brown, M.S., Flocchini, R.G., 2004. Measurement of $PM_{2.5}$ emission potential from soil using the UC Davis resuspension test chamber. Geomorphology 59, 75-80.

Celo, V., Dabek-Zlotorzynska, E., Zhao, J., Bowman, D., 2012. Concentration and source origin of lanthanoids in the Canadian atmospheric particulate matter: A case study. Atmospheric Pollution Research 3, 270-278.

Chow, J.C., Watson, J.G., Houck, J.E., Pritchett, L.C., Rogers, C.F., Frazier, C.A., Egami, R.T., Ball, B.M., 1994. A laboratory resuspension chamber to measure fugitive dust size distributions and chemical compositions. Atmospheric Environment 28, 3463-3481.

Danadurai, K.S.K., Chellam, S., Lee, C.-T., Fraser, M.P., 2011. Trace elemental analysis of airborne particulate matter using dynamic reaction cell inductively coupled plasma - mass spectrometry: Application to monitoring episodic industrial emission events. Analytica Chimica Acta 686, 40-49.

Henry, R.C., Chang, Y.S., Spiegelman, C.H., 2002. Locating nearby sources of air pollution by nonparametric regression of atmospheric concentrations on wind direction. Atmospheric Environment 36, 2237-2244.

Huang, X., Olmez, I., Aras, N.K., Gordon, G.E., 1994. Emissions of trace elements from motor vehicles: Potential marker elements and source composition profile. Atmospheric Environment 28, 1385-1391.

Kim, E., Hopke, P.K., 2004. Comparison between Conditional Probability Function and Nonparametric Regression for Fine Particle Source Directions. Atmospheric Environment 38, 4667-4673.

Kitto, M.E., Anderson, D.L., Gordon, G.E., Olmez, I., 1992. Rare-Earth Distributions in Catalysts and Airborne Particles. Environmental Science & Technology 26, 1368-1375.

Kotchenruther, R.A., 2013. A regional assessment of marine vessel $PM_{2.5}$ impacts in the U.S. Pacific Northwest using a receptor-based source apportionment method. Atmospheric Environment 68, 103-111.

Kowalczyk, G.S., Gordon, G.E., Rheingrover, S.W., 1982. Identification of Atmospheric Particulate Sources in Washington, Dc, Using Chemical-Element Balances. Environmental Science & Technology 16, 79-90.

Kulkarni, P., Chellam, S., Flanagan, J.B., Jayanty, R.K.M., 2007a. Microwave digestion - ICP-MS for elemental analysis in ambient airborne fine particulate matter: Rare earth elements and validation using a filter borne fine particle certified reference material. Analytica Chimica Acta 599, 170-176.

Kulkarni, P., Chellam, S., Fraser, M.P., 2006. Lanthanum and lanthanides in atmospheric fine particles and their apportionment to refinery and petrochemical operations in Houston, TX. Atmospheric Environment 40, 508-520.

Kulkarni, P., Chellam, S., Fraser, M.P., 2007b. Tracking petroleum refinery emission events using lanthanum and lanthanides as elemental markers for $PM_{2.5}$. Environmental Science & Technology 41, 6748-6754.

Kulkarni, P., Chellam, S., Mittlefehldt, D.W., 2007c. Microwave-assisted extraction of rare earth elements from petroleum refining catalysts and ambient fine aerosols prior to inductively coupled plasma-mass spectrometry. Analytica Chimica Acta 581, 247-259.

Martuzevicius, D., Kliucininkas, L., Prasauskas, T., Krugly, E., Kauneliene, V., Strandberg, B., 2011. Resuspension of particulate matter and PAHs from street dust. Atmospheric Environment 45, 310-317.

Moreno, T., Querol, X., Alastuey, A., Gibbons, W., 2008a. Identification of FCC refinery atmospheric pollution events using lanthanoid- and vanadium-bearing aerosols. Atmospheric Environment 42, 7851-7861.

Moreno, T., Querol, X., Alastuey, A., Pey, J., Minguillón, M.C., Pérez, N., Bernabé, R.M., Blanco, S., Cárdenas, B., Gibbons, W., 2008b. Lanthanoid geochemistry of urban atmospheric particulate matter. Environmental Science and Technology 42, 6502-6507.

Olmez, I., Gordon, G.E., 1985. Rare earths: Atmospheric signatures for oil-fired power plants and refineries. Science 229, 966-968.

Taylor, S.R., McLennan, S.M., 1985. Continental crust: its composition and evolution. An examination of the geochemical record preserved in sedimentary rocks.

United States Environmental Protection Agency, 2005. Code of Federal Regulations, Title 40, Part 136, Appendix B. Definition and Procedure for the Determination of the Method Detection Limit.

United States Geological Survey, 2014. Geochemical and mineralogical data for soils of the conterminous United States.

Wu, S., Zhao, Y.H., Feng, X.B., Wittmeier, A., 1996. Application of inductively coupled plasma mass spectrometry for total metal determination in silicon-containing solid samples using the microwave-assisted nitric acid hydrofluoric acid hydrogen peroxide boric acid digestion system. Journal of Analytical Atomic Spectrometry 11, 287-296.

2.8. Supplementary Material

2.8.1. Relationships between FCC Impacts and Wind Direction

Figure 2-6 shows expected values with 95% confidence intervals for ambient $PM_{2.5}$ La, Ce and the La/Ce ratio using both on-site (Roxana) winds and Lambert St. Louis International Airport winds. Henry *et al.* (2002) describe how the confidence intervals can be used to determine whether the local maxima in the NWR plots correspond to actual emission sources. However, wide confidence intervals can also result from periodic – rather than continuous – emissions and the persistence of hourly wind

direction over the 24-hour sampling period which modulates the impacts. A small number of data points from a specific wind direction can also lead to wide confidence intervals. Thus, the relatively wide confidence intervals for winds from the direction of the FCC unit are to be expected. NWR results for $PM_{2.5}$ mass (Figure 2-7) do not show a strong directional pattern including no strong feature from the direction of the FCC unit.

Figure 2-8 is the same data as Figure 2-4(c) but shown as a Cartesian plot to better visualize the expected values as a function of wind direction. Maximum expected values correspond to winds from ~125°N for Roxana winds and ~140°N for Lambert winds.

Figure 2-9 is similar to Figure 2-5, in this case using Lambert meteorological data instead of Roxana meteorological data. Similar patterns are observed for the two winds datasets.

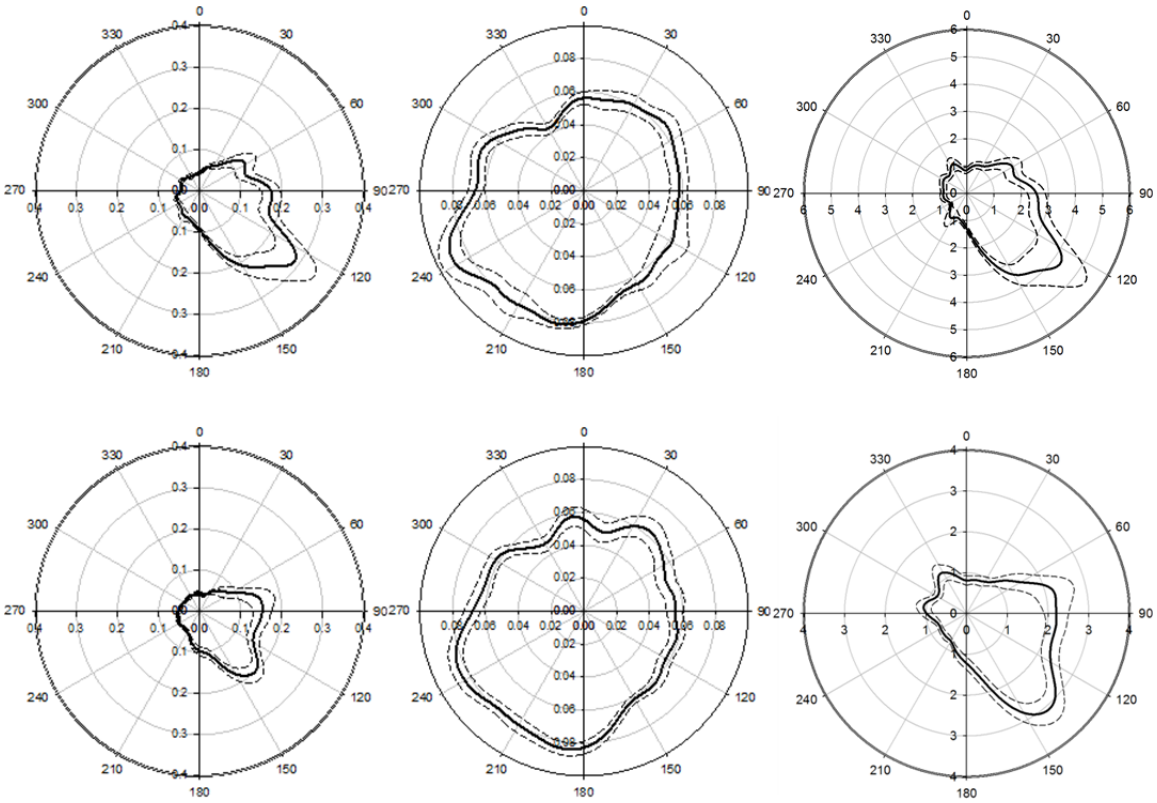

Figure 2-6. NWR analysis on La ambient concentration (left), Ce ambient concentration (center), and La/Ce ratio (right) based on Roxana meteorological data (top row) and Lambert St. Louis International Airport meteorological data (bottom row). The dashed lines are 95% confidence intervals generated from 1000 iterations of bootstrapping. Concentrations have units of ng/m^3.

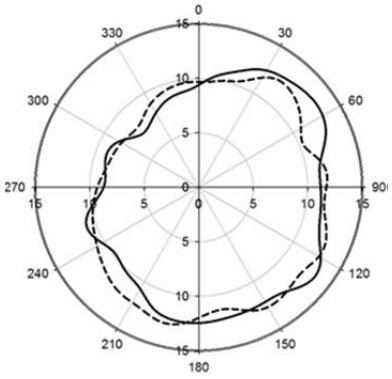

Figure 2-7. NWR expected values for ambient $PM_{2.5}$ mass concentration based on Roxana meteorological data (solid curve) and Lambert St. Louis International Airport meteorological data (dashed curve). Concentrations have units of $\mu g/m^3$.

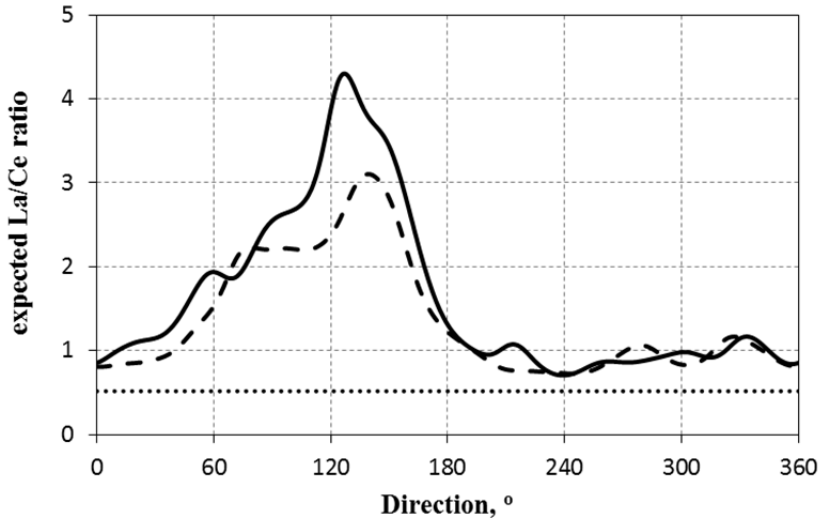

Figure 2-8. NWR analysis on the ambient $PM_{2.5}$ La/Ce using Roxana meteorological data (solid line) and Lambert St. Louis International Airport meteorological data (dashed line). The La/Ce ratio for Roxana soil is the horizontal dotted line.

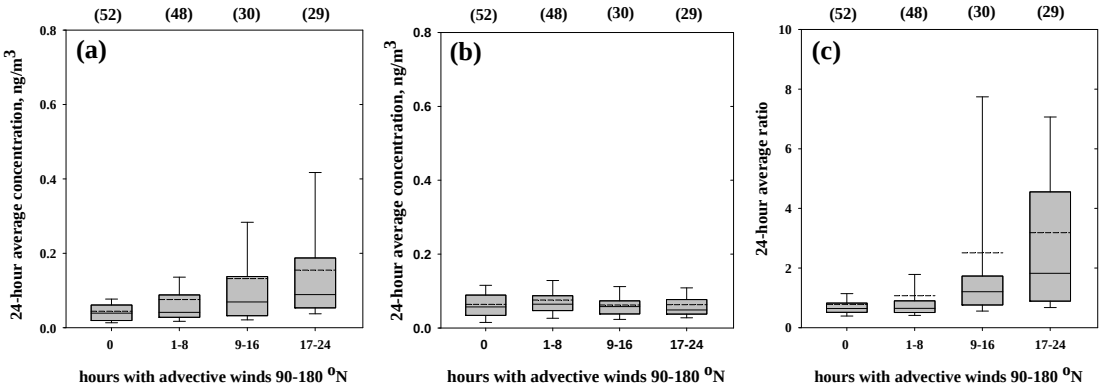

Figure 2-9. Distributions for 24-hour integrated ambient $PM_{2.5}$ La (a), Ce (b), and the La/Ce ratio (c) after stratifying the data by the number of hours with advective winds (speeds > 0.5 m/s) from the southeast quadrant. Analysis conducted using Lambert St. Louis International Airport meteorological data. Interior solid lines are medians and dashed lines are arithmetic means. The numbers of samples in each distribution are denoted in parenthesis.

2.8.2. Roxana Soil Analyses

Table 2-2. Lanthanoid elements profiles (ng/mg) in soil samples collected in Roxana, IL. Resuspension and analysis was performed in triplicate for each sample. "-" denotes the element was not detected.

	La	Ce	Pr	Nd	Sm	Eu	Gd	Tb	Dy	Ho	Er	Tm	Yb	Lu
Soil #1														
1	14.88	26.19	3.22	11.42	1.69	0.51	1.55	–	1.43	–	0.13	–	1.37	0.23
2	21.21	40.42	4.57	16.21	2.14	0.55	2.86	0.22	1.74	0.17	0.49	–	0.68	0.05
3	24.94	42.84	5.35	18.78	3.05	0.70	3.73	0.29	2.62	0.22	1.23	–	1.10	0.13
Soil #2														
1	24.46	48.30	5.84	22.13	4.40	0.99	4.42	0.50	3.29	0.48	1.47	0.13	1.75	0.23
2	30.04	60.01	7.56	27.47	5.65	1.24	5.70	0.65	3.73	0.63	1.96	0.22	1.61	0.22
3	29.73	58.95	7.27	27.80	5.69	1.29	5.31	0.63	3.82	0.65	2.01	0.17	1.76	0.23
Soil #3														
1	12.39	22.53	2.60	11.39	1.62	0.42	–	–	1.04	–	0.16	–	0.27	–
2	15.35	33.22	3.63	14.35	1.93	0.30	2.08	–	1.32	–	0.50	–	0.56	–
3	24.44	51.85	5.61	22.39	3.55	0.91	4.36	0.28	3.09	0.23	1.15	–	1.65	0.16

2.8.3. Source Apportionment Modeling

Datasets

$PM_{2.5}$ species data from 1-in-6 day sampling over the period July 14, 2012 – June 28, 2014 (N=98) were used for source apportionment modeling. The CSN dataset includes $PM_{2.5}$ gravimetric mass and 52 chemical components: five ions measured by ion chromatography (IC); 33 elements measured by x-ray fluorescence (XRF); and total carbon (TC) and 13 carbon fractions measured by the IMPROVE_A thermal-optical analysis protocol. The carbon data included elemental carbon (EC), organic carbon (OC), and pyrolytic carbon (OP) measured by both thermal-optical reflectance (TOR) and thermal-optical transmittance (TOT) methods; three carbon sub-fractions for EC; and four carbon sub-fractions for OC. Modeling was conducted using EC-TOR and OC-TOR for the carbonaceous PM data. The following species were excluded because of low detectability: Ag, Ba, Cd, Ce, Cs, Cr, Co, In, P, Rb, Se, Sn, Sr, Ti, V, and Zr. For components measured as both an element and an ion, only one species was retained: specifically, either K^+ or elemental K was removed; and SO_4^{2-} was retained and elemental S was removed. Both Na^+ and elemental Na were removed because they are noisy measurements and for PMF modeling tended to be resolved as a factor with only sodium. For PMF modeling, the CSN sample-specific uncertainties were used except for the carbon data because uncertainties are currently not reported; in this case we used collocated data from the G.T. Craig CSN site in Cleveland, OH to generate concentration-dependent error structures for the EC-TOR and OC-TOR. The data were not blank-corrected.

In addition to the CSN data, the following lanthanoids from the ICP-MS analysis were included in the modeling: La, Ce, Pr, and Nd. Concentration-dependent error structures were generated

for these species using our collocated data collected using separate channels of the SASS sampler.

The dataset for modeling included: $PM_{2.5}$ mass, NH_4^+, NO_3^-, SO_4^{2-} , EC-TOR, OC-TOR, Al, As, Br, Ca, Cl, Cr, Cu, Fe, K^+ or K, Mg, Mn, Ni, Pb, Si, and Zn from the CSN data; and La, Ce, Pr and Nd from our ICP-MS analysis.

Positive Matrix Factorization (PMF) Modeling

Source apportionment was performed using EPA PMF (Version 5.0). Based on the signal-to-noise ratio (S/N) calculated by the model, species with S/N value less than 0.5 were excluded (As, Mg, Pb) and species with S/N values larger than 0.5 but less than 2.0 were assigned as "weak" (Al, Cr, Cu, Mn and Ni). Elemental K was included and K^+ was rejected because of the higher S/N for elemental K. Chlorine was excluded because it was consistently resolved as a standalone factor with no additional species loaded and therefore did not provide value to the apportionment. For the base case all the concentration values – even when below the MDL – were used in the PMF modeling. A sensitivity study was conducted with the commonly used data conditioning approach of imputing concentration values below MDL with 1/2 MDL and setting the corresponding uncertainties to 5/6 MDL. Very similar results were obtained for the base case and the modeling run with low concentration data conditioning.

An eight-factor solution was deemed optimal. Figure 2-10 shows the source profiles as concentrations (bars) and the explained mass distributions (closed circles). Table 2-3 summarizes the $PM_{2.5}$ mass source contribution estimates and the La loaded onto each factor. 60% of the La loaded onto La-rich factor which presumably includes FCC emissions. However, ammonium, sulfate, and organic carbon account for about 40% of the $PM_{2.5}$ mass apportioned to

this factor and this suggests it is an admixture of FCC emissions and secondary particulate matter. Figure 2-11 shows the NWR results for this factor. In contrast to the results for La concentration and the La/Ce ratio, there is no distinct feature towards the southeast where the FCC unit is located and instead the dominant feature is to the south which is consistent with prevailing summertime winds conducive to regional transport of secondary sulfate and secondary organic carbon to St. Louis. Thus, PMF cannot reliably isolate the $PM_{2.5}$ mass contributions from FCC emissions.

Furthermore, a comparison of sample-specific modeled and observed La concentrations showed that PMF failed to capture most high La days which appear to be impacts from the FCC unit.

Table 2-3. Sources and contribution estimates by PMF.

Factor/source	Source contribution estimate		Percentage of explained La (%)
	$\mu g/m^3$	%	
Biomass burning and vehicle emissions	1.9	18	0
Metal processing	0.7	7	0
Secondary sulfate	3.8	35	0
Brass production	0.1	0.9	5
Calcium-rich	0.1	0.9	9
Resuspended soil	0.6	5	11
Secondary nitrate	2.4	22	15
La-rich	1.2	11	60

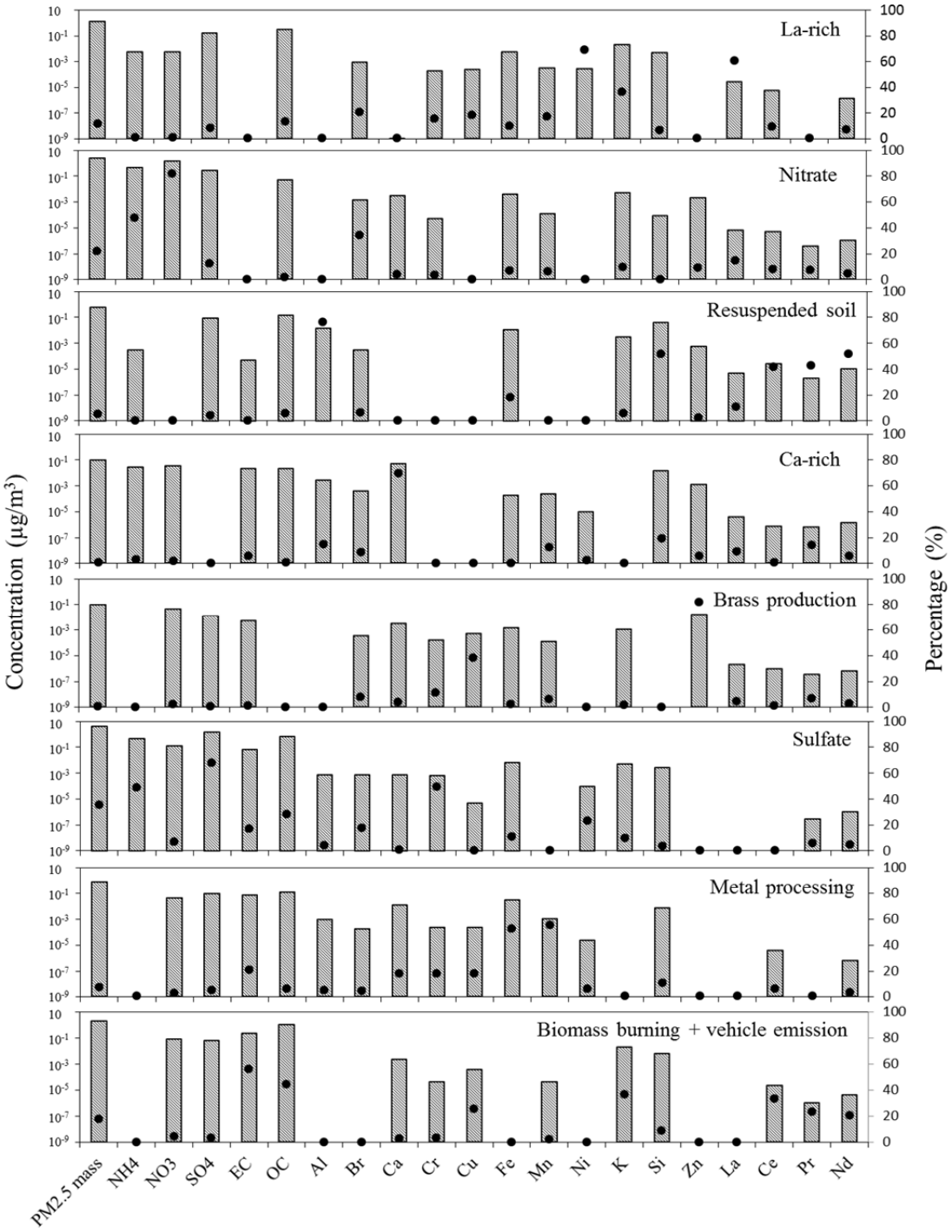

Figure 2-10. Profiles for the PMF-resolved factors and the emission source categories assigned to each factor. Bars represent concentrations (μg/m^3) and correspond to the left y-axis; solid circles represent the explained mass contributions (%), i.e. the percentage of a given species that loads onto the factor, and correspond to the right y-axis.

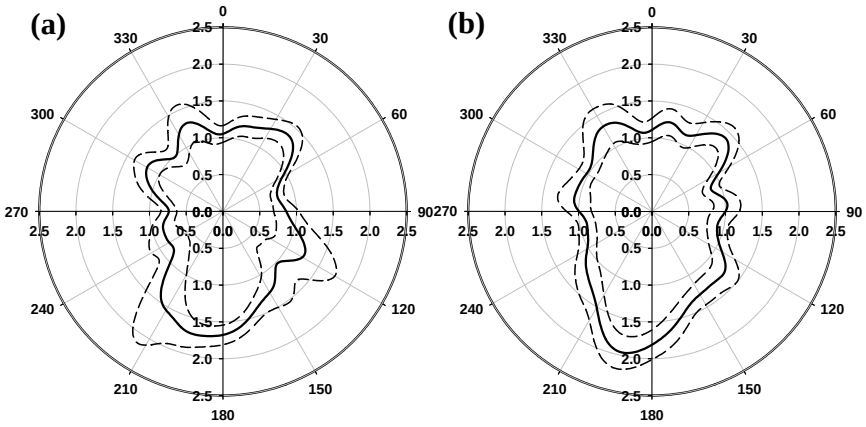

Figure 2-11. WR results for the La-rich factor resolved by PMF using Roxana meteorological data (a) and Lambert St. Louis International Airport meteorological data (b). The dashed lines are 95% confidence intervals generated from 1000 iterations of bootstrapping. Concentrations have units of $\mu g/m^3$.

Kulkarni et al. (2006) conducted source apportionment modeling of their $PM_{2.5}$ dataset by including only those chemical components (elements) that would be emitted exclusively by primary emission sources and subtracting sulfate and OC from the total (gravimetric) $PM_{2.5}$ mass. OC was subtracted instead of organic matter OM because of the ambiguity in the OM/OC ratio. Source apportionment was conducted using principle components analysis with absolute principle components scores (PCA-APCS). This approach uses a multivariable regression of PM mass (in this case, the adjusted $PM_{2.5}$ mass) on the PCA-resolved factor scores to estimate $PM_{2.5}$ mass source contribution estimates (SCEs). The multivariable regression seeks the best fit of a linear combination of factor scores to the adjusted $PM_{2.5}$ mass. Thus, the lack of adjustment for the non-carbonaceous component of OM and secondary ammonium can bias the $PM_{2.5}$ mass SCEs for the resolved primary emission sources. Bozlaker et al. (2013) conducted source apportionment modeling of their PM_{10} dataset using positive matrix factorization (EPA PMF 3.0). Again, the modeling included only those chemical components (elements) that would be

emitted exclusively by primary emission sources. In this case total PM_{10} mass was apportioned with no adjustments for secondary contributions. The modeling apportioned 73.2% of the total PM_{10} mass to the resolved primary sources with the modeling residual of 26.8% attributed to secondary PM. It is not clear how the omission of secondary PM species from the modeling affects the quantitative apportionment of total PM_{10} mass to primary emission sources and that residual that can be physically interpreted as a quantitative estimate of secondary PM contributions; the modeling is less constrained and this could potentially positively or negatively impact the robust apportionment of total PM_{10} mass. The approach is intriguing, however, and serves as a reference case for future source apportionment studies that could explore the approaches to quantifying SCEs for primary emission sources.

Despite these concerns, PMF modeling sensitivity studies were conducted which excluded the major secondary species (NH_4^+, NO_3^-, SO_4^{2-} and OC) with these species also subtracted from the reported $PM_{2.5}$ mass. For modeling with 1×OC subtracted from the $PM_{2.5}$ mass the La-rich SCE was 0.84 $\mu g/m^3$ and for modeling with 1.8×OC subtracted from the $PM_{2.5}$ mass (to account for non-carbonaceous components in the organic matter) the La-rich factor SCE was 0.21 $\mu g/m^3$. The relatively large range of La-rich factor SCEs across the base case and sensitivity studies further confounds the interpretation of source apportionment modeling results.

UNMIX Modeling

Source apportionment modeling was conducted using EPA UNMIX (Version 6). UNMIX does not necessarily produce a feasible solution for any combination of species and for any number of factors. Instead the model generates interpretable solutions when the species combinations and the number of chosen factors allow for suitable hyperplanes (Pancras et al., 2013). In this case,

the model retained $PM_{2.5}$ mass and fifteen species (NH_4^+, NO_3^-, SO_4^{2-}, K^+, OC, EC, Br, Cu, Fe, Si, Zn, Mn, Pb, La and Ce) - with Mn and Pb added from the ICP-MS data – and suggested a five-factor solution. One factor had high loadings from numerous species and could not be interpreted, and a four-factor solution was eventually selected which had the following SCEs and other characteristics.

- Factor 1 (SCE = 6.3 $\mu g/m^3$, 59% of $PM_{2.5}$ mass) included all of the nitrate and had significant loadings of other species such as sulfate and carbon.
- Factor 2 (SCE = -1.77 $\mu g/m^3$) included more than 90% of the Zn and about 50% of the Cu. While the species loadings onto this factor are consistent with a brassworks located 4 km from the site – and NWR for this factor exhibited a strong feature pointing towards the brassworks – the relatively large negative SCE is unrealistic and suggests problems with the overall solution.
- Factor 3 (SCE = 5.6 $\mu g/m^3$, 52% of $PM_{2.5}$ mass) appeared to be an admixture of vehicle emissions and resuspended road dust.
- Factor 4 (SCE was 0.6 $\mu g/m^3$, 5% of $PM_{2.5}$ mass) included about 80% of the La and presumably includes FCC emissions. However, this factor had significant loadings of sulfate, nitrate and organic carbon which suggest an admixture of FCC emissions and secondary particulate matter. Therefore, the SCE for this factor likely overestimates impacts from the FCC unit.

Overall, the UNMIX modeling results were deemed unreliable for apportioning $PM_{2.5}$ mass because of significant admixing of sources within factors and a negative SCE for one factor (hence the remaining three factors sum to 116% of the $PM_{2.5}$ mass).

2.8.4. Additional References

Henry, R.C., Chang, Y.S., Spiegelman, C.H., 2002. Locating nearby sources of air pollution by nonparametric regression of atmospheric concentrations on wind direction. Atmospheric Environment 36, 2237-2244.

Pancras, J.P., Landis, M.S., Norris, G.A., Vedantham, R., Dvonch, J.T., 2013. Source apportionment of ambient fine particulate matter in Dearborn, Michigan, using hourly resolved PM chemical composition data. Sci. Total Environ. 448, 2-13.

Chapter 3 : Measurement of Selenium in Ambient Fine Particulate Matter by Inductively Coupled Plasma Mass Spectrometry (ICP-MS) under Standard Mode

3.1. Abstract

Selenium in ambient particulate matter has been included in epidemiological and air quality studies because of its toxic effects to human health and its role as a tracer for fossil fuel combustion emissions. Selenium concentration in $PM_{2.5}$ is reported by the Chemical Speciation Network (CSN). However, for most sites low selenium mass loadings often lead to concentrations near or below the detection limit for X-Ray Fluorescence (XRF), the trace elements analytical method for CSN. In this chapter, a selenium measurement methodology using inductively coupled plasma mass spectrometry (ICP-MS), which has superior detection limits compared to XRF, was adopted from a study of selenium in aquatic environments. It was optimized for the analysis of $PM_{2.5}$ filter samples collected from a CSN protocol site. The method features a two-stage hot-plate acid digestion followed by filtering and dilution. Spiking the sample solution with 3% (v/v) methanol improved the sensitivity of selenium signal intensity as well as the linearity of the calibration curve using the standard mode of ICP-MS. Consequently, this led to enhanced detectability of selenium and improved precision for collocated samples.

3.2. Introduction

Selenium (Se) can have toxic effects on human health in the case of excessive intake (Amouroux et al., 2001; Ohlendorf et al., 1986). Se in the ambient particulate matter (PM) raises potential concern on a regional and global scale because of the contamination by deposition as well as human exposure via inhalation (Wen and Carignan, 2007). In consideration of selenium's adverse health effects the US Environmental Protection Agency (EPA) currently categorizes selenium as a Hazardous Air Pollutant (HAP). Previous research has indicated fossil fuel combustion as one of the major contributors to atmospheric Se (Ellis et al., 1993). Indeed, many air quality studies (Eldred, 1997; Ondov et al., 1989) and air pollution epidemiological studies have used Se as a tracer species for fossil fuel combustion.

US EPA has established nationwide air monitoring networks to measure ambient PM and its components, including Se, across the United States. Among current networks, $PM_{2.5}$ speciation datasets collected from Chemical Speciation Network (CSN), starting in 1999, have been widely used in both air quality and epidemiological studies because of its relatively extensive coverage of populated urban areas. However, with increased adoption of advanced emission control technologies since the establishment of the CSN, the commensurate reduction of ambient PM Se concentration values has created a challenge for routine detection by X-Ray Fluorescence (XRF) which is the analytical method for elemental analysis in CSN. As an example, during the 3-year time period from 2009 to 2011, 58 CSN sites had more than 200 valid samples, but only three of these sites had Se concentration values above the detection limit for more than 25% of the samples. Degraded detectability caused by a large number of Se concentration values below the analytical detection limit also leads to increased uncertainty for source apportionment modeling and perhaps greater measurement error for epidemiological studies. Recent epidemiological

research (Ito et al., 2011; Lippmann et al., 2013) focused on associations between mortality and hospitalization health endpoints and $PM_{2.5}$ mass and its components as measured by CSN. It was reported that from 2000 to 2007, more than 69% of Se measurements were below the detection limit and for more than 20% of the measurements Se was not detected (reported as zero).

Inductively Coupled Plasma Mass Spectrometry (ICP-MS), with superior detection limits compared to XRF for many elements, is an attractive option for elemental analysis of $PM_{2.5}$ samples with low mass loading. However, measurement of trace-level Se is still challenging in spite of the generally excellent detection capability of ICP-MS because of polyatomic interferences introduced by the instrument. Table 3-1 summarizes the major interfering species for each of the stable Se isotopes. The two most abundant isotopes of Se, ^{78}Se (23.6%) and ^{80}Se (49.7%), are by convention favored for analysis, but polyatomic ions produced from the ICP-MS argon (Ar) plasma source, which are present in high abundance, overlap with the spectra of these two Se isotopes. Similar interferences are also observed for the less abundant isotopes.

Several studies focusing on the analysis of trace level Se in the atmosphere and in aquatic environments used ICP-MS equipped with a dynamic reaction cell (DRC) to remove spectral interferences, making feasible the measurement of higher abundance isotopes (Danadurai et al., 2011; Wan, 2007). However, given the complexity of environmental samples DRC-ICP-MS usually requires prudent selection of reaction gases and optimal operation conditions. The optimization process can be even more complicated and laborious for instruments that are in heavy use or are routinely challenged with a variety of sample matrices. In addition, Wan (2007) investigated the efficiencies of measuring Se by both DRC-ICP-MS and standard-mode ICP-MS and found that the removal of Ar_2 background signals might be at the expense of large loss of net Se signal intensities in DRC mode. One way to circumvent the DRC-related complications is to

operate ICP-MS under standard mode (i.e. without DRC) but focus on increasing the signal intensity of less abundant isotopes such as ^{82}Se. The relatively low abundance of ^{82}Se leads to low instrument signal and thus potentially raises the detection limits (D'Ilio et al., 2011), but the polyatomic interferences are less common.

Se is known as a hard-to-ionize element under standard ICP-MS conditions. Carbon sources such as methanol can be added to the aqueous analyte solutions to enhance the signal sensitivity of selenium and improve the detection limit (Grindlay et al., 2013; Larsen and Stürup, 1994; Wan, 2007). To our knowledge, this method remains largely un-recognized in the atmospheric research field. Therefore, we adopted and evaluated this method of adding 3% methanol to ambient $PM_{2.5}$ sample solutions. Our approach was to evaluate this method using one of our long-term air monitoring studies to provide a reference case of analyzing PM samples with low Se mass loadings (e.g. CSN samples) using standard mode ICP-MS.

Table 3-1. Stable Se isotopes and major spectral interferences (D'Ilio et al., 2011).

Isotopes	Abundance (%)	Major interferences
^{80}Se	49.7	$^{40}Ar^{40}Ar^{+}$, $^{40}Ar^{40}Ca^{+}$
^{78}Se	23.6	$^{40}Ar^{38}Ar^{+}$
^{82}Se	9.2	$^{40}Ar^{42}Ca^{+}$, $^{34}S^{16}O_3^{+}$
^{76}Se	9.0	$^{40}Ar^{36}Ar^{+}$
^{77}Se	7.6	$^{40}Ar^{37}Cl^{+}$
^{74}Se	0.9	$^{38}Ar^{36}Ar^{+}$

3.3. Experimental

Methanol addition was evaluated using samples collected during the Roxana Air Quality Study (RAQS) (Du and Turner, 2015). The RAQS monitoring station is located at the fenceline of the

Philips 66 Wood River Refinery in Roxana, Illinois. Measurements included, but were not limited to, $PM_{2.5}$ speciation following the CSN sampling and analytical protocols. 24-hour integrated $PM_{2.5}$ samples were collected onto filters every sixth day using a five-channel Met One Spiral Ambient Speciation Sampler (SASS) (Met One Instruments Inc., Grants Pass, OR). Two of the five filters (one Teflon and one nylon) were analyzed by RTI International for gravimetric mass, elements by XRF, and water soluble ions by ion chromatography. Teflon filters (MTL, Minneapolis, MN) were used in the remaining three sampling channels. One filter was digested and analyzed by ICP-MS for lanthanoid elements (Du and Turner, 2015) and the remaining two filters were archived for future use.

Particle-laden Teflon filter samples were extracted using the two-stage digestion protocol described by Du and Turner (2015). To summarize, the samples were first extracted using concentrated (69.0~70.0%) nitric acid (Trace metal analysis, J.T. Baker, Center Valley, PA) and concentrated (47 ~ 51%) hydrofluoric acid (Suprapur Grade, BDH, UK) with a second stage using 5% (m/v) boric acid (J.T. Baker, Center Valley, PA). Each stage was 2 hours duration and was conducted at a digestion temperature of 90 °C and atmospheric pressure using a hot plate digestion system (ModBlock™, CPI International, Santa Rosa, CA). After the digestion process, the sample solutions were diluted with DI water to a final HNO_3 concentration of 5% (v/v) and filtered using Acrodisc (Pall Corporation, Port Washington, NY) syringe filters. Wan (2007) concluded in a study of aquatic organisms that spiking the sampling solutions with 3% (v/v) methanol greatly improved the sensitivity and detectability of Se by ICP-MS. Therefore, this analytical method was adopted and 3% methanol was added to the filtered sample solutions before ICP-MS analysis.

Elemental analysis was performed using an Elan DRC II ICP-MS (Perkin Elmer, Norwalk, CT). Prior to analysis the instrument was optimized using a SmartTune solution (Perkin Elmer, Norwalk, CT) containing 10 μg/L Ba and 1 μg/L Be, Ce, Co, Fe, In, Mg, Pb, Th, and U, respectively. Nebulizer gas flow rate and auto lens voltages were adjusted to reduce the formation of double-charged ions and oxides as well as to maximize the detection sensitivity. Rhodium (Rh) was used as the internal standard to correct for the non-spectral interference such as instrumental drift. In order to minimize the effect of different acid matrices in the sample solutions, calibration standard solutions were made using a multi-element stock standard solution of 18 elements (CPI International, Santa Rosa, CA) and digested blank solution with acid matrix (5% HNO_3, 0.025% HF and 0.25% H_3BO_3) that are identical to the samples.

The optimized analytical protocol was validated using standard reference material (SRM) 1648a purchased at the National Institute of Standard and Technology (NIST). SRM 1648a was collected as total suspended particulate (TSP) from St. Louis and provided as homogenized powder. The recovery of Se was 85.64 ± 3.78% (1σ) based on the measured reference concentrations in SRM, which demonstrated the efficacy of the analytical protocol.

3.4. Results and Discussion

Figure 3-1 shows the instrument calibration with and without methanol spiked in the calibration standards. In the absence of methanol the sensitivity is poor, especially at low selenium concentrations. A low fraction of selenium ionization may lead to low signal-to-noise ratios which would be amplified at lower concentrations. In contrast, the calibration curve for selenium in the presence of methanol exhibits good linearity down to 0.05 ppb.

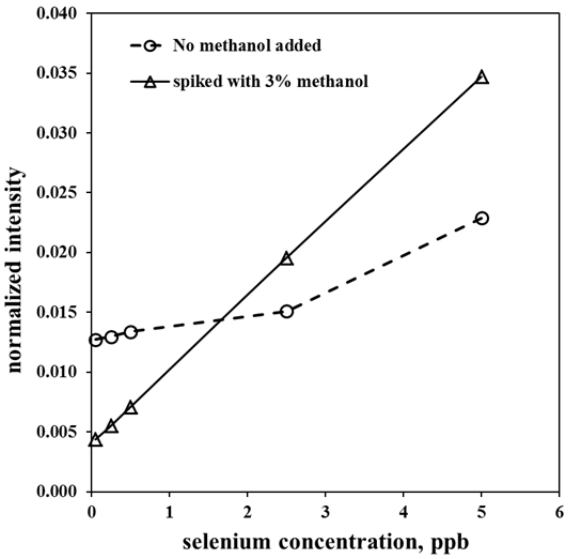

Figure 3-1. ICP-MS instrument calibration using standards with methanol (triangle and solid line) and without methanol (circles and dashed line) added as a carbon source. Vertical axis represents the sample signal intensity normalized by the internal standard. 1 ppb in analyte solution equals 6.2 ng/m^3 for a standard air sampling flow rate (6.7 lpm) and 24 hour sampling duration.

Method detection limits (MDL) were evaluated using the protocol recommended by US EPA (40 CFR) and were calculated as 3σ of the analysis of seven replicates digested acid matrix matched blank solutions spiked with the lowest Se concentrations used to calibrate the ICP-MS instrument. The MDL of Se without methanol addition was 4.97 ng/m^3 (assuming a default flow rate of 6.7 lpm and 24-hour sample) whereas methanol addition improved the MDL by more than an order of magnitude to 0.36 ng/m^3.

Samples from multiple channels of the Met One SASS sampler were analyzed to assess the effect of methanol addition on Se collocated precision. From the 165 valid sampling events during 10/01/2011 ~ 06/30/2014, 29 samples collected on a secondary channel were drawn and analyzed together with samples from the primary channel both with and without methanol addition. Figure 3-2 compares the comparison of the two methods. In the absence of methanol

the Se concentrations were below the corresponding MDL and poor collocated precision was observed (Figure 3-2a). In contrast, in the presence of methanol most samples were above the MDL and exhibited dramatically improved collocated precision as shown by data points in good alignment with 1:1 line in Figure 3-2b. This demonstrates the power of adding methanol as a carbon source to increase the detection sensitivity of Se by ICP-MS.

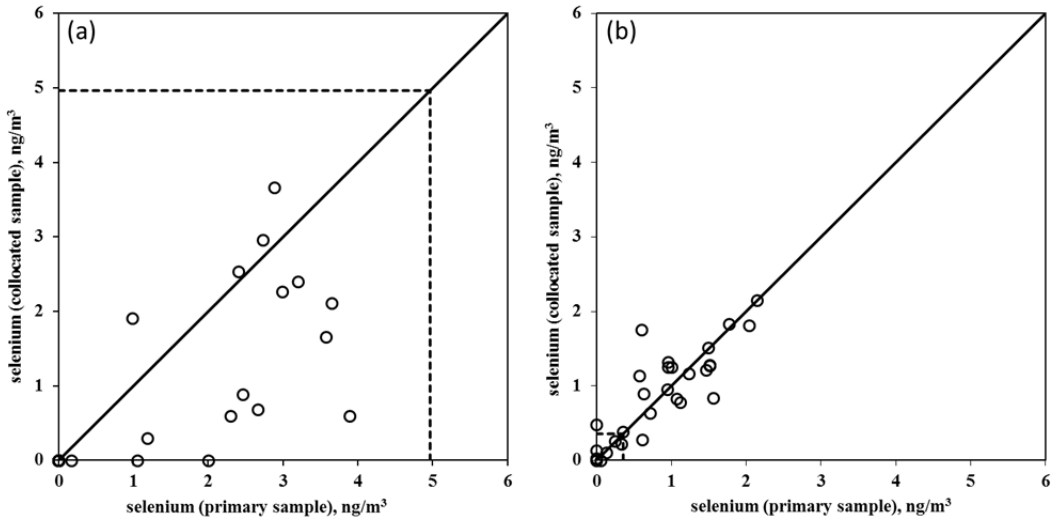

Figure 3-2. Comparison of duplicate sample precision: (a) without methanol; and (b) with methanol spiked in the sample solutions. Dashed lines represent the respective MDL values. Non-detected values are marked as zeros in the plots. The numbers of pairs with both primary and duplicate samples having non-detected values are 13 in (a) and 1 in (b).

Ambient $PM_{2.5}$ selenium concentrations measured by XRF as implemented by CSN and by standard mode ICP-MS with methanol addition are plotted in Figure 3-3. MDL values for ICP-MS and XRF are shown as solid and dashed lines, respectively. Since the MDL for XRF analysis provided by RTI varies with each sample (range 1.01 – 2.63 ng/m^3), the median MDL over the studied time period, 1.96 ng/m^3, is shown. For the time period when the two datasets overlap (07/14/2012 ~ 06/28/2014), 48% of the samples exhibited concentration levels above the

MDL for ICP-MS whereas only 8% of the samples were above the MDL for XRF. The ICP-MS protocol exhibits superior Se detectability compared to XRF in this study. The large fraction of data below MDL for XRF poses challenges to utilizing that dataset for source apportionment studies. For all samplers analyzed by ICP-MS with methanol addition over the period 10/06/2011 – 06/28/2014 (n=165), 56% of the Se concentration values were above the MDL; while this is a dramatic improvement compared to the XRF data, the detection frequency is below our threshold for inclusion in source apportionment modeling.

It should be noted that despite the limited performance for Se measurement by XRF as implemented in CSN, XRF as an analytical method in general is capable of providing superior detectability. In this case, however, longer sample analysis times and perhaps optimization of other instrument conditions are needed. The limited detectability of Se by XRF as implemented in CSN is a result for the need for analysis conditions suitable to high throughput to meet the demands of a large national monitoring network.

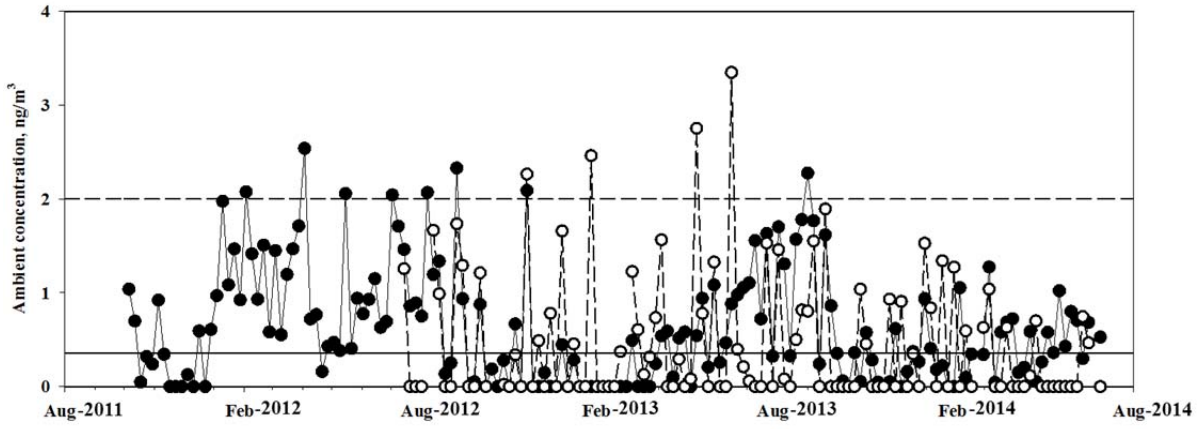

Figure 3-3. Se in Roxana ambient $PM_{2.5}$ as measured by XRF (triangles connected with dashed lines) and standard model ICP-MS with methanol addition (circles connected by solid lines).

The Roxana CSN data cannot be used to evaluate the ICP-MS protocol because of the low frequency of detection for XRF. Thus, to establish further confidence in the method, ambient PM_{10} Se concentrations from a National Air Toxics Trend Sites (NATTS) station in the City of St. Louis was compared to the Roxana $PM_{2.5}$ Se data. The NATTS site is located north of downtown St. Louis and is 15 km southwest of the Roxana station. 24-hour integrated low-volume (16.7 lpm) PM_{10} samples were collected and analyzed by ICP-MS under standard mode at Eastern Research Group, Inc. A recent study on the spatial variability of air toxic metals in PM in St. Louis suggested that ambient PM_{10} Se in the St. Louis area, including at the NATTS station, is dominated by regional sources and thus accumulation of Se in the fine PM size fraction can also be inferred (Yadav and Turner, 2014). Therefore, general comparability between PM_{10} Se from downtown St. Louis and $PM_{2.5}$ Se from Roxana can be expected and used as evidence to support the efficacy of the customized ICP-MS protocol.

Figure 3-4 shows time series of PM_{10} Se concentration from downtown St. Louis and $PM_{2.5}$ Se concentrations from Roxana. Given the distance between the two sites as well as the different ambient PM size ranges measured, the two time series display good overall agreement. The lowest reported MDL for the NATTS dataset is 0.29 ng/m^3 compared to the MDL obtained for this study of 0.36 ng/m^3. By converting the higher flow rate of the sampler at the NATTS site and using 6.7 lpm which is the flow rate of Met One SASS as a reference, an equivalent NATTS MDL is 0.75 ng/m^3 which is a factor of two higher than the MDL obtained in house with methanol addition.

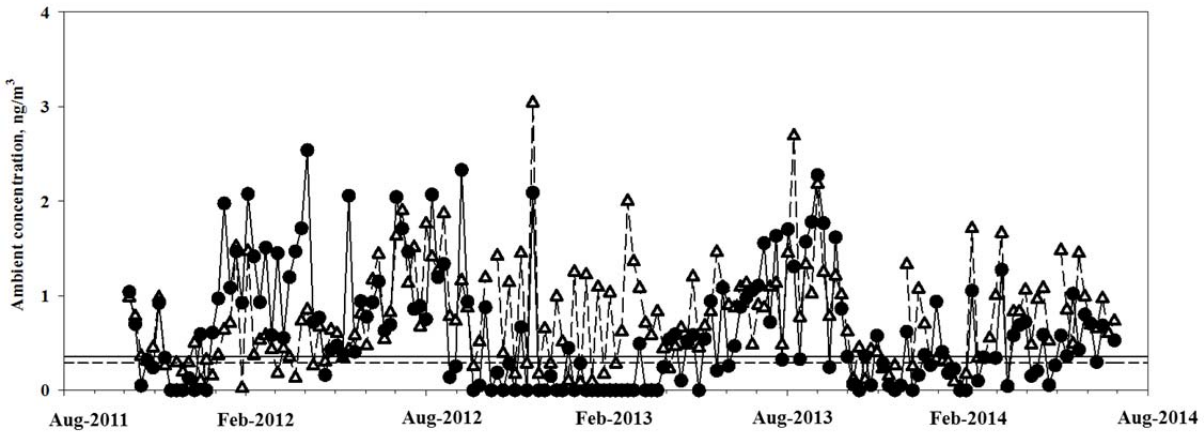

Figure 3-4. Se concentrations in PM_{10} at downtown St. Louis (triangles connected by dashed lines) and in $PM_{2.5}$ at Roxana (circles connected by solid lines). MDLs are marked as a dashed line and a solid line for NATTS ICP-MS protocol and in-house ICP-MS protocol, respectively.

3.5. Conclusions

An analytical method was adopted from disciplines related to aquatics organisms to achieve better detectability of a less abundant Se isotope, ^{82}Se, in ambient PM when analyzed by standard mode ICP-MS. The method was evaluated using $PM_{2.5}$ samples collected at the RAQS monitoring site. In this protocol, extraction solutions from a previously-optimized digestion process were spiked with 3% methanol. Calibration data for Se with methanol addition exhibited significantly improved sensitivity compared to calibration data in the absence of methanol. A significantly lower MDL was obtained by the ICP-MS with methanol protocol compared to both the ICP-MS without methanol protocol and the XRF protocol as implemented in CSN, resulting in about 50% of the ambient $PM_{2.5}$ sample concentration values being above MDL. The inter-comparison between $PM_{2.5}$ Se at Roxana and PM_{10} Se in the City of St. Louis showed good overall agreement considering the distance between the two sites and size difference of PM sampled; this provided confidence in the application of this method to the atmospheric research

field and confirmed the added value to the detection of trace to ultra-trace level Se in ambient PM using standard-mode ICP-MS.

3.6. Acknowledgement

The Roxana Air Quality Study is funded by the ConocoPhillips Company (former Wood River Refinery operator) in response to a settlement agreement with American Bottom Conservancy, the Sierra Club, the Environmental Integrity Project, and the Natural Resources Defense Council. None of these five entities have formally reviewed or approved this manuscript and their approval or endorsement should not be inferred. We also acknowledge the ICP-MS facility support by Nano Research Facility (NRF) at Washington University in St. Louis, a member of the National Nanotechnology Infrastructure Network (NNIN).

3.7. References

Amouroux, D., Liss, P.S., Tessier, E., Hamren-Larsson, M., Donard, O.F.X., 2001. Role of oceans as biogenic sources of selenium. Earth and Planetary Science Letters 189, 277-283.

D'Ilio, S., Violante, N., Majorani, C., Petrucci, F., 2011. Dynamic reaction cell ICP-MS for determination of total As, Cr, Se and V in complex matrices: Still a challenge? A review. Analytica Chimica Acta 698, 6-13.

Danadurai, K.S.K., Chellam, S., Lee, C.-T., Fraser, M.P., 2011. Trace elemental analysis of airborne particulate matter using dynamic reaction cell inductively coupled plasma - mass spectrometry: Application to monitoring episodic industrial emission events. Analytica Chimica Acta 686, 40-49.

Du, L., Turner, J., 2015. Using $PM_{2.5}$ lanthanoid elements and nonparametric wind regression to track petroleum refinery FCC emissions. Sci. Total Environ. 529, 65-71.

Eldred, R.A., 1997. Comparison of Selenium and Sulfur at Remote Sites. Journal of the Air & Waste Management Association 47, 204-211.

Ellis, W.G., Arimoto, R., Savoie, D.L., Merrill, J.T., Duce, R.A., Prospero, J.M., 1993. Aerosol Selenium at Bermuda and Barbados. Journal of Geophysical Research-Atmospheres 98, 12673-12685.

Grindlay, G., Mora, J., de Loos-Vollebregt, M., Vanhaecke, F., 2013. A systematic study on the influence of carbon on the behavior of hard-to-ionize elements in inductively coupled plasma–mass spectrometry. Spectrochimica Acta Part B: Atomic Spectroscopy 86, 42-49.

Ito, K., Mathes, R., Ross, Z., Nádas, A., Thurston, G., Matte, T., 2011. Fine particulate matter constituents associated with cardiovascular hospitalizations and mortality in New York City. Environmental Health Perspectives 119, 467-473.

Larsen, E.H., Stürup, S., 1994. Carbon-enhanced inductively coupled plasma mass spectrometric detection of arsenic and selenium and its application to arsenic speciation. Journal of Analytical Atomic Spectrometry 9, 1099-1105.

Lippmann, M., Chen, L.C., Gordon, T., Ito, K., Thurston, G.D., 2013. National Particle Component Toxicity (NPACT) Initiative: integrated epidemiologic and toxicologic studies of the health effects of particulate matter components. Research report (Health Effects Institute), 5-13.

Ohlendorf, H.M., Hoffman, D.J., Saiki, M.K., Aldrich, T.W., 1986. Embryonic mortality and abnormalities of aquatic birds: Apparent impacts of selenium from irrigation drainwater. Sci. Total Environ. 52, 49-63.

Ondov, J.M., Choquette, C.E., Zoller, W.H., Gordon, G.E., Biermann, A.H., Heft, R.E., 1989. Atmospheric behavior of trace elements on particles emitted from a coal-fired power plant. Atmospheric Environment (1967) 23, 2193-2204.

Wan, L., 2007. Determination of Total Selenium and Seleno-amino Acids in Yeast and Aquatic Organisms by Liquid Chromatography and Inductively Coupled Plasma Mass Spectrometry, Department of Chemistry. University of Missouri-Columbia.

Wen, H., Carignan, J., 2007. Reviews on atmospheric selenium: Emissions, speciation and fate. Atmospheric Environment 41, 7151-7165.

Yadav, V., Turner, J., 2014. Gauging intraurban variability of ambient particulate matter arsenic and other air toxic metals from a network of monitoring sites. Atmospheric Environment 89, 318-328.

Chapter 4 : Measurement of Lead Isotopes in $PM_{2.5}$

4.1. Introduction

Lead has been associated with adverse health effects especially to neurological systems. Historically, airborne lead has been a major source of concern although the route of exposure is predominantly indirect with lead particles depositing onto surfaces and then being ingested. Leaded gasoline was a significant contributor to airborne lead before the 1970's (Nriagu, 1996). Ambient lead levels decreased dramatically in the United States after leaded gasoline was phased out. However, lead exposure and poisoning may persist especially in the neighborhood of lead emitting point sources. Accumulated lead in the soil and crustal materials in areas where facilities used to be located may also enter the ambient air through resuspension and be redistributed. Therefore, the study of lead in the ambient particulate matter is still of significant interest. There is a rich history of lead mining in Eastern Missouri and lead smelting near the mines and in the Metropolitan St. Louis area.

Lead isotopes are used to identify and sometimes quantify lead sources. Previous global-scale studies have demonstrated that lead isotopic compositions could be related to the long range transport of different types of both natural and anthropogenic sources (Bollhöfer and Rosman, 2001; Mukai et al., 1994; Sturges and Barrie, 1989a, b). Mukai et al. (1994) found the different lead isotope ratios in PM collected in a Northern Pacific island were associated with air masses transported from different areas of north Asia. Lead isotope ratios were also widely used as tracers for anthropogenic point sources in source apportionment studies focusing on finer-scale environments (Bollhöfer et al., 2006; Widory et al., 2010; Xu et al., 2012). With the advent of

sophisticated analytical techniques, lead isotope ratios have become reliable tracers for source apportionment analysis.

4.1.1. Instrumentation for the measurement of isotopic compositions

Inductively coupled plasma mass spectrometry (ICP-MS) is a widely accepted and efficient technique for elemental and isotopic analyses. Its cost-effective operation, relatively easy maintenance as well as excellent accuracy make it a good choice for analytical research. While ICP-MS instruments are commonly equipped with single collectors and quadrupole-based mass filters, because of the increasing needs for high-quality and high-resolution data, technical improvements have been made to achieve better precision and accuracy of elemental and isotopic measurements. The quadrupole mass filter is based on voltages applied to four rods which allow only ions of a single m/z to have a path that exit the quadrupole. However, measurements by quadrupole-based ICP-MS have a relatively high level of noise and the precision of the analyzed isotope ratios is not always sufficient for geological dating and determining nuclear properties (Hirata, 1996). Instead, isotopic analysis is commonly performed using magnetic sector field ICP-MS which has higher resolution (Feldmann et al., 1994). In the sector field ICP-MS, a magnetic field is applied perpendicularly to the ion beam so that the filtering of ions is based on m/z, the magnetic field and the kinetic energy of the ions. Mass resolution can be controlled by modifying the width of the slit where the filtered ions enter the detector (Linge and Jarvis, 2009). In studies that focused on isotope ratios, multi-collector ICP-MS were commonly employed. Improved precision can be achieved by multi-collector ICP-MS instruments which simultaneously collect ions filtered for particular m/z ratios and convert these ions into voltages (Ingle et al., 2003). Multi-collector ICP-MS instruments are more expensive

and are typically used in fields such as geochemistry, geochronology or cosmochemistry where the accurate determination of isotopic compositions is required.

4.1.2. Correction for mass bias effect

Mass bias, also referred to as mass discrimination or mass fractionation, arises in ICP-MS when ions of different mass are transmitted through the spectrometer with different efficiencies, resulting in non-uniform sensitivity across the mass range and inaccurate isotope ratio measurements (Ingle et al., 2003). Mass bias arises from instrumental effects and numerous studies have focused on understanding its mechanisms (Gillson et al., 1988; Heumann et al., 1998; Jakubowski et al., 1998; Maréchal et al., 1999). It has been reported that non-analyte species in the ion beam can contribute to the total mass bias (Evans and Giglio, 1993).

A common practice to correct for the mass bias of lead is to use thallium (Tl) with known isotope composition as an internal standard because the isotopes of Tl and Pb cover similar atomic mass ranges. However, the mathematical models for accurate correction are still subject to debate (Gallon et al., 2008; Ingle et al., 2003; Margui et al., 2007; Rehkämper and Mezger, 2000; Terán-Baamonde et al., 2015). Three common correction models are the linear model, power law model and exponential law model which differ in the specific form of the correction formula. The exponential law model has been demonstrated to be effective for correcting the mass bias of Pb (Chernyshev et al., 2007; Gallon et al., 2008; Rehkämper and Mezger, 2000; Tanimizu and Ishikawa, 2006) because it takes into account the *ratio* between ^{205}Tl and ^{203}Tl instead of the absolute mass difference.

4.2. Method

An analytical protocol for Pb isotope ratios in analyte solutions was implemented in this study as constrained by the available instrumentation (a single collector quadrupole ICP-MS) and the available standards. An internal standard solution with 20 pp Tl was made from a 1000 ppm Tl stock standard solution (Alfa Aesar, Ward Hill, MA) and a 10 ppb Pb check standard solution was made from a 100 ppm Pb stock solution with certified isotopic composition (Alfa Aesar, Ward Hill, MA). Before each ICP-MS analysis batch, multiple Pb check standards were analyzed to obtain a batch-specific Tl isotope ratio for the internal standard which was subsequently used to correct the mass bias for Pb in the analyte solutions. A Pb check standard was inserted into the sample sequence after every 10 regular samples.

The exponential correction method as described by Rehkämper and Mezger (2000) was used. The corrected isotopic ratio R_i is calculated as shown in Equation (1) where r_i is the measured, uncorrected isotope ratio, M_i is the atomic mass of the measured isotope, and β is the mass bias coefficient. Using ^{208}Pb and ^{206}Pb as an example, the ^{208}Pb /^{206}Pb ratio is -

$$R_{Pb} = r_{Pb}\left[\frac{M_{208}}{M_{206}}\right]^{\beta_{Pb}} \quad (1)$$

The mass bias coefficient β_{Pb} is obtained from thallium using -

$$\beta_{Pb} \approx \beta_{Tl} = \frac{ln\left(\frac{R_{Tl}}{r_{Tl}}\right)}{ln\left(\frac{M_{205}}{M_{203}}\right)} \quad (2)$$

The assumption that mass bias effects for the Tl isotopes are similar to those for Pb isotopes implies that $\beta_{Pb} \approx \beta_{Tl}$. The batch-specific Tl isotope ratio is obtained by this exponential law using a Pb isotope standard with certified Pb isotope ratios.

Pb in 61 $PM_{2.5}$ samples collected on Teflon filters from the Roxana Air Quality Study (RAQS) (1-in-6 day samples for year 2012) and 12 $PM_{2.5}$ samples collected at East St. Louis during September 2011 were extracted following the procedure described by Du and Turner (2015). $^{208}Pb/^{206}Pb$ and $^{207}Pb/^{206}Pb$ ratios were obtained by ICP-MS analysis followed by mass bias corrections using the aforementioned exponential method.

4.3. Results and Recommendations

Figure 4-1 shows $^{208}Pb/^{206}Pb$ versus $^{207}Pb/^{206}Pb$ for $PM_{2.5}$ samples collected at Roxana and East St. Louis along with these ratios from other earlier studies compiled by Prapaipong (2001) for both atmospheric aerosols historic (US emissions) and crustal materials common in Eastern Missouri. Pb ratios from a variety of sources generally follow a mixing line. Natural materials such as rocks have ratios corresponding to the data points located to the bottom left side. Lead ores from Viburnum, MO bounded the lower end of the mixing line. In contrast, Pb isotope ratios measured in urban aerosols collected at Los Angeles, San Francisco and San Diego characterize the upper end of this mixing line. Since these data were collected from the 1970's when the leaded gasoline was not phased out, the characteristic ratios of these Pb isotopes in these urban aerosols are likely affected by the lead emitted from motor vehicle exhaust.

Pb isotope ratios measured in ambient $PM_{2.5}$ at Roxana and East St. Louis area both fall along the mixing line between historical US emissions and Lamotte sandstone/Viburnum ore. The wide ranges covered by these ratios suggest a mixture of impacts from various sources including resuspended crustal materials and industrial emissions. However, an apportionment cannot be conducted because it is not clear whether the crustal material end member should be the Lamotte sandstone or Viburnam ore.

The Roxana data were further analyzed for regressing $^{208}Pb/^{206}Pb$ onto $^{207}Pb/^{206}Pb$ and then using a least-square criterion to project the data on the regression line. This approach ordered the data from low-to-high ratios and relationships to wind speed (daily average and daily 1 hour maxiumum) and wind direction (nonparametric wind regression) were examined. No clear patterns were discerned and more analysis is needed to determine the factors influencing sample location along the mixing line.

It is also notable that the instrument used in this study was a quadrupole ICP-MS with a single collector which has relatively low precision compared to a multi-collector ICP-MS. A certified

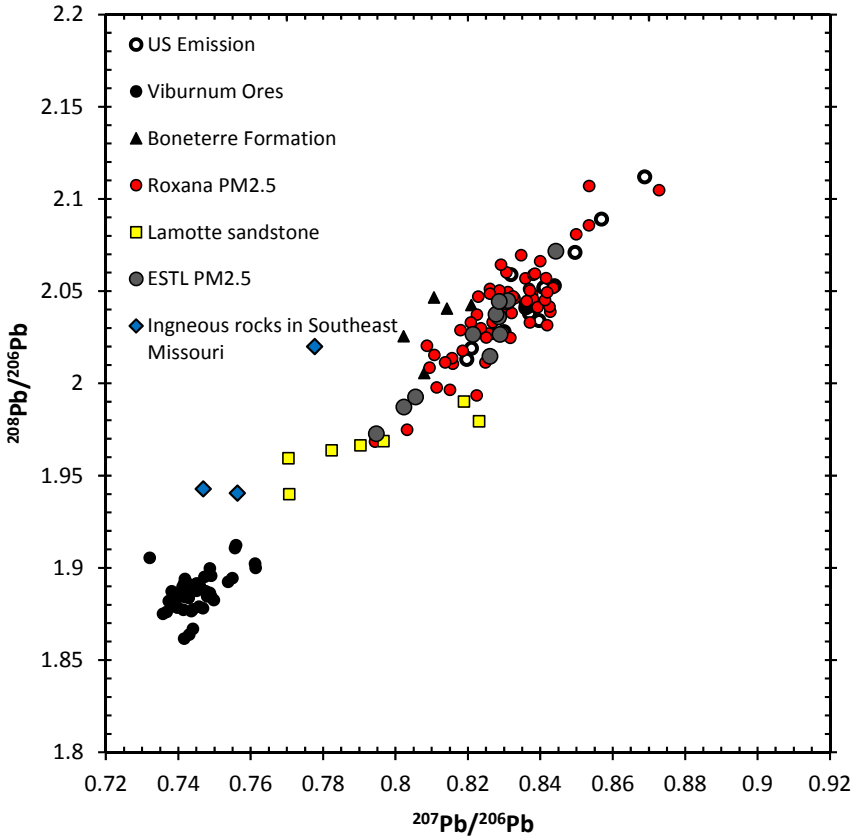

Figure 4-1. $^{208}Pb/^{206}Pb$ versus $^{207}Pb/^{206}Pb$ in ambient $PM_{2.5}$ samples collected in Roxana (IL) and East St. Louis (IL) and from other materials as reported by Prapaipong (2001).

Pb isotopic standard was used to calibrate the isotopic composition of the Tl internal standard and this could add additional measurement error. Finally, the exponential law model was used and any model for mass bias correction will have associated uncertainty. Therefore, the method applied in this study provides a semi-quantitative estimate of Pb isotope ratios but the quantitative results should be interpreted with caution. For future work, it is recommended that: (1) a Tl standard with certified isotopic ratios be obtained to reduce the errors from the calculations of these values; (2) a ICP-MS instrument with higher precision (e.g. multi-collector ICP-MS) be used for more accurate determination of the elemental isotope ratios; and (3) propagation of errors should be systematically performed to provide statistical support to the quantification of Pb isotope ratios.

4.4. References

Bollhöfer, A., Honeybun, R., Rosman, K., Martin, P., 2006. The lead isotopic composition of dust in the vicinity of a uranium mine in northern Australia and its use for radiation dose assessment. Sci. Total Environ. 366, 579-589.

Bollhöfer, A., Rosman, K.J.R., 2001. Isotopic source signatures for atmospheric lead: The Northern Hemisphere. Geochimica et Cosmochimica Acta 65, 1727-1740.

Chernyshev, I.V., Chugaev, A.V., Shatagin, K.N., 2007. High-precision Pb isotope analysis by multicollector-ICP-mass-spectrometry using Tl-205/Tl-203 normalization: Optimization and calibration of the method for the studies of Pb isotope variations. Geochemistry International 45, 1065-1076.

Evans, E.H., Giglio, J.J., 1993. Interferences in inductively coupled plasma mass spectrometry. A review. Journal of Analytical Atomic Spectrometry 8, 1-18.

Feldmann, I., Tittes, W., Jakubowski, N., Stuewer, D., Giessmann, U., 1994. Performance characteristics of inductively coupled plasma mass spectrometry with high mass resolution. Journal of Analytical Atomic Spectrometry 9, 1007-1014.

Gallon, C., Aggarwal, J., Flegal, A.R., 2008. Comparison of mass discrimination correction methods and sample introduction systems for the determination of lead isotopic composition using a multicollector inductively coupled plasma mass spectrometer. Analytical Chemistry 80, 8355-8363.

Gillson, G.R., Douglas, D.J., Fulford, J.E., Halligan, K.W., Tanner, S.D., 1988. Nonspectroscopic interelement interferences in inductively coupled plasma mass spectrometry [1]. Analytical Chemistry 60, 1472-1474.

Heumann, K.G., Gallus, S.M., Rädlinger, G., Vogl, J., 1998. Precision and accuracy in isotope ratio measurements by plasma source mass spectrometry. Journal of Analytical Atomic Spectrometry 13, 1001-1008.

Hirata, T., 1996. Lead isotopic analyses of NIST standard reference materials using multiple collector inductively coupled plasma mass spectrometry coupled with a modified external correction method for mass discrimination effect. Analyst 121, 1407-1411.

Ingle, C.P., Sharp, B.L., Horstwood, M.S.A., Parrish, R.R., Lewis, D.J., 2003. Instrument response functions, mass bias and matrix effects in isotope ratio measurements and semi-quantitative analysis by single and multi-collector ICP-MS. Journal of Analytical Atomic Spectrometry 18, 219-229.

Jakubowski, N., Moens, L., Vanhaecke, F., 1998. Sector field mass spectrometers in ICP-MS. Spectrochimica acta, Part B: Atomic spectroscopy 53, 1739-1763.

Linge, K.L., Jarvis, K.E., 2009. Quadrupole ICP-MS: Introduction to instrumentation, measurement techniques and analytical capabilities. Geostandards and Geoanalytical Research 33, 445-467.

Maréchal, C.N., Télouk, P., Albarède, F., 1999. Precise analysis of copper and zinc isotopic compositions by plasma-source mass spectrometry. Chemical Geology 156, 251-273.

Margui, E., Iglesias, M., Queralt, I., Hidalgo, M., 2007. Precise and accurate determination of lead isotope ratios in mining wastes by ICP-QMS as a tool to identify their source. Talanta 73, 700-709.

Mukai, H., Tanaka, A., Fujii, T., Nakao, M., 1994. Lead isotope ratios of airborne particulate matter as tracers of long-range transport of air pollutants around Japan. Journal of Geophysical Research 99, 3717-3726.

Nriagu, J.O., 1996. A history of global metal pollution. Science 272, 223-224.

Prapaipong, P., 2001. Roles of organic compounds in metal transport during water/rock reactions, Department of Earth and Planetary Sciences. Washington University in St. Louis.

Rehkämper, M., Mezger, K., 2000. Investigation of matrix effects for Pb isotope ratio measurements by multiple collector ICP-MS: Verification and application of optimized analytical protocols. Journal of Analytical Atomic Spectrometry 15, 1451-1460.

Sturges, W.T., Barrie, L.A., 1989a. Stable lead isotope ratios in arctic aerosols: evidence for the origin of arctic air pollution. Atmospheric Environment (1967) 23, 2513-2519.

Sturges, W.T., Barrie, L.A., 1989b. The use of stable lead 206 207 isotope ratios and elemental composition to discriminate the origins of lead in aerosols at a rural site in eastern Canada. Atmospheric Environment (1967) 23, 1645-1657.

Tanimizu, M., Ishikawa, T., 2006. Development of rapid and precise Pb isotope analytical techniques using MC-ICP-MS and new results for GSJ rock reference samples. Geochemical Journal 40, 121-133.

Terán-Baamonde, J., Andrade, J.M., Soto-Ferreiro, R.M., Carlosena, A., Prada, D., 2015. A simple procedure to select a model for mass discrimination correction in isotope dilution inductively coupled plasma mass spectrometry. Journal of Analytical Atomic Spectrometry 30, 1197-1206.

Widory, D., Liu, X., Dong, S., 2010. Isotopes as tracers of sources of lead and strontium in aerosols (TSP & PM2.5) in Beijing. Atmospheric Environment 44, 3679-3687.

Xu, H.M., Cao, J.J., Ho, K.F., Ding, H., Han, Y.M., Wang, G.H., Chow, J.C., Watson, J.G., Khol, S.D., Qiang, J., Li, W.T., 2012. Lead concentrations in fine particulate matter after the phasing out of leaded gasoline in Xi'an, China. Atmospheric Environment 46, 217-224.

Chapter 5 : Gaseous Air Toxics in the St. Louis Area

5.1. Introduction

Volatile organic compounds (VOCs) play an important role in the formation of secondary air pollutants such as ozone and secondary organic aerosols via photochemical processes in the atmosphere (Carter, 1994; Chameides et al., 1988). Carbonyl compounds serve as another major source of free radicals and precursors to secondary organic aerosols (Ban-Weiss et al., 2008; Grosjean, 1982). Adverse health effects associated with VOCs including carbonyl compounds have been suggested by previous studies (Morello-Frosch et al., 2000; Woodruff et al., 1998). The 1990 Clean Air Act Amendments designated 188 toxic chemicals as hazardous air pollutants (HAPS) including, but not limited to, select VOCs including carbonyl compounds. To comply with related statutory requirements, the US Environmental Protection Agency (EPA) initiated the National Air Toxics Trends Station (NATTS) Program in 2003. This network was developed to fulfill the need for long-term ambient air toxics monitoring data acquired using consistent measurement approaches, and to provide information about trends in HAPs concentrations.

While carbonyl compounds are products gas-phase hydrocarbons photooxidation, primary emissions such as motor vehicle exhaust are also major contributors to ambient carbonyls especially in urban areas (Ban-Weiss et al., 2008; Grosjean, 1982). Other VOCs such as benzene are emitted by a wide range of sources including: motor vehicle exhaust; fossil fuel combustion; manufacturing, storage and use of petrochemical products; other industrial processes; and even biogenic emissions (Davis and Otson, 1996; Mohamed et al., 2002; Winer et al., 1992).

Petroleum refineries are associated with the emissions of various substances to the atmosphere. While they are not considered to be major sources of carbonyls, they are major sources of many

other VOCs with emissions originating from the production processes, storage tanks, transport pipelines and waste areas (Kalabokas et al., 2001). A number of studies have demonstrated elevated concentrations of select VOC mixing ratios in the vicinity of petroleum refineries (Baltrenas et al., 2011; Cetin et al., 2003; Kalabokas et al., 2001; Lin et al., 2004). Source apportionment modeling of VOC data using tools such as positive matrix factorization (PMF) have identified factors related to refinery emissions at urban receptors (Jorquera and Rappenglück, 2004; Xie and Berkowitz, 2006) and in industrialized areas where refineries and petrochemical industries are located (Buzcu and Fraser, 2006; Leuchner and Rappenglück, 2010). For example, Buzcu and Fraser (2006) apportioned 26 - 35% of the measured VOCs mixing ratio at three sites in an industrial area of Houston to refineries. The majority of these studies were short-term campaigns that spanned at most several months and the sampling as well as analytical protocols were also customized according to the specific objectives of the campaign.

In this study, data for gaseous air toxics including VOCs and carbonyls were routinely collected over a 2.5 year period at the fenceline of a petroleum refinery in Roxana, Illinois. Sampling and analysis followed the NATTS protocols and data obtained from a nearby NATTS site were used to place the fenceline data in context. Surface winds were used to determine the influence from emission sources including refinery operations.

5.2. Sampling and methods

5.2.1. Gaseous air toxics sampling

Gaseous air toxics samples were collected at Roxana, Illinois (USA) during the Roxana Air Quality Study (RAQS) (Du and Turner, 2015). The village of Roxana is located ~ 25km to the

northeast of downtown St. Louis, Missouri and the monitoring site (38º50´54.20´´ N, 90º04´35.50´´ W) is located at the fenceline of a petroleum refinery and next to a residential neighborhood (Figure 5-1). 1-in-6 day 24-hour integrated VOCs and carbonyl samples were collected in passivated stainless steel canisters and onto DNPH cartridges following the US EPA compendium methods TO-15 and TO-11A, respectively. A total of 58 VOCs and 13 carbonyl compounds were measured for each sample. Identical sampling and analytical protocols are used in the NATTS program and samples were analyzed by the Eastern Research Group, Inc. (ERG) which is the US EPA NATTS contract laboratory. For the period of interest (June 8th 2012 – Feb 23rd 2015), 159 and 164 valid sampling events were conducted for VOCs and carbonyls, respectively, out of 171 events attempted. Additional measurements included 1-in-6 day 24-hour integrated ambient $PM_{2.5}$ sampling for speciation analysis and continuous H_2S/ SO_2 and meteorological parameters.

Figure 5-1. Air monitoring at Roxana (IL) and the adjacent refinery. The think black line is the refinery boundary for the main operations; refinery satellite operations are not marked.

Gaseous air toxics samples were also collected by the Missouri Department of Natural Resources (MDNR) at the Blair Street site which is a NATTS site located just north of the City of St. Louis, Missouri, central business district (Figure 5-1). Data for VOCs including carbonyls were provided by MDNR. During the time period of interest (June 8th 2012 – Feb 23rd 2015), 162 and 166 valid sampling events were conducted for VOCs and carbonyls, respectively, out of 168 events attempted.

Carbon disulfide and acetonitrile were not included because of possible measurement artifacts observed at Roxana and Blair Street, respectively. 38 carbonyl samples collected at Roxana from June 8th 2012 to Dec 29th 2012 were invalidated because of measurement artifacts from a spent ozone scrubber. Therefore, a total number of 159 VOCs samples and 129 carbonyl samples at Roxana were included in the analysis.

5.2.2. Nonparametric wind regression

Nonparametric wind regression was introduced by Henry et al. (2002) as a type of pollution rose that does not require *a priori* binning of the data into discrete wind direction sectors. A Gaussian kernel is used in conjunction with a user-defined smoothing parameter to generate a smooth curve relating the expected (mean) concentration to wind direction. NWR was initially implemented on hourly concentration data and hourly winds data but has also been used on 24-hour integrated concentration data and hourly winds data. The latter approach can lead to smearing across wind directions yet often generates interpretable results including good agreement with the conditional probability function (CPF) approach for locating the bearings of emission sources (Kim and Hopke, 2004).

In this study, NWR was conducted on 24-hour integrated mixing ratio data using hourly surface winds data. The daily mixing ratio value is equally assigned to each hour of the day. Hours with calm winds (operationally defined as wind speeds less than 0.5m/s) were excluded from the analysis. Confidence intervals were generated as 1σ values of the expected concentrations. Analyses were conducted using hourly 10m surface winds data collected at the Roxana and Blair Street stations for the air toxics collected at each corresponding site.

5.2.3. Principle Component Analysis (PCA/APCS)

PCA is a statistical technique for analyzing structure in multivariate datasets. It seeks to reduce the dimensions of a dataset by identifying a smaller number of factors that are independent of each other based on the correlations between the variables included in the dataset. In the application of source apportionment to air quality data, a factor may not necessarily represent a specific emission source but rather an association of one or multiple emission sources that are closely correlated (Guo et al., 2004b), or even an atmospheric process. In this study, source apportionment modeling was performed using PCA combined with the absolute principal component scores (APCS) method. Detailed descriptions of PCA/APCA model are given elsewhere (Guo et al., 2004a; Miller et al., 2002; Thurston and Spengler, 1985).

VOCs and carbonyl compounds were combined for the PCA analysis. The data were conditioned to retain only those species with >90% detection rate. Sample days with one or more values missing or below MDL were also excluded. Because of a sampling artifact, 38 samples collected before December 2012 were excluded from the Roxana dataset and acetonitrile was also excluded from the Blair Street dataset. The final datasets for PCA included 31 variables (species) and 77 samples for Roxana, and 31 variables and 87 samples for Blair Street.

5.3. Results and Discussion

5.3.1. Spatial variability of gaseous air toxics

Table 1 summarizes the basic statistics of the gaseous air toxics with more than 60% of the measured concentration values above MDL at both Roxana and Blair. Two nonparametric statistical tests - the Wilcoxon paired signed-rank test and the Mann-Whitney U test - were used to categorize the spatial variability. Both tests were utilized to assess whether the two population means are equal with the difference being the Wilcoxon paired signed-rank test compares the date-matched sample pairs and the Mann-Whitney U test treats the two populations as independent distributions. The categorization shown in the table is based on the Wilcoxon paired signed-rank test with significance at the 95^{th} percent confidence level whereas the species that were categorized otherwise by the Mann-Whitney U test are marked by asterisks.

Seven species were deemed spatially homogeneous by both tests including five halogenated hydrocarbons and two aldehydes. Some of these halogenated hydrocarbons such as dichlorodifluoromethane, trichlorotrifluoroethane and dichlorotetrafluoroethane were used as refrigerants; the manufacture and use of these compounds were banned decades ago because they are on stratospheric ozone depletors. However, their chemical inertness allows them to reside in the atmosphere for several decades to even over a hundred years (Elkins et al. 1993). The monitored mixing ratios for carbon tetrachloride and chloromethane at both sites are already lower than the tropospheric abundances of 0.146 ± 0.015 ppb and 0.602 ± 0.015 ppb, respectively, at 1990 level (Fabian et al., 1996). Indeed, the global mean mixing of dichlorodifluoromethane mixing ratio is about 0.52 ppb as of March 2015 (National Oceanic and Atmospheric Administration, 2015) which agrees with the mean mixing ratios of 0.50 and 0.51 ppb measured at Roxana and Blair Street, respectively.

Table 5-1. Descriptive statistics for species above MDL and spatial variability assignments based on Wilcoxon paired signed-rank test.

	Roxana (ppb)				Blair Street (ppb)				Spatial Variability
	N	Mean	25th Perc.	75th Perc.	N	Mean	25th Perc.	75th Perc.	
Carbon tetrachloride	159	0.102	0.096	0.111	162	0.102	0.096	0.110	
Chloromethane	159	0.568	0.519	0.603	162	0.568	0.506	0.618	
Dichlorodifluoromethane	159	0.502	0.469	0.534	162	0.509	0.466	0.551	
Trichlorotrifluoroethane	159	0.081	0.077	0.085	161	0.081	0.076	0.087	Homogeneous
Dichlorotetrafluoroethane	159	0.017	0.015	0.019	155	0.017	0.015	0.020	
Propionaldehyde	129	0.145	0.087	0.180	166	0.147	0.092	0.182	
Hexaldehyde	129	0.031	0.018	0.041	166	0.035	0.023	0.046	
n-Octane	156	0.070	0.031	0.093	130	0.036	0.023	0.042	
Propylene	159	0.650	0.354	0.805	162	0.389	0.275	0.455	
Benzene	159	0.384	0.221	0.470	162	0.219	0.154	0.263	
Ethylbenzene	159	0.079	0.042	0.096	149	0.059	0.037	0.069	
m,p-Xylene	159	0.205	0.099	0.251	161	0.147	0.086	0.176	
o-Xylene	159	0.081	0.040	0.101	155	0.062	0.036	0.073	Heterogeneous Roxana > Blair
Toluene	159	0.540	0.246	0.689	162	0.396	0.238	0.496	
1,2,4-Trimethylebezene	136	0.074	0.041	0.094	133	0.059	0.033	0.069	
1,2-Dichloroethane	124	0.023	0.020	0.025	126	0.022	0.018	0.025	
Benzaldehyde	128	0.053	0.027	0.072	163	0.034	0.023	0.043	
Tolualdehyde*	112	0.033	0.018	0.033	139	0.027	0.016	0.032	
Acetylene	159	0.543	0.329	0.672	162	0.729	0.404	0.904	
1,3-Butadiene	141	0.035	0.020	0.040	150	0.041	0.022	0.051	
Methyl Isobutyl Ketone	121	0.047	0.024	0.041	146	0.068	0.030	0.080	
Dichloromethane	159	0.145	0.092	0.164	161	0.467	0.183	0.442	
Chloroform	139	0.025	0.020	0.029	157	0.057	0.025	0.050	
Trichlorofluoromethane	159	0.245	0.225	0.264	162	0.286	0.235	0.311	
Valeraldehyde*	129	0.028	0.019	0.034	155	0.031	0.021	0.039	Heterogeneous Blair > Roxana
Crotonaldehyde*	129	0.156	0.021	0.149	165	0.200	0.025	0.217	
Acetaldehyde*	129	1.026	0.725	1.220	166	1.112	0.726	1.448	
Butyraldehyde	128	0.086	0.064	0.104	166	0.102	0.078	0.122	
Formaldehyde*	129	2.463	1.340	3.140	166	2.741	1.515	3.490	
Acetone	129	0.876	0.547	1.150	166	1.098	0.715	1.370	
2-Butanone	129	0.127	0.076	0.166	165	0.167	0.100	0.207	

*Mean of the two concentration distributions are not statistically different (homogeneous) based on the Mann-Whitney U test.
Statistical tests were conducted for days when samples from both sites were available. Summary statistics were calculated using available samples at each site.

The homogeneity suggests negligible local source contributions to these species and the observed mixing ratios are very likely to be the regional (or larger scale) background representing residues in the atmosphere from much earlier time emissions.

While carbonyls, to some extent, originate from photochemical conversion of hydrocarbons, motor vehicle emissions are also significant emission sources (Mohamed et al., 2002). Most aldehydes exhibit higher mixing ratios at Blair Street (Table 5-1) which is consistent with contributions from traffic emissions at in the St. Louis urban core. However, the excess of these carbonyls at Blair Street were only marginal and Mann-Whitney U test indicated homogeneity across the two sites. VOCs such as acetylene and 1, 3-butadiene which are commonly found in motor vehicle exhaust (Liu et al., 2008) and were higher at Blair Street compared to Roxana. Other gaseous air toxics typically associated with various chemical and industrial processes were present in elevated mixing ratios at downtown St. Louis likely because of a number of local anthropogenic activities including facilities along the industrialized Mississippi riverfront.

The VOCs which showed statistically higher concentrations at Roxana are predominantly aromatics and other petroleum related hydrocarbons, indicating potential contributions from the refinery. Figure 5-2 shows the expected mixing ratios as a function of wind direction from NWR analysis for a subset of these species at Roxana (solid lines) and Blair Street (dashed lines) using surface winds from the corresponding sites. The expected mixing ratio profiles at Roxana exhibit maxima at ~150ºN whereas there is no dominant wind direction for maximum impacts for these species at Blair Street. The wind direction associated with maximum impact at Roxana is consistent with the bearings of the main unit operations area of the refinery; this demonstrates the influence from refinery emissions. The variations in maxima across these profiles probably arise from wind direction smearing from using hourly winds but daily concentration data. Mixing

ratio maxima for benzene, propylene and n-octane are not as sharp compared to other species; this reflect multiple point sources or non-point sources that are distributed across the refinery footprints. For most species the expected mixing ratios at Roxana and Blair are quite similar when the Roxana monitoring site is upwind of the refinery (i.e. northwest winds), and the Roxana mixing ratios are up to 2-to-3 times higher than the Blair mixing ratios when the Roxana monitoring site is downwind of the refinery. An exception to this pattern is benzene which has higher expected concentrations at Roxana for all wind directions; this suggests there might be additional benzene sources in the Roxana area located off the refinery footprint. Figures 5-9 and 5-10 show the NWR expected concentrations for these compounds at the two locations along with their 95% confidence intervals.

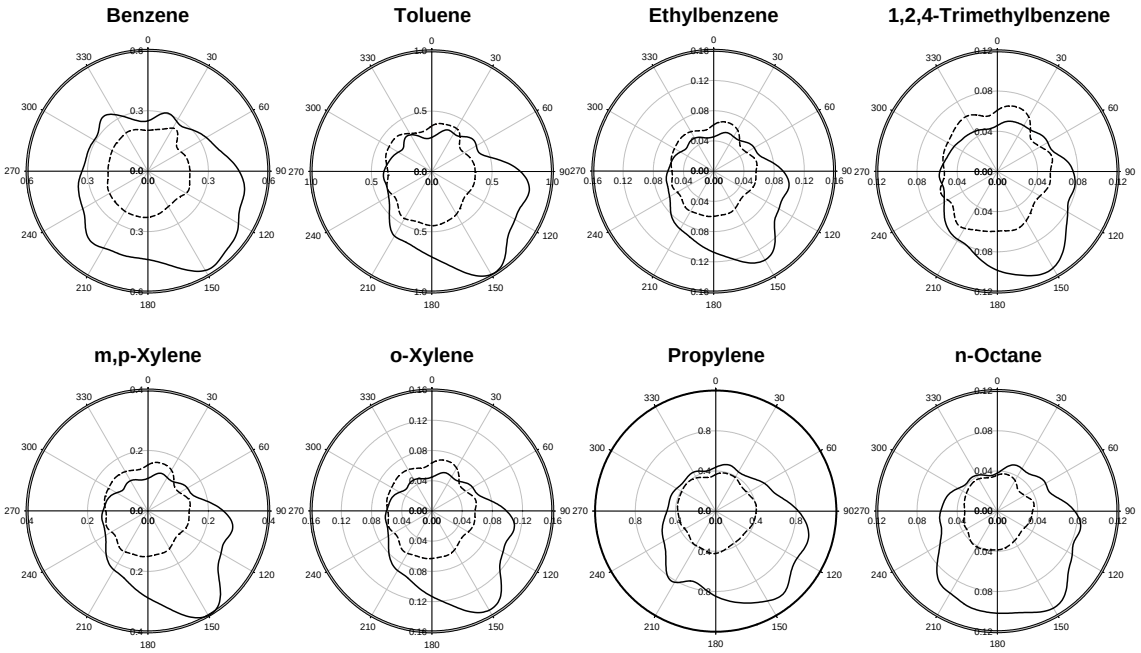

Figure 5-2. Nonparametric wind regression expected values for select aromatics and petroleum related hydrocarbons. Solid lines at Roxana data and dashed lines are at Blair Street (City of St. Louis) data. The radial axes have the units of ppb

NWR profiles for the two aldehydes on days when samples from both sites were available (Figure 5-3) showing relatively higher mixing ratios at Roxana do not point towards impacts from the refinery main operations area. The pattern may be the coupling of seasonal trends for photochemical reactions and prevailing winds which will be discussed in Section 5.3.3.

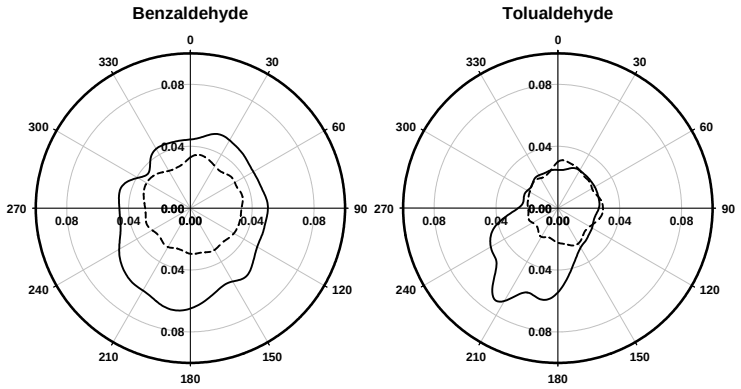

Figure 5-3. Nonparametric wind regression expected values for benzaldehyde and tolualdehyde. Solid lines are at Roxana data and dashed lines are Blair Street data. The radial axes have the units of ppb.

A semi-quantitative estimation of the local contributions at Roxana is based on the assumption that the species measured at Blair Street represent urban-scale contributions. Because both sites could have local influences, differences should be considered as the minimum local contribution at the higher mixing ratios site and this approach serves as a conservative estimate for local contributions. The median of the daily differences between paired samples at Roxana and Blair Street were used to represent the Roxana excess and urban scale contributions were estimated by the Roxana median minus Roxana excess.

Figure 5-4 shows the semi-quantitative split between local and urban-scale contributions for the eleven species deemed to have higher mixing ratios at Roxana (Table 5-1). Local contributions were up to ~50% of the observed mixing ratios. Significant relative contributions were observed

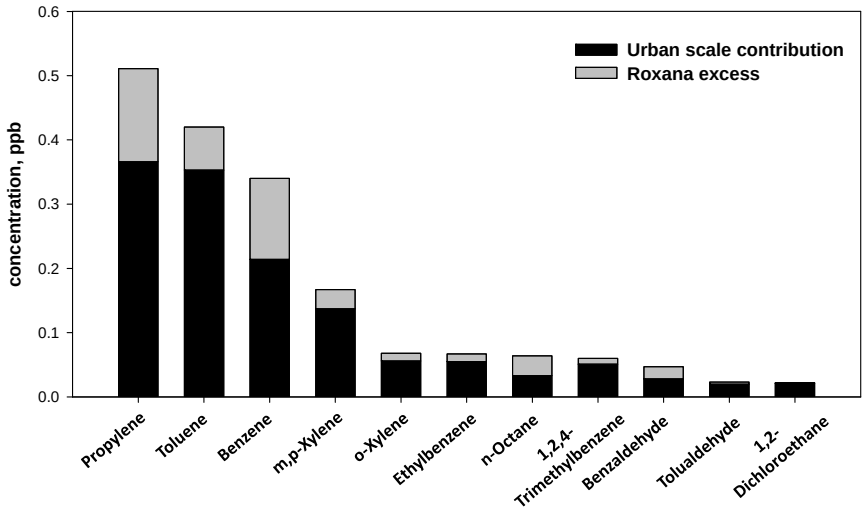

Figure 5-4. Estimation of local contributions to select gaseous air toxics observed at Roxana.

for n-octane (48%), benzaldehyde (40%) and benzene (37%) while small local contributions were associated with tolualdehyde (13%) and 1,2-dichloroethane (4%). Using this metric the local contributions were smaller than the urban-scale contributions for all of the species despite being at the fenceline of the refinery and downwind of the main unit operations area for prevailing southerly winds.

5.3.2. Benzene and Toluene at Roxana

Figure 5-5 is a scattergram of benzene against toluene at Blair Street and Roxana for June 2012 – February 2015. The two species are moderately well correlated (r = 0.59) at Blair Street. A Theil regression of benzene on toluene yields [B] = 0.276 [T] + 0.106. In contrast to Blair Street, there appears to be an edge which defines the minimum benzene/toluene (B/T) ratio at Roxana. The Theil regression line obtained by Blair Street data is consistent with the edge for Roxana. Therefore, the B/T pattern at Roxana suggests benzene is a mixture of contributions that can be

modeled as two sources with no discrimination whether these are real sources or admixture of many sources.

One source has the B/T ratio that is consistent with measurement at Blair Street and is likely influenced by traffic emissions and other sources such as fugitive emissions from the storage and transportation of fuels and biomass burning. For this analysis it is sufficient to define it as a combined source that consists of a mixture of hydrocarbons with presumably a consistent urban-scale pattern. The second source is assumed to be pure benzene. This is supported by the NWR analysis shown in Figure 5-2 which shows higher expected benzene mixing ratios at Roxana even when the refinery is not upwind of the monitoring station. However, at Roxana the two-source pattern is confounded by emissions from the refinery as is indicated by high expected mixing ratios for winds from the southeast where the main unit operations area is located.

The NWR analysis also provides evidence that the main unit operations area was the only local emission source zone that strongly impacts the benzene mixing ratio measured at the Roxana

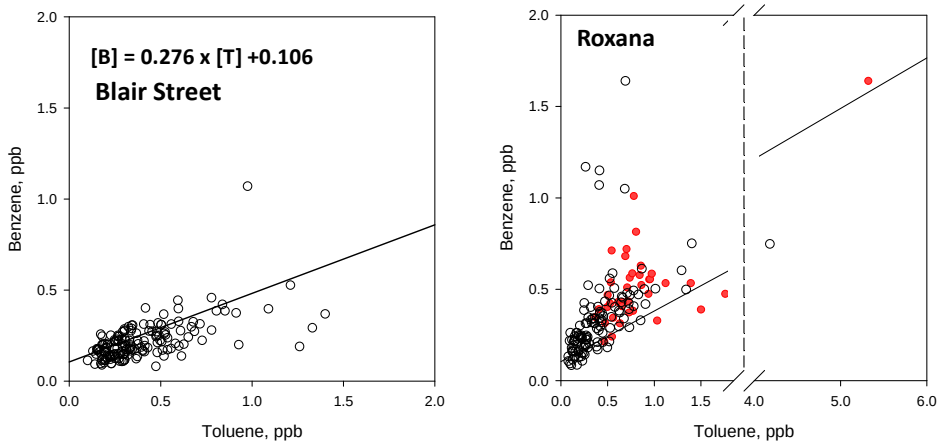

Figure 5-5. Benzene versus toluene measured at Blair Street and Roxana. The solid line is a Theil regression on the Blair Street data. Red closed circles indicate samples that were considered to be significantly impacted by refinery emissions.

site. Therefore, samples on days with over 12 hours of advective winds (wind speed > 0.5m/s) coming from the range 90ºN - 180ºN were identified (closed red circles in Figure 5-4) and considered as "refinery - influenced" samples. These 38 "refinery – influenced" samples were removed from the dataset.

The corrected two-source model (i.e model with refinery influenced samples removed) can be used to apportion the benzene in each sample. For the remaining 121 "non-refinery influenced"

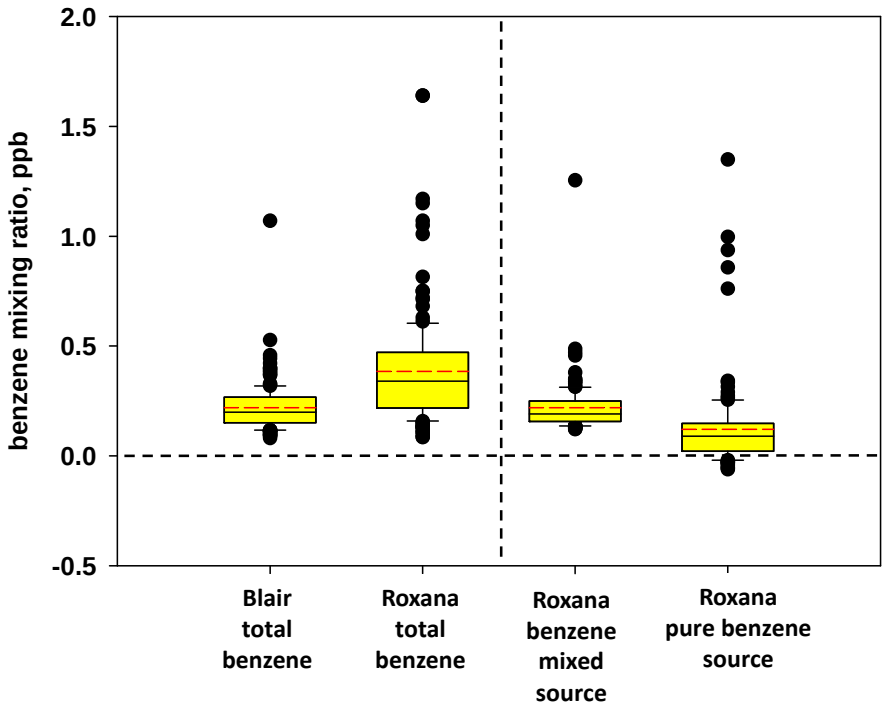

Figure 5-6. Distribution of benzene mixing ratios apportioned to the mixed hydrocarbon source and pure benzene source using the pseudo two-source model with benzene/toluene relation of [B] = 0.276 [T] + 0.106 for the mixed hydrocarbon source (N = 121). 38 refinery-influenced samples were excluded from the analysis. The top and bottom of each box are the 75th and 95th percentiles, the solid black interior line is the median, the dashed red interior line is the arithmetic mean, whiskers are 10th and 90th percentiles, and the closed circles are individual samples above the 90th percentile or below the 10th percentile.

samples the measured toluene at Roxana is multiplied by the Blair B/T ratio to estimate benzene from the mixed hydrocarbon source (which again, likely represents admixing of several actual sources). Subsequently, this contribution is subtracted from the measured total benzene to estimate the contribution from the pure-benzene source. Figure 5-6 shows the distributions of benzene mixing ratios for the two sources. The estimated contribution from the mixed hydrocarbon source at Roxana is consistent with that at Blair Street, which could support the pseudo-two source assumption. Mean mixing ratios from the pure benzene source (mean = 0.09 ppb) was lower than the mixed hydrocarbon source (mean = 0.22 ppb) and displayed greater variability.

5.3.3. PCA/APCS analysis

PCA was conducted for data collected from January 2013 to February 2015 at Roxana and from June 2012 to February 2015 at Blair Street. Four factors were resolved at both sites. Table 5-2 summarizes the factor loadings of analyzed compounds. Four factors were extracted at both sites. The first factor (PC1) at both sites is characterized by high loadings of aromatics and n-octane which are all petroleum related compounds. Propylene was categorized in this factor at Blair Street but smeared across all the factors at Roxana. It is possible that propylene is emitted by distinct sources within the refinery and thus did not load onto this factor. At Blair Street, besides the aromatic compounds, n-octane and propylene that dominated this factor, 2-butanone, acetone, acetylene and 1, 3-butadiene have loadings greater than 0.5 on this factor. These compounds are often associated with motor vehicle emissions, and the PC1 factor at Blair Street likely includes contributions from traffic related emissions.

In contrast, PC1 at Roxana had high loadings of only aromatics and n-octane without the tracer

Table 5-2. PCA results for Roxana and Blair Street. Only those factor loadings >0.5 are reported.

	Roxana				Blair Street			
	PC1	PC2	PC3	PC4	PC1	PC2	PC3	PC4
1,2,4 -Trimethylbenzene	0.95				0.87			
Ethylbenzene	0.98				0.88			
m,p-Xylene	0.98				0.89			
n-Octane	0.94				0.79			
o-Xylene	0.98				0.89			
Propylene					0.82			
Toluene	0.97				0.77			
Benzene	0.86				0.63			
Chloroform		0.56						0.67
Chloromethane							0.71	
Dichlorodifluoromethane			0.87				0.92	
Dichloromethane								0.62
Dichlorotetrafluoroethane			0.79				0.71	
Trichlorofluoromethane			0.91					
Trichlorotrifluoroethane			0.91				0.89	
Carbon tetrachloride							0.57	
2-Butanone				0.84	0.56			
Acetone		0.91			0.55			
Acetaldehyde				0.79		0.78		
Benzaldehyde		0.84				0.66		
Butyraldehyde		0.75		0.51		0.57		
Crotonaldehyde		0.81				0.78		
Formaldehyde		0.94				0.92		
Hexaldehyde		0.91				0.69		
Propionaldehyde		0.97				0.94		
Tolualdehyde		0.75				0.72		
Valeraldehyde		0.89				0.88		
Acetylene				0.81	0.53			
1,3-Butadiene				0.55	0.83			
Carbon disulfide*								
Acetonitrile*								
Methyl Isobutyl Ketone**								0.69
Acrolein**								
% of variance	31	35	18	16	39	32	16	13
Cumulative %	31	66	84	100	39	71	87	100

* Carbon disulfide was included only for the Blair Street dataset and acetonitrile were included only for Roxana dataset.
**Methyl isobutyl ketone and acrolein were only included for Blair Street dataset.

compounds for motor vehicle exhausts. This is consistent with impacts from refinery operations. Figure 5-7 shows the time series for the three major components (PC1-PC3) at both sites. The PC1 median mixing ratio of Roxana was 1.54 ppb compared to 2.12 ppb at Blair Street. At both sites the factor does not have a strong seasonal trend but does exhibit relatively high day-to-day variations. NWR analysis on the source contribution estimates (SCE) are shown in Figure 5-8 (first column – aromatics) did not reveal a well-defined dependence of wind direction at Blair Street which supports the conclusion of no major point sources contributing to the PC1 factor. However, at Roxana the NWR analysis clearly demonstrates impacts from the refinery with an SCE maximum in the direction of the main unit operations zone located to the southeast of the monitoring site. In summary, the PC1 (aromatics) factors at Blair Street and Roxana represent different admixtures with Blair Street influenced by motor vehicle exhaust emissions and Roxana influenced by the refinery.

The second factor (PC2) is dominated by carbonyl compounds and aldehydes in particular. The time series for this factor (Figure 5-7) exhibits a strong seasonal pattern at both locations with a summertime maximum and winter time minimum. This is consistent with the enhanced

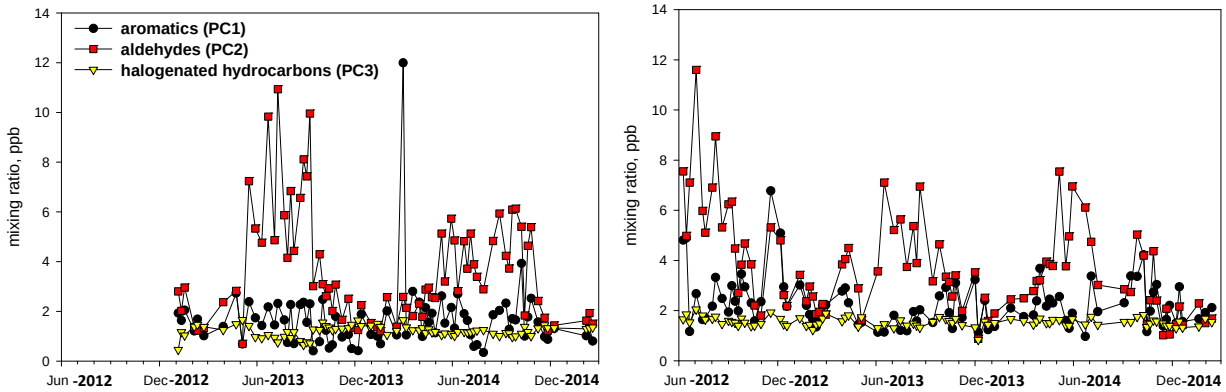

Figure 5-7. Time series for the three major factors resolved by PCA at Roxana (left) and Blair Street (right).

photochemistry in the summertime that coverts hydrocarbons to carbonyl species. The aldehyde factor NWR profile at Blair Street lacks strong features whereas this factor at Roxana display higher mixing ratios for winds from the south – southwest (Figure 5-8 – middle column) which could possibly be attributed to: (1) coupling of summertime high aldehyde mixing ratios with the prevailing southerly winds during the summer; and (2) the summertime prevailing southerly winds transporting aldehydes from St. Louis urban core to the downwind Roxana site. The weight of evidence might be in favor of the second explanation but a more detailed analysis using data with higher temporal resolution is needed.

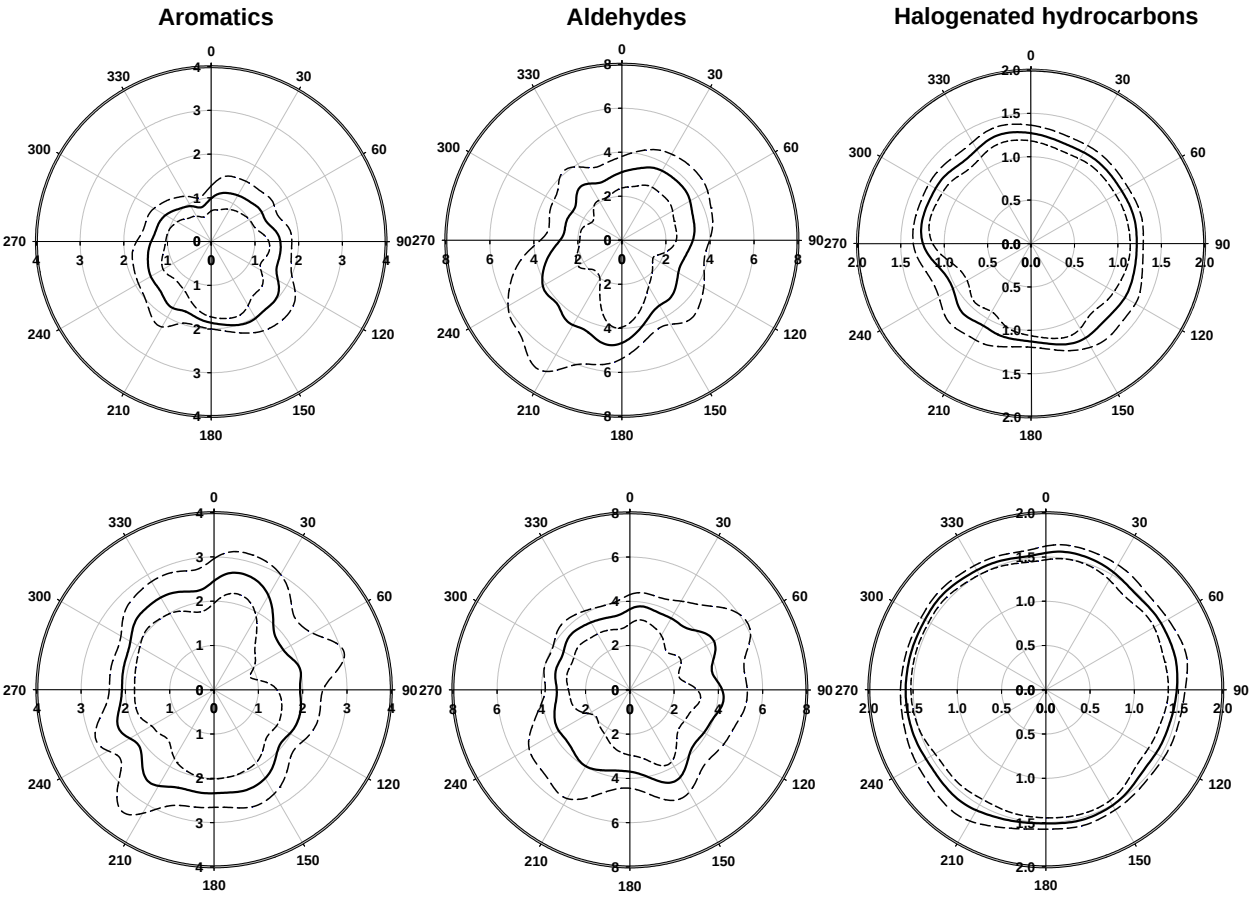

Figure 5-8. Nonparametric wind regression on three major PCA-resolved factors at Roxana (top) and Blair Street (bottom). Solid lines are the expected mixing ratios (ppb) and dashed represent 95% confidence intervals.

The profile for the third factor (PC3) varied slightly between the two sites but is generally represented by several halogenated hydrocarbons most of which are CFCs. Because of their impact on the stratospheric ozone layer depletion, most of these halogenated compounds have been prohibited from use and manufacture. Thus, the measured mixing ratios should be close to the atmospheric background levels. This is well supported by the spatial homogeneity discussed in the previous section, weak seasonal and day-to-day variations, and a lack of strong features in the NWR profiles (Figure 5-7 – right column).

The fourth factor (PC4) was relatively ill-defined at both sites and included a mixture of various compounds that showed weak inter-correlation. At Roxana, these compounds are perhaps more related to motor vehicle emissions whereas at Blair Street only two halogenated hydrocarbons and one ketone had loadings greater than 0.5. The day-to-day contributions from this factor at both sites were close to or less than zero, and therefore an interpretation is not warranted.

Seasonal variations for the compounds of interest have been well summarized by those for the PCA factors: the factor characterized by aldehydes displays strong seasonal patterns with a summertime maximum; the factor characterized by aromatics and hydrocarbons shows moderate levels of seasonal variation; and the factor represented primarily by halogenated hydrocarbons has an indistinguishable pattern. Specific to individual compounds, aromatics, alkanes and alkenes display moderate seasonal patterns with a summertime minimum. This is consistent to the observation by previous studies most likely due to: enhanced chemical reactions in the atmosphere that convert these hydrocarbons to other oxidative products; and increased mixing heights during the summer which leads to the dilution of the compounds. Significant weekday-weekends patterns were observed for 1, 3-butadiene and acetylene at Blair Street (City of St.

Louis) which provided evidence for these two compounds having major contributions from traffic related emissions.

5.4. Summary

Gaseous air toxics such as VOCs including carbonyls were sampled and analyzed at two sites in the St. Louis area – the fenceline of a petroleum refinery in Roxana and near the City of St. Louis central business district (Blair Street station). In general, most of the halogenated hydrocarbons showed homogeneity between the two sites. Aromatic compounds and other petroleum related hydrocarbons such as n-octane and propylene displayed higher mixing ratios at Roxana compared to Blair Street while most of the carbonyls and motor vehicle exhaust related hydrocarbons such as acetylene and 1,3-butadiene showed higher mixing ratios at Blair Street. It was estimated that local contributions to compounds with higher mixing ratios at Roxana were up to about 50%. Nonparametric wind regression analysis provided supporting evidence for refinery operation impacts for the aromatics, n-octane and propylene when the receptor site is downwind of the refinery during the 24-hour sampling period.

A pseudo-two source model for benzene at Roxana was proposed with data from Blair Street as a context. Benzene from a source with mixed hydrocarbons that appears to be homogeneous between the two sites was estimated to contribute about 70% of the total benzene at Roxana that was not “refinery-influenced” while the median contribution from the local pure benzene source was 0.09 ppb.

Based on the principle component analysis, similar source profiles were resolved at both Roxana and Blair Street with aromatics and aldehydes collectively responsible for up to 71% of the variance in gaseous air toxics. The factor characterized by aldehydes display strong seasonal

cycles which was affected by photochemical reactions modulated by seasonal cycle of meteorology. NWR provided evidence that the factor dominated by aromatic compounds is impacted by refinery operations at Roxana while it showed no wind direction dependence at downtown St. Louis. Halogenated hydrocarbons were identified as minor contributors to gaseous air toxics and are likely dominated by regional background.

5.5. References

Baltrenas, P., Baltrenaite, E., Šerevičiene, V., Pereira, P., 2011. Atmospheric BTEX concentrations in the vicinity of the crude oil refinery of the Baltic region. Environmental Monitoring and Assessment 182, 115-127.

Ban-Weiss, G.A., McLaughlin, J.P., Harley, R.A., Kean, A.J., Grosjean, E., Grosjean, D., 2008. Carbonyl and nitrogen dioxide emissions from gasoline- and diesel-powered motor vehicles. Environmental Science and Technology 42, 3944-3950.

Buzcu, B., Fraser, M.P., 2006. Source identification and apportionment of volatile organic compounds in Houston, TX. Atmospheric Environment 40, 2385-2400.

Carter, W.P.L., 1994. Development of ozone reactivity scales for volatile organic compounds. Journal of the Air and Waste Management Association 44, 881-899.

Cetin, E., Odabasi, M., Seyfioglu, R., 2003. Ambient volatile organic a petrochemical (VOC) concentrations around compound complex and a petroleum refinery. Sci. Total Environ. 312, 103-112.

Chameides, W.L., Lindsay, R.W., Richardson, J., Kiang, C.S., 1988. The role of biogenic hydrocarbons in urban photochemical smog: Atlanta as a case study. Science 241, 1473-1475.

Davis, C.S., Otson, R., 1996. Estimation of emissions of volatile organic compounds (VOCs) from Canadian residences. ASTM Special Technical Publication 1261, 55-65.

Du, L., Turner, J., 2015. Using $PM_{2.5}$ lanthanoid elements and nonparametric wind regression to track petroleum refinery FCC emissions. Sci. Total Environ. 529, 65-71.

Elkins, J.W., Thompson, T.M., Swanson, T.H., Butler, J.H., Hall, B.D., Cummings, S.O., Fisher, D.A., Raffo, A.G., 1993. Decrease in the growth rates of atmospheric chlorofluorocarbons 11 and 12. Nature 364, 780-783.

Fabian, P., Borchers, R., Leifer, R., Subbaraya, B.H., Lal, S., Boy, M., 1996. Global Stratospheric distribution of halocarbons. Atmospheric Environment 30, 1787-1796.

Grosjean, D., 1982. Formaldehyde and other carbonyls in los angeles ambient air. ES and T Contents 16, 254-262.

Guo, H., Wang, T., Louie, P.K.K., 2004a. Source apportionment of ambient non-methane hydrocarbons in Hong Kong: Application of a principal component analysis/absolute principal component scores (PCA/APCS) receptor model. Environmental Pollution 129, 489-498.

Guo, H., Wang, T., Simpson, I.J., Blake, D.R., Yu, X.M., Kwok, Y.H., Li, Y.S., 2004b. Source contributions to ambient VOCs and CO at a rural site in eastern China. Atmospheric Environment 38, 4551-4560.

Henry, R.C., Chang, Y.S., Spiegelman, C.H., 2002. Locating nearby sources of air pollution by nonparametric regression of atmospheric concentrations on wind direction. Atmospheric Environment 36, 2237-2244.

Jorquera, H., Rappenglück, B., 2004. Receptor modeling of ambient VOC at Santiago, Chile. Atmospheric Environment 38, 4243-4263.

Kalabokas, P.D., Hatzianestis, J., Bartzis, J.G., Papagiannakopoulos, P., 2001. Atmospheric concentrations of saturated and aromatic hydrocarbons around a Creek oil refinery. Atmospheric Environment 35, 2545-2555.

Kim, E., Hopke, P.K., 2004. Comparison between Conditional Probability Function and Nonparametric Regression for Fine Particle Source Directions. Atmospheric Environment 38, 4667-4673.

Leuchner, M., Rappenglück, B., 2010. VOC source–receptor relationships in Houston during TexAQS-II. Atmospheric Environment 44, 4056-4067.

Lin, T.Y., Sree, U., Tseng, S.H., Chiu, K.H., Wu, C.H., Lo, J.G., 2004. Volatile organic compound concentrations in ambient air of Kaohsiung petroleum refinery in Taiwan. Atmospheric Environment 38, 4111-4122.

Liu, Y., Shao, M., Fu, L., Lu, S., Zeng, L., Tang, D., 2008. Source profiles of volatile organic compounds (VOCs) measured in China: Part I. Atmospheric Environment 42, 6247-6260.

Miller, S.L., Anderson, M.J., Daly, E.P., Milford, J.B., 2002. Source apportionment of exposures to volatile organic compounds. I. Evaluation of receptor models using simulated exposure data. Atmospheric Environment 36, 3629-3641.

Mohamed, M.F., Kang, D., Aneja, V.P., 2002. Volatile organic compounds in some urban locations in United States. Chemosphere 47, 863-882.

Morello-Frosch, R.A., Woodruff, T.J., Axelrad, D.A., Caldwell, J.C., 2000. Air toxics and health risks in California: The public health implications of outdoor concentrations. Risk Analysis 20, 273-291.

National Oceanic and Atmospheric Administration, 2015. Chlorofluorcarbon-12 (CCl_2F_2) — Combined Data Set.

Thurston, G.D., Spengler, J.D., 1985. A quantitative assessment of source contributions to inhalable particulate matter pollution in metropolitan Boston. Atmospheric Environment (1967) 19, 9-25.

Winer, A.M., Arey, J., Atkinson, R., Aschmann, S.M., Long, W.D., Morrison, C.L., Olszyk, D.M., 1992. Emission rates of organics from vegetation in California's Central Valley. Atmospheric Environment Part A, General Topics 26, 2647-2659.

Woodruff, T.J., Axelrad, D.A., Caldwell, J., Morello-Frosch, R., Rosenbaum, A., 1998. Public health implications of 1990 air toxics concentrations across the United States. Environmental Health Perspectives 106, 245-251.

Xie, Y., Berkowitz, C.M., 2006. The use of positive matrix factorization with conditional probability functions in air quality studies: An application to hydrocarbon emissions in Houston, Texas. Atmospheric Environment 40, 3070-3091.

5.6. Supplemetary Material

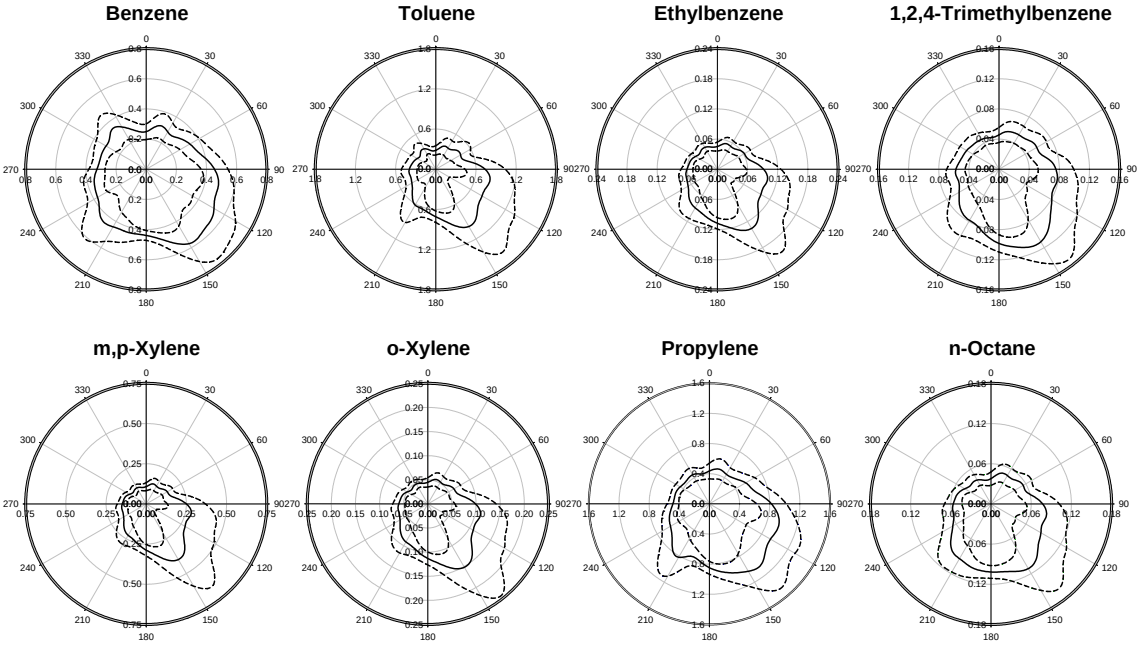

Figure 5-9 Nonparametric wind regression expected values for select aromatics and petroleum related hydrocarbons at Roxana. Solid lines are the expected mixing ratios (ppb) and dashed lines represent 95% confidence intervals.

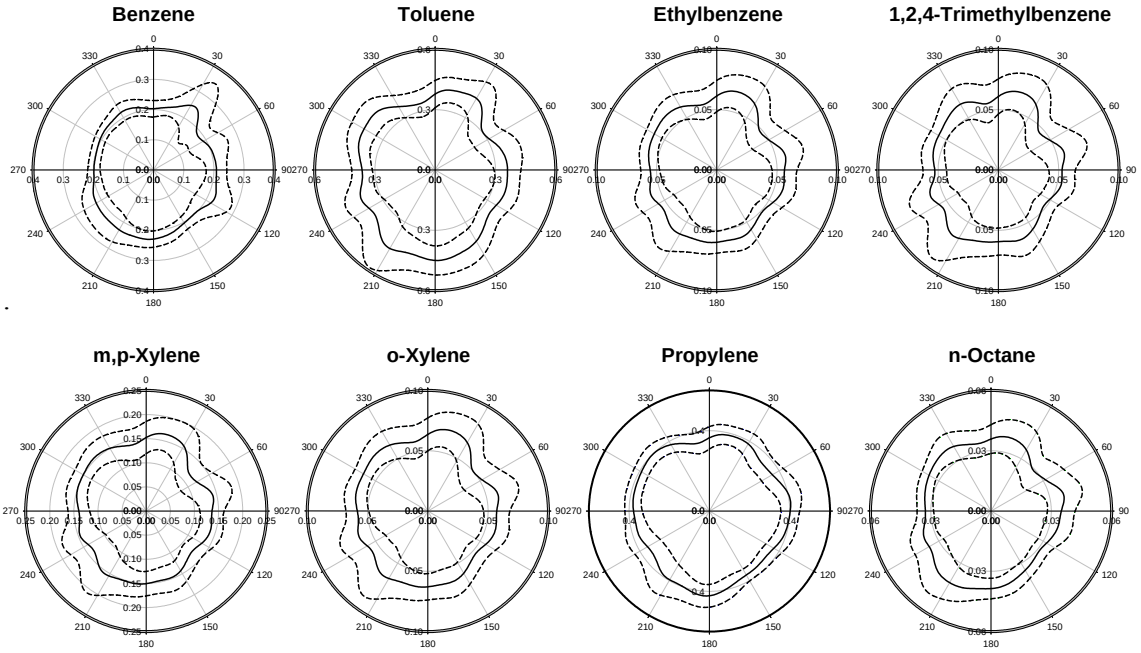

Figure 5-10 Nonparametric wind regression expected values for select aromatics and petroleum related hydrocarbons at Blair Street. Solid lines are the expected mixing ratios (ppb) and dashed lines represent 95% confidence intervals.

Chapter 6 : Special Topics in PM Spatial Variability Assessment

6.1. Introduction

Many epidemiological studies have linked adverse health effects, including mortality and morbidity, to ambient particulate matter (PM) exposures (Dockery et al., 1993; Pope et al., 2002; Zanobetti et al., 2003). Advances in both monitoring techniques and statistical methods have made the analyses more sensitive and often led to adverse effects being found at lower exposures (World Health Organization, 2000). Early ambient PM epidemiological studies focused on ambient PM mass concentration and used data from a single monitoring site (typically called the "central" site) to represent population exposures over relatively large study areas (Pope et al., 2002; Roosli et al., 2001; Zanobetti et al., 2003) while other studies simply averaged the concentrations monitored at multiple sites over the study area to estimate human exposure (Burnett et al., 2001). These approaches assumed the ambient PM mass was homogeneously distributed across the study area (or at least nearly so). In some cases this approach appears justified because the pollutant of interest is nearly homogeneous or at least well correlated (Burton et al., 1996; Pope et al., 2002). However, in other cases the spatial variability can be relatively large and lead to potential misclassification of exposure levels based on the homogenous distribution assumption (Ito et al., 2004; Pinto et al., 2004; Zhu et al., 2002). Ambient particulate matter is a complex mixture of numerous chemical components and there has been a growing focus on understanding the relationships between specific PM components, or emissions from specific emission source categories such as coal-fired power plants or diesel vehicles, and adverse health effects (Aschner et al., 2005; Burnett et al., 2000; Ito et al., 2006; Ostro et al., 2007). Therefore, considerable effort has focused on developing more sophisticated

approaches to estimating exposures including, but not limited to, developing a better understanding of the spatial variability of both PM mass and its components.

Pinto et al. (2004) has grouped the factors that could influence spatial variability of PM on urban and finer spatial scales into six categories: (1) local sources of primary PM; (2) transient emission events that differentially impact some sites more than others; (3) differences in the behavior of semi-volatile components; (4) topographical barriers separating sites; (5) meteorological phenomena; and (6) measurement error. These factors can individually and collectively lead to spatial variability. Metrics such as the Pearson correlation coefficient (PCC) and coefficient of Divergence (COD) have been developed to gauge temporal and spatial variability, respectively. Methods such as the conditional probability function (CPF) and nonparametric wind regression (NWR) are used to characterize the wind direction dependence of the pollutant concentration, and can lead to the identification of local emission source zones which can drive spatial variability. Graphical tools such as time series and scattergrams have been applied to datasets collected at multiple locations as a simple representation of the spatial variability. Based on a survey of numerous previous studies (Houthuijs et al., 2001; Pakbin et al., 2010; Wang et al., 2011; Wilson and Suh, 1997), it is clear that PM spatiotemporal variability is typically investigated using several metrics because each metric captures only some aspects of the variability. Factors such as outliers and measurement error can distort or confound the outcomes of these metrics or methods, and a comprehensive understanding of the nature of these metrics in the context of specific datasets is necessary.

This chapter presents examples of several issues that can arise when assessing spatial variability using conventional metrics. Section 6.3 demonstrates the sensitivity of the Pearson correlation coefficient to extreme values. Section 6.4 examines the concentration dependence of precision

and implications to using a single-valued estimate of precision. Finally, Section 6.5 shows a case where concentrations at two sites would be deemed homogeneous by most metrics but the differences that do exist cannot be explained by measurement error and appear to arise from small and largely offsetting local source impacts.

6.2. Datasets and method

6.2.1. $PM_{2.5}$ speciation datasets

The US Environmental Protection Agency (EPA) Chemical Speciation Network (CSN) was implemented in 1999 to provide insights into fine particulate matter ($PM_{2.5}$) chemical composition in urban areas and to support air quality management and health related studies. 24 hour integrated samples are collected on a 1-in-3 day or 1-in-6 day schedule and $PM_{2.5}$ gravimetric mass, water soluble ions, elements and carbon fractions are reported at each site. Details of the samplers and analytical protocols were described in detail in prior reports and publications (Birch and Cary, 1996; Chow et al., 1993; Solomon et al., 2014; Solomon et al., 2000).

For the CSN, six collocated sites (sites that collect side-by-side samples using two identical collocated samplers) across the United States have been in operation since around 2001 – Bakersfield, CA, Riverside, CA, Cleveland, OH, Houston, TX, Boston, MA and New Brunswick, NJ – and these data collected through late 2013 were extracted from US EPA Air Quality System (AQS). Collocated data provide important information on assessing measurement error in the CSN. Currently in the St. Louis area there are three CSN sites and two additional sites that follow the CSN sampling and analysis protocols. The temporal coverage of

these sites varies from 2 to 15 years and collectively provide a relatively rich dataset to explore patterns and issues in assessing spatiotemporal variability.

6.2.2. Key Metrics to Gauge Spatial and Temporal Variability

The Pearson correlation coefficient (PCC) is a commonly used metric to describe the linear correlation or dependence between two variables. In air quality studies focusing on spatiotemporal variability, PCC is defined by Equation (1) where C_{ij} is the concentration for sample *i* measured at site *j*; $\bar{C}_j$ is the average concentration at site *j*; and *j* and *k* represent two sites and *n* is the total number of paired samples.

$$PCC_{jk} = \frac{\sum_{i=1}^{n}(C_{ij}-\bar{C}_j)\times(C_{ik}-\bar{C}_k)}{\sqrt{\sum_{i=1}^{n}(C_{ij}-\bar{C}_j)^2\times\sum_{i=1}^{n}(C_{ik}-\bar{C}_k)^2}} \quad (1)$$

The metric typically involves concentration time series measured at two locations and describes the temporal similarity between them. It is bounded by [-1, 1] where -1 and 1 indicate perfect negative and positive correlations, respectively, and 0 means no correlation.

Coefficient of divergence (COD) is a metric to gauge the inter-site variability in the concentration between two sites (Wongphatarakul et al., 1998). COD is defined by Equation (2):

$$COD_{jk} = \sqrt{\frac{1}{n}\sum_{i=1}^{n}\left\{\frac{(C_{ij}-C_{ik})}{(C_{ij}+C_{ik})}\right\}^2} \quad (2)$$

COD has a range of zero to one with zero representing perfect agreement between the two sites (absolute homogeneity) and unity meaning absolute spatial heterogeneity.

6.2.3. Quantifying Measurement Error using Precision

Precision and uncertainty are methods used to estimate measurement error with the former focusing on observed differences between collocated samples and the latter describing the predicted or calculated differences among repeated measurements. There is no single prescribed formula for reporting precision; two definitions are the root mean square (RMS) precision and the percentile precision (Hyslop and White, 2009). The RMS precision is the EPA-recommended formula for calculating precision of the collocated Federal Reference Method (FRM) samplers. It is defined as the root mean square of the sample-specific *scaled relative difference* D_i as shown in Equation (3) and (4) where C_{i1} and C_{i2} are the i^{th} paired collocated samples, $\overline{C_i}$ is average concentration of the i^{th} paired samples and n is total number paired collocated samples.

$$RMS\ precision = \sqrt{\frac{1}{n}\sum_{i=1}^{n} {D_i}^2} \times 100\% \tag{3}$$

$$D_i = \frac{(C_{i1} - C_{i2})/\sqrt{2}}{\overline{C_i}} \tag{4}$$

RMS precision is sensitive to deviations from normality and outliers (data pairs with large *relative* differences) will be influential. Therefore, when calculating the RMS precision only sample pairs with average concentration values at least three times the method detection limit (MDL) were included to minimize the impact from large relative differences that can arise at low concentrations. Percentile precision focuses on the central tendencies of the data and estimates 1σ precision using the 16^{th} and 84^{th} percentiles of the scaled relative difference (D_i) distribution. Assuming a normal distribution for the scaled relative difference, this method ignores the outer edges of the distributions and, therefore, reduces the influence of outliers.

$$Percentile\ precision = \frac{1}{2}[P_{84}(D_i) - P_{16}(D_i)] \times 100\% \tag{5}$$

6.3. Pearson Correlation Coefficient and Extreme Values

Species dominated by regional-scale sources that simultaneously impact multiple sites could lead to PCC values close to unity, whereas concentration pairs for species differentially influenced by local sources or activities would have values closer to zero. One disadvantage of the PCC is its sensitivity to extreme values in the time series, such large concentration values caused by exceptional or episodic events. Failure to consider the effect from these samples could result in misinterpretation of variability when using the PCC metric. Statistical tests such as the Grubb's test and the Tiejen-Moore test have been developed to test for and identify outliers in a dataset. However, these statistical tests do not provide insights to how the identified outliers influence the PCC. Therefore, a systematic, semi-graphical method with statistical support was developed to test the sensitivity of datasets to outlier pairs and thereby inform the stability of the correlation calculation.

St. Louis area CSN speciation data were screened to keep only concentration values above the sample-specific MDL. PCC was calculated for only those species with more than 60% of the samples above the MDL. For each species, concentrations were paired between any two selected sites, resulting in nine site pairs (the temporal coverage of data collected at Granite City and Roxana did not overlap). Bootstrapping was used to resample each original dataset by pairs with replacement to create new datasets of the same size. In this study 1000 iterations of bootstrapping were performed and the PCC was calculated for each of the 1000 synthetic datasets. The frequency distributions of these PCC values provide insights into the sensitivity to outliers. A relatively narrow, single-mode distribution suggests a robust PCC estimate whereas noisy or multi-mode distribution of PCC values often indicates that one or more outliers are having influence on the PCC. Figure 6-1 shows scattergrams of $PM_{2.5}$ Si at Blair and Arnold as

well as the frequency distribution of PCC values derived from the original dataset and after removing extreme values.

Airmass back-trajectory analysis indicated that two of the identified extreme values (marked on Figure 6-1) were from long-range transport of Saharan dust which resulted in elevated regional-level Si concentrations. The event showing high Si concentration at Arnold was possibly due to local activity because the airmass was relatively stagnant and conditions were unfavorable for dispersion; another possible explanation is a measurement error. The noisy frequency distribution of bootstrapped PCC values clearly illustrates the influence of the three

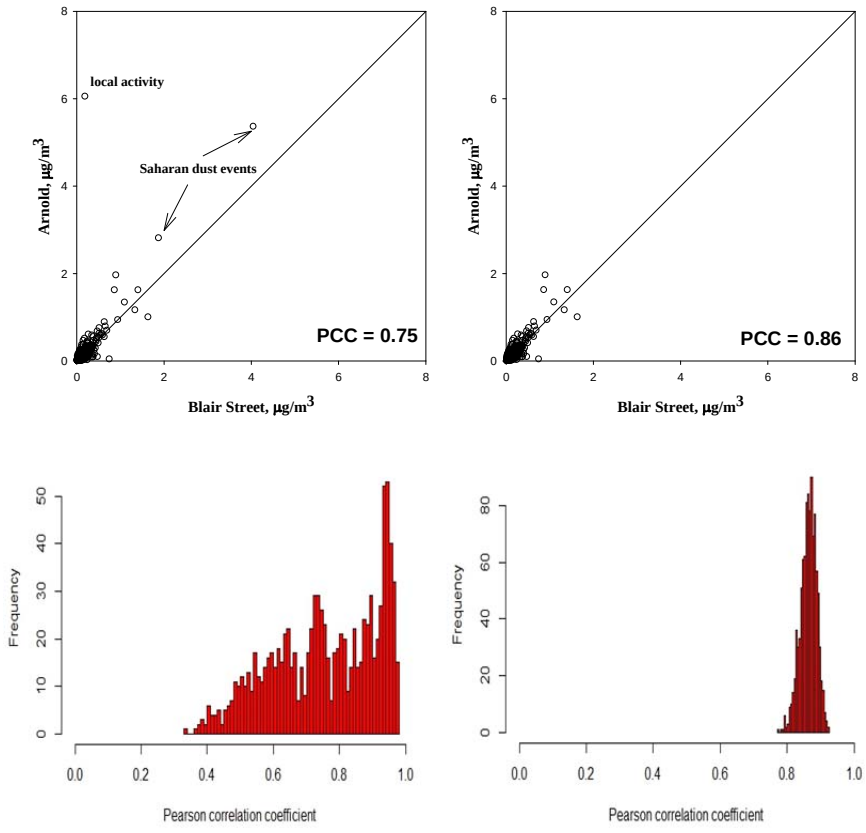

Figure 6-1. Scattergrams and frequency distributions of PCC values derived from bootstrapping on $PM_{2.5}$ Si observed at Blair Street and Arnold using original dataset (left column) and with three outliers removed (right column).

extreme values on PCC (Figure 6-1 left). Upon excluding these three sample pairs the PCC distribution is unimodal with a narrow distribution. Similarly, fireworks on July 4th weekend often leads to elevated potassium concentrations that exert high influence on the PCC. A failure to exclude these events could cause a misclassification of variability in biomass burning impacts for which potassium is a commonly used (albeit imperfect) tracer species. Table 6-1 summarizes the correlations for select species between all the available site pairs. Each dataset was evaluated using the bootstrapping method described above and was subsequently conditioned to minimize the influence from extreme values.

Table 6-1. Summary of Pearson correlation coefficient for select species between site pairs[1].

	BL-AR	BL-BV	BL-GC	BL-RX	AR-BV	AR-GC	AR-RX	BV-GC	BV-RX
$PM_{2.5}$ mass	0.84	0.81	0.74	0.86	0.80	0.67	0.80	0.67	0.91
NH_4	0.96	0.97	0.94	0.97	0.96	0.89	0.96	0.92	0.97
NO_3	0.97	0.98	0.96	0.96	0.98	0.93	0.98	0.93	0.99
SO_4	0.96	0.96	0.96	0.93	0.93	0.89	0.85	0.92	0.93
Ca	*0.48(1)*[2]	*0.65(1)*	0.33	0.38	0.55	0.33	0.20	*0.50(1)*	*0.48(1)*
Fe	0.23	0.20	-0.06	-0.01	0.25	0.17	0.39	0.05	0.34
K	*0.65(9)*	*0.85(1)*	*0.67(4)*	*0.74(1)*	*0.87(5)*	*0.60(7)*	*0.79(3)*	*0.24*	*0.74(1)*
Si	*0.86(3)*	0.84	*0.53(1)*	0.84	*0.92(1)*	0.60	0.80	0.60	0.80
Zn	0.41	0.41	-0.12	-0.17	0.33	-0.04	-0.10	-0.02	0.12
OC(NIOSH)	0.74								
EC(NIOSH)	0.59								
OC(IMPROVE)	0.88	0.55	*0.90(1)*	0.87	0.86	*0.83(1)*	0.90	*0.81(1)*	0.85
EC(IMPROVE)	0.70	0.85	0.71	0.43	*0.72(1)*	0.56	0.63	0.43	0.65

1. BL-Blair; AR-Arnold; GC-Granite City; BV-Belleville; RX-Roxana
2. PCC calculated using conditioned datasets are in italics and values in parentheses indicate number of outlier pairs excluded.

Ammonium, nitrate and sulfate showed very high correlation (0.85-0.99) for all the site pairs, consistent with these species being dominated by regional-scale sources. $PM_{2.5}$ mass is generally well correlated among all the sites with PCC > 0.8 except for site pairs involving Granite City which has high impacts from the nearby Granite City steelworks. Both K and Si exhibit

relatively high intersite correlation after conditioning the data to remove extreme values with Granite City pairs again having lower correlations because of the steelworks influences. Correlations for Ca among all the sites were moderately low and the source apportionment analysis in Chapter 7 indicates it has contributions from both local resuspended soil and a regional-scale feature that is not yet fully understood. In the St. Louis area, metals such as Fe and Zn have contributions from local industries including but not limited to a steel mill, copper production and a zinc smelter; relatively low correlations are observed. Source apportionment analysis also indicated that carbonaceous species, including organic carbon (OC) and elemental carbon (EC), are primarily attributed to biomass burning (and unresolved secondary OC) and local traffic related emissions, respectively, which could possibly explain the high but noisy correlation of these two species for some site pairs as evidenced by unimodal but relatively broad PCC distributions.

In summary, this analysis demonstrates a simple methodology to evaluate the sensitivity of the PCC to outlier data pairs. While in principle PCC confidence intervals could be used as a measure of stability, the bootstrapped distributions are a powerful visual tool.

6.4. Spatial Variability in the Context of Measurement Error – Concentration Dependence of Precision

Measurement error is associated with all sampling and monitoring processes and results in differences between the reported and true concentration. Properly characterizing measurement error is important because source apportionment modeling and other data analyses can be considerably influenced by measurement error. Also, some analyses methods, including certain source apportionment models, use uncertainty estimates to constrain the solutions. The primary

sources of measurement error may be attributed to instrument imprecision which includes that for a single type of instrument and analytical protocol, as well as that stemming from the use of different instruments or analytical procedures for a single analyte (Wade et al., 2006). For continuous and semicontinuous measurements, instrument error typically results from calibration drift, flow rate changes, and changes in atmospheric conditions (such as relative humidity), that can affect the instrument response. Instrument precision can be quantified using data from collocated instruments. For example, Hyslop and White (2011) used $PM_{2.5}$ speciation data from collocated samplers at a subset of sites in the Interagency Monitoring of Protected Visual Environments (IMPROVE) network and Speciation Trends Network (STN; a subset of the CSN) to examine interspecies covariance. At one site the high covariance of measurement differences between collocated samplers for the soil elements (Fe, Ca, Si, etc.) suggests a common error in the particle size discrimination between collocated samplers. Haddad (2015) identified periods of systematic bias between collocated samples at six sites in the CSN. $PM_{2.5}$ gravimetric mass and sulfur behaved nearly ideally with small persistent bias whereas crustal elements such as Si, Ca and Fe displayed persistent bias (i.e periods on the order of one year) as well as abrupt changes in the magnitude and direction of bias. If these samplers were not collocated but rather were placed at different sites, the measurement error might be interpreted as spatial variability.

As another example, Pinto et al. (2004) suggested using COD of 0.2 as a threshold value with spatial homogeneity at lower COD and spatial heterogeneity at higher COD. A number of studies focusing on $PM_{2.5}$ as well as its components adopted this threshold value for the classification of spatial variability (Cheung et al., 2011; Hudda et al., 2010; Lagudu et al., 2011; Mendoza et al., 2010; Moore et al., 2009). However, this cutoff value was originally developed in a study on FRM $PM_{2.5}$ gravimetric mass concentration data and extending the application of this cutoff

value to PM components has not been thoroughly discussed and validated. In addition, using COD values without considering the contribution of measurement error could lead to misclassification of spatial variability. Haddad (2015) demonstrated that for certain species (e.g. Cu, Cl, Fe) reported by CSN, the COD could exceed the threshold of 0.2 even when including only collocated sample pairs with both concentrations greater than 3×MDL.

A study was conducted to examine whether there is a concentration dependence on precision, in this case focusing on values greater than the MDL. This assessment is important because previous approaches typically condition the data to include concentrations greater than 3×MDL assume the precision is well-represented by a single-valued metric.

CSN collocated data were extracted from AQS. Table 6-2 provides summary statistics for sulfate and nitrate which was the focus of this study because these species have a wide range in mean concentrations between sites (1.7 to 3.8 $\mu g/m^3$ for sulfate and 0.7 to 7.7 $\mu g/m^3$ for nitrate). Thus, they can be used to test how pooling data across sites influences the precision estimates.

Figure 6-2 illustrates the relationships between the scaled relative difference (Equation 4) and concentration for nitrate and sulfate. This measure of relative precision exhibits a concentration dependence which is strong for nitrate and not distinguishable for sulfate. In particular, nitrate measurements are more imprecise at low concentrations whereas the data are more precise at higher concentrations. This suggests that it is difficult to define a single-valued precision metric even when restricting the analysis to concentrations greater than 3×MDL. *Assuming the collocated data can be pooled across sites*, one refinement to a single-valued metric is to draw collocated samples from the pooled dataset to match the concentration distributions for the network site pairs of interest. In this study, paired samples for two St. Louis sites were used to

Table 6-2. Summary statistics for the primary sampler at each of the six collocated CSN sites.

	Number of paired samples	Concentration, μg/m^3		
		Mean	25th percentile	75th percentile
Bakersfield, CA				
05/25/2001 - 09/07/2013				
Sulfate	604	1.70	1.04	2.14
Nitrate	738	5.29	1.17	6.53
Houston, TX				
12/14/2000 - 12/06/2013				
Sulfate	748	3.07	1.81	3.91
Nitrate	685	0.73	0.39	0.84
Cleveland, OH				
05/01/2001 - 12/06/2013				
Sulfate	770	3.78	2.01	4.74
Nitrate	738	2.21	0.80	2.92
New Brunswick, NJ				
06/18/2001 - 12/06/2013				
Sulfate	624	3.09	1.36	3.66
Nitrate	574	1.28	0.42	1.71
Riverside, CA				
05/19/2001 - 12/06/2013				
Sulfate	919	2.52	0.83	3.64
Nitrate	848	7.67	2.46	10.40
Boston, MA				
05/18/2000 - 12/06/2013				
Sulfate	694	2.40	1.07	2.82
Nitrate	637	0.95	0.35	1.27

construct a distribution of pairwise average concentration values. The distribution was segmented into concentration bins (the "two-site data" bins). Identical binning was applied to the pooled collocated dataset (the "collocated data" bins). A synthetic collocated dataset was constructed by randomly drawing a sample pair from the corresponding collocated data bin for each data pair in the two-site data bin. 1000 synthetic collocated datasets – each with a concentration distribution matching the two-site data (at the concentration bin level) – were used for the precision calculations.

This "binning-sampling" method was validated using a "leave-one-out" approach based on the jackknife technique. Each of the six collocated sites was treated as the target (i.e. two-site) dataset and the synthetic collocated datasets were created by pooling data from the remaining five collocated sites following the method described above. Figure 6-3 shows the actual precision for the target dataset on the x-axis and the precision predicted from concentration-dependent sampling of the remaining five collocated datasets on the y-axis. Error bars represent 1σ of the distribution of precision values derived from bootstrapping. Percentile

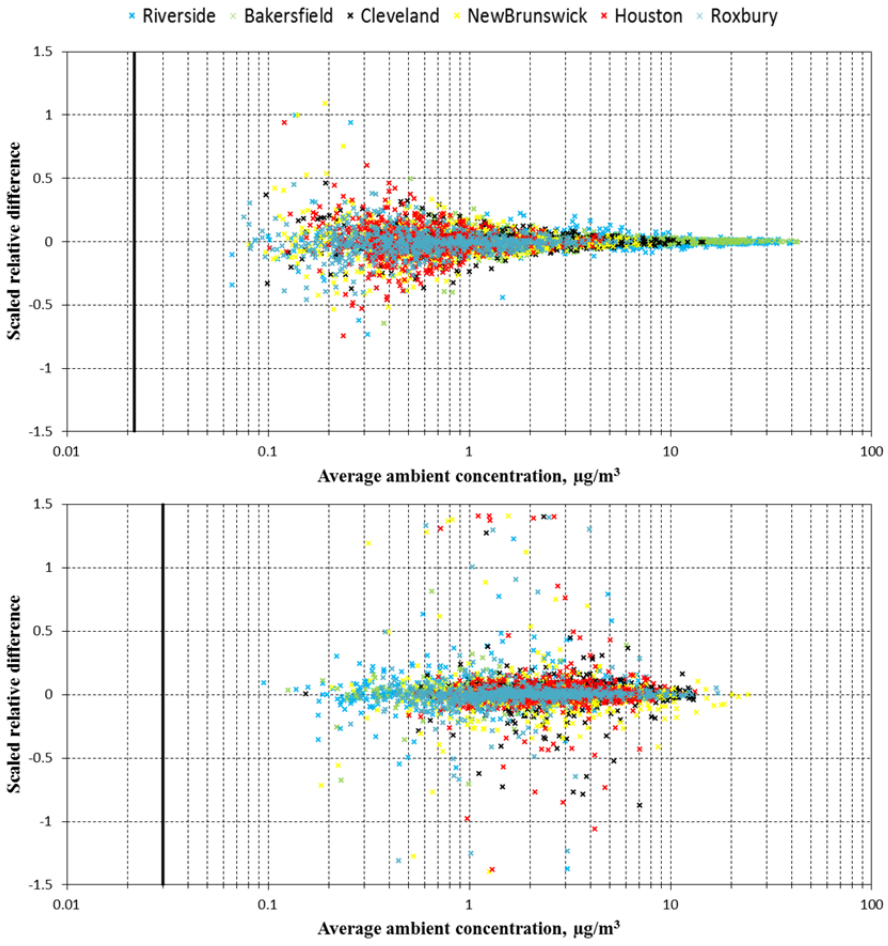

Figure 6-2. Scaled relative difference vs. average concentration for the collocated measurements of $PM_{2.5}$ nitrate (top) and sulfate (bottom) from six collocated CSN sites. Thick black lines are 3 times the mode MDLs.

precision shows relatively good agreement between the actual precision and the precision estimated by concentration matching of collocated data from the remaining sites. For sulfate this refinement is incremental because the precision range across sites is only 3-7% and the all-sites pooled precision of 4% is a reasonable estimate for each site (again, consistent with no distinguishable concentration dependence of precision). For nitrate, however, this refinement is more substantial because the precision range across sites is 3-12% and the all-sites pooled precision of 5% poorly represents some sites. For both species the results are inferior for the RMS precision because it is influence by both outliers and persistent bias between the collocated samplers which varies across sites (Haddad 2015). This is demonstrated in Figure 6-2 where at a given concentration the Riverside data are more tightly clustered around the zero line and the New Brunswick data tends to have the largest deviations from the zero line.

The applicability of this approach has been demonstrated for sulfate and nitrate, especially for the predicted precision, but needs to be examined for species such as Fe and Si which are more strongly influenced by persistent collocated sampler bias. Haddad (2015) showed that collocated sampler bias is less pronounced for species primarily found in fine PM but can be quite large for crustal species which are present in both fine and coarse PM. Possible causes include, but are not limited to, maintenance issues such as miscalibration of flow rate that changes the sampler cut point. At this time it is not clear whether the precision for such species can be reliably estimated from the collocated data.

In summary, it has been demonstrated that some species, such as nitrate, exhibit a concentration dependent relative precision even for concentrations greater than 3×MDL. Bootstrapping the pooled collocated datasets to match the concentration distributions for the site pairs of interest yields a better single-value precision estimate.

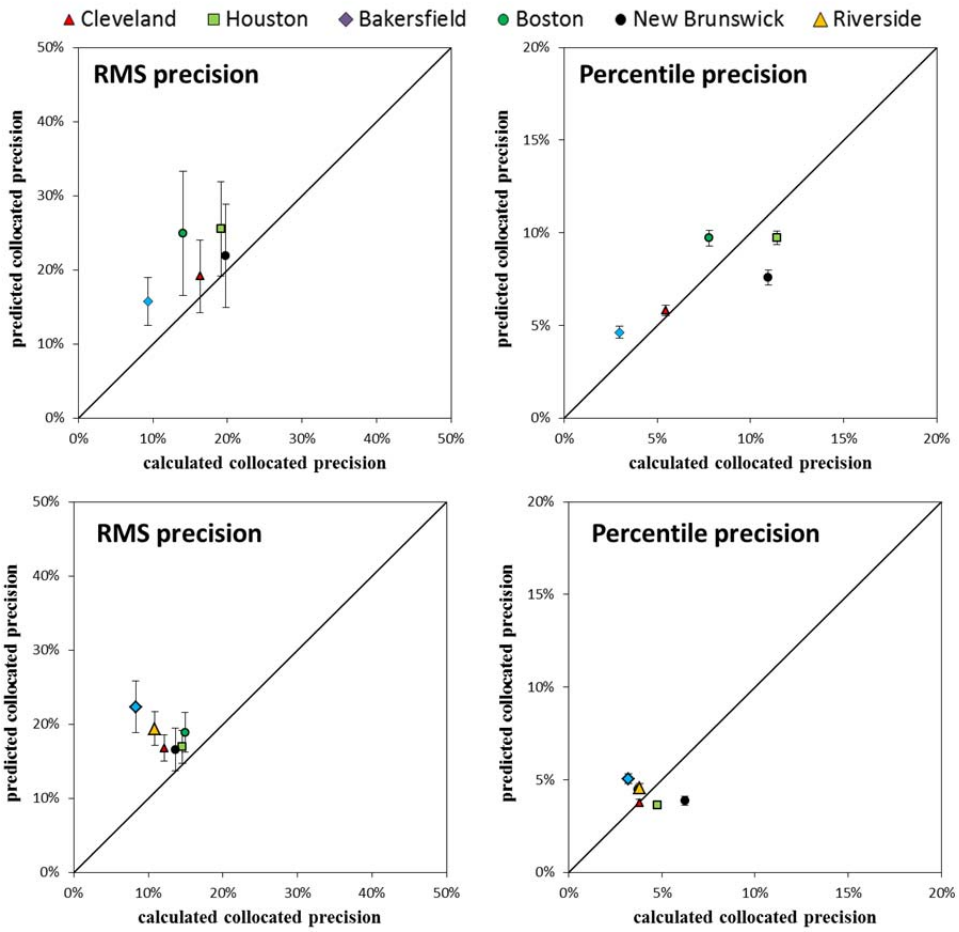

Figure 6-3. Calculated vs. predicted RMS precision and percentile precision for nitrate (top) and sulfate (bottom). Riverside, CA was not included in the nitrate comparison because there were insufficient samples from other sites to match the Riverside concentration distribution.

6.5. Spatial Variability in the Context of Measurement Error – Resolving Small Impacts

While measurement error can be a significant source of variability as demonstrated in the previous sections of this chapter, measurement error also provides a context for assessing spatial variability. Turner (2008) demonstrated that small day-to-day differences in PM sulfate concentrations between two sites in Cleveland (OH) separated by only 1.7 km could not be

explained by measurement error estimated from collocated samples. While on average there was negligible difference in sulfate levels between the sites, the day-to-day variations could be explained by differential impacts from sources that cancelled out when time averaging the data. Nonparametric wind regression was used on the daily differences in sulfate concentration between the sites to identify the emission sources, only one of which was previously identified by source apportionment modeling. In contrast to PM sulfate, PM organic carbon showed much higher day-to-day variability between the two sites but collocated data showed these measurements were much less precise and the observed intersite differences could be explained by measurement error. For species such as sulfate and nitrate that trend towards spatial homogeneity by commonly used metrics (e.g. PCC and COD) in the St. Louis area, measurement error can have significant contributions to the variability that is observed. Characterizing measurement error is crucial to unravelling small contributions from local sources for these species.

Random measurement error may become crucial in the interpretation of spatial varaibility especially for species that are less affected by systematic measurement errors which are often observed as collocated sampler bias. It may confound the conclusion of homogeneity derived by other metrics or approaches. Meanwhile, for species dominated by regional sources, weak signals from local contribuions are superposed on the considerably stronger regional backgound baseline. The day-to-day variations should be brought into the context of random measurement error to reliably identify contributions from local sources.

Figure 6-4 shows the scattergram for sulfate concentrations observed at Arnold and Belleville. The dataset was censored to include only those days with valid data above detection limit at both sites. The regression coefficients were obtained from a reduced major axis regression which

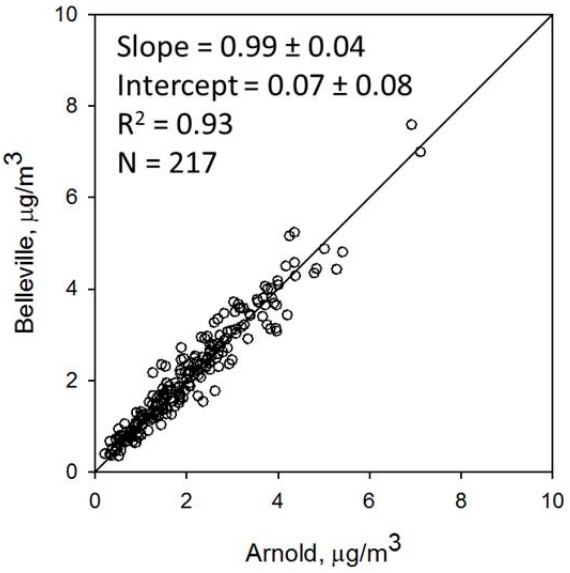

Figure 6-4. Scatter plot for the $PM_{2.5}$ sulfate data collected at Arnold and Belleville from 2010 through 2013. The solid line is the 1:1 relationship. Uncertainties in the regression coefficients are reported as 95% confidence intervals.

takes into consideration that both variables have uncertainty. The top 5th percentiles of the concentration difference distribution (two-way) were trimmed to reduce the impact from extreme values. The regression intercept is statistically indistinguishable from zero and the slope is statistically indistinguishable from unity (95% C.I.). For the time period of interest, the observed sulfate concentration at Arnold is 2.13 ± 1.29 µg/m^3 compared to 2.19 ± 1.27 µg/m^3. Based on these observations, it would be concluded that sulfaute is spatially homogeneous. However, this should not be interpreted as meaning there are no impacts from local sources and random measurement error provides a framework for assessing whether local source impacts can be discerned from these data.

Random measurement error was evaluated using the six site CSN collocated dataset. The collocated dataset was censored to include only those days with valid data above detection limit

at both sites to be consistent with the target dataset. The "binning-sampling" method as described in the previous section was then applied to create new collocated datasets that matched the concentration distribution of the target dataset. The collocated precision was calculated as 4% with standard deviation of 0.5% based on 1000 iterations of random sampling. Figure 6-5 shows the cumulative distribution of the concentration differences scaled to the expected concentration difference calculated from the collocated precision. This analysis approach was motivated by the methodology of White et al. (2005) to compare CSN and IMPROVE network data in the context of in-network precision data. The unit normal variate is calculated using the collocated precision with a mean of zero and a standard deivuation of unity, N(0,1). Cumulative distributions that fall on the unit normal variate line suggest nomally distributed error. The binning-sampling method results in a distribution of precision estimates and this taken into account by: sorting sample pairs by the observed concentration difference for each iteration of the random sampling; and calculating the 5^{th} and 95^{th} percentile at each position along the cumulative distribution. The 5^{th} and 95^{th} percentile cumulative distributions are shown by the closed black circles in Figure 6-5 and form "edges" and a distribution would be expected to fall in the area ("the unit normal variate zone") normal error can be implied for the interior area between these curves. Concentration differences beween sulfate measured at Arnold and Belleville exhibit significant deviation from the unit normal variate zone, suggesing that the day-to-day variations cannot be explained soley by measurement error. This motivates a closer examination of the data to identify local source influences.

Nonparametric wind regression was performed on the sulfate concentration difference distributions to identify local sources that might differentially impact the two sites,. Nonparametric wind regression (NWR) was first introduced by Henry et al. (2002) as a pollution

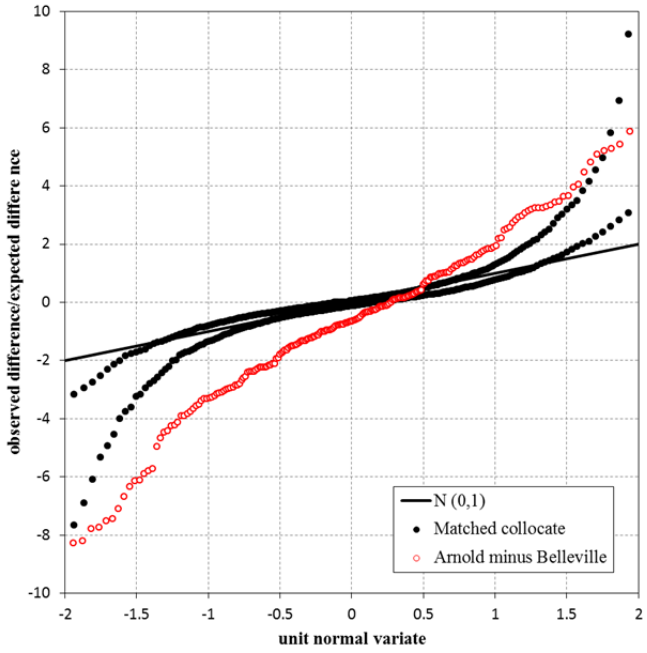

Figure 6-5. Cumulative concentration difference distributions for sulfate: Arnold minus Belleville (red open circles) and matched collocated dataset as described in the text (closed black circles) and. The solid black line is the unit normal variate for 4% precision.

rose which does not require the binning of the pollution data into wind direction sectors. In this study, NWR was conducted using 24-hour integrated concentration data with hourly winds data. Hours with calm winds (operationally defined as wind speeds less than 0.5 m/s) were excluded from the analysis.10m winds data were available for downtown St. Louis (Blair) and Arnold. Confidence intervals were generated by bootstrapping the dataset; no blocking was needed because the 1-in-3 day (Arnold, Blair) and 1-in-6 day (Belleville) concentration values for the parameters of interest were not serially correlated.

Figure 6-6 shows the wind direction dependence of expected concentration for excess sulfate at Arnold derived from NWR. Figure 6-6a corresponds to the concentration difference at Arnold relative to Belleville with positive values indicating excess at Arnold and negative values

indicating excess at Belleville; Figure 6-6b shows the excess concentration for Arnold relative to Blair. Figure 6-7 shows the locations of the five $PM_{2.5}$ speciation sites. Arnold and Belleville are located on opposite sides of the Mississippi River and the shift between positive Arnold excess and positive Belleville excess is at a wind direction of ~170 °N with the other shift occurring at ~10 °N (Figure 6a). In both cases the site downwind of the riverfront shows higher sulfate

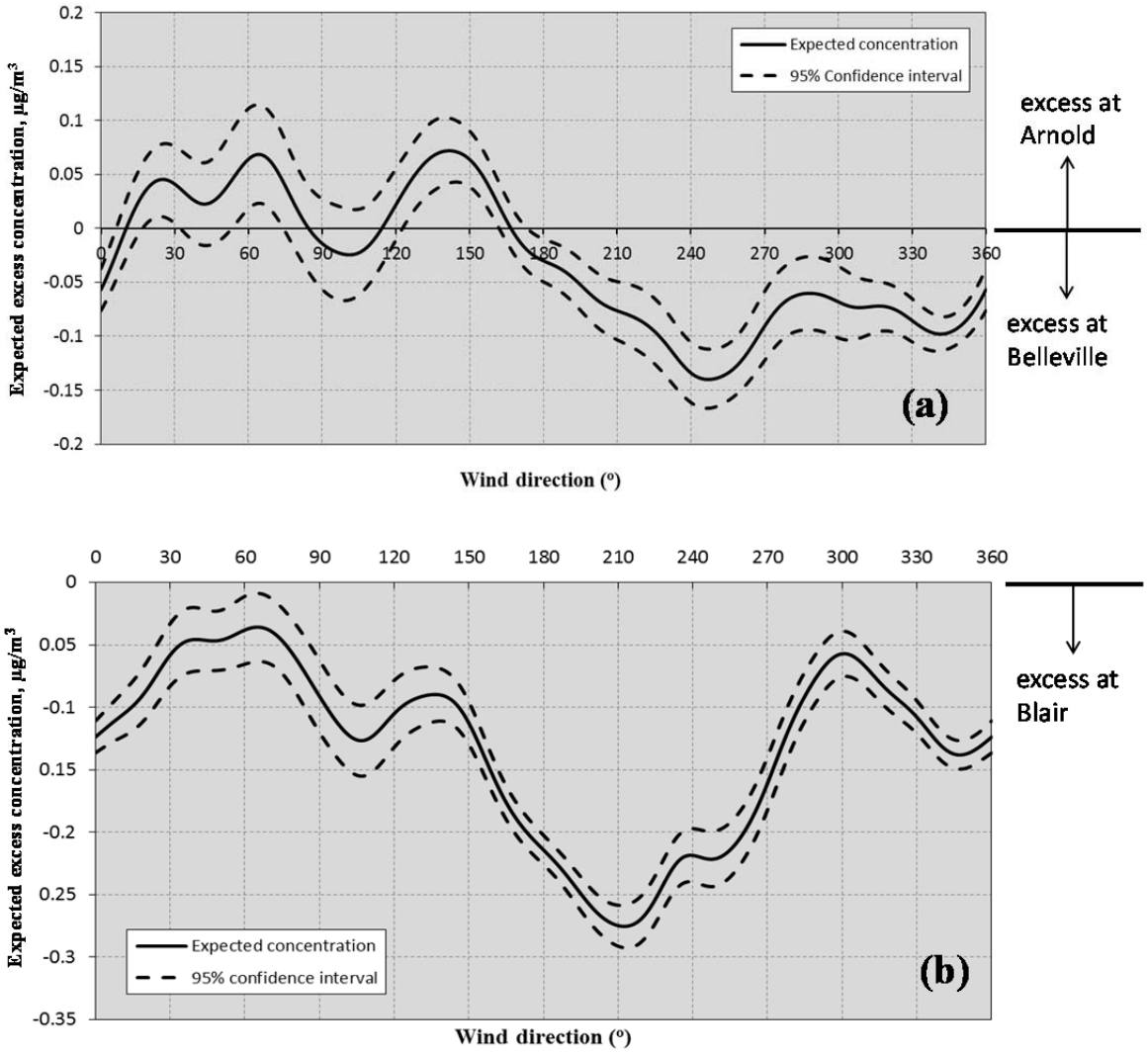

Figure 6-6. Expected concentrations for excess sulfate at Arnold compared to Belleville (a) and Arnold compared to Blair (b) as a function of wind direction. Solid lines are the expected concentrations and dashed lines are 95% confidence intervals calculated from 1000 bootstrap runs.

concentration, suggesting sulfate emissions from industries in the riverfront corridor and/or barge traffic on the river including dock facilities. In this case, a change in wind direction across the north/south line would cause local sources near the riverfront to impact the two sites differentially with the greatest difference occurring in the presence of easterly or westerly winds and minimum difference observed when the winds are from the due south or due north. Figure 6-6(b) shows the excess sulfate concentration at Arnold relative to Blair. All values are negative because the expected sulfate concentration is consistently higher at Blair which may be attributed to industries and other local activities at or near the St. Louis urban core. A peak of excess sulfate at Arnold compared to Blair (albeit still negative) corresponds to wind directions from 270 ^{o}N clockwise to 150 ^{o}N which points back to downtown St. Louis. Overall, the NWR pattern suggests impacts from local sources when a site is downwind of the urban core. While the sources that differentially impact the sites are the same, meteorological conditions such as wind direction varies the influences at each receptor site.

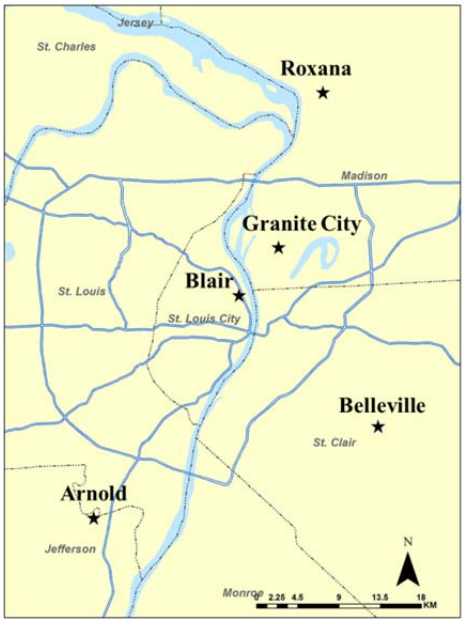

Figure 6-7. Locations of five $PM_{2.5}$ speciation sites in the St. Louis area.

In summary, following upon the work of Turner (2008) this analysis shows another case where two sites have nearly identical average sulfate concentrations but the day-to-day differences cannot be explained by measurement error. There are small but discernable impacts from local sources that cancel out (at least for Arnold vs. Belleville) from day-to-day variations in surface winds.

6.6. Summary

Commonly used metrics such as Pearson correlation coefficient (PCC) were applied to chemical speciation data collected at five $PM_{2.5}$ speciation sites in the St. Louis area. Bootstrapping is an effective tool to explore the sensitivity of PCC to extreme values, and this study demonstrates that efforts should be taken to understand, and possibly censor, the data so the PCC can be properly interpreted depending on the study objectives. Strong temporal similarity was implied by large PCC values for $PM_{2.5}$ mass and species such as sulfate, nitrate, and ammonium, whereas species dominated by local sources such as iron and zinc exhibited weaker correlations.

Measurement error should be considered when interpreting metrics for spatial variability such as the COD. For nitrate, collocated precision has a concentration dependence even for concentrations greater than 3×MDL and thus the use of a single-valued precision derived from data pooled across all collocation sites would be would be inappropriate. A "binning-sampling" approach was developed to harmonize the collocated precision from the six collocated CSN sites to the match concentration distributions for the site pairs of interest. This approach is effective for characterizing measurement error for species that exhibit concentration dependent of precision and are relatively free of bias in the collocated data. More work is needed to examine the applicability of this approach when bias in the collocated data is large.

Measurement error was used as a context to interpret sulfate inter-site differences for two sites in the St. Louis area. While the average concentration difference between the sites was very small, the distribution of sample-specific concentration differences could not be explained by measurement error as estimated using the "binning-sampling" approach. Wind regression analysis indicated the sites experienced differential impacts from local industries and activities located between the sites and variations in wind direction across the dataset caused these impacts to largely cancel out when calculating mean metrics.

The implications of this chapter may apply to all studies focusing on spatial variability. Conventional metrics to gauge spatial variability should be used with caution and exploratory data analysis needs to be conducted to understand the data structure. Measurement error should always be considered and assessed when monitoring datasets are utilized because it artificially contributes to spatial variability and may result in misleading interpretations.

6.7. References

Aschner, M., Erikson, K.M., Dorman, D.C., 2005. Manganese dosimetry: Species differences and implications for neurotoxicity. Crit. Rev. Toxicol. 35, 1-32.

Birch, M.E., Cary, R.A., 1996. Elemental carbon-based method for monitoring occupational exposures to particulate diesel exhaust. Aerosol Science and Technology 25, 221-241.

Burnett, R., Ma, R.J., Jerrett, M., Goldberg, M.S., Cakmak, S., Pope, C.A., Krewski, D., 2001. The spatial association between community air pollution and mortality: A new method of analyzing correlated geographic cohort data. Environmental Health Perspectives 109, 375-380.

Burnett, R.T., Brook, J., Dann, T., Delocla, C., Philips, O., Cakmak, S., Vincent, R., Goldberg, M.S., Krewski, D., 2000. Association between particulate- and gas-phase components of urban air pollution and daily mortality in eight Canadian cities. Inhalation Toxicology 12, 15-39.

Burton, R.M., Suh, H.H., Koutrakis, P., 1996. Spatial variation in particulate concentrations within metropolitan Philadelphia. Environmental Science & Technology 30, 400-407.

Cheung, K., Daher, N., Kam, W., Shafer, M.M., Ning, Z., Schauer, J.J., Sioutas, C., 2011. Spatial and temporal variation of chemical composition and mass closure of ambient coarse

particulate matter (PM10-2.5) in the Los Angeles area. Atmospheric Environment 45, 2651-2662.

Chow, J.C., Watson, J.G., Pritchett, L.C., Pierson, W.R., Frazier, C.A., Purcell, R.G., 1993. The dri thermal/optical reflectance carbon analysis system: description, evaluation and applications in U.S. Air quality studies. Atmospheric Environment Part A, General Topics 27, 1185-1201.

Dockery, D.W., Pope III, C.A., Xu, X., Spengler, J.D., Ware, J.H., Fay, M.E., Ferris Jr, B.G., Speizer, F.E., 1993. An association between air pollution and mortality in six U.S. cities. N. Engl. J. Med. 329, 1753-1759.

Haddad, K., 2015. An assessment of air pollution databases to inform their use in epidemiological studies, Department of Energy, Environmental and Chemical Engineering. Washington University in St. Louis.

Houthuijs, D., Breugelmans, O., Hoek, G., Vaskovi, E., Mihalikova, E., Pastuszka, J.S., Jirik, V., Sachelarescu, S., Lolova, D., Meliefste, K., Uzunova, E., Marinescu, C., Volf, J., de Leeuw, F., van de Wiel, H., Fletcher, T., Lebret, E., Brunekreef, B., 2001. PM10 and PM2.5 concentrations in Central and Eastern Europe: results from the Cesar study. Atmospheric Environment 35, 2757-2771.

Hudda, N., Cheung, K., Moore, K.F., Sioutas, C., 2010. Inter-community variability in total particle number concentrations in the eastern Los Angeles air basin. Atmospheric Chemistry and Physics 10, 11385-11399.

Hyslop, N.P., White, W.H., 2009. Estimating Precision Using Duplicate Measurements. Journal of the Air & Waste Management Association 59, 1032-1039.

Ito, K., Christensen, W.F., Eatough, D.J., Henry, R.C., Kim, E., Laden, F., Lall, R., Larson, T.V., Neas, L., Hopke, P.K., Thurston, G.D., 2006. PM source apportionment and health effects: 2. An investigation of intermethod variability in associations between source-apportioned fine particle mass and daily mortality in Washington, DC. Journal of Exposure Science and Environmental Epidemiology 16, 300-310.

Ito, K., Xue, N., Thurston, G., 2004. Spatial variation of PM 2.5 chemical species and source-apportioned mass concentrations in New York City. Atmospheric Environment 38, 5269-5282.

Lagudu, U.R.K., Raja, S., Hopke, P.K., Chalupa, D.C., Utell, M.J., Casuccio, G., Lersch, T.L., West, R.R., 2011. Heterogeneity of coarse particles in an urban area. Environmental Science and Technology 45, 3288-3296.

Mendoza, A., Pardo, E.I., Gutierrez, A.A., 2010. Chemical characterization and preliminary source contribution of fine particulate matter in the Mexicali/Imperial Valley border area. Journal of the Air and Waste Management Association 60, 258-270.

Moore, K., Krudysz, M., Pakbin, P., Hudda, N., Sioutas, C., 2009. Intra-Community Variability in Total Particle Number Concentrations in the San Pedro Harbor Area (Los Angeles, California). Aerosol Science and Technology 43, 587-603.

Ostro, B., Feng, W.-Y., Broadwin, R., Green, S., Lipsett, M., 2007. The effects of components of fine particulate air pollution on mortality in California: Results from CALFINE. Environmental Health Perspectives 115, 13-19.

Pakbin, P., Hudda, N., Cheung, K.L., Moore, K.F., Sioutas, C., 2010. Spatial and Temporal Variability of Coarse (PM(10-2.5)) Particulate Matter Concentrations in the Los Angeles Area. Aerosol Science and Technology 44, 514-525.

Pinto, J.P., Lefohn, A.S., Shadwick, D.S., 2004. Spatial variability of PM2.5 in urban areas in the United States. Journal of the Air & Waste Management Association 54, 440-449.

Pope III, C.A., Burnett, R.T., Thun, M.J., Calle, E.E., Krewski, D., Ito, K., Thurston, G.D., 2002. Lung cancer, cardiopulmonary mortality, and long-term exposure to fine particulate air pollution. Jama-Journal of the American Medical Association 287, 1132-1141.

Roosli, M., Theis, G., Kunzli, N., Staehelin, J., Mathys, P., Oglesby, L., Camenzind, M., Braun-Fahrlander, C., 2001. Temporal and spatial variation of the chemical composition of PM10 at urban and rural sites in the Basel area, Switzerland. Atmospheric Environment 35, 3701-3713.

Solomon, P.A., Crumpler, D., Flanagan, J.B., Jayanty, R.K., Rickman, E.E., McDade, C.E., 2014. U.S. national PM2.5 Chemical Speciation Monitoring Networks-CSN and IMPROVE: description of networks. Journal of the Air & Waste Management Association (1995) 64, 1410-1438.

Solomon, P.A., Mitchell, W., Tolocka, M., Norris, G.A., Gemmill, D., Wiener, R., Vanderpool, R., Murdoch, R., Natarajan, S., Hardison, E., 2000. Evaluation of $PM_{2.5}$ chemical speciation samplers for use in the EPA National $PM_{2.5}$ Chemical Speciation Network. EPA-454/R-01-005. Office of Air Quality Planning and Standards, US Environmental Protection Agency, Research Triange Park, NC.

Turner, J.R., 2008. Measurement Error as a Context for Assessing Intraurban Variability in Chemical Speciation Network Data. Air & Waste Management Association.

Wade, K.S., Mulholland, J.A., Marmur, A., Russell, A.G., Hartsell, B., Edgerton, E., Klein, M., Waller, L., Peel, J.L., Tolbert, P.E., 2006. Effects of instrument precision and spatial variability on the assessment of the temporal variation of ambient air pollution in Atlanta, Georgia. Journal of the Air & Waste Management Association 56, 876-888.

Wang, G., Hopke, P.K., Turner, J.R., 2011. Using highly time resolved fine particulate compositions to find particle sources in St. Louis, MO. Atmospheric Pollution Research 2, 12.

White, W.H., Hyslop, N.P., McDade, C.E., 2005. Using in-network precision data as a basis for cross-network comparisons. See http://vista.cira.colostate.edu/improve/publications/graylit/027_IMPROVE_STN/WHW-Atlanta-AAAR.ppt (accessed June 2, 2015).

Wilson, W.E., Suh, H.H., 1997. Fine particles and coarse particles: Concentration relationships relevant to epidemiologic studies. Journal of the Air & Waste Management Association 47, 1238-1249.

Wongphatarakul, V., Friedlander, S.K., Pinto, J.P., 1998. A comparative study of PM2.5 ambient aerosol chemical databases. Environmental Science & Technology 32, 3926-3934.

Zanobetti, A., Schwartz, J., Samoli, E., Gryparis, A., Touloumi, G., Peacock, J., Anderson, R.H., Le Tertre, A., Bobros, J., Celko, M., Goren, A., Forsberg, B., Michelozzi, P., Rabczenko, D., Hoyos, S.P., Wichmann, H.E., Katsouyanni, K., 2003. The temporal pattern of respiratory and heart disease mortality in response to air pollution. Environmental Health Perspectives 111, 1188-1193.

Zhu, Y.F., Hinds, W.C., Kim, S., Shen, S., Sioutas, C., 2002. Study of ultrafine particles near a major highway with heavy-duty diesel traffic. Atmospheric Environment 36, 4323-4335.

Chapter 7 : Source Apportionment of $PM_{2.5}$ in the St. Louis Area using Chemical Speciation Datasets

7.1. Introduction

Many epidemiological studies found positive associations between exposure to ambient fine particulate matter ($PM_{2.5}$) and mortality and morbidity (USEPA, 2009), which resulted in the promulgation of a $PM_{2.5}$ National Air Quality Standard (NAAQS) starting from 1997. Ambient PM is a complex mixture of species originating from different emission sources and atmospheric processes. Therefore, a comprehensive understanding of its composition that varies both temporally and spatially could provide enormous insights towards $PM_{2.5}$ air quality management, especially in the areas designated to be in non-attainment of the $PM_{2.5}$ NAAQS. Some early studies indicated composition- and source-oriented health effects of PM (Mar et al., 2000), further suggesting the need of a nationwide $PM_{2.5}$ speciation dataset. In 1999 the US Environmental Protection Agency (EPA) initiated a national chemical speciation program to address these needs. Data collected from the nationwide Chemical Speciation Network (CSN) has been used in numerous air quality and health studies which led to better interpretation and understanding of the sources of $PM_{2.5}$ as well as its health effects, and provided more sophisticated support to the regulatory decision-making by state and local agencies (Hopke et al., 2006; Ito et al., 2006; Ito et al., 2011; Ito et al., 2004; Kim et al., 2003; Thurston et al., 2011).

The greater St. Louis area spans counties and cities in Missouri and Illinois, USA. This area was historically heavily industrialized and was a major transportation hub on the Mississippi River. Local industries included, but were not limited to, steel manufacturing, metal processing, oil refining and coal-fired electric utility power generation over the past several decades. The

clustering of industries as well as a wide range of socio-economic classes made the area an attractive case for both air quality research (Lee et al., 2006; Trijonis et al., 1980) and air pollution health effects studies (Ferris Jr et al., 1979). The greater St. Louis area was designated by the US EPA as a non-attainment area under 1997 $PM_{2.5}$ NAAQS standard; revisions to the NAAQS in 2012 again posed challenges to the air quality administrations.

Positive matrix factorization (PMF) has been applied to many ambient PM datasets and has been shown to be a powerful receptor modeling tool for source apportionment analysis (Kim et al., 2003; Polissar et al., 1998; Wang and Hopke, 2013). Prior source apportionment studies on the St. Louis area data using PMF analyzed $PM_{2.5}$ data from two CSN sites in St. Louis (Blair Street in the City of St. Louis, and Arnold in Jefferson County) and the St. Louis-Midwest Supersite in East St. Louis (Amato and Hopke, 2012; Lee and Hopke, 2006; Lee et al., 2006). The analyses focused on the time period from 2000 to 2003. However, the emission control programs implemented over the past decade have dramatically altered the contributions from both local and regional sources. Data collected at Blair Street and Arnold now spans more than ten years, providing a wonderful opportunity to update the source apportionment analyses performed by prior research. Besides the extended time period available for analysis, three additional monitoring sites which follow the CSN sampling and analytical protocols (hereafter called CSN-protocol sites) are now operational in the St. Louis area. The number of speciation sites is unusually large among cities of comparable size, allowing the exploration of the spatial variability and a more comprehensive interpretation of apportioned sources. Furthermore, a recent update to the EPA PMF program (EPA PMF 5.0) incorporates a suite of advanced statistical methods for analysis of uncertainty estimates which were not included in previous versions of PMF. These tools help users to better understand sources of variability in the results

and to obtain more robust apportionment but to date there is little experience applying these tools and interpreting their results. EPA PMF 5.0 also features easy accessibility to conduct multi-site analysis which was rarely included in prior studies.

In this study, speciation data collected at five sites in the greater St. Louis area were analyzed using PMF to identify emission sources and their contributions to $PM_{2.5}$ concentrations as well as to update the results from prior studies. The option of performing multi-site as opposed to single-site analysis was also explored to elucidate its effects on and implications to the source apportionment results. Nonparametric wind regression coupling surface meteorology data and the PMF analysis results was used to confirm and locate resolved local sources. Uncertainties associated with the analysis were characterized using the tools now available in EPA PMF 5.0 and additional approaches to provide more insight into the results.

7.2. Methods

7.2.1. $PM_{2.5}$ speciation data

$PM_{2.5}$ speciation data were collected at three CSN sites and two CSN-protocol sites in the St. Louis area. The Blair Street site (cited as Blair hereafter) is a CSN site located in the City of St. Louis, MO, and is ~ 3km north of the Central Business District. Interstate Highway I-70 runs along the east side of the site (closest distance of 200m) and several industries are nearby. The original Arnold Street (cited as Arnold hereafter) site was in a suburban residential area in Jefferson County, located about 30 km to the southeast of downtown St. Louis. Because of interferences to the microscale surface meteorology caused by the surrounding topography and obstructions from trees, in 2008 the site was moved 3 km westward to its current location. The Granite City site is located in downtown Granite City Illinois. The site is about 10 km to the

northeast of downtown St. Louis and < 1km from major emission points at the Granit City Steelworks. The three sites described above are CSN sites operated by state agencies while the two CSN-protocol sites are operate by non-governmental organizations. The site in the Village of Roxana, IL (cited as Roxana hereafter) is currently operated by the Turner group at Washington University in St. Louis and is located at the fenceline of the Phillips 66 Wood River Refinery. Details of the sampling and data collection are described elsewhere (Du and Turner, 2015). The other CSN-protocol site is in suburban area of the City of Belleville, IL (cited as Belleville hereafter) and located about 25 km to the southeast of downtown St. Louis. The Belleville site is currently operated by Atmospheric Research and Analysis, Inc. on behalf of the Prairie State Generating Station. In order to provide a baseline to the analysis of sites in the St. Louis area, a background CSN site located in Bonne Terre, MO (cited as Bonne Terre hereafter), about 80 km south of downtown St. Louis, was also included in the analysis. The Bonne Terre site is surrounded by open fields with no major industries and provides insights into the regional background. Figure 7-1 shows locations of the sampling sites and select major industries relevant to the analysis.

24-hour integrated $PM_{2.5}$ samples were collected on Teflon, nylon, and quartz filters every 3 or 6 days and the temporal coverage of the datasets at each site also vary. The sampling specifications of each site are summarized in Table 7-1. Teflon filters were used for gravimetric analysis of mass concentration and for elemental analysis by X-ray fluorescence. Nylon filters were analyzed for water-soluble ions such as sulfate, nitrate, ammonium, potassium, and sodium. Quartz filters collected during earlier time periods were analyzed by the National Institute of Occupational Safety and Health (NIOSH) /Thermal Optical Transmittance protocol (Birch and Cary, 1996) for organic and elemental carbon (OC and EC). Starting from 2007 the CSN adopted

the IMPROVE thermal/optical protocol for the analysis of OC and EC to replace the NIOSH. The transition was also accompanied by the deployment of a modified IMPROVE carbon sampler (i.e. URG 3000N carbon sampler; URG Corp.) instead of using a sampling channel in the conventional speciation sampler. A detailed description of the samplers and analytical protocols for the filters can be found in prior reports and publications (Chow et al., 1993; Solomon et al., 2014; Solomon et al., 2000). The transition in carbon sampling and analysis methods created a discontinuity in the OC and especially EC data time series; thus, the speciation data from each site were divided into two datasets based on the carbon measurement transitions.

Figure 7-1. Locations of the monitoring sites and select relevant facilities. Monitoring sites are represented by stars and facilities are represented by crosses.

Datasets consisting of data from multiple sites were created by matching the time period as well as the sampling events. The sampling frequencies of combined datasets were matched to those of the individual sites with the lowest sampling frequency. For example, 1-in-3 day samples from Blair and Arnold with were filtered to retain only the 1-in-6 day samples when combined with other sites into a multisite dataset. Four multisite datasets were created for this study (Table 7-1).

Table 7-1.Summary of the datasets.

Dataset	Sites	Temporal coverage	Sampling frequency	Type	No. of samples
Single-site datasets					
BL1	Blair	Feb 2000 - Jul 2007	1-in-3 day	urban	804
BL2	Blair	Jul 2007 - Sep 2014	1-in-3 day	urban	802
AR1	Arnold	Apr 2001 - Feb 2009	1-in-3 day	suburban	881
AR2	Arnold	Apr 2009 - Sep 2014	1-in-3 day	suburban	632
GC	Granite City	Oct 2007 - Jul 2012	1-in-6 day	industrial	209
RX	Roxana	Jul 2012 - Nov 2014	1-in-6 day	industrial	121
BV	Belleville	Feb 2010 - Oct 2014	1-in-6 day	suburban	264
BT1	Bonne Terre	Feb 2003 - Jul 2007	1-in-3 day	rural	460
BT2	Bonne Terre	Jul 2007 - Sep 2014	1-in-3 day	rural	632
Multisite datasets					
BLAR1		Apr 2001 - Jul 2007	1-in-3 day	–	1400
	Blair				707
	Arnold				693
BLAR2		Apr 2009 - Sep 2014	1-in-3 day	–	1257
	Blair				625
	Arnold				632
MULT1		Feb 2010 - Jul 2012	1-in-6 day	–	523
	Blair				139
	Arnold				141
	Belleville				144
	Granite City				99
MULT2		Jul 2012 - Sep 2014	1-in-6 day	–	491
	Blair				121
	Arnold				127
	Belleville				122
	Roxana				121

Samples for which $PM_{2.5}$ mass concentration or one or more species concentrations were not available were excluded from the analysis. Samples collected on July 4 and proximate days (± 3 d) were also excluded from the analysis because the July 4th fireworks featuring high potassium and carbon content can significantly distort the biomass burning factor. Species with data above MDLs for less than 50% of samples were excluded from the analysis.

Sample-specific method detection limit (MDL) and uncertainty values are reported for $PM_{2.5}$ mass concentration, ions, elements and NIOSH carbon species. However, MDL and uncertainties for carbon species analyzed after the transition to IMPROVE protocol are currently not available. Because of the similarity in sampler configurations and analytical protocols to the IMPROVE networks MDL values for the IMPROVE network carbon fractions were adopted. Carbon data from the six collocated sites in IMPROVE network were used to generate concentration-dependent uncertainty estimates for carbon species. The data were not blank-corrected.

7.2.2. Positive matrix factorization

Positive matrix factorization framework

Positive matrix factorization (PMF) is a multivariate factor analysis tool that is widely used to identify emission sources and quantify their contributions. The goal of the model is to decompose the matrix of sample data into two matrices: factor profiles (F) and factor contributions (G). Users need to interpret the factor profiles to identify the types of emission sources and/or atmospheric processes they represent, typically using tracer species information and emission inventories. The theoretical basis of the method is described in greater detail elsewhere (Paatero, 1997; Paatero and Tapper, 1994). For ambient PM speciation data, the model decomposes the data matrix into a source profile (F matrix) containing the species composition

profile for each source and a contribution profile (G matrix) indicating the amount of mass contributed by each source to each sample. Non-negative constraints are imposed by the model so that there are no negative species concentrations in any of the source profiles and no source contributions that are significantly negative. In PMF, each sample concentration is individually weighted by its uncertainty which provide users the flexibility to adjust the weight of each data point and potentially minimize the influence of extreme values to the model. The model searches for a solution by minimizing the sum of the square of the uncertainty-weighted residual between modeled and observed data from each sample.

In this study, the optimal number of factors for a given dataset was selected based on several criteria. The number of factors was systematically varied and the modeling output was inspected for goodness of fit between the modeled and measured species concentrations, distribution of source contribution estimates in G-space scatter plots, distribution of residuals, and interpretability of the factors based on tracer species loadings. Uncertainty matrix perturbation and uncertainty estimation tools incorporated by EPA PMF 5.0 were also used to support the selection of number of factors.

Handling and selection of input data

Previous source apportionment analyses normally conditioned the datasets by imputing concentrations below MDL with half of the MDL values and setting their uncertainties to 5/6 of the MDL (Buzcu et al., 2003; Kim and Hopke, 2007; Kim et al., 2003; Wang and Hopke, 2013). However, Brown et al. (2015) recently suggested no proven advantages to this substitution practice but possible disadvantages such as introducing biases. Thus, in this study the analysis was performed by retaining all the reported concentration (including zero) values and uncertainty

values. However, additional source apportionment analyses were also performed as sensitivity studies following the conventional practice described above to condition the datasets.

A revised calculation of signal-to-noise ratio (S/N) is implemented in EPA PMF 5.0 which is different from the conventional definition applied in prior studies (Lee and Hopke, 2006). The new S/N calculation takes into account the difference between concentration and uncertainty values and uses it as the signal, down-weighting the influence from negative and extreme values. The detailed calculation is given by Norris et al. (2014). In this study, species with S/N values larger than 2.0 were assigned as "strong" variables and species with S/N larger than 0.5 but smaller than 2.0 were assigned as "weak" variables. "Bad" variables were species with S/N values less than 0.5 and were excluded from the analysis. $PM_{2.5}$ mass was always selected as the "total variable" and given extra uncertainty. In addition, an extra 10% overall modeling uncertainty was added to account for the temporal variation of the source profiles. More details are provided in the Supplementary Materials.

Uncertainty estimates for the modeling results

EPA PMF 5.0 incorporated displacement analysis (DISP) and bootstrapping enhanced with displacement (BS-DISP) for the estimation of variability in PMF solutions based on the discussion by Paatero et al. (2014). The classical bootstrapping (BS) method and the two additional methods focus on uncertainties arising from different sources and are therefore complementary to each other. BS analysis characterizes the effects from random errors introduced in the measurement process and part of the effects from rotational ambiguity arising from rotationally non-unique solutions to the model. DISP analysis provides information on the rotational ambiguity of the solutions but not on the random error. BS-DISP as a combination of the BS and DISP methods; it is less sensitive to inaccuracies in data uncertainties and is believed

to be more robust than DISP results. Key output parameters from these three methods were used in this study to obtain a deeper insight of the uncertainty of source apportionment results. 100 bootstrap runs were made for each dataset and a minimum correlation of 0.8 for mapping factors generated by bootstrap runs (BS and BS-DISP) were used.

Christensen et al. (2008) proposed perturbing the species uncertainty matrix as a tool for evaluating the stability of PMF solutions. This approach might complement the variability estimation methods provided by EPA PMF v5.0 especially towards identifying the optimal number of factors. This approach perturbs the uncertainty matrices by inserting noise based on a lognormal distribution while keeping the original concentration matrices. The distributions of source contributions from perturbed datasets and the similarity between the solutions generated by perturbed datasets compared to the original datasets reflects the stability of the analysis. In this study, we explored this approach using the St. Louis datasets as a complement to the error estimation approaches provided by the PMF program. For each dataset runs were made using ten perturbed uncertainty matrices.

Nonparametric wind regression (NWR)

Nonparametric wind regression (NWR) was first introduced by Henry et al. (2002) as a pollution rose which does not require the binning of the pollution data into wind direction sectors. NWR uses a Gaussian kernel and a user-defined smoothing parameter to generate a smooth and continuous curve for the expected concentration as a function of the wind direction. Hourly wind data and hourly concentration data are normally applied together for the analysis. When applied with 24-hour integrated concentration data, each hour is equally assigned as the daily concentration value. The potential smearing effect caused by using 24-hour integrated data has been discussed and in general good agreement with the conditional probability function (CPF)

method to locate the bearings of the emission sources has been observed (Kim and Hopke, 2004).

In this study, NWR was conducted using source contribution estimates (SCE) derived from 24-hour integrated concentration data from CSN in conjunction with hourly winds data. Hours with calm winds (operationally defined as wind speeds less than 0.5 m/s) were excluded from the analysis. 10m winds data were available for Blair, Arnold and Roxana. Because of the proximity and geographical similarity, Blair winds were used for Granite City and Arnold winds were used for Belleville and Bonne Terre sites. However, variability has been observed for wind patterns at different locations which may cause mild shifts in the NWR profiles. For example, the channeling effect caused by the Mississippi River results in higher frequency of north-south winds for sites located in or close to the Mississippi River valley. Thus, NWR patterns should be interpreted with caution. Confidence intervals on the SCEs were generated as 1σ of the expected concentrations; no blocking was needed because the 1-in-6 and 1-in-3 day concentration values for the parameters of interest were not serially correlated.

7.3. Results and Discussion

7.3.1. Source apportionment using single-site datasets

The source apportionment analyses resulted in five to eight factor solutions deemed to be optimal at the six sites using unconditioned datasets. Runs using different FPEAK values were conducted for these solutions to evaluate and confirm and evaluate the uniqueness of the solutions. Figure 7-2 and Figure 7-3 show the sources profiles identified at Blair, Arnold and Bonne Terre for the pre- and post- carbon methods transition, respectively. Because these three sites are representative of urban, suburban and rural environments, presenting the source profiles together

enables better comparison among the source contributions, especially for the sources identified to be regional. Table 7-2 summarizes the identified sources and their average contributions to $PM_{2.5}$ SCEs for each of the six sites. Results for source apportionment analysis using Belleville, Granite City, and Roxana datasets are shown in Figures 7-9 to 7-11, respectively.

The secondary sulfate factor was characterized by high loadings of sulfate and ammonium ions at all six sites. This factor is one of the major contributors to $PM_{2.5}$ mass and accounts for 34 ~ 42% of $PM_{2.5}$ mass concentration. The time series (Figures 7-12, through 7-14) of this secondary sulfate factor at all sites exhibits a seasonal pattern with summer maximum when photochemical conversion of SO_2 from primary emissions is enhanced. Figure 7-2 and Figure 7-3 show that sulfate factor contributions from urban, suburban and rural environments are in good agreement which suggests at most small impact from local activities. General agreement of sulfate factor SCEs at the three Illinois sites was also observed and suggests spatial homogeneity across the St. Louis area. Lee and Hopke (2006) attributed the dominant source of the secondary sulfate in the St. Louis area to regional transport from Ohio River Valley which has a high density of coal-fired power plants; Appendix B includes analyses supporting this attribution. The secondary nitrate factor was identified by high loadings of nitrate and ammonium ions. A seasonal pattern with winter/spring maximum was observed because of the low temperature and high humidity which enhances the gas-to-particle conversion of ammonium nitrate. Modestly higher SCEs were observed at the downtown (Blair) site was observed and can be attributed to nitrogen oxides from local traffic. The Upper Midwest/Central Plains was identified as the dominant source region in a previous study using air mass back trajectory based tools (Lee and Hopke, 2006); again, analyses in Appendix B support the attribution.

A biomass burning factor was resolved at all sites expect Granite City. K and high loadings of OC and EC are usually tracers for this source type. This factor accounts for 20 to 40% of the total $PM_{2.5}$ mass concentration. However, this biomass burning factor is not be well-defined in many datasets with some species such as sulfate, nitrate and ammonium as well as inorganic elements loading onto this factor. The association of carbon species and sulfate and nitrate could be the result of gas-to-particle condensation since both sulfate and nitrate are regional contributors to $PM_{2.5}$. Many inorganic elements were present in ambient PM at trace levels which often resulted in the assignment as "weak" species. With the extra uncertainty applied to these species, they are more poorly fitted to factors. Therefore, these elements were either smeared across multiple factors or grouped into a few regional factors. High loadings of many inorganic elements onto the biomass burning factors at Bonne Terre compared to Blair and Arnold shown in Figure 7-2 and Figure 7-3 are good illustrations. At some sites, traffic related sources were not resolved by PMF, possible resulting in smearing of OC and EC and overestimation of biomass burning contributions. Secondary OC was not resolved as a unique source and likely loads strongly onto the biomass burning factor. At all five sites, there were no significant temporal patterns and occasional spikes were observed, indicating minor local contributions on top of a regional background. A biomass burning factor was not identified at Granite City (resolved profiles shown in Figure 7-10). A factor with over 50% of the OC and over 65% of the EC was resolved whereas K largely smeared across all six factors. Steelmaking emissions exert high influence at Granite City and might interfere with the resolution of other factors.

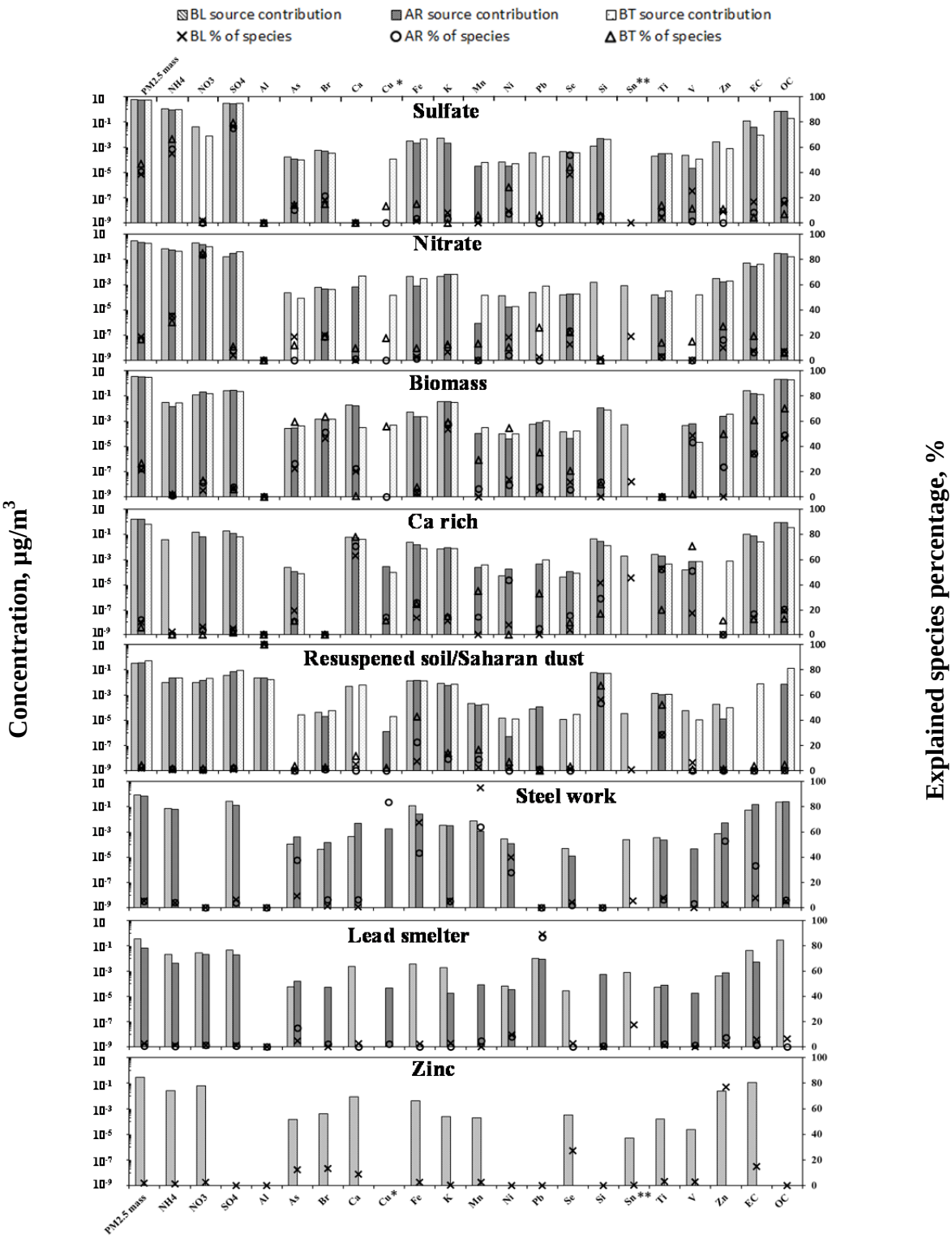

Figure 7-2. Source profiles identified at Blair, Arnold and Bonne Terre using BL1, AR1 and BT1. The steel factor and lead smelter factor were not resolved at Bonne Terre; the zinc factor was not resolved at Arnold and Bonne Terre. *Cu is modeled only for AR2 and BT2; **Sn is modeled only for BT2.

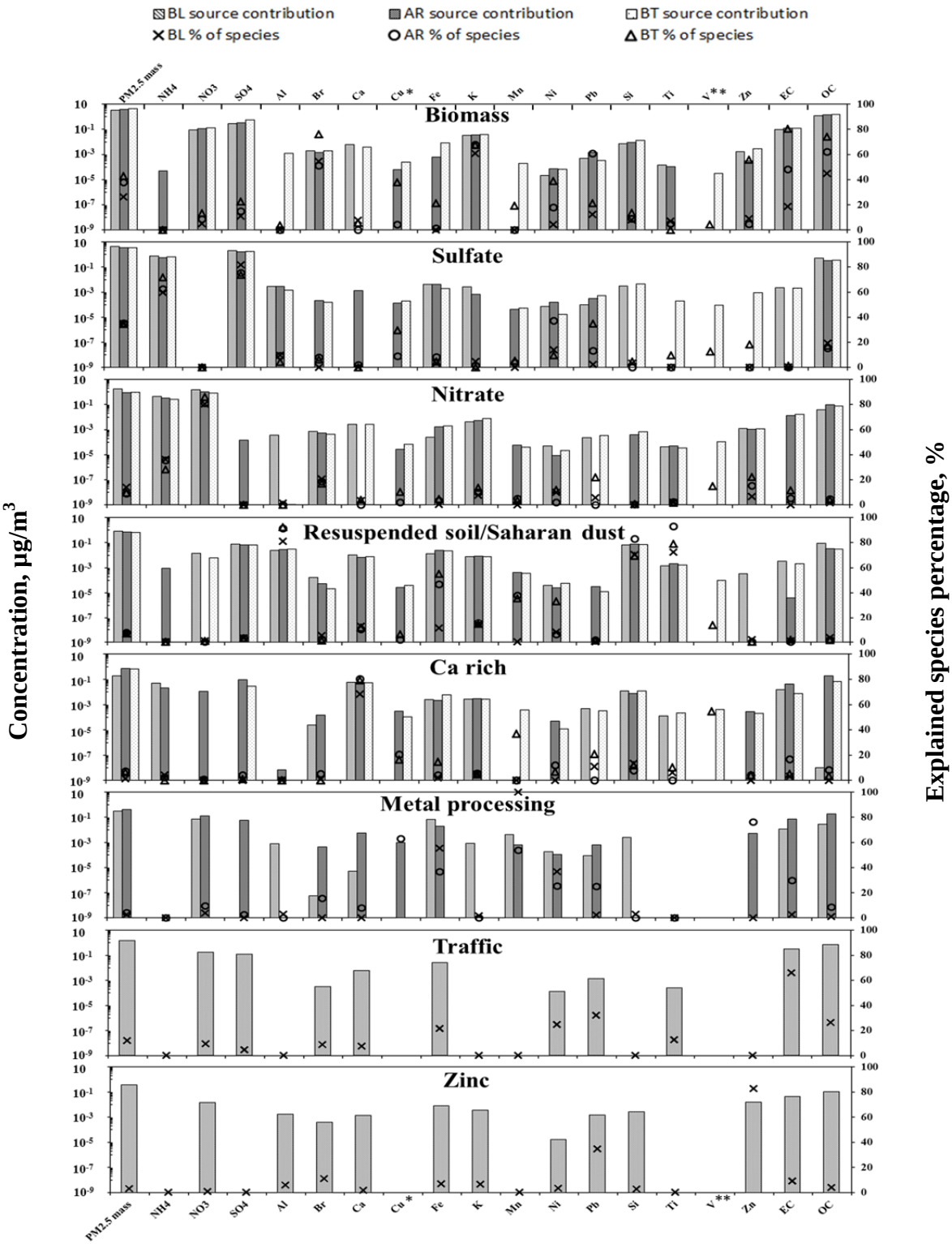

Figure 7-3. Source profiles identified at Blair, Arnold and Bonne Terre using BL2, AR2 and BT2. The traffic factor and the zinc factor were not resolved at Arnold and Bonne Terre. *Cu is modeled only for AR2 and BT2; **V is modeled only for BT2.

Table 7-2. Average source contribution estimates (SCEs) to $PM_{2.5}$ mass concentration. Values in parentheses represent the percentage of $PM_{2.5}$ mass explained by each factor.

Blair Street			
BL1 (2000 – 2007)		**BL2 (2007 – 2014)**	
Secondary sulfate	6.0 (39)	Secondary sulfate	4.3 (35)
Secondary nitrate	2.9 (19)	Secondary nitrate	1.7 (14)
Biomass burning	3.3 (21)	Biomass burning	3.2 (26)
Resuspended soil + Saharan dust	0.3 (2)	Resuspended soil + Saharan dust	0.8 (6)
Ca-rich	1.5 (10)	Ca-rich	0.2 (1)
Metals processing	0.8 (5)	Metals processing	0.3 (2)
Zinc smelting	0.2 (2)	Zinc smelting	0.4 (3)
Pb	0.4 (2)	Traffic	1.5 (12)
Arnold			
AR1 (2001 – 2009)		**AR2 (2009 – 2014)**	
Secondary sulfate	5.5 (41)	Secondary sulfate	3.4 (35)
Secondary nitrate	2.2 (17)	Secondary nitrate	0.9 (9)
Biomass burning	3.1 (23)	Biomass burning	3.7 (38)
Resuspended soil + Saharan dust	0.3 (3)	Resuspended soil + Saharan dust	0.7 (7)
Ca-rich	1.6 (12)	Ca-rich	0.7 (7)
Metals processing	0.7 (5)	Metals processing	0.4 (4)
Bonne Terre			
BT1 (2003 – 2007)		**BT2 (2007 – 2014)**	
Secondary sulfate	5.3 (47)	Secondary sulfate	3.4 (34)
Secondary nitrate	1.9 (17)	Secondary nitrate	1.0 (10)
Biomass burning + Mixed sources	3.0 (26)	Biomass burning + Mixed sources	4.2 (43)
Resuspended soil	0.5 (4)	Resuspended soil	0.7 (7)
Ca-rich	0.6 (6)	Ca-rich	0.6 (7)
Granite City (GC)			
Secondary sulfate	4.3 (34)		
Secondary nitrate	1.6 (12)		
Resuspended soil	2.3 (18)		
Metals #1	1.0 (8)		
Metals #2	0.8 (6)		
Carbon	2.8 (22)		
Belleville (BV)			
Secondary sulfate	5.0 (42)		
Secondary nitrate	1.0 (8)		
Biomass burning	2.8 (22)		
Resuspended soil	1.0 (8)		
Ca-rich	1.1 (9)		
metals	1.3 (10)		
Roxana (RX)			
Secondary sulfate	3.9 (37)		
Secondary nitrate	2.4 (23)		
Biomass burning	1.8 (17)		
Metal processing	1.0 (10)		
Resuspended soil	0.9 (9)		
Ca-rich	0.3 (3)		
Brass manufacturing	0.1 (1)		

An airborne soil factor was characterized by the presence of Al, Si and Fe. Ti was often excluded from PMF modeling because of its low S/N ratio; otherwise it was associated with this factor as well. The time series of this factor at Blair, Arnold and Bonne Terre (shown in Figure 7-12, 7-13 and 7-14) displays a seasonal pattern with summer maximum which is consistent with increased soil dryness. This airborne soil factor in St. Louis during the summertime is significantly influenced by long-range transport of Saharan dust from Africa. The occasional spikes in the source contributions time series agree with these events. For example, at the rural site Bonne Terre the average observed Si/Fe ratios on days when soil contributions rank in the top 5% is 3.31 which is similar to the ratios (3.25 – 4.53) observed by Perry et al. (1997) in Eastern US and Virgin Islands during Saharan dust events. In addition, ratios between Al, Si, Fe and Ca on these days are within or similar to the ranges reported in the aforementioned study. At Blair Street, Arnold and Bonne Terre, there are 27 days on which $PM_{2.5}$ mass concentration apportioned to the soil factor at all three sites are in the top 5% of the respective time series. Back trajectory analysis suggests that on those days the air masses predominantly came from the south/gulf area which is consistent with the typical path for inter-continental transport of Saharan dust.

In some source apportionment studies, Ca was also used as a chemical tracer for road dust and resuspended soil (Lee et al., 2006; Pancras et al., 2013). However, in this study Ca was separately resolved by the model and a "Ca-rich" factor with 70 to 80% of the total Ca load was identified at five of the six sites with Granite City again as the exception. Previous source apportionment studies focusing on the St. Louis area identified a Ca-rich factor at the Arnold site using CSN data from 2001 to 2003 and concluded that this factor may result from the local activities such as a cement kiln, quarries and a pigment factory (Amato and Hopke, 2012; Lee and Hopke, 2006). In this study, however, a Ca-rich factor was resolved at multiple sites

including the rural site which is about 100 km outside the urban core which suggests that this factor is likely not driven by one or more point sources. Instead, it may serve as the evidence of a regional scale source or a regional scale behavior common to all of the sites. Nonparametric wind regression analysis for this factor at multiple sites is shown in Figure 7-13. The results did not display patterns that are distinguishable and consistently indicative of point sources. One possible explanation to the ubiquitous Ca-rich factor is the prevalence Karst topography throughout the St. Louis area. Karst is rich in limestone which is a sedimentary rock primarily in the form of calcium carbonate. Particles from limestone attrition can be resuspended under certain physical conditions such as dryness and high winds. However, based on the limited evidence it is difficult to draw any definitive conclusion regarding the origin of this source. It is notable that a Ca-rich factor was not identified at Granite City site. Instead, the majority of Ca merged into the resuspended soil factor which might be influenced by slag piles from the steelworks. In addition, PMF might differently apportion species as well as $PM_{2.5}$ mass to Ca rich and soil factors in different datasets. For example, discontinuities in the SCE time series for the Ca rich factor at Blair Street (Figure 7-12) and Arnold (Figure 7-13) correspond to the change of carbon analytical protocols and are attributed to the discrepancies of loadings of other elements onto this factor. The Ca rich factor resolved using dataset BL1 and AR1 resembles the soil factor because it has higher loadings of Ti, Si and carbon species.

A factor characterized by metals such as Cu, Fe, Mn and Zn was identified at Blair, Arnold and Belleville. The Granite City Steelworks might be one of the major contributors to this factor although source-receptor distances to Arnold and Belleville are relatively large. Meanwhile, other metal manufacturing industries such as Cerro Copper Products and Big River Zinc Corporation were quite active during the earlier time period. At Blair NWR analysis (shown in

Figure 7-14) suggests contributions from metal processing industries to the east and possible local activities to the west of the site. Contributions from the east were an artifact from a small fabrication shop 50m from the site. This facility caused microscale influences prior to its shutdown in 2006. The zinc smelter and copper production industries were shut down in 2006 and 2003, which is consistent with the decrease in metals processing SCEs between the two time periods that were modeled. The metal processing factors that appeared at both Arnold and Belleville are most likely admixtures of metal processing and possibly other activities in the urban core when the sites were downwind since Zn, Cu, Fe and Mn were all included in the metal processing factor. The large spatial variability in SECs for this factor could possibly be explained by other non-metal species loading on this factor. An example would be Belleville where a large fraction (~40%) of the EC loads onto the metal processing factor.

A Zn factor was identified at Blair for both modeled time periods. NWR analysis indicated that the observed Zn at Blair is primarily attributed to the emissions from the Granite City steel mill to the northeast and Big River Zinc Corporation to the southeast. The NWR profile (shown in Supplementary Material Figure 7-15) has only a northeasterly feature during 2007 to 2014 which is after the zinc production facility had shut down. The NWR plots for lead factor identified at Arnold before 2009 points to the south, suggesting the lead smelter in Herculaneum, MO as a major contributor. Emissions from this smelter were reduced by more than six-fold from year 2000 to 2003 based on the data provided by the EPA Toxics Release Inventory (TRI). As a potential result of the lower emissions, a lead factor could not be resolved for the 2009 – 2014 dataset. A lead factor was also identified at Blair during 2000 – 2007. Because of the distance between the lead smelter and the receptor site, the NWR plot has a less distinctive southerly pattern but is in general agreement with the lead smelter location.

A traffic factor was resolved by PMF for the most contemporary data at Blair site with about 70% of EC and 25% of OC included in its profile. The contribution from this traffic factor is estimated to be 12% of the average $PM_{2.5}$ mass concentration. Figure 7-4 shows the daily SCEs and observed EC concentrations distributed by day of week. The SCEs exhibit a weekly pattern with low levels on weekends compared to weekdays and is consistent with the EC pattern which serves as a tracer species for motor vehicle emissions.

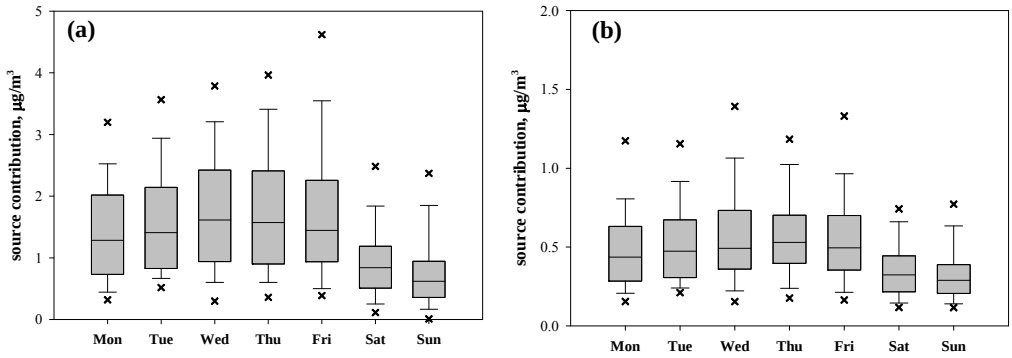

Figure 7-4. Weekly pattern of the (a) SCE of the traffic related factor and (b) observed EC. The upper and lower edges of the boxes indicate the 75th percentile and 25th percentile of the distribution. The whiskers represent 90th and 10th percentile and the crosses are 95th and 5th percentiles of the distribution. Medians are shown as a solid line in the boxes.

Wind regression profiles are shown in Figure 7-5 for the traffic related factor SCEs at Blair. High expected contributions are for winds from the southwest (~100^{o} N) where a scrap metal recycling facility is located in Figure 7-1. The similar patterns for weekdays and weekends imply an emission source that is operated each day of week. The difference between the expected concentrations on weekdays versus weekends (Figure 7-5b) shows relatively low directional variation, suggesting the contributions from local traffic on weekdays. In addition, the larger excess during weekdays for the northeast through southwest direction agrees well with bearings

of the interstate highway I-70 to the east of the Blair site. The weight of evidence indicates that this factor is an admixture of a local point and on top of traffic related.

At Granite City two metal processing factors were resolved (Figure 7-10). One of the features is primarily characterized by Fe, Cu and Co (Metals #1). The other metal processing factor has high loadings of Mn and Zn (Metals #2). NWR plots for both factors (shown in Figure 7-16) point to the south of the site which is consistent with the footprint of the Granite City steelworks.

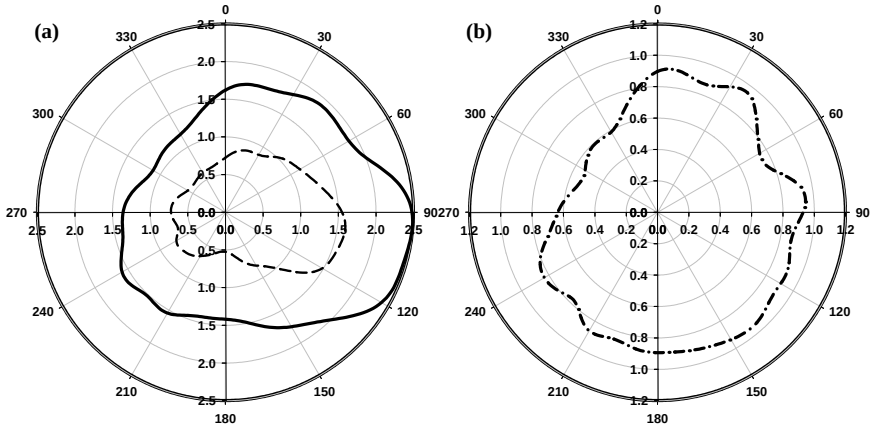

Figure 7-5. Nonparametric wind regression profiles for (a) traffic factor at Blair on weekdays (solid line) and weekends (dashed lines) and (b) difference of the expected concentrations between weekdays and weekends (dotted dashed line). Radial axes units are $\mu g/m^3$.

The high expected concentration with a wide confidence interval shown around 0°N in the NWR plot for Metal #2 is attributed to a small number of exceptional episodes and cannot be explained. Taiwo et al (2014) considered Fe as marker for blast furnace (BF) emissions and Zn as a tracer element for basic oxygen furnace (BOF) emissions in a source apportionment analysis using data collected at multiple sites in the vicinity of a steelworks. However, the two identified metal factors in this study show different profiles compared to prior source apportionment and

source characterization studies. In this work, Metals #1 bearings are broadly consistent with the BOF and finishing operations whereas Metals #2 bearings are consistent with the BOF location.

In summary, source apportionment analysis using single-site datasets demonstrate that $PM_{2.5}$ in the St. Louis area is dominated by regional sources including secondary sulfate and secondary nitrate with generally consistent source contribution estimates across the sites when modeling similar time periods. A Ca factor was resolved and served as evidence of a regional scale source (or a source having regional characteristics) instead of contributions from one or more point sources which was inferred in previous studies. Local point sources exhibit different impacts across the five sites depending on source-receptor separation. A traffic factor was resolved only at the downtown St. Louis site with a strong weekday-weekend pattern. Several subtle features to the modeling results were noted that are consistent with known changes in local emissions over time.

7.3.2. Source apportionment using multi-site datasets

There have been an increasing number of source apportionment studies using datasets comprised of multiple receptor sites in order to enhance the robustness of the analysis by increasing the size of the dataset as well as to characterize sources at a regional scale (Escrig et al., 2009; Minguillón et al., 2012; Mooibroek et al., 2011; Xie et al., 2012). However, the effect of pooling data from multiple receptor sites on the identification of sources by PMF has been less studied. Tian et al. (2014) used synthetic datasets and concluded that the PMF analyses using single-site and multi-site datasets agreed well for regional sources with relatively homogeneous profiles but might be sensitive to the spatial variability of source profiles. Xie et al. (2012) compared PMF solutions for a pooled dataset and those for its component single site datasets using speciated carbonaceous aerosol data. Factor contributions derived from single-site datasets and from the

pooled dataset were highly correlated and supported the assumption of homogeneity of source types across the region of interest. However, this comparison enforced identical numbers of factors to both scenarios. Independent evaluations using observed multi-site air quality datasets have yet to be thoroughly conducted.

In this study site-specific datasets with overlaps in time coverage were pooled to generate several multisite datasets. Each pooled dataset was modeled as an independent dataset without inferring the same number of factors that were resolved for the component single sites. Table 7-3 shows the solutions to the four pooled datasets and their contributions to $PM_{2.5}$ mass.

Table 7-3. Sources and their contributions identified from pooled datasets. Values in parentheses indicate percentage of $PM_{2.5}$ mass explained.

Blair Street + Arnold			
BLAR1 (2001 – 2007)		**BLAR2 (2009 – 2014)**	
Secondary sulfate	6.0 (41)	Secondary sulfate	3.4 (33)
Secondary nitrate	2.2 (15)	Secondary nitrate	1.1 (11)
Biomass burning	3.5 (24)	Biomass burning	2.4 (23)
Resuspended soil + Saharan dust	0.3 (2)	Resuspended soil + Saharan dust	0.7 (6)
Ca-rich	1.3 (9)	Ca-rich	0.4 (3.5)
Metals processing	0.5 (4)	Metals processing	0.2 (1.9)
Zinc smeltering	0.7 (5)	Zinc	0.3 (2)
Pb	0.2 (1)	Traffic	2.1 (19)

Blair Street + Arnold + Belleville + Granite City	
MULT1 (2010 – 2012)	
Secondary sulfate	3.9 (33)
Secondary nitrate	1.3 (11)
Biomass burning	3.6 (30)
Resuspended soil + Saharan dust	0.7 (6)
Ca-rich	0.2 (2)
Metals processing	0.5 (4)
Zinc rich	0.2 (1)

Blair Street + Arnold + Belleville + Roxana	
MULT2 (2012 – 2014)	
Secondary sulfate	3.2 (33)
Secondary nitrate	1.2 (12)
Biomass burning	1.3 (13)
Resuspended soil	0.9 (9)
Ca-rich	0.3 (3)
Metal processing	0.2 (2)
Zinc rich	0.1 (1)
Traffic	2.6 (26)

Source apportionment studies using pooled datasets assume homogeneity among profiles a given source category and allow spatial heterogeneity in the contributions for these sources. This source profile homogeneity assumption might lead to biased results in areas where local sources within a given source category differentially impacts different sites. Two metal processing factors characterized by Fe/Cu and Mn/Zn respectively were identified at Granite City using the site-specific dataset, whereas multisite datasets including Blair, Arnold, Belleville and Granite City sites identified one metal processing factor on which larger percentages of Cu (44%), Fe (72%) and Mn (66%) were loaded. A zinc-rich factor explaining 78% of the observed Zn also appeared in the solution to the multisite dataset. It is very likely that the covariance of Mn and Zn which defines the metal processing factor (Metals#2 shown in Figure 7-10) becomes confounded by pooling data from three other sites which are not influenced by the steelworks or are at source –receptor distances that blend together the two steelworks factors. Using factors resolved from the multisite analysis could potentially distort the interpretation of the sources at Granite City.

Meanwhile, there do appear to be some advantages to pooling data across sites. As shown in Table 7-2 and Figure 7-3, traffic-related factors characterized by high EC were not resolved at Arnold during 2009 - 2014 using the single-site dataset. However, they do appear in the solutions for the Blair-Arnold multisite analyses. The observed weekly pattern at Arnold (shown in Figure 7-6) with weekend minima is attributed to traffic related emissions. As a suburban site, traffic contributions were smaller than at Blair. It is possible that the small contribution of local traffic at Arnold did not provide sufficient “covariance” for PMF to resolve a well-defined factor and tracer species such as EC and OC were smeared across other factors. When the single-site dataset was combined with Blair where traffic related source contributions are significant, the data from

Blair assisted in detecting the covariance and resolving a traffic-related factor in this pooled dataset.

It is also notable that multisite PMF analysis may result in source contribution estimates that disagree with those from single site analysis even when both cases were able to resolve the same set of factors. The Blair Street was selected to demonstrate the effect of pooling data from multiple sites in the study area because identical sources were resolved for the four multisite datasets and corresponding single-site dataset with the same temporal coverage. This provides an ideal case for the comparison (Figure 7-7).

PMF modeling was conducted on four pooled datasets: BLAR1, BLAR2, MULT1 and MULT2. Modeling was also performed using only the Blair samples included in each of the above four multisite datasets. Table 7-3 shows results as well as the number of samples used in each of the cases. To assess the effect of pooling data from multiple sites, two metrics were used: Pearson correlation coefficient and relative average absolute error (RAAE). RAAE is defined as:

$$\text{RAAE} = \frac{\frac{1}{n}\sum_{i=1}^{n}|M_i - S_i|}{\frac{1}{n}\sum_{i=1}^{n} S_i}$$

where n is the total number of samples at Blair, M_i is the SCE of a factor resolved from multisite analysis and S_i is the SCE of a factor resolved from single-site analysis. Correlation is an indicator for the agreement of day-to-day co-variance of source contributions and RAAE is a measure of differences in the two contribution time series.

Generally, factors for regional sources such as sulfate, nitrate, resuspended soil and calcium-rich materials showed minimum variation. However, factors with local emissions impacts such as

traffic related sources displayed increased bias and weaker correlation in the day-to-day contributions between SCEs from multisite and single-site analyses. Including more sites from a larger geographical area which potentially include sources profiles with larger spatial variability in the multisite analyses could also lead to different SCEs compared to single-site analyses. This is consistent with previous observations in the sensitivity study by Tian et al. (2014) which ascribed sensitivity of multisite PMF analysis to the spatial variability of source profiles.

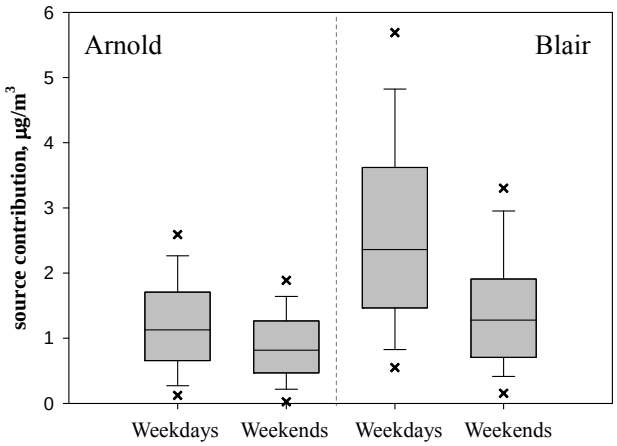

Figure 7-6. Weekly patterns for the traffic related factor SCEs at Arnold and Blair based on the analysis using pooled data from these two sites. The upper and lower edges of the boxes indicate the 75th percentile and 25th percentile of the distribution. The whiskers represent 90th and 10th percentile and the crosses are 95th and 5th percentiles of the distribution. Medians are shown as a solid line in the boxes.

Therefore, pooling data from multiple sites in order to increase the size of the dataset and to enhance the stability of the solutions might lead to different SCEs at individual sites and caution should be used when interpreting these results.

In summary, source apportionment analyses using multisite datasets assume homogeneous source profiles at all sites and this can lead to biased results at sites differentially impacted by local sources. The advantage of using multisite datasets for source apportionment analyses are

demonstrated by resolving a traffic factor at a suburban site where such factor could not be resolved using the corresponding single-site dataset. While the source contribution estimates from multisite datasets may differ with those obtained from single-site datasets, regional scale sources typically show good agreement with poorer agreement for the local sources.

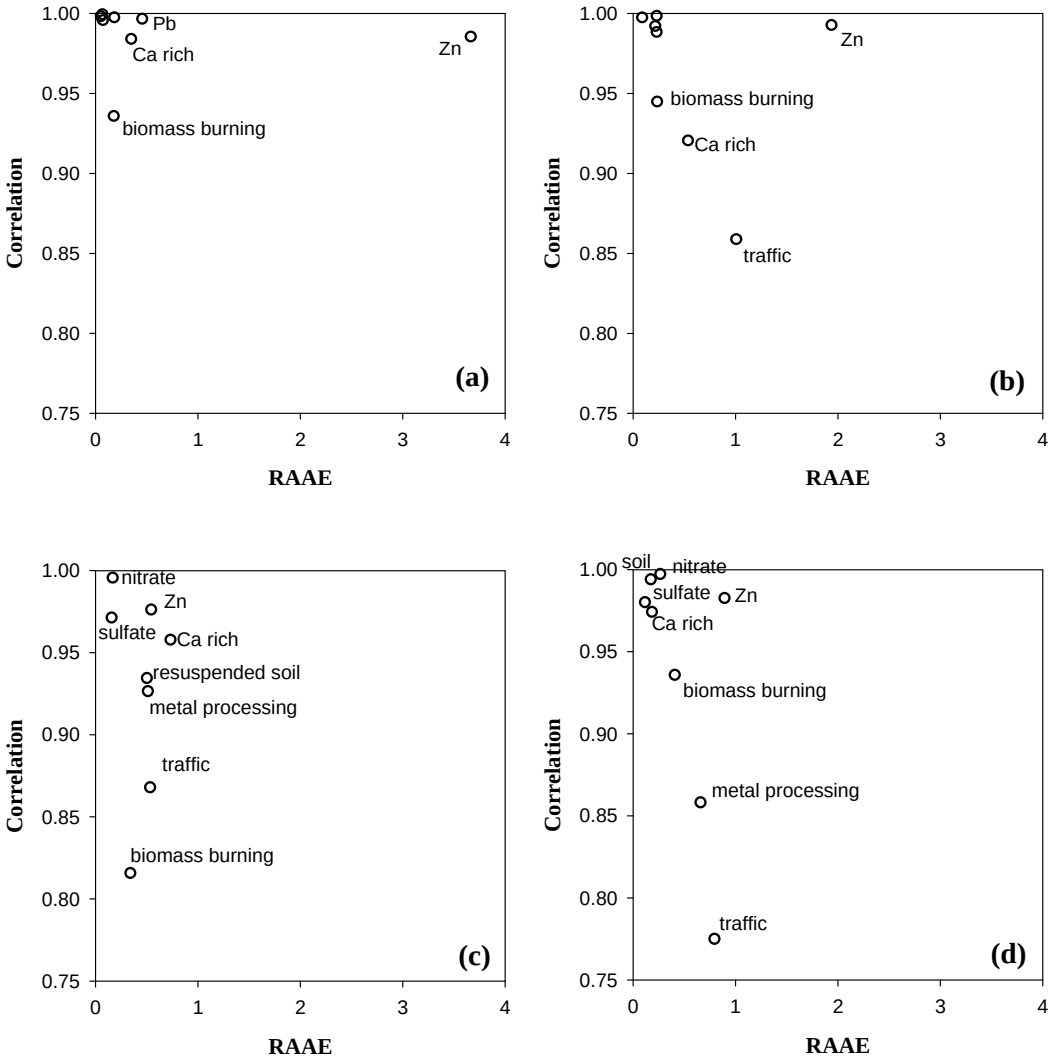

Figure 7-7. RAAE and correlation of factors resolved at Blair using the site-specific dataset and pooled datasets: (a) BLAR1; (b) BLAR2; (c) MULT1 and (d) MULT2. Only select factors are labeled in (a) and (b).

7.3.3. PMF Modeling Uncertainties

Error estimation results and diagnostics are summarized in Table 7-4. Generally good stability was observed for all the optimal runs which were selected based on diagnostic parameters such as goodness of fit to the observations and the distribution of residues. All the factors in 13 datasets had more than 80% of the bootstrap runs successfully mapped which indicates that the BS uncertainty could be interpreted and the number of factors may be appropriate (Norris et al., 2014). As discussed in Section 7.2, DISP and BS-DISP attempted to transform the solution gradually without significant increase of Q which is the objective function being minimized. Swap refers to extreme cases in these calculations when the factors change so much that they exchange identities. The extent of factor swapping is an indicator of whether a solution is well-defined. In this study, no swaps occurred with DISP and the decrease in Q approached or was equal to zero, suggesting minimum rotational ambiguity. The majority of BS-DISP runs were successful with no swaps, except two single-site datasets and three multisite datasets. In spite of the swaps observed, runs with Belleville and Blair + Arnold suggested only minor instability with less than five swaps and a high proportion of accepted cases. Moderate instability was observed with runs at Roxana where 17 swaps occurred and 83 cases were considered acceptable. BS results confirmed this instability with metal processing factor mapped only in 81% of BS runs. Similar levels of instability were also exhibited by with the two pooled datasets comprised of four sites where spatial variability of source profiles may affect the identification of factors and are likely responsible for the increased uncertainties.

These methods provide only semi-quantitative measures of the uncertainty associated with PMF modeling and are best interpreted in a relative sense (Norris et al., 2014). Therefore, sensitivity studies were conducted that applied three error estimation methods to ten solutions to a given

dataset that were generated using different seeds. Table 7-5 summarizes the sensitivity study conducted using the Blair+Arnold+Belleville+Granite City dataset. While BS and DISP are relatively stable, the result indicated that BS-DISP was sensitive to the variability of source profiles caused by using different seeds. Thus, BS-DISP may not be a robust method to quantify the modeling uncertainty and care should be taken to avoid overinterpreting the BS-DISP results.

In addition to the three uncertainty estimation methods implemented by EPA PMF 5.0, the uncertainty matrix perturbation method described by Christensen et al. (2008) was also explored. Results for one of the datasets (Blair + Arnold + Belleville + Roxana) are shown in Figure 7-8 as an illustration and Table 7-6 summarizes the results for all datasets. The explained mass correlation (EMC) is a metric for the similarity or correlation between the factor profiles (F matrix) of an alternative solution from the perturbation and the standard (base) solution; the relative average absolute error (RAAE) is an indicator for the relative difference of the day-to-day source contributions (G matrix) between the two cases Christensen et al. (2008).

Figure 7-7 shows the calculated RAAE vs. correlation for four multisite – single-site pairs. Points at the upper left corner are in best agreement with high correlation and minimum difference in SCEs. Factors that show excellent agreement (sulfate, nitrate, resuspended soil and metal processing) are not labeled in Figure 7-7 (a) and (b).

Both source factor contribution estimates (Figure 7-8a) and EMC values (Figure 7-8b) display a wide range for biomass burning factor and to a lesser extent the traffic factor. RAAE (Figure 7-8c) values showed more variability as well as wider range for several factors. However, the wide range of RAAE values for calcium, zinc and metal processing factor is not suprising because the RAAE is a relative scaled metric and inherently has high variability for small SCEs.

Collectively, these three metrics suggested moderate instability for the biomass burning factor and a lesser extent the traffic factor. This finding is consistent with the three error estimation methods. Consistency between the two sets of error estimation methods was also observed for the other studied datasets. While a limited number of runs (10) can inform the stability of factors resolved by PMF and could be used as a qualitative check on the selection of the optimal number of factors, a larger number of perturbation runs are needed to establish robust statistical evaluation of the solutions.

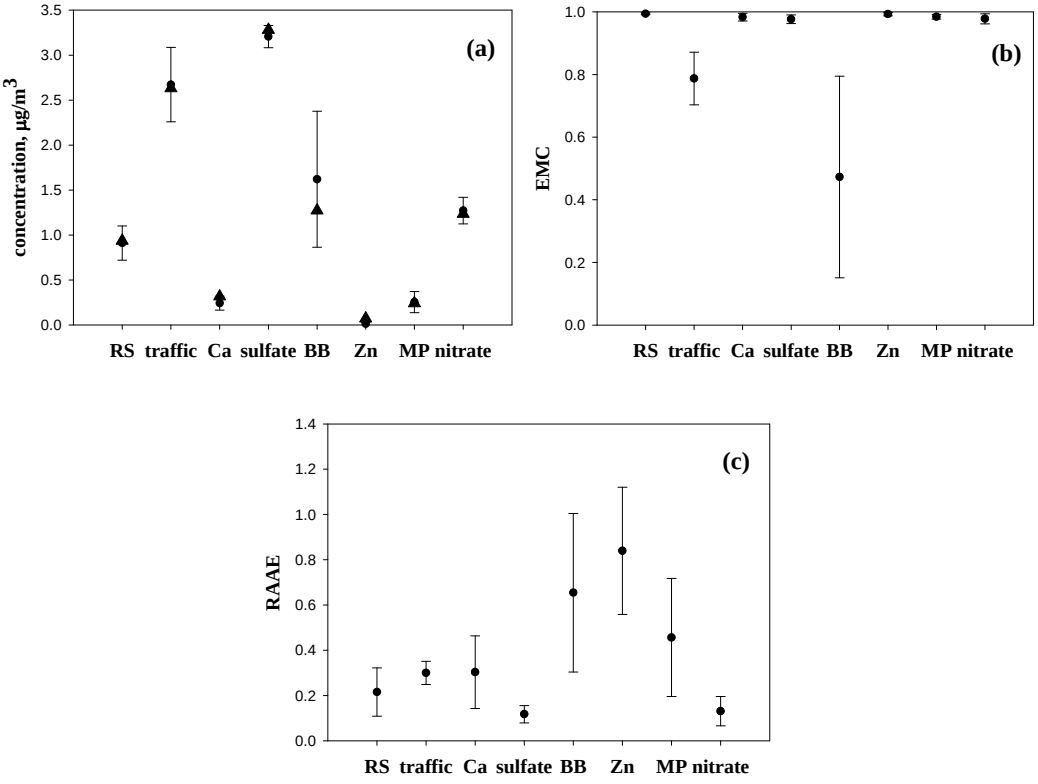

Figure 7-8. Results for the uncertainty matrix perturbations runs for Blair+Arnold+Belleville+Roxana. (a) average factor contributions; (b) EMC; (c) RAAE. The base case is represented by triangles and the alternative runs (average ± 1σ) are shown as closed circles with error bars. The resolved factors are: resuspended soil (RS), traffic related emissions (traffic), secondary sulfate (sulfate), biomass burning (BB), Zn rich (Zn), metal processing (MP) and secondary nitrate (nitrate).

7.4. Conclusions

$PM_{2.5}$ speciation data collected at six sites in the St. Louis area were analyzed by PMF to identify emission sources and apportion their contributions. Wind regression was also utilized to locate the local emission sources. Three regional-scale sources - sulfate, biomass burning and nitrate - were identified at the majority of the sites and collectively accounted for 72~91% of the $PM_{2.5}$ mass. These factors presumably also include regional secondary organic aerosol. A resuspended soil factor that is significantly affected by the intercontinental transport of Saharan dust contributes 2~8% of $PM_{2.5}$ mass. Because of the benefit from the extended spatial and temporal coverage of the current datasets, a Ca-rich factor which was previously attributed to point sources appears to have regional source characteristics. Point sources such as steel processing, brass production, lead smelting and zinc smelting were resolved at some sites. A factor dominated by traffic but mixed with a local point source was identified at downtown St. Louis for the most contemporary time period and was estimated to contribute to 12% of total $PM_{2.5}$.

Datasets pooled from the multiple single-site datasets were also analyzed by PMF. Additional factors were identified at certain sites likely because of the strengthened covariance by the pooling of multiple datasets. However, multisite analysis may result in differences in contribution estimates at individual sites compared to the corresponding single-site analysis. Regional sources often exhibit good agreement in the SCE between single-site and multisite analyses whereas discrepancies were found for SCEs from factors representing local sources such as traffic related emissions. Caution must be used when interpreting SCEs derived from a multisite analysis for any individual site.

Modeling uncertainties were evaluated using BS, DISP and BS-DISP implemented by EPA PMF 5.0. Stability was generally observed for all of the optimal solutions. Higher uncertainties are more likely to be associated with the solutions to multisite datasets. Sensitivity studies indicate instability of BS-DISP and, therefore, values generated by BS-DISP should be used a reference instead of a stringent standard. PMF runs with perturbed uncertainty matrices led to similar observations as the PMF 5.0 tools and have been demonstrated as a potentially alternative method to evaluate modeling uncertainties.

7.5. Acknowledgements

The Roxana Air Quality Study is funded by ConocoPhillips in response to a settlement agreement with American Bottom Conservancy, the Sierra Club, the Environmental Integrity Project, and the Natural Resources Defense Council. None of these five entities have formally reviewed or approved this manuscript and their approval or endorsement should not be inferred. We would also acknowledge Dr. Gary Norris for the discussion about the EPA PMF software including the uncertainty estimation tools.

7.6. References

Amato, F., Hopke, P.K., 2012. Source apportionment of the ambient PM2.5 across St. Louis using constrained positive matrix factorization. Atmospheric Environment 46, 329-337.

Birch, M.E., Cary, R.A., 1996. Elemental carbon-based method for monitoring occupational exposures to particulate diesel exhaust. Aerosol Science and Technology 25, 221-241.

Buzcu, B., Fraser, M.P., Kulkarni, P., Chellam, S., 2003. Source identification and apportionment of fine particulate matter in Houston, TX, using positive matrix factorization. Environmental Engineering Science 20, 533-545.

Chow, J.C., Watson, J.G., Pritchett, L.C., Pierson, W.R., Frazier, C.A., Purcell, R.G., 1993. The dri thermal/optical reflectance carbon analysis system: description, evaluation and applications in U.S. Air quality studies. Atmospheric Environment Part A, General Topics 27, 1185-1201.

Christensen, W.F., Schauer, J.J., 2008. Impact of species uncertainty perturbation on the solution stability of positive matrix factorization of atmospheric particulate matter data. Environmental Science and Technology 42, 6015-6021.

Du, L., Turner, J., 2015. Using $PM_{2.5}$ lanthanoid elements and nonparametric wind regression to track petroleum refinery FCC emissions. Sci. Total Environ. 529, 65-71.

Escrig, A., Monfort, E., Celades, I., Querol, X., Amato, F., Minguillón, M.C., Hopke, P.K., 2009. Application of optimally scaled target factor analysis for assessing source contribution of ambient PM10. Journal of the Air and Waste Management Association 59, 1296-1307.

Ferris Jr, B.G., Speizer, F.E., Spengler, J.D., Dockery, D., Bishop, Y.M., Wolfson, M., Humble, C., 1979. Effects of sulfur oxides and respirable particles on human health. Methodology and demography of populations in study. American Review of Respiratory Disease 120, 767-779.

Hopke, P.K., Ito, K., Mar, T., Christensen, W.F., Eatough, D.J., Henry, R.C., Kim, E., Laden, F., Lall, R., Larson, T.V., Liu, H., Neas, L., Pinto, J., Stölzel, M., Suh, H., Paatero, P., Thurston, G.D., 2006. PM source apportionment and health effects: 1. Intercomparison of source apportionment results. Journal of Exposure Science and Environmental Epidemiology 16, 275-286.

Ito, K., Christensen, W.F., Eatough, D.J., Henry, R.C., Kim, E., Laden, F., Lall, R., Larson, T.V., Neas, L., Hopke, P.K., Thurston, G.D., 2006. PM source apportionment and health effects: 2. An investigation of intermethod variability in associations between source-apportioned fine particle mass and daily mortality in Washington, DC. Journal of Exposure Science and Environmental Epidemiology 16, 300-310.

Ito, K., Mathes, R., Ross, Z., Nádas, A., Thurston, G., Matte, T., 2011. Fine particulate matter constituents associated with cardiovascular hospitalizations and mortality in New York City. Environmental Health Perspectives 119, 467-473.

Ito, K., Xue, N., Thurston, G., 2004. Spatial variation of PM 2.5 chemical species and source-apportioned mass concentrations in New York City. Atmospheric Environment 38, 5269-5282.

Kim, E., Hopke, P.K., 2004. Comparison between Conditional Probability Function and Nonparametric Regression for Fine Particle Source Directions. Atmospheric Environment 38, 4667-4673.

Kim, E., Hopke, P.K., 2007. Comparison between sample-species specific uncertainties and estimated uncertainties for the source apportionment of the speciation trends network data. Atmospheric Environment 41, 567-575.

Kim, E., Hopke, P.K., Edgerton, E.S., 2003. Source identification of Atlanta aerosol by positive matrix factorization. Journal of the Air & Waste Management Association 53, 731-739.

Lee, J.H., Hopke, P.K., 2006. Apportioning sources of $PM_{2.5}$ in St. Louis, MO using speciation trends network data. Atmospheric Environment 40, Supplement 2, 360-377.

Lee, J.H., Hopke, P.K., Turner, J.R., 2006. Source identification of airborne PM 2.5 at the St. Louis-Midwest Supersite. Journal of Geophysical Research-Part D-Atmospheres 111, 12 pp.-12 pp.

Mar, T.F., Norris, G.A., Koenig, J.Q., Larson, T.V., 2000. Associations between air pollution and mortality in Phoenix, 1995-1997. Environmental Health Perspectives 108, 347-353.

Minguillón, M.C., Querol, X., Baltensperger, U., Prévôt, A.S.H., 2012. Fine and coarse PM composition and sources in rural and urban sites in Switzerland: Local or regional pollution? Sci. Total Environ. 427-428, 191-202.

Mooibroek, D., Schaap, M., Weijers, E.P., Hoogerbrugge, R., 2011. Source apportionment and spatial variability of PM2.5 using measurements at five sites in the Netherlands. Atmospheric Environment 45, 4180-4191.

Norris, G.A., Duvall, R.M., Brown, S.G., Bai, S., 2014. EPA Positive Matrix Factorization (PMF) 5.0 Fundamental and User Guide. Prepared for the U.S. Environmental Protection Agency Office of Research and Development, Washington, DC (EPA/600/R-14/108;STI-910511-5594-UG, April).

Paatero, P., 1997. Least squares formulation of robust non-negative factor analysis. Chemometrics and Intelligent Laboratory Systems 37, 23-35.

Paatero, P., Eberly, S., Brown, S.G., Norris, G.A., 2014. Methods for estimating uncertainty in factor analytic solutions. Atmospheric Measurement Techniques 7, 781-797.

Paatero, P., Tapper, U., 1994. Positive matrix factorization - a nonnegative factor model with optimal utilization of error-estimates of data values. Environmetrics 5, 111-126.

Pancras, J.P., Landis, M.S., Norris, G.A., Vedantham, R., Dvonch, J.T., 2013. Source apportionment of ambient fine particulate matter in Dearborn, Michigan, using hourly resolved PM chemical composition data. Sci. Total Environ. 448, 2-13.

Perry, K.D., Cahill, T.A., Eldred, R.A., Dutcher, D.D., Gill, T.E., 1997. Long-range transport of North African dust to the eastern United States. Journal of Geophysical Research: Atmospheres 102, 11225-11238.

Polissar, A.V., Hopke, P.K., Paatero, P., Malm, W.C., Sisler, J.F., 1998. Atmospheric aerosol over Alaska 2. Elemental composition and sources. Journal of Geophysical Research D: Atmospheres 103, 19045-19057.

Solomon, P.A., Crumpler, D., Flanagan, J.B., Jayanty, R.K., Rickman, E.E., McDade, C.E., 2014. U.S. national PM2.5 Chemical Speciation Monitoring Networks-CSN and IMPROVE: description of networks. Journal of the Air & Waste Management Association (1995) 64, 1410-1438.

Solomon, P.A., Mitchell, W., Tolocka, M., Norris, G.A., Gemmill, D., Wiener, R., Vanderpool, R., Murdoch, R., Natarajan, S., Hardison, E., 2000. Evaluation of $PM_{2.5}$ chemical speciation

samplers for use in the EPA National $PM_{2.5}$ Chemical Speciation Network. EPA-454/R-01-005. Office of Air Quality Planning and Standards, US Environmental Protection Agency, Research Triange Park, NC.

Taiwo, A.M., Beddows, D.C.S., Calzolai, G., Harrison, R.M., Lucarelli, F., Nava, S., Shi, Z., Valli, G., Vecchi, R., 2014. Receptor modelling of airborne particulate matter in the vicinity of a major steelworks site. Sci. Total Environ. 490, 488-500.

Thurston, G.D., Ito, K., Lall, R., 2011. A source apportionment of U.S. fine particulate matter air pollution. Atmospheric Environment 45, 3924-3936.

Tian, Y.-Z., Shi, G.-L., Han, B., Wang, W., Zhou, X.-Y., Wang, J., Li, X., Feng, Y.-C., 2014. The accuracy of two- and three-way positive matrix factorization models: Applying simulated multisite data sets. Journal of the Air & Waste Management Association 64, 1122-1129.

Trijonis, J., Eldon, J., Gins, J., Berglund, G., 1980. Analysis of the St. Louis RAMS (Regional Air Monitoring System) ambient particulate data. Volume I: final report.

USEPA, 2009. Integrated Science Assessment for Particulate Matter.

Wang, Y., Hopke, P.K., 2013. A ten-year source apportionment study of ambient fine particulate matter in San Jose, California. Atmospheric Pollution Research 4, 398-404.

Xie, M., Coons, T.L., Hemann, J.G., Dutton, S.J., Milford, J.B., Peel, J.L., Miller, S.L., Kim, S.Y., Vedal, S., Sheppard, L., Hannigan, M.P., 2012. Intra-urban spatial variability and uncertainty assessment of PM 2.5 sources based on carbonaceous species. Atmospheric Environment 60, 305-315.

7.7. Supplementary Materials

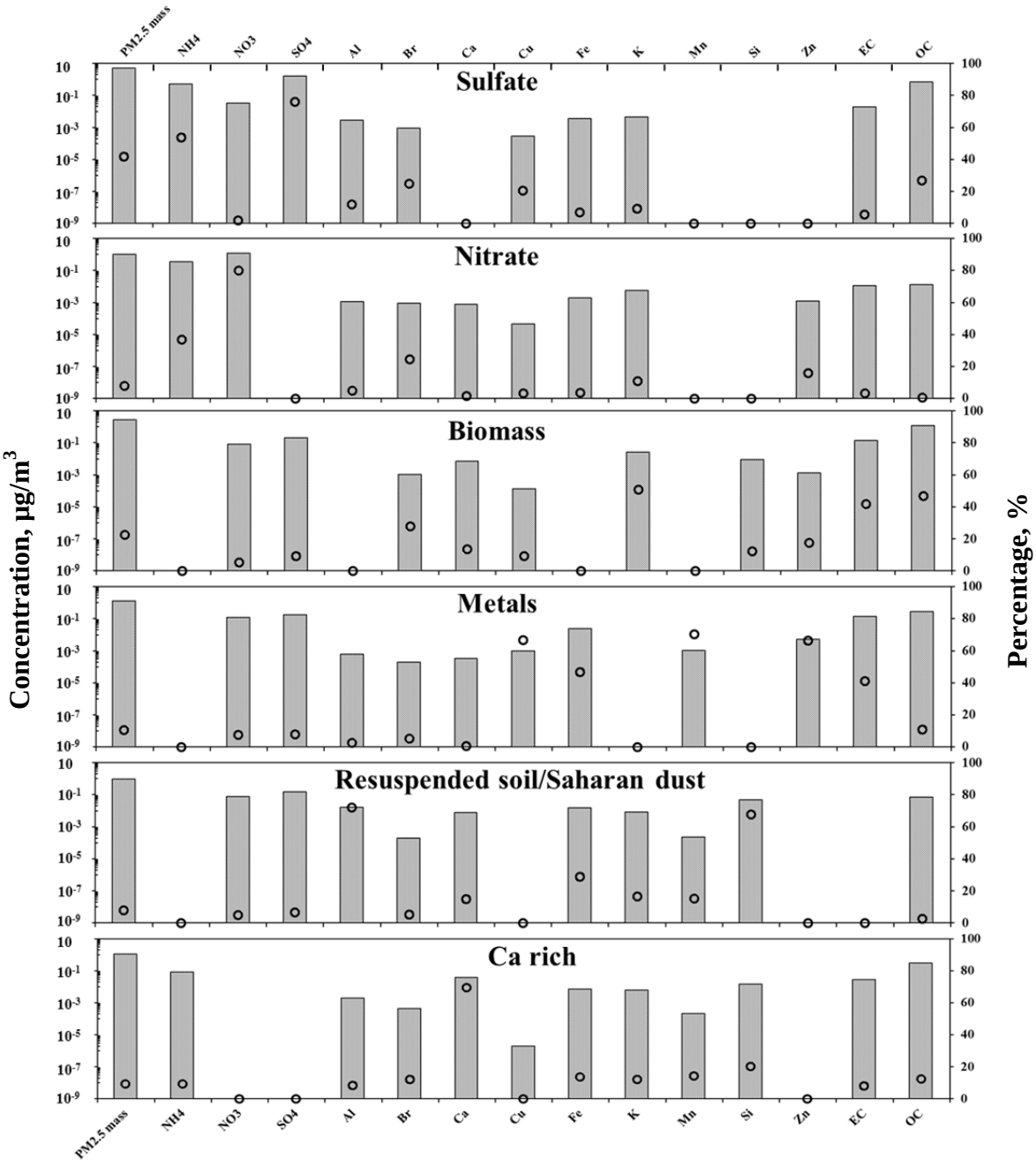

Figure 7-9. Factor resolved at Belleville using dataset BV.

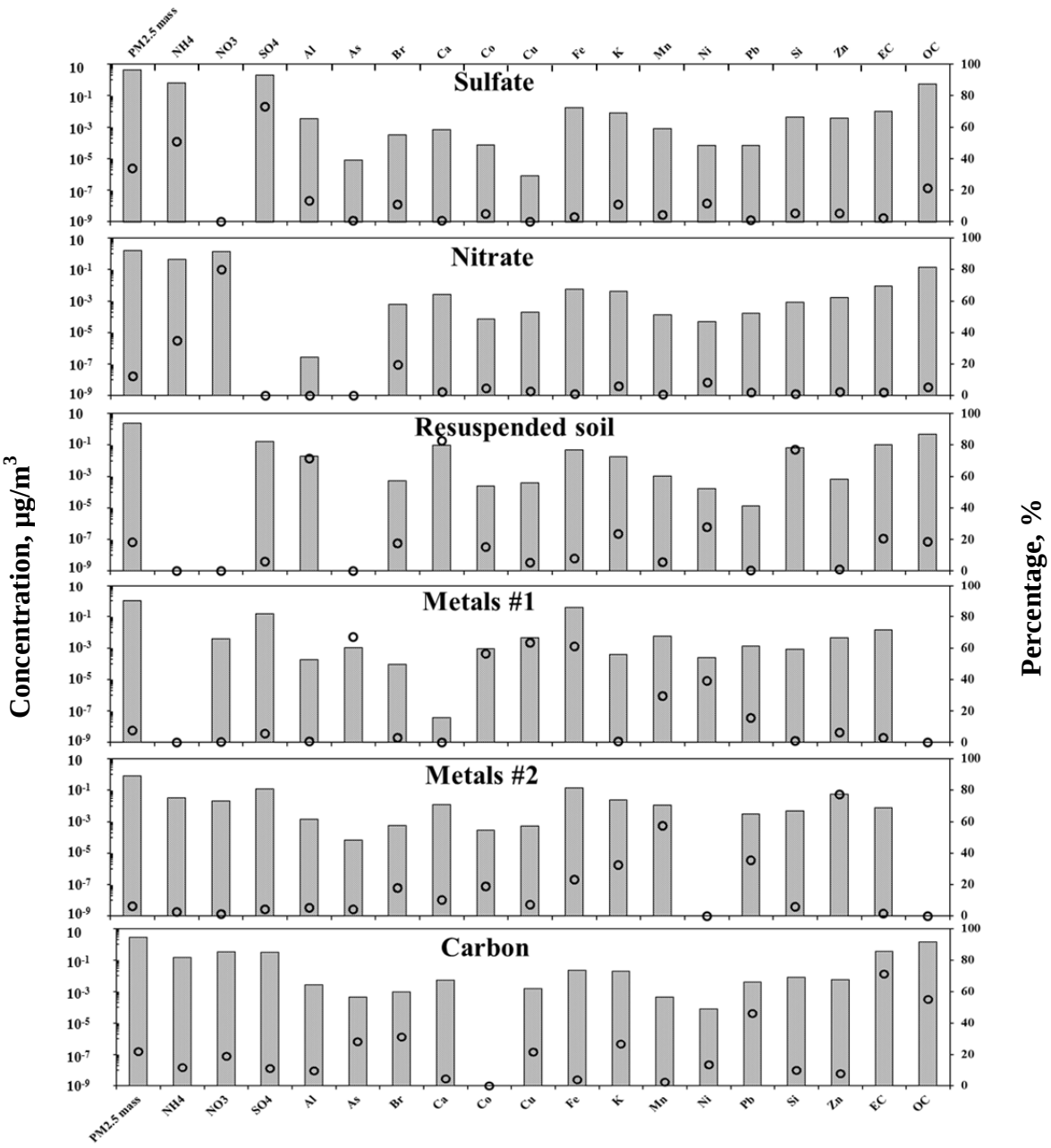

Figure 7-10. Factor resolved at Granite City using dataset GC.

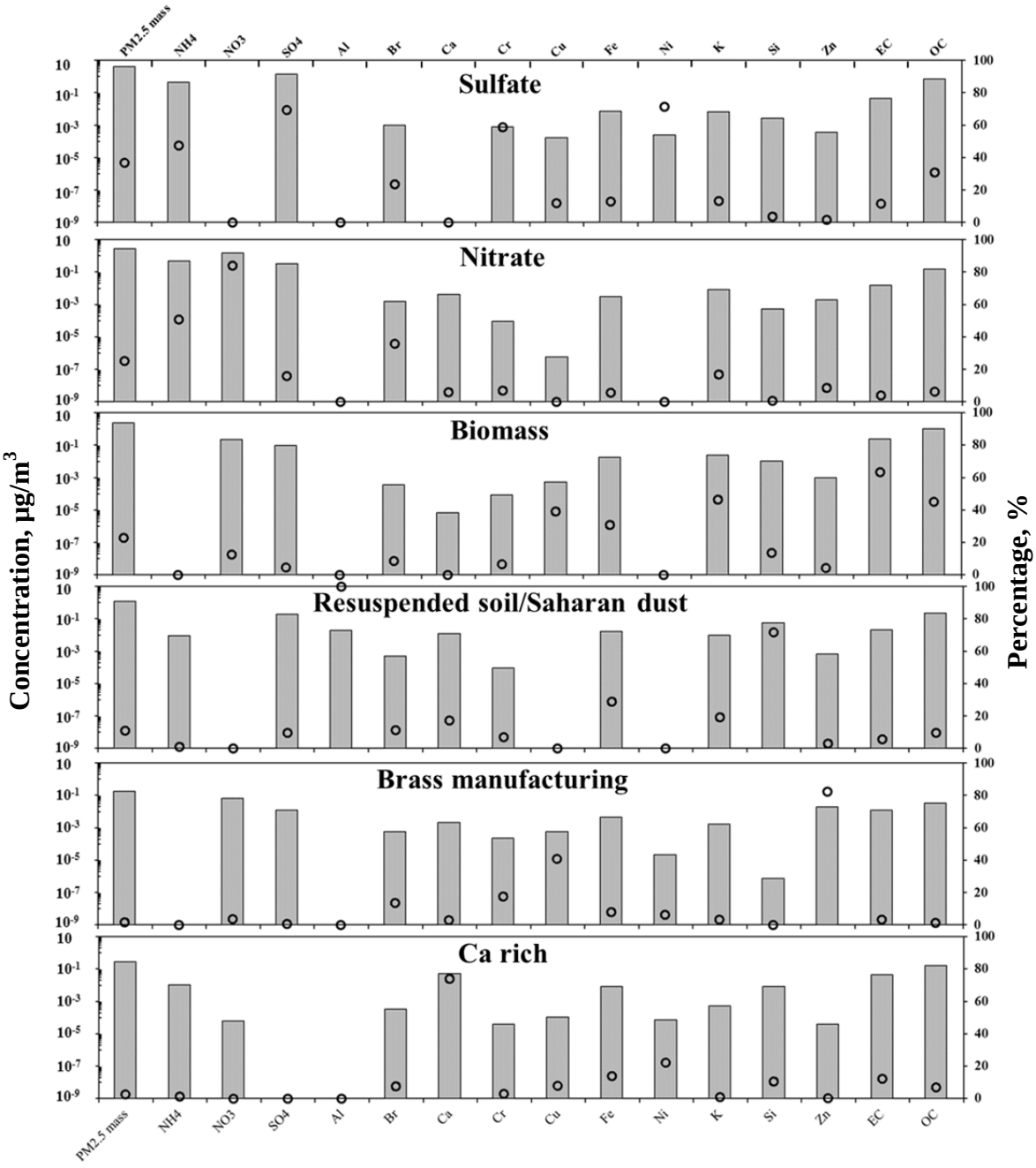

Figure 7-11. Factor resolved at Roxana using dataset RX.

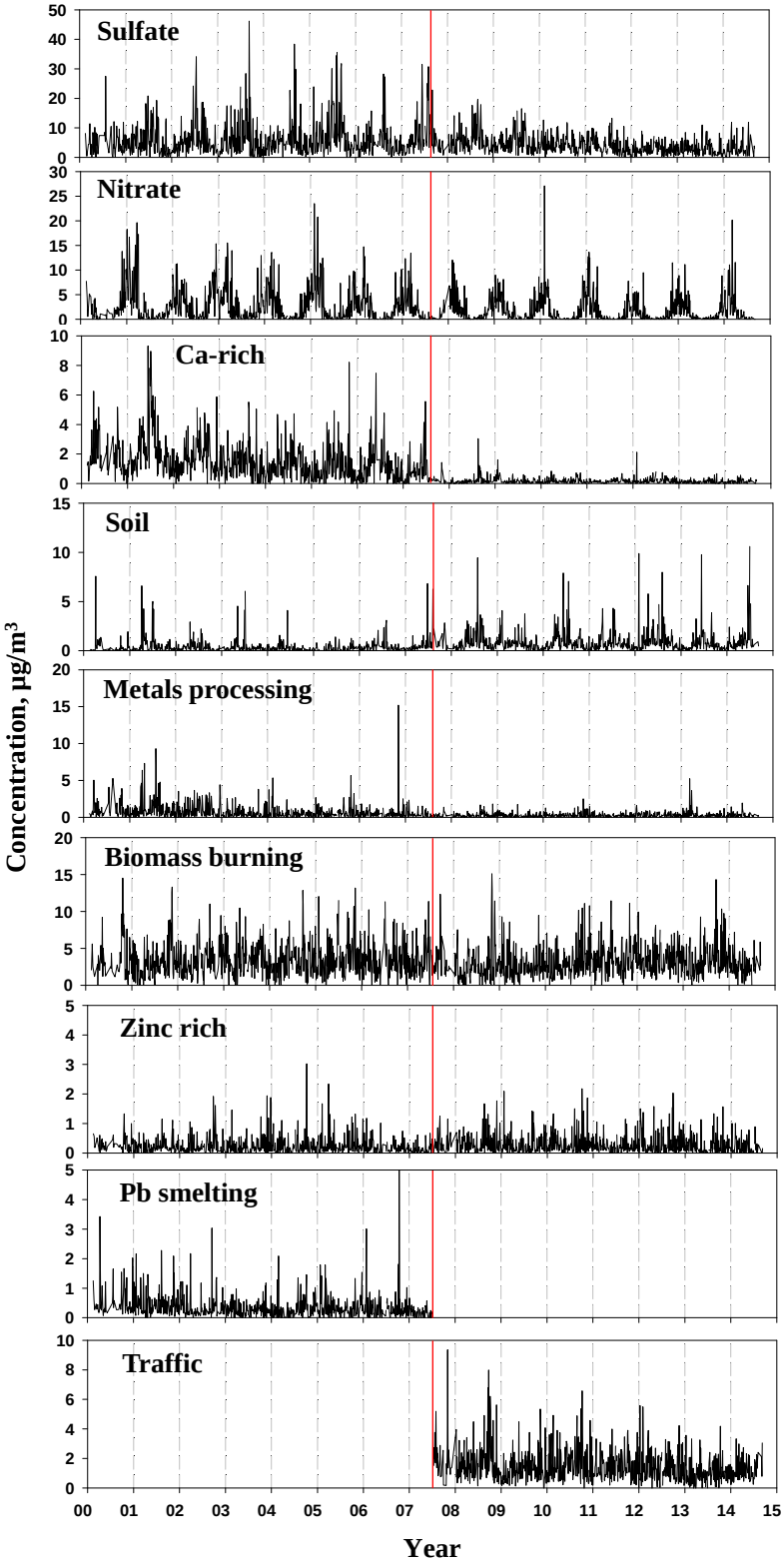

Figure 7-12. Time series for factors identified at Blair Street. The red vertical lines denote the carbon analysis method transition. SCE values less than 0 are not shown.

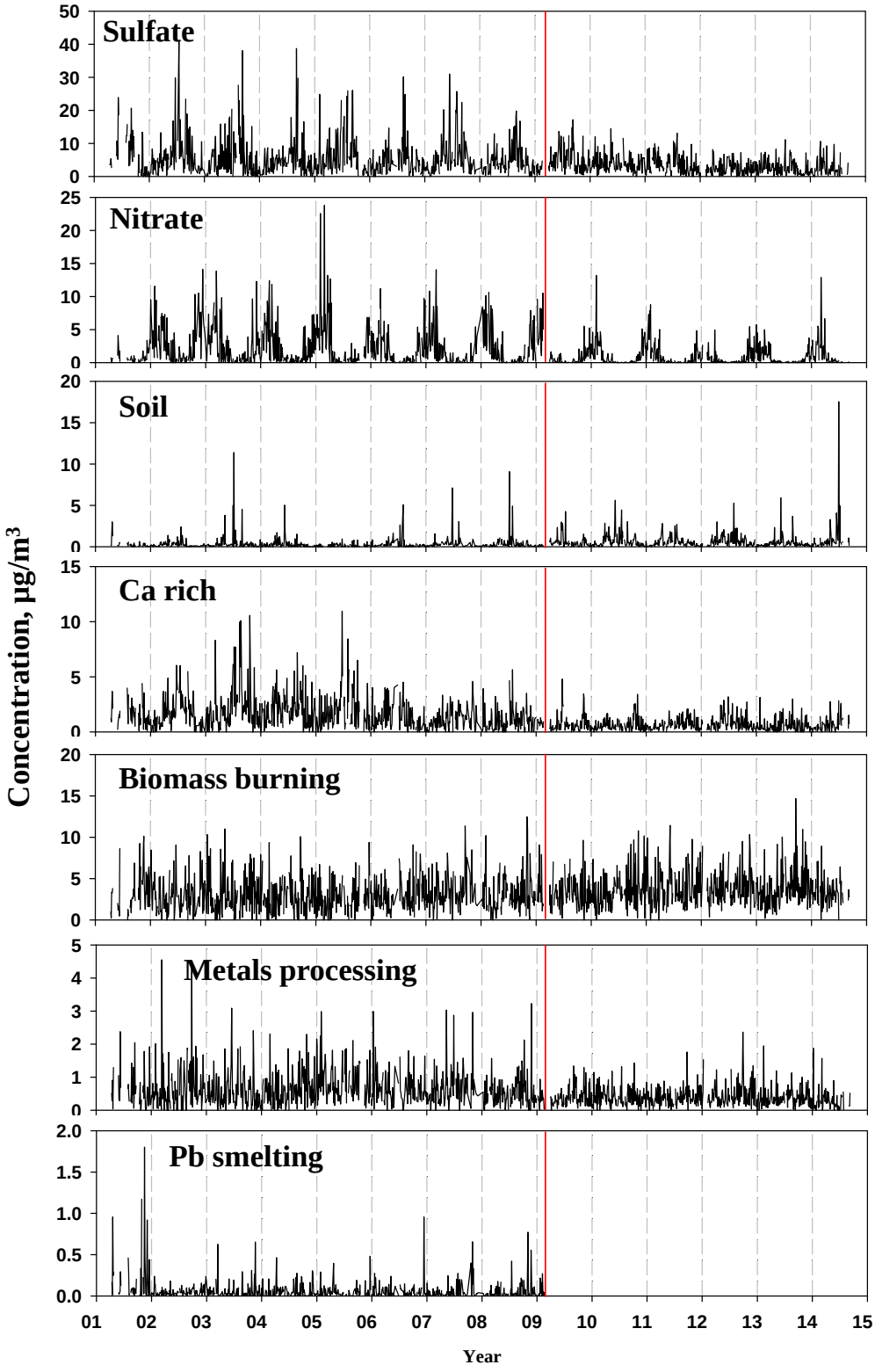

Figure 7-13. Time series for factors identified at Arnold. The red vertical lines denote the carbon analysis method transition. SCE values less than 0 are not shown.

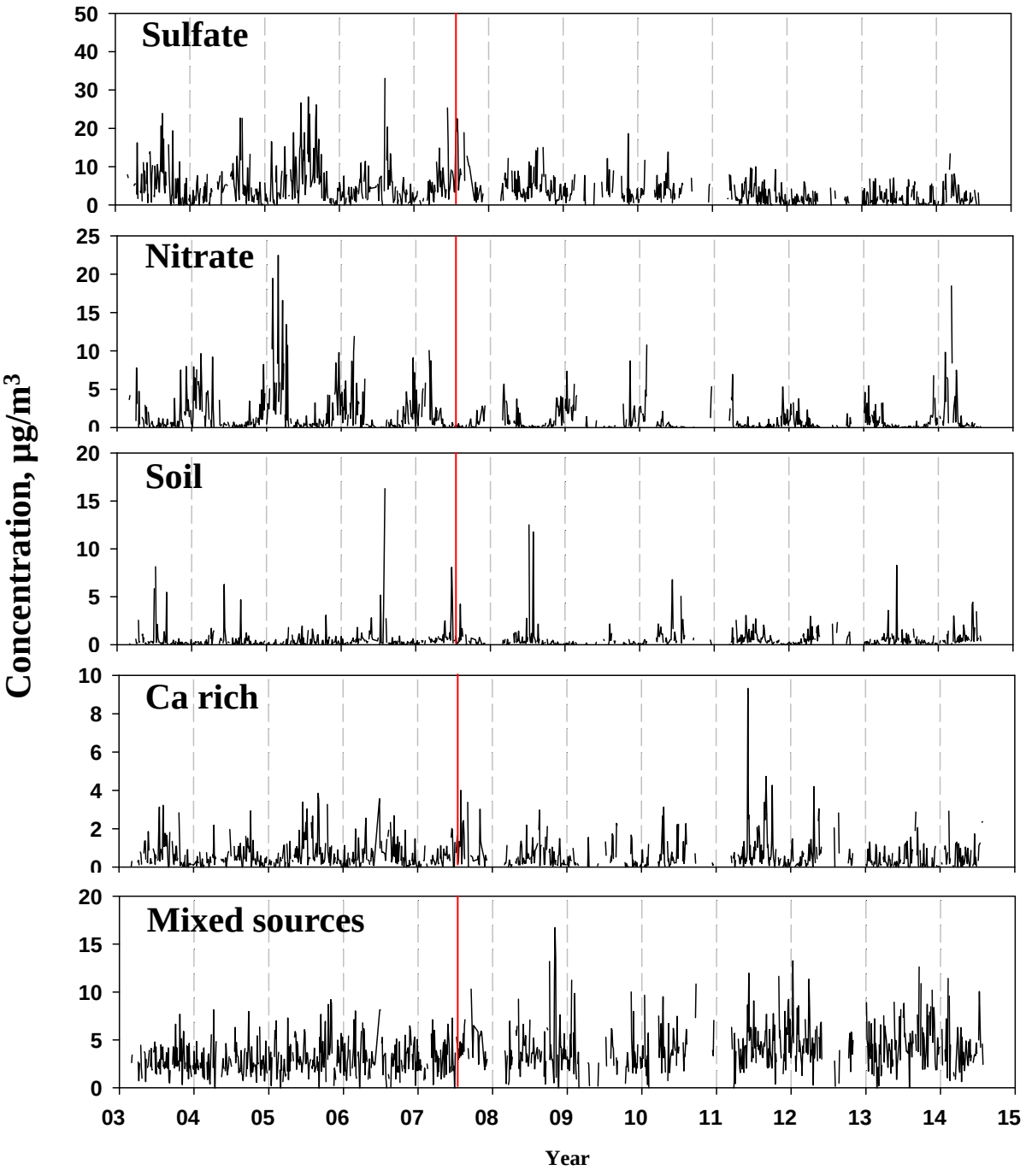

Figure 7-14. Time series for factors identified at Bonne Terre. The red vertical lines denote the carbon analysis method transition. SCE values less than 0 are not shown.

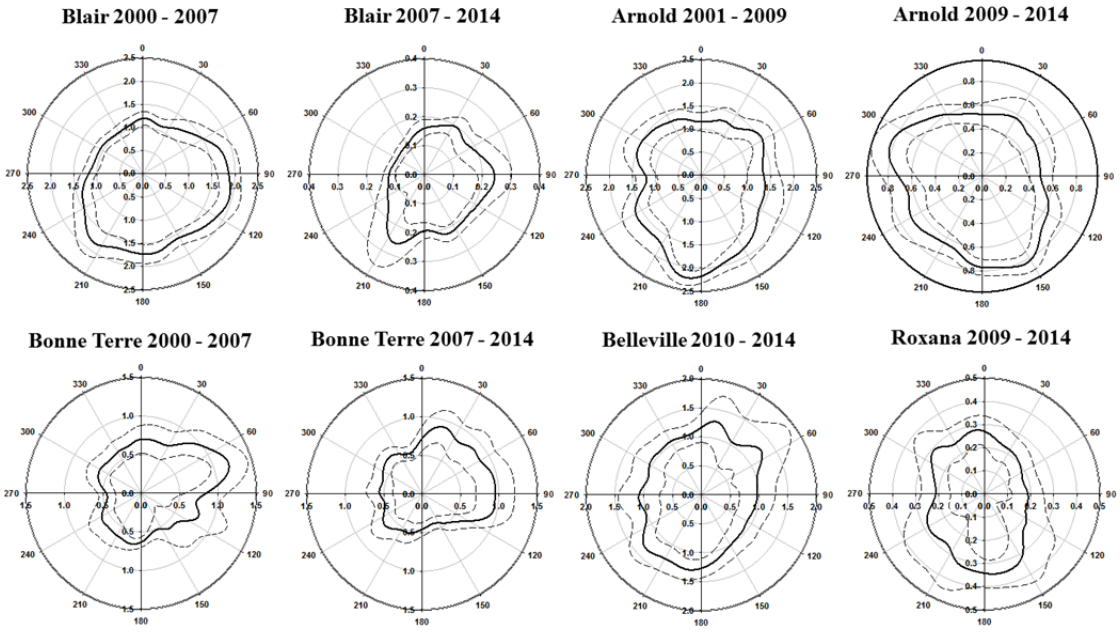

Figure 7-15. Nonparametric wind regression for Ca-rich factors resolved at five locations. Solid black lines represent expected concentrations and dashed black lines indicate 95th confidence intervals. The radial axes have concentration units of µg/m^3.

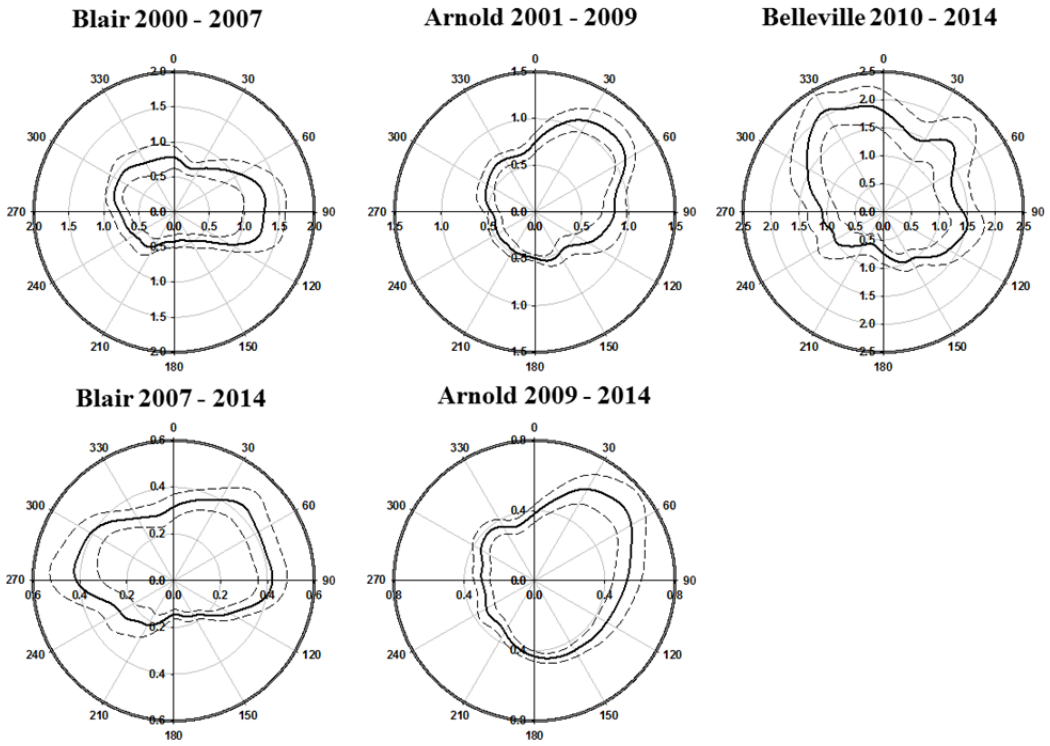

Figure 7-16. Nonparametric wind regression for metal processing factors resolved at three locations. Solid black lines represent expected concentrations and dashed black lines indicate 95th confidence intervals. The radial axes have concentration units of µg/m^3.

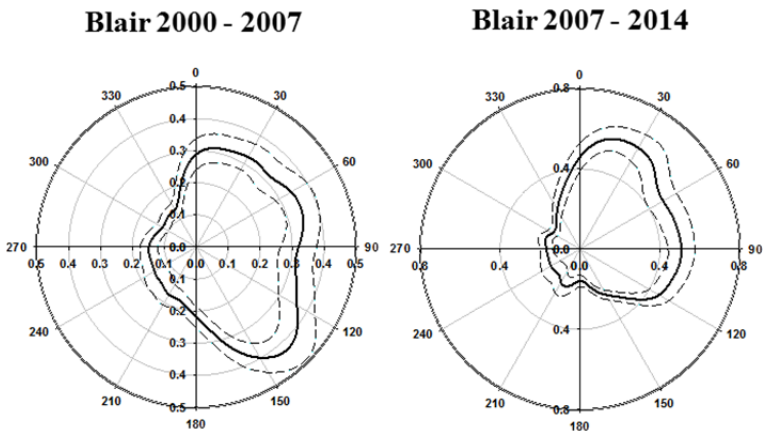

Figure 7-17. Nonparametric wind regression for Zn factors resolved at the Blair site. Solid black lines represent expected concentrations and dashed black lines indicated 95th confidence intervals. The radial axes have concentration units of µg/m^3.

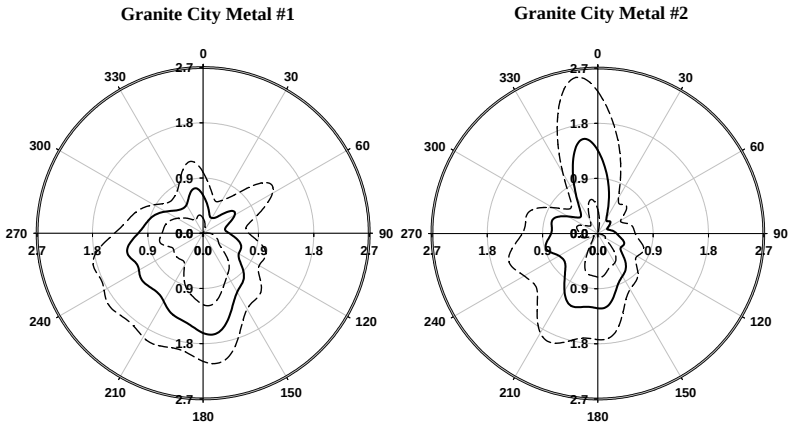

Figure 7-18. Nonparametric wind regression for the two metal factors resolved at Granite City. Solid black lines represent expected concentrations and dashed black lines indicated 95th confidence intervals. The radial axes have concentration units of µg/m^3.

Table 7-4. Summary of EPA PMF 5.0 error estimates diagnostics by datasets.

	BS		DISP			BS-DISP	
	mapping	error limits*	DISP species	dQ%	DISP swaps	dQ%	% cases with swaps
Blair 2000-2007							
Ca rich	100%	0.86, 2.41	NH_4, NO_3	-0.000	0	-0.35	2
metal processing	100%	0.33, 1.02	SO_4, Al, Br				
resuspended dust	98%	0.28, 0.91	Ca, Fe, K, Mn				
biomass burning	99%	2.43, 4.02	Pb, Si, Ti, Zn				
Pb	92%	0.24, 0.89	EC, OC				
nitrate	100%	2.43, 3.49					
sulfate	100%	5.14, 6.19					
Zn	100%	0.19, 0.74					
Blair 2007-2014							
Ca rich	100%	0.11, 0.54	NH_4, NO_3	-0.001	0	-0.002	0
metal processing	100%	0.24, 0.65	SO_4, Br, Ca				
resuspended dust	100%	0.50, 1.09	Fe, K, Mn				
biomass burning	100%	2.47, 3.63	Si, Ti, Zn				
nitrate	100%	1.53, 1.91	EC, OC				
sulfate	100%	3.93, 4.69					
Zn	100%	0.09, 0.60					
traffic	100%	0.97, 1.93					
Arnold 2001-2009							
Ca rich	100%	0.92, 2.57	NH_4, NO_3	-0.000	0	-0.001	0
metal processing	100%	0.10, 1.17	SO_4, Al, Br				
resuspended dust	100%	0.29, 0.63	Ca, Cu, Fe, K				
biomass burning	99%	2.58, 3.86	Mn, Pb, Si, Ti				
Pb	100%	0.03, 0.45	Zn, EC, OC				
nitrate	100%	1.53, 2.52					
sulfate	100%	4.94, 6.07					
Arnold 2009-2014							
Ca rich	100%	0.29, 1.01	NH_4, NO_3	-0.000	0	-0.019	0
metal processing	100%	0.06, 1.06	SO_4, Ca, Fe				
resuspended dust	100%	0.56, 1.10	K, Si, Zn				
biomass burning	100%	2.80, 4.05	EC, OC				
nitrate	100%	0.68, 1.13					
sulfate	100%	3.05, 3.87					

Table 7-4 (continued)

	BS		DISP			BS-DISP	
	mapping	error limits*	DISP species	dQ%	DISP swaps	dQ%	% case with swaps
Bonne Terre 2003-2007							
resuspended dust	98%	0.31, 1.13	NH_4, NO_3	-0.000	0	-0.208	0
biomass burning	100%	2.48, 3.74	SO_4, Al, Br				
Ca rich	100%	0.35, 1.13	Ca, Cu, Fe, K				
nitrate	100%	1.09, 2.11	Mn, Pb, Si, Ti				
sulfate	100%	4.94, 5.88	V, Zn, EC, OC				
Bonne Terre 2007-2014							
resuspended dust	100%	0.47, 1.47	NH_4, NO_3	-0.000	0	-0.005	0
biomass burning	100%	3.31, 4.42	SO_4, Al, Br				
Ca rich	100%	0.48, 1.15	Ca, Fe, K, Si				
nitrate	100%	0.74, 1.15	Zn, EC, OC				
sulfate	100%	3.38, 4.04					
Belleville							
resuspended dust	99%	0.57, 2.12	NH_4, NO_3	-0.001	0	-0.364	1
biomass burning	100%	1.88, 3.66	SO_4, Br, Ca				
Ca rich	94%	0.11, 1.66	Fe, K, Si, Zn				
metal processing	100%	0.27, 2.27	EC, OC				
nitrate	100%	0.78, 1.30					
sulfate	100%	3.88, 5.41					
Granite City							
resuspended soil/Ca rich	100%	1.66, 3.03	NH_4, NO_3	-0.000	0	-0.001	0
Metals #1	100%	0.85,1.49	SO_4, Ca, Cu				
Metals #2	100%	0.54, 1.18	Fe, K, Mn, Si				
Carbon	100%	1.25, 3.30	Zn, EC, OC				
nitrate	100%	1.54, 2.50					
sulfate	100%	3.69, 5.11					
Roxana							
resuspended dust	100%	0.71, 1.74	NH_4, NO_3	-0.001	0	-0.304	17
biomass burning	99%	1.31, 2.51	SO_4, Br, Ca				
Ca rich	99%	0.15, 1.44	Fe, K, Si, Zn				
metal processing	81%	0.39, 1.86	EC, OC				
brass production	100%	0.02, 0.33					
nitrate	100%	1.78, 2.97					
sulfate	100%	2.57, 4.09					

Table 7-4 (continued)

	BS		DISP			BS-DISP	
	mapping	error limits*	DISP species	dQ%	DISP swaps	dQ%	% case with swaps
Blair + Arnold 2001-2007							
Ca rich	99%	0.64, 2.05	NH_4, NO_3	0.000	0	-0.183	3
metal processing	98%	0.17, 0.96	SO_4, Al, Br				
resuspended dust	100%	0.24, 0.88	Ca, Fe, K, Mn				
biomass burning	99%	2.92, 4.21	Ni, Pb, Si, Ti				
Pb	96%	0.12, 0.46	Zn, EC, OC				
nitrate	100%	1.79, 2.68					
sulfate	100%	5.45, 6.23					
Zn	97%	0.20, 1.07					
Blair + Arnold 2009-2014							
Ca rich	100%	0.08, 0.59	NH_4, NO_3	-0.000	0	-0.109	0
metal processing	100%	0.15, 0.39	SO_4, Br, Ca				
resuspended dust	100%	0.55, 1.02	Fe, K, Mn, Si				
biomass burning	100%	1.56, 3.57	Zn, EC, OC				
Zn	100%	0.07, 0.43					
nitrate	100%	0.98, 1.35					
sulfate	100%	3.20, 3.90					
traffic	99%	1.13, 3.14					
Blair + Arnold + Belleville + Granite City							
Ca rich	100%	0, 0.56	NH_4, NO_3	-0.000	0	-0.029	17
metal processing	100%	0.17, 0.60	SO_4, Br, Ca				
resuspended dust	95%	0.59, 3.32	Cu, Fe, K, Mn				
biomass burning	98%	0.32, 4.01	Si, Zn, EC, OC				
Zn	99%	0.06, 0.33					
nitrate	100%	0.93, 1.49					
sulfate	100%	3.34, 4.41					
traffic	99%	1.14, 3.77					
Blair + Arnold + Belleville + Roxana							
Ca rich	92%	0.15, 0.47	NH_4, NO_3	0	0	-0.391	4
metal processing	92%	0.17, 0.74	SO_4, Br, Ca				
resuspended dust	92%	0.37, 1.32	Fe, K, Si, Zn				
biomass burning	86%	1.06, 3.14	EC, OC				
Zn	92%	0, 0.25					
nitrate	92%	0.78, 1.73					
sulfate	92%	2.28, 3.92					
traffic	86%	1.24, 3.06					

*error limits are represented by 5^{th} and 95^{th} percentiles of the $PM_{2.5}$ concentration assigned to each factor from the bootstrapped runs. Concentration units in $\mu g/m^3$

Table 7-5. Summary of diagnostics for sensitivity study of error estimation methods.

	seed number	BS	DISP		BS-DISP		
		minimum mapping %	%dQ	swaps	% of case accepted	%dQ	# of swaps
base	55	95	0	0	69	-0.029	14
test run #1	13	97	0	0	88	-0.2	10
test run #2	90	94	0	0	89	-0.334	6
test run #3	80	97	0	0	92	-0.155	6
test run #4	5	93	0	0	92	-0.242	1
test run #5	100	96	-0.001	0	79	-0.085	9
test run #6	10	81	0	0	85	-0.213	9
test run #7	500	87	0	0	93	-0.274	6
test run #8	205	80	0	0	88	-0.740	10
test run #9	20	79	0	0	84	-0.255	14
test run #10	70	82	0	0	86	-0.903	12

%dQ is calculated as (the largest observed decrease of Q value during DISP)/(Q value of the base run).

Table 7-6. Summary of uncertainty matrix perturbation runs, ten perturbation runs for each model solution.

	contribution, µg/m^3					EMC				RAAE			
	base	average	std. dev	min	max	average	std. dev	min	max	average	std. dev	min	max
Blair 2000-2007													
metals processing	0.78	0.57	0.18	0.28	0.77	0.99	0.00	0.99	1.00	0.29	0.20	0.09	0.64
sulfate	5.93	5.72	0.26	5.38	6.10	0.98	0.01	0.97	0.99	0.09	0.02	0.07	0.14
Pb	0.36	0.64	0.19	0.38	1.01	0.98	0.02	0.92	1.00	0.82	0.53	0.11	1.86
resuspended soil	0.39	0.28	0.08	0.19	0.46	0.99	0.00	0.98	0.99	0.39	0.09	0.27	0.56
Ca rich	1.50	1.75	0.22	1.45	2.11	0.95	0.01	0.93	0.96	0.34	0.12	0.21	0.54
Zn	0.25	0.29	0.09	0.16	0.45	0.96	0.03	0.91	0.99	0.31	0.26	0.12	0.82
biomass burning	3.46	3.29	0.33	2.84	3.89	0.95	0.02	0.92	0.98	0.21	0.02	0.18	0.24
nitrate	2.84	2.98	0.33	2.70	3.70	0.99	0.01	0.98	1.00	0.11	0.08	0.05	0.31
Blair 2007-2014													
resuspended soil	0.690	0.76	0.10	0.63	0.95	0.97	0.01	0.96	0.98	0.24	0.05	0.19	0.36
Ca rich	0.302	0.20	0.06	0.11	0.29	0.96	0.01	0.94	0.99	0.33	0.18	0.07	0.65
nitrate	1.756	1.60	0.08	1.54	1.76	0.99	0.01	0.98	1.00	0.13	0.03	0.08	0.17
biomass burning	3.248	3.50	0.18	3.25	3.77	0.96	0.02	0.93	0.98	0.19	0.03	0.14	0.22
metals processing	0.297	0.26	0.03	0.22	0.30	0.99	0.01	0.97	1.00	0.20	0.06	0.11	0.29
traffic	1.584	1.60	0.11	1.49	1.88	0.92	0.04	0.82	0.96	0.17	0.03	0.13	0.25
Zn	0.336	0.17	0.05	0.05	0.23	0.99	0.01	0.97	1.00	0.48	0.16	0.29	0.85
sulfate	4.164	4.29	0.10	4.11	4.45	0.99	0.00	0.98	1.00	0.08	0.02	0.05	0.11
Arnold 2001-2009													
Pb	0.066	0.22	0.08	0.04	0.30	0.98	0.02	0.94	1.00	2.45	1.08	0.35	3.67
nitrate	2.234	2.31	0.29	1.85	2.62	0.99	0.01	0.98	1.00	0.16	0.05	0.08	0.24
metals processing	0.662	0.36	0.10	0.14	0.52	0.98	0.01	0.94	0.99	0.48	0.14	0.27	0.80
biomass burning	3.066	2.79	0.33	2.42	3.47	0.96	0.01	0.93	0.97	0.24	0.02	0.21	0.27
resuspended soil	0.343	0.31	0.04	0.21	0.37	0.98	0.01	0.96	0.99	0.24	0.07	0.19	0.43
sulfate	5.480	5.55	0.15	5.24	5.75	0.99	0.00	0.99	0.99	0.09	0.03	0.07	0.15
Ca rich	1.650	2.01	0.26	1.69	2.39	0.91	0.02	0.87	0.94	0.41	0.12	0.30	0.62
Arnold 2009-2014													
Ca rich	0.681	0.63	0.15	0.37	0.84	0.98	0.01	0.95	1.00	0.20	0.13	0.07	0.46
biomass burning	3.665	3.77	0.22	3.40	4.16	0.98	0.01	0.97	0.99	0.09	0.02	0.07	0.15
metals processing	0.395	0.32	0.12	0.16	0.54	0.98	0.01	0.97	0.99	0.33	0.15	0.11	0.61
resuspended soil	0.698	0.66	0.04	0.63	0.75	1.00	0.00	1.00	1.00	0.10	0.01	0.08	0.12
nitrate	0.859	0.95	0.13	0.69	1.13	1.00	0.00	0.99	1.00	0.17	0.10	0.04	0.32
sulfate	3.407	3.42	0.15	3.20	3.71	0.98	0.01	0.96	1.00	0.07	0.02	0.04	0.10

Table 7-6. (continued)

	contribution, μg/m^3					EMC				RAAE			
	base	average	std. dev	min	max	average	std.dev	min	max	average	std.dev	min	max
Belleville													
biomass burning	2.709	2.82	0.37	2.12	3.23	0.98	0.01	0.95	0.99	0.21	0.05	0.14	0.28
sulfate	5.035	4.91	0.25	4.48	5.40	0.99	0.01	0.98	1.00	0.08	0.02	0.05	0.12
metals processing	1.267	1.32	0.46	0.72	2.32	0.98	0.01	0.95	1.00	0.33	0.21	0.15	0.85
nitrate	0.976	1.04	0.11	0.84	1.20	1.00	0.00	0.99	1.00	0.13	0.06	0.06	0.25
resuspended soil	0.963	1.08	0.25	0.80	1.63	0.99	0.01	0.96	0.99	0.26	0.16	0.11	0.70
Ca rich	1.107	0.98	0.28	0.53	1.40	0.93	0.03	0.87	0.97	0.27	0.12	0.08	0.53
Granite City													
Metals #1	1.074	1.25	0.19	0.87	1.62	0.98	0.01	0.97	0.99	0.27	0.12	0.16	0.55
resuspended soil	2.471	2.38	0.15	2.09	2.55	0.99	0.02	0.94	1.00	0.13	0.04	0.08	0.23
carbon	1.917	1.53	0.34	1.15	2.18	0.93	0.04	0.84	0.97	0.29	0.09	0.15	0.41
sulfate	4.435	4.66	0.27	4.15	4.98	0.98	0.02	0.92	0.99	0.11	0.03	0.05	0.15
nitrate	2.105	2.20	0.14	2.01	2.43	0.99	0.00	0.99	1.00	0.12	0.05	0.07	0.24
Metals #2	0.880	0.86	0.21	0.40	1.16	0.99	0.00	0.99	0.99	0.23	0.15	0.10	0.58
Roxana													
brass production	0.078	0.07	0.04	0.01	0.14	0.98	0.01	0.96	0.99	0.43	0.28	0.09	0.92
biomass burning	1.976	1.99	0.24	1.64	2.29	0.92	0.05	0.82	0.98	0.22	0.06	0.16	0.36
resuspended soil	0.919	0.88	0.18	0.59	1.15	0.98	0.02	0.94	0.99	0.24	0.09	0.10	0.39
metal processing	1.180	0.99	0.31	0.64	1.68	0.87	0.03	0.80	0.91	0.36	0.11	0.22	0.54
Ca rich	0.255	0.28	0.14	0.15	0.59	0.92	0.05	0.82	0.98	0.45	0.37	0.13	1.33
sulfate	3.868	3.87	0.31	3.38	4.35	0.96	0.02	0.93	0.99	0.11	0.03	0.07	0.18
nitrate	2.172	2.31	0.15	2.10	2.62	0.99	0.01	0.97	1.00	0.10	0.05	0.04	0.21
Bonne Terre 2003-2007													
resuspended soil	0.505	0.46	0.06	0.37	0.56	0.99	0.00	0.99	0.99	0.24	0.05	0.19	0.34
biomass burning	3.014	3.03	0.30	2.45	3.41	0.97	0.02	0.95	0.99	0.17	0.03	0.13	0.23
sulfate	5.316	5.76	0.20	5.52	6.08	0.98	0.01	0.96	0.99	0.17	0.03	0.10	0.20
nitrate	1.899	1.30	0.30	1.01	1.86	0.97	0.00	0.97	0.98	0.34	0.12	0.11	0.48
Ca rich	0.634	0.89	0.16	0.55	1.09	0.96	0.02	0.93	0.98	0.58	0.20	0.23	0.84
Bonne Terre 2007-2014													
biomass burning	4.202	4.00	0.14	3.78	4.17	0.98	0.01	0.96	1.00	0.10	0.02	0.08	0.13
nitrate	0.959	0.91	0.06	0.82	1.02	0.99	0.00	0.99	1.00	0.09	0.03	0.07	0.15
sulfate	3.378	3.53	0.13	3.38	3.76	0.98	0.01	0.95	0.99	0.07	0.03	0.04	0.12
Ca rich	0.640	0.77	0.12	0.52	0.91	0.98	0.01	0.96	0.99	0.28	0.08	0.16	0.44
resuspended soil	0.652	0.67	0.06	0.57	0.74	0.99	0.00	0.99	1.00	0.13	0.03	0.09	0.18

Table 7-6. (continued)

	contribution, µg/m^3					EMC				RAAE			
	base	average	std.dev	min	max	average	std. dev	min	max	average	std. dev	min	max
Blair + Arnold 2001-2007													
Zn	0.700	0.32	0.07	0.22	0.44	0.97	0.03	0.89	0.99	0.55	0.10	0.38	0.70
sulfate	6.009	6.01	0.24	5.48	6.35	0.99	0.01	0.98	1.00	0.10	0.01	0.08	0.12
resuspended soil	0.307	0.23	0.03	0.19	0.27	0.99	0.00	0.98	0.99	0.33	0.07	0.23	0.43
nitrate	2.224	2.32	0.22	1.97	2.66	0.99	0.00	0.99	1.00	0.12	0.05	0.06	0.22
biomass burning	3.513	3.34	0.22	2.98	3.74	0.95	0.02	0.92	0.97	0.22	0.03	0.17	0.26
Pb	0.169	0.54	0.16	0.32	0.82	0.98	0.01	0.95	1.00	2.50	1.27	0.90	4.94
metal processing	0.528	0.29	0.08	0.19	0.43	1.00	0.00	0.99	1.00	0.46	0.15	0.21	0.65
Ca rich	1.271	1.75	0.20	1.53	2.04	0.93	0.01	0.91	0.95	0.54	0.14	0.38	0.78
Blair + Arnold 2009-2014													
metal processing	0.200	0.19	0.05	0.09	0.24	0.98	0.01	0.97	0.99	0.25	0.12	0.17	0.58
resuspended soil	0.565	0.67	0.04	0.61	0.73	0.99	0.00	0.99	0.99	0.23	0.06	0.14	0.31
nitrate	1.088	1.06	0.03	1.04	1.14	1.00	0.00	0.99	1.00	0.07	0.01	0.06	0.09
biomass burning	2.837	3.55	0.15	3.28	3.72	0.95	0.02	0.92	0.97	0.34	0.04	0.27	0.38
sulfate	3.542	3.58	0.12	3.47	3.80	0.99	0.01	0.98	1.00	0.08	0.01	0.06	0.10
Zn	0.314	0.15	0.05	0.07	0.24	0.96	0.02	0.93	0.99	0.53	0.16	0.25	0.78
Ca rich	0.384	0.39	0.11	0.27	0.60	0.96	0.01	0.94	0.98	0.30	0.15	0.15	0.66
traffic	1.774	1.13	0.25	0.73	1.55	0.84	0.02	0.80	0.88	0.46	0.08	0.34	0.61
Blair + Arnold + Belleville + Granite City													
Zn	0.166	0.09	0.08	0.00	0.22	0.98	0.01	0.97	1.00	0.58	0.30	0.19	1.02
biomass burning	3.619	3.18	0.60	2.16	3.78	0.90	0.02	0.87	0.93	0.34	0.06	0.24	0.44
Ca rich	0.179	0.24	0.23	0.00	0.61	0.97	0.02	0.93	0.99	1.19	0.54	0.38	2.47
metal processing	0.453	0.42	0.16	0.19	0.59	0.97	0.02	0.94	0.99	0.41	0.12	0.26	0.60
traffic	1.592	1.24	0.62	0.57	2.06	0.80	0.09	0.62	0.96	0.49	0.09	0.36	0.65
sulfate	3.880	3.94	0.26	3.50	4.31	0.98	0.01	0.96	0.99	0.11	0.03	0.07	0.16
resuspended soil	0.662	1.59	0.45	1.02	2.12	0.96	0.01	0.93	0.98	1.35	0.63	0.60	2.26
nitrate	1.282	1.16	0.11	1.07	1.46	0.99	0.00	0.99	1.00	0.13	0.04	0.07	0.20
Blair+Belleville+Arnold+Roxana													
resuspended soil	0.937	0.91	0.19	0.53	1.16	0.99	0.00	0.99	1.00	0.22	0.11	0.11	0.44
traffic	2.632	2.67	0.41	2.15	3.25	0.79	0.08	0.65	0.90	0.30	0.05	0.20	0.37
Ca rich	0.317	0.24	0.08	0.11	0.39	0.98	0.01	0.96	1.00	0.30	0.16	0.09	0.65
sulfate	3.281	3.21	0.12	3.00	3.37	0.98	0.01	0.96	0.99	0.12	0.04	0.07	0.17
biomass burning	1.273	1.62	0.76	0.70	2.92	0.47	0.32	-0.09	0.86	0.65	0.35	0.28	1.20
Zn	0.071	0.01	0.02	0.00	0.06	0.99	0.01	0.98	1.00	0.84	0.28	0.20	1.01
metal processing	0.241	0.25	0.12	0.10	0.46	0.99	0.01	0.97	1.00	0.46	0.26	0.22	0.98
nitrate	1.236	1.27	0.15	0.99	1.46	0.98	0.02	0.95	0.99	0.13	0.07	0.06	0.23

Chapter 8 : Summary, Implications, and Recommendations

8.1. Summary

The Roxana Air Quality Study (RAQS) has provided an understanding of air quality impacts from a major point source in the St. Louis area – the Wood River petroleum refinery. The refinery is an insignificant contributor to $PM_{2.5}$ mass even at the facility fenceline. $PM_{2.5}$ FCC emissions were observed using lanthanum in excess of the characteristic lanthanum/cerium ratio in soil as a tracer. Excellent detectability of lanthanoids in $PM_{2.5}$ was achieved using a hot plate digestion protocol followed by ICP-MS. Nonparametric wind regression on lanthanum concentration and the lanthanum/cerium ratio provided evidence of FCC impacts when winds placed the monitoring station downwind of the refinery core unit operations. Lanthanum concentration and the lanthanum/cerium ratio were strongly coupled to frequency of hourly winds from the refinery during the 24-hour sampling period; thus, days with high impacts do not necessarily correspond to days with higher emissions. For the samples collected in this study, there was no evidence of non-routine, episodic (i.e. startup/shutdown/malfunction) emissions from the FCC.

Analytical methods using a single collector quadrupole ICP-MS operating in standard mode were customized for selenium and for lead isotopes using RAQS samples. Spiking the analyte solution with 3% methanol achieved good detectability of a low abundance Se isotope, ^{82}Se, for analysis by standard-mode ICP-MS. This approach is promising for selenium analysis in samples with low mass loadings such as the CSN. Analysis by single collector quadrupole ICP-MS using Tl to correct for the mass bias effects provides a good semi-quantitative method for the characterization of Pb isotope ratios $^{208}Pb/^{206}Pb$ and $^{207}Pb/^{206}Pb$. Pb isotope ratios derived from

ambient $PM_{2.5}$ samples collected at two locations in the St. Louis area – including RAQS – fall along a mixing line with end members corresponding to US urban aerosols and geological formations common to Eastern Missouri.

For the gaseous air toxics, aromatic compounds and other petroleum related hydrocarbons such as n-octane and propylene displayed higher mixing ratios at Roxana compared to downtown St. Louis. Nonparametric wind regression provides supporting evidence for refinery impacts at the Roxana site. Local contributions to compounds with higher mixing ratios at Roxana compared to downtown St. Louis were up to 50% of the downtown mixing ratios. A pseudo two-source model for benzene at the two contrasting sites was proposed based on the benzene-toluene relationship. Benzene from a mixed hydrocarbons source appears to be homogeneous between the two sites and was estimated to contribute to about 70% of the total benzene at Roxana that was not "refinery-influenced". Principle component analysis resolved factors with similar source profiles at both Roxana and Blair Street with aromatics and aldehydes factors collectively responsible for up to 71% of the variance in gaseous air toxics. There were differences between the sites in how species related to vehicle exhaust load onto the factors.

Commonly used metrics such as Pearson correlation coefficient (PCC) were applied to $PM_{2.5}$ chemical speciation data collected at five speciation sites in the St. Louis area. Bootstrapping was used to examine the sensitivity of PCC to extreme values. Cases were observed where a few samples had very high influence on the PCC and efforts should be taken to screen for and possibly exclude such values depending on the study objectives. Measurement error characterized using collocated precision data was shown to be dependent on measured concentrations for some species, including nitrate. A "binning-sampling" approach was developed to harmonize the collocated precision estimate from six collocated CSN sites to be

compatible with the concentration ranges observed for the site pairs of interest. It was also demonstrated that in at least one case – sulfate for the Arnold and Belleville sites – spatial variability metrics would suggest the sites are homogeneous but the intersite differences could not be fully explained by measurement error. Emission sources located between the two sites differentially impact the sites depending on wind direction but these impacts cancel out when averaged over the entire dataset. These analyses demonstrate that care must be used when applying even the most conventional metrics for spatiotemporal variability and it is sometimes possible to extract details about local emission sources from data that appear spatially homogeneous in the absence of considering the measurement error as a frame of reference.

Finally, source apportionment analysis by PMF on five $PM_{2.5}$ speciation sites in the St. Louis area revealed that three regional-scale sources – sulfate, biomass burning and nitrate – were identified at the majority of the sites and accounted for about 72-91% of the $PM_{2.5}$ mass. Because of the benefit from having datasets with extended spatial and temporal coverage, a Ca-rich factor which was explained as a point source contribution in other previous work appears to have strong regional-scale contributions or at least a similar emission source profiles over large spatial scales. Datasets pooled from multiple single-site datasets were also analyzed by PMF. Additional factors were identified at certain sites likely because of the strengthened covariance by pooling across multiple datasets. However, multisite analysis may result in differences in the source contribution estimates at individual sites compared to the corresponding single-site analysis; it is not clear which estimates are most representative but the multi-site analyses do appear to have biases for the source contribution estimates from local point sources. Perturbations to the uncertainty matrix were demonstrated to be an effective approach towards determining of optimal number of factors which is inherently a subjective process. Uncertainty

estimation tools available in the newest version of EPA PMF were applied to all of the datasets. Sensitivity studies indicate instability of BS-DISP and, therefore, values generated by BS-DISP should be used in a relative sense rather than as a stringent standard.

8.2. Implications and Recommendations

1. *Characterizing the coupling between emissions and impacts*. Both emission strength and dispersion modulate the observed impacts at the receptor. Meteorological conditions, especially surface winds, largely determine the near-field dispersion of pollutants emitted from local sources. It was clear from RAQS that elevated La concentrations were observed only when the winds placed the monitoring site downwind of the FCC unit. However, the La concentrations during such periods could not be reliably compared to the La concentrations reported by other studies because the role of emissions could not be disentangled from the role of meteorology for all of these studies. For example, consider the relationship $C(x,t) = D(x,t)E(t)$ where C is the concentration, D is the dispersion and E is the emission rate. Previous studies at most qualitatively related concentration to wind direction and thus provided no information about dispersion. For RAQS, the wind direction variability during the 24-hour sampling period means that the concentration can be coupled to the emissions only if the latter are assumed constant which is likely a poor assumption. This dissertation has demonstrated that surface winds data can be used to characterize *impacts* from a point source but higher time resolution concentration data, such as hourly data, would also be needed to better characterize the *emissions*. Higher time resolution measurements would also have a greater likelihood of capturing episodic emission events. These implications from RAQS apply to all stationary monitors aimed at characterizing contributions from local point sources.

La/Ce ratios in ambient $PM_{2.5}$ samples that were concluded to be impacted by refinery emissions are reported as 2.9 ± 1.8 (1σ) (Kulkarni et al., 2006) and 1.37 ± 2.60 (1σ) (Moreno et al., 2008) compared to 1.49 ± 2.11 (1σ) in RAQS. However, the comparison of La/Ce ratios reported by RAQS and previous studies is limited by the insufficient characterization of dispersion conditions in the latter. In contrast, La-Ce relationship in FCC catalysts has been relatively less studied. Kulkarni et al. (2006) reported La/Ce ratios in FCC catalysts as 4.3 ± 4.6 (1σ) which demonstrates large variability among the six catalysts measured. Although this value provided the evidence of lanthanum being concentrated in FCC catalysts, catalysts used at the Roxana refinery operations would need to be analyzed to obtain the profile of lanthanoids specific to the FCC unit in this study. The St. Louis area is occasionally impacted by the inter-continental transport of Saharan dust and these events may result in possible elevation of lanthanoids concentration and the variation of La/Ce ratios in ambient $PM_{2.5}$. Air mass back trajectories generated by the HYSPLIT model for days with high La concentration (top 5%) did not provide consistent evidence of long range transport on those days. For future work, obtaining the profile of lanthanoids in $PM_{2.5}$ samples collected at other speciation monitoring sites in the St. Louis area could provide additional insights towards determining the impact of Saharan dust.

2. *Placing the RAQS air toxics data in broader context*. This dissertation exploited the NATTS air toxics data collected in the City of St. Louis to place the RAQS data in a St. Louis context. Another dimension would be to place the RAQS data in the context of measurements conducted near other petroleum refineries. This is actually quite difficult because of the source-receptor relationship presented in the first recommendation. For example, the distance between the emission point(s) and the monitoring station and also the distribution of wind directions will both significantly influence the observed impacts. That stated, there would be value in comparing

RAQS data to other sites if the site characteristics are adequately described and qualified. As a starting point, Figure 8-1 shows the cumulative distribution of annual average benzene mixing ratios reported to AQS for sites nationwide with 24-hour average sampling durations. Blair Street (City of St. Louis) is at the 59th percentile and RAQS is at the 88th percentile. These monitoring sites include the full spectrum of land use classifications ranging from rural to urban to industrial. However, six of the eight highest-concentration sites are in Texas and are presumably near petroleum and/or petrochemical facilities. Future work should condition the data to include only those monitoring sites located in industrial areas and then a more-detailed site-by-site assessment could be conducted.

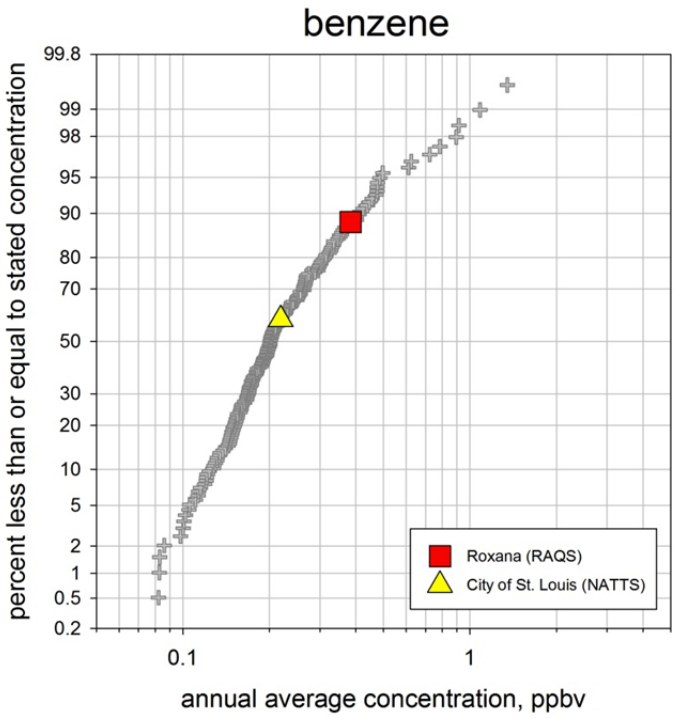

Figure 8-1. Cumulative distribution of year 2013 annual average benzene mixing ratios for sites reporting data to AQS plus the RAQS data. Data were screened to include only those sites operating on a 1-in-6 or 1-in-12 day sampling schedule with 24-hour integrated sampling and at least 85% data completeness (n = 196).

3. *Probing the robustness of spatiotemporal variability metrics*. The role of extreme values or outliers merits greater attention when calculating spatiotemporal variability metrics. For example, extreme values are known to strongly influence the Pearson correlation coefficient (PCC) and therefore are often excluded from such calculations. In many air quality analyses, however, the exclusion of these values is simply based on subjectively chosen cutoff values for absolute or relative differences. Conversely, an argument against this approach is that censoring a dataset by a particular cutoff value inherently changes the dataset. In most cases, it is usually the central tendency of the dataset distribution that is of most interest. Therefore, an alternative way of censoring the dataset is identify extreme values based on how they influence deviations from the representativeness of the central tendency; this requires study of the *sensitivity* of the metrics to potential outliers. For example, in Chapter 6 the distribution of PCC values obtained from numerous bootstrapped datasets demonstrated that only a small number of samples – usually much smaller than would be designated by a cutoff percentile – exert strong influence on the PCC. The identified outliers can then be screened for physical interpretation of their drivers such as the Saharan dust events that influence the $PM_{2.5}$ silicon in St. Louis. While in principle confidence intervals on the metric (e.g. PCC) could be used as a measure of influence from extreme values, the bootstrapped distributions provide insights into the nature of the influence including whether they result in multi-model versus uni-modal distributions.

4. *Understanding opportunities and limitations of using collocated data to estimate network precision*. Measurement error is ubiquitous in all monitoring networks. Measurement precision often exhibits concentration dependence, in some cases even when the concentration values are well above the MDL. Previous work on the collocated CSN data revealed periods of persistent bias which are site- and species-specific. Therefore, in general the error associated with each

measurement is a combined effect of both concentration-dependent random error and systematic bias (e.g. flow rate) error. The two aspects have varying influence on the observed measurement error and will depend on the species and network configurations.

Collocated data can be used to estimate measurement precision. However, if there is concentration dependence for the precision than the precision estimate from collocated data might not be representative for a dataset of interest if the concentration distributions are different. This mismatch can be reconciled by creating a synthetic collocated dataset that matches the concentration distribution for the sites of interest. However, the aforementioned bias that is observed for some species in the CSN cannot be addressed using this approach. Future work should examine the species-specific coupling of concentration dependent precision and measurement bias to determine cases where the precision from pooled collocated data can be used, cases where the precision should be calculated from bootstrapping the collocated data to match the concentration distribution of interest, and cases where bias is so large that the collocated data should not be used to infer precision at another site.

5. *Source apportionment modeling on multisite datasets should be conducted with caution*. Source apportionment modeling on datasets pooled from multiple sites is attractive but has limitations. It can stabilize regional source factors by forcing all sites to have the same profile and thus not be differentially influenced by spurious loading of species onto such factors. Mixing sites with distinct and less distinct but ubiquitous impacts like this – such as traffic at a downtown site and suburban site – can better resolve the impacts at the less distinct site. However, sources that impact only specific monitoring sites can be confounded by the presence of other sites, leading to a degradation of source resolution at the impacted site and/or the spurious presence of that source impacting the other sites. Therefore, source profiles and source

contribution estimates from multisite PMF analysis should be interpreted with caution especially when seeking to quantify the behavior at individual sites.

6. *Refining tools to choose optimal PMF solutions and estimate uncertainties in the modeling results*. BS, DISP and BS-DISP tools implemented in the US EPA PMF v5.0 serve as semi-quantitative metrics for modeling uncertainty estimation. To date there is very little user experience with DISP and BD-DISP and there is a need to examine them in the context of numerous actual datasets. These metrics collectively provide information on the uncertainty associated with the modeling results with each metric focusing on different aspects of the modeling. However, these estimates should only be elements in a weight-of-evidence approach to characterizing uncertainty and the quantitative estimates from the tools should be not be over-interpreted. For example, using the standard deviation (or certain percentile values) of factor loadings across several BS runs as error estimates, which is a common practice in many source apportionment studies, is not fully justified because the intent of BS is to assure the stability of the solutions and it does not capture all sources of uncertainty inherent in the modeling. BS, DISP and BS-DISP results should be reported and over time a meta-analysis could be performed across studies to determine the utility of these metrics. The tools do appear to have value in the subjective process of selecting optimal solutions; it is recommended that perturbation on the uncertainty matrix also be used to examine the stability of solutions.

7. *Suggested procedure for the evaluation of intraurban spatiotemporal variability based on data collected at multiple locations.*

It is challenging to develop a unified approach to evaluate spatiotemporal variability. As has been demonstrated by this thesis work, each dataset needs to be investigated from different

perspectives which require the use of one or multiple tools. Chapter 6 provided an example showing how the differential impacts from local sources to two locations could be teased out using specific technique while other tools suggested spatial homogeneity. The selection of the tool(s) is largely determined by the characteristics of the datasets as well as the objectives of the analyses. For example, source apportionment analysis is limited by the availability of speciated datasets in air quality studies and could not be implemented with concentration data only. In some other cases where the concentration variability of a specific pollutant is of greater interest, statistical analyses and graphical tools could be prioritized compared to source apportionment analysis. Therefore, instead of providing a predefined procedure for the evaluation of spatiotemporal variability, this thesis work suggests a conceptual framework which encourages the thorough understanding of the datasets and applying analytical tools that best accommodate the target of the study.

Appendix A: Estimation of Exposure to Environmental Risk Factors for Respiratory Syncytial Virus (RSV) Bronchiolitis in Early Life (RBEL) Study

A.1. Introduction

Asthma is the most common childhood diseases and is responsible for significant mortality and morbidity of children, especially at an early age (Akinbami, 2006). Children 0-4 years of age are more vulnerable to asthma as demonstrated by a higher rate of hospitalization compared to older children (Akinbami and Schoendorf, 2002). Wheezing is a common symptom associated with asthma diagnosis in early childhood. Many children experience wheezing for the first time during the course of acute bronchiolitis which is a lower respiratory tract infection typically caused by respiratory syncytial virus (RSV). A severe RSV illness in early childhood is risk factor for subsequent wheezing (Sigurs, 2001; Sigurs et al., 1995; Sigurs et al., 2005). Children with RSV infection in early life either eventually develop asthma or recover without further symptoms. It was proposed that the inception of asthma is likely to be influenced by genetic susceptibility, environmental influences, and complex interactions between genetics and environmental exposures. Exposure to tobacco smoke has been demonstrated to increase the severity of RSV bronchiolitis (Bradley et al., 2005). Exposure to ambient fine particulate matter ($PM_{2.5}$) and ozone are also linked to increased risk of developing asthma (Brauer et al., 2007; McConnell, 2002). Andersen et al. (2008) demonstrated an association between exposure to air pollutants and wheezing symptom in infants during the first year of life.

One of the hypotheses for the RBEL study is that exposure to air pollutants in early life could be a risk factor for inception of asthma in children after being infected by RSV. Therefore, besides characterizing the genetic aspects of asthma inception during post-RSV childhood, environmental exposure to key air pollutants such as $PM_{2.5}$, ozone and to traffic emissions should be evaluated. The expected outcome of the environmental risk evaluation was to identify and quantify metrics to represent the exposure of a specific cohort to $PM_{2.5}$, ozone and traffic emissions and to use the exposure estimates as inputs to epidemiological models to identify potential associations between asthma and these exposures.

A.2. Experimental design

Starting from 1998, researchers at the School of Medicine at Washington University in St. Louis recruited infants, primarily from the St. Louis area, with severe RSV bronchiolitis in two study phases, RBEL1 and RBEL2. The recruitment processes were typically during December and May of the next year because these are time periods with the high hospitalization rates of infants with RSV bronchiolitis. RBEL1 enrolled 206 participants with recruitment starting in December 1999 and ending in April 2001. 200 participants were planned to be recruited for RBEL2 starting Jan 2010, and only the first 159 participants were included in this analysis. These participants were followed up regularly after being released from the hospital including data collection about occurring wheezing symptoms and diagnosis of asthma symptoms. Records from these follow-ups indicate the geographical address of the participants, date of entry into the study, date for the diagnosis of asthma, and date and frequency of recurring wheezing symptoms.

24-hour integrated $PM_{2.5}$ mass concentration measured by the Federal Reference Method (FRM) at 13 sites and hourly ozone concentration at 9 sites from 1999 to 2011 were retrieved from US Environmental Protection Agency (EPA) Air Quality System (AQS). These sites cover the metropolitan St. Louis area spanning across Missouri and Illinois. Daily 8-hour maximum concentrations for ozone were calculated based on hourly ozone concentration values to be consistent with 24-hour averaged $PM_{2.5}$ concentrations being a daily metric.

A.3. Results

A.3.1 Spatiotemporal variability analysis

Figure A-1 shows the distribution of the valid physical addresses (not including P.O. boxes as addresses) of the participants in RBEL1 and RBEL2. The majority of the patients recruited for both studies reside in the City of St. Louis and counties close to the urban core. RBEL2 recruited more patients from Illinois compared to RBEL1.

Table A-1 shows the annually averaged ozone concentration at six sites. The maximum inter-site difference is 0.007 ppm observed between East St. Louis and Jerseyville in 2001 and the maximum site-specific interannual temporal difference is 0.012 ppm, which suggests temporal variability is comparable to or slightly greater than spatial variability for ozone in St. Louis. In contrast, for $PM_{2.5}$ mass (Table A-1) the temporal variability is significantly greater than the spatial variability. Since the temporal variability has a larger contribution to in the overall observed variability, as a crude approximation spatial homogeneity was assumed and exposure was evaluated based on the time series from one representative site. In this study, $PM_{2.5}$ and ozone concentrations from the East St. Louis site were used because it is located close to downtown St. Louis and has ozone concentrations reported throughout the year.

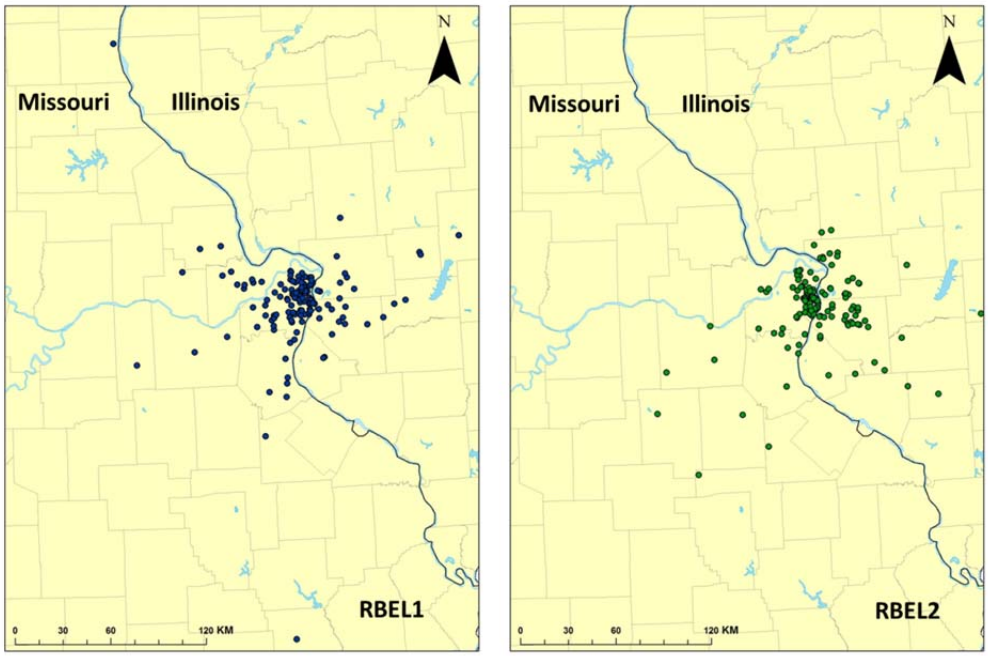

Figure A-1. Residential locations of RBEL1 and RBEL2 participants.

Table A-1. Annual average of the daily 8-hour max ozone concentration calculated for ozone season months (OS: May to Oct) and non-ozone season months (NS: Nov to Apr). Units are in ppm.

	RBEL1								RBEL2			
Year	**1999**		**2000**		**2001**		**2002**		**2010**		**2011**	
	OS	NS	OS	NS	OS	NS	OS	NS	OS	NS	OS	NS
Jerseyville	0.054	N/A	0.049	N/A	0.052	N/A	0.053	N/A	0.042	N/A	0.048	N/A
Edwardsville	0.053	0.032	0.047	0.029	0.045	0.029	0.049	0.029	N/A	N/A	N/A	N/A
Wood River	0.051	0.027	0.045	0.025	0.049	0.027	0.048	0.026	0.043	0.029	0.049	0.034
East St. Louis	0.050	0.026	0.045	0.025	0.048	0.026	0.050	0.025	0.049	0.029	0.045	0.03
St. Louis City	N/A	N/A	N/A	N/A	N/A	N/A	N/A	N/A	0.042	N/A	0.048	N/A

1.All Missouri sites and Jerseyville, IL only monitor ozone during the ozone season.
2.The City of St. Louis Blair Street site started reporting ozone concentrations in 2005.

Table A-2. Annual average $PM_{2.5}$ concentration for select sites in the St. Louis area. Units are $\mu g/m^3$.

	RBEL1				RBEL2	
	1999	**2000**	**2001**	**2002**	**2010**	**2011**
St. Louis City	17.28	16.41	15.20	15.40	12.60	11.91
Clayton	15.39	15.13	13.83	15.05	11.87	11.64
Arnold	15.19	15.26	14.47	15.70	11.19	10.42
East St. Louis	17.91	17.41	16.88	16.86	12.99	12.75
Wood River	15.87	15.93	14.98	15.20	12.03	12.41

A.3.2 Relationship between exposure and asthma/wheezing symptoms

The exposure for each participant was estimated using the average pollutant concentration during a one-year period starting with the date of entry into the study because the hypothesis is that exposure to air pollutants after RSV infection could influence the development of more severe diseases such as asthma. Participants recruited after May 2013 were excluded from the analysis because the air quality data were not available to calculate a one-year average at the time of the analysis. In addition, records such as the diagnosis of asthma for certain participants were missing because the regular follow-up visits or communication were not successfully completed at the time of this analysis. The numbers of cases with sufficient information for analysis the results are summarized in Table A3. Relationships between air quality parameters and dichotomized health outcomes were examined using the Mann-Whitney U test. For RBEL1 none of the comparisons were statistically different at the 99% confidence level. For RBEL2 there was one comparison with a statistically significant difference at the 95% confidence level - asthma/no asthma for $PM_{2.5}$ – but this case was very unbalanced with only 10% of participants in one category.

Table A-3. Summary of exposure estimates for participants categorized based on diagnosed asthma and reported wheezing symptom. Units are $\mu g/m^3$ for $PM_{2.5}$ and ppm for ozone.

			$PM_{2.5}$		Ozone	
		N	Average	p value	Average	p value
RBEL1						
	Asthma	101	14.1	0.261	0.036	0.812
	No asthma	92	14.4		0.036	
	Wheezing	181	14.6	0.266	0.036	0.527
	No wheezing	17	14.1		0.037	
RBEL2						
	Asthma	15	12.1	<0.001	0.039	0.346
	No asthma	130	11.7		0.039	
	Wheezing	96	11.8	0.74	0.039	0.900
	No wheezing	51	11.7		0.039	
RBEL1&RBEL2						
	No wheezing	68	12.3	<0.001	0.038	0.002
	Wheezing	277	13.6		0.037	

The skewed distribution for RBEL2 asthma is likely from limitations on making asthma diagnoses. RBEL2 participants were typically newborn to 3 years old at the time of enrollment and there may be a few years lag before the inception of asthma. The time of asthma diagnosis itself is a variable that is a complicated function of potentially many factors including but not limited to exposure to environment risks. Similarly, over 90% of the participants in RBEL1 reported the symptom of wheezing during the 10+ years after their entry into the study. These symptoms could be induced by exposure to other factors such as tobacco smoke as study time period extended. A pooled analysis using data from RBEL1 and RBEL2 yielded statistically significant differences for wheezing/no wheezing for both $PM_{2.5}$ and ozone. $PM_{2.5}$ displayed a positive association with the occurrence of wheezing, whereas ozone was deemed protective for wheezing which is inconsistent with expectations. These results suggest that this simple exposure-symptom relationship may be confounded by other factors and causation should not be inferred.

A.4. Discussion and recommendations

1. The statistical analysis was underpowered because of the small cohort size and the relatively homogeneous pollutant levels. For the air quality condition in St. Louis, a larger cohort would be needed to adequately test the hypothesis.

2. The residential addresses of the participants are clustered which reduced the variability of exposure to air pollutants. This problem is compounded by the sparse monitoring network which precluded incorporation of fine-scale spatial variability of exposure into the modeling

3. More stable and representative variables might be needed as indicators for air pollution exposure. Both the diagnosis of asthma and wheezing are variables that evolve with time. There appears to be a positive correlation between the occurrence of asthma symptoms and length of the post-RSV period during which many confounding factors could have impacts. In addition, the appearance of asthma symptoms may also be a function of total time of exposure. Thus, integrated exposure after the infection of RSV might be a relevant metric but it will exhibit lower variability across the cohort.

4. The exposure estimates could be used as input parameters in more advanced statistical models that take into account a wider range of factors such as genetic information, allergic reactions and tobacco exposure.

A.5. References

Akinbami, L., 2006. The state of childhood asthma, United States, 1980-2005. Advance data, 1-24.

Akinbami, L.J., Schoendorf, K.C., 2002. Trends in childhood asthma: Prevalence, health care utilization, and mortality. Pediatrics 110, 315-322.

Bradley, J.P., Bacharier, L.B., Bonfiglio, J., Schechtman, K.B., Strunk, R., Storch, G., Castro, M., 2005. Severity of respiratory syncytial virus bronchiolitis is affected by cigarette smoke exposure and atopy. Pediatrics 115, e7-e14.

Brauer, M., Hoek, G., Smit, H.A., de Jongste, J.C., Gerritsen, J., Postma, D.S., Kerkhof, M., Brunekreef, B., 2007. Air pollution and development of asthma, allergy and infections in a birth cohort. European Respiratory Journal 29, 879-888.

McConnell, R., 2002. Erratum: Asthma in exercising children exposed to ozone (The Lancet (Feb. 2) (386)). Lancet 359, 896.

Sigurs, N., 2001. Epidemiologic and clinical evidence of a respiratory syncytial virus-reactive airway disease link. American Journal of Respiratory and Critical Care Medicine 163, S2-S6.

Sigurs, N., Bjarnason, R., Sigurbergsson, F., Kjellman, B., Bjorksten, B., 1995. Asthma and immunoglobulin E antibodies after respiratory syncytial virus bronchiolitis: A prospective cohort study with matched controls. Pediatrics 95, 500-505.

Sigurs, N., Gustafsson, P.M., Bjarnason, R., Lundberg, F., Schmidt, S., Sigurbergsson, F.,

Kjellman, B., 2005. Severe respiratory syncytial virus bronchiolitis in infancy and asthma and

allergy at age 13. American Journal of Respiratory and Critical Care Medicine 171, 137-141.

Appendix B: Identification of Potential Source Areas for Elevated Sulfate, Nitrate and Air toxic Elements in the United States

B.1. Introduction

Numerous previous studies have suggested adverse health effects of fine particulate matter ($PM_{2.5}$) (Burnett et al., 2001; Dockery et al., 1993; Pope III et al., 2002; Pope III et al., 2013; Pope III et al., 1995). There is a growing interest in health effects associated with $PM_{2.5}$ chemical components as well as sources of $PM_{2.5}$ (Aschner et al., 2005; Bollati et al., 2010; Thurston et al., 2011). Source apportionment studies using models such as Positive Matrix Factorization (PMF) have demonstrated the strength of identifying potential sources (Brown et al., 2007; Buzcu et al., 2003; Gu et al., 2011; Kim et al., 2003; Lee and Hopke, 2006). Secondary nitrate and sulfate are commonly considered to have regional impacts with spatial homogeneity often observed or inferred at the urban scale (Heo et al., 2013; Lee and Hopke, 2006; Lee et al., 2006). For example, Lee et al. (2006) concluded that $PM_{2.5}$ nitrate and sulfate in the metropolitan St. Louis area are attributed to regional sources originating from the Upper Midwest/Central Plains and Ohio River Valley, respectively. Most studies have focused on a single site or city and a comprehensive multisite study at a larger spatial scale to examine potential source regions has not been performed.

Trace metals such as selenium (Se) and arsenic (As) have been used as chemical signatures for emissions from coal-fired power plants (Ondov et al., 1989). Ambient data-driven identification of potential source regions now has incremental value for sulfate and nitrate because these parameters are well-captured by contemporary chemical transport modeling which can be run with source apportionment tools to quantify source-receptor relationships. In contrast, there have

been few studies on the identification of potential source areas for trace elements. With more stringent control strategies being implemented, primary PM emissions have been significantly reduced, which may be accompanied by changes in source profiles and source locations. Therefore, a data-driven analysis of sources regions for these air toxic elements that spans several years is desired.

There are several wind-based statistical tools to identify the bearings or locations of potential sources. Conditional probability function (CPF) and nonparametric wind direction (NWR) are prevailing methods for the identifying the bearings of local sources and are often performed a source apportionment modeling results (Kim and Hopke, 2004; Lee and Hopke, 2006; Wang et al., 2011). These methods provide limited information about sources or species exerting regional scale influences. Potential source contribution function (PSCF), a statistical model that incorporates air mass back trajectories, residence times over certain areas and the observed concentration (Ashbaugh et al., 1985), provides insights into the sources that are from regional transport and has the advantage of identifying the specific geographical areas compared to CPF and NWR.

In this preliminary study, $PM_{2.5}$ sulfate and nitrate as well as PM_{10} Se obtained from multiple routine monitoring sites were analyzed using the PSCF model to identify potential source regions in the US. Sulfate and nitrate were used to evaluate model results in the context of known source regions. Analysis of PM_{10} Se is motivated by the work of Yadav and Turner (2014) which suggested that in St. Louis these species are dominated by regional transport. This study aims to examine the validity of Se and As as tracers for coal-fired power plant emissions for future source apportionment studies.

B.2. Dataset and method

B.2.1 Monitoring datasets

Five sites that are both the Chemical Speciation Network (CSN) and National Air Toxics Trends Stations (NATTS) sites were selected for the preliminary study. 24-hour integrated $PM_{2.5}$ sulfate and nitrate data were obtained at the five sites from the CSN dataset. Se in 24-hour integrated 1-in-6 day PM_{10} samples were retrieved only for select NATTS sites because Se is not one of the species mandated to be reported. The sampling and analytical protocols of these networks are described in detail elsewhere (Solomon et al., 2014; United States Environmental Protection Agency, 2015). In contrast, PM_{10} arsenic compounds are one of the 18 HAPs required by the US EPA to measure and report at NATTS sites. Table B-1 summarizes the sites and the temporal coverage of the select data.

Table B-1. Summary of the studies sites.

Site Name	NO_3 and SO_4				Se	
	Sampling Frequency	Temporal coverage	N(NO_3)	N(SO_4)	Temporal Coverage	N
St. Louis, MO	1-in-3	2000.2 – 2014.9	1606	1606	2000.2 – 2014.9	618
Atlanta, GA	1-in-3	2001.3 – 2014.12	1628	1623	2004.5 - 2013.12	533
Chesterfield, SC	1-in-6	2002.1 – 2014.12	751	751	2005.1 – 2014.9	459
Dearborn, MI	1-in-6	2003.1 – 2014.12	695	698		
Milwaukee, WI	1-in-3	2001.1 – 2014.12	1642	1642		

B.2.2 Potential source contribution function (PSCF)

The PSCF model (Ashbaugh et al., 1985) was applied to identify the source regions associated with elevated $PM_{2.5}$ sulfate, nitrate and PM_{10} Se concentrations. Airmass back trajectories were generated with the Hybrid Single-Particle Lagrangian Integrated Trajectory (HYSPLIT) model

using 80 km gridded meteorological data (EDAS 80km) and 40 km gridded meteorological data (EDAS 40km) for the periods before 2004 and after 2004, respectively. Five day (120 hour) back trajectories arriving at 500m above ground level were calculated at each of the five monitoring sites. One trajectory per day arriving at noon local time at each site was computed. The measured daily concentration values were assigned to the corresponding back trajectories. The PSCF value in each 1° x 1° grid cell was calculated using PSCF = m_{ij}/n_{ij}, where n_{ij} is the total number of the trajectory endpoints in the grid cell (i, j) and m_{ij} is the number of endpoints associated with the concentration values that exceed a threshold value. In this study, the top 25% of the concentration values was used as the threshold criterion. In order to reduce the potential bias of PSCF calculations caused by the small number of endpoints in certain grid cells, a weighting function based on previous studies (Ashbaugh et al., 1985; Heo et al., 2013; Lee and Hopke, 2006) was customized and applied in this study:

$$W(n_{ij}) = \begin{cases} 1 & n_{av} < n_{ij} \\ 0.7 & n_{mid} < n_{ij} \leq n_{av} \\ 0.4 & n_{med} < n_{ij} \leq n_{mid} \\ 0.2 & 5 < n_{ij} \leq n_{med} \\ 0 & n_{ij} \leq 5 \end{cases}$$

where n_{av} is the average number of endpoints across each grid cells having at least one endpoint, n_{med} is the median number of endpoints across grid cells having at least one endpoint, and n_{mid} is the midpoint between n_{av} and n_{med}.

Previous studies suggested that one of the limitations of using the weighting function is the possibility of eliminating real source regions which few trajectories pass through. In addition, the pattern suggested by PSCF might be dominated by the pattern of air mass trajectories for small datasets (Hsu et al., 2003). In this study with large datasets this issue should be minimized.

However, caution should be used if further analysis will be conducted on shorter time periods for these datasets.

B.3. Preliminary results and discussion

Figure B-1 shows the PSCF spatial pattern for elevated concentrations of $PM_{2.5}$ nitrate, sulfate and PM_{10} Se measured at Blair Street, a site located in downtown St. Louis. One area with high nitrate PSCF values is located in the Upper Midwest/Central Plains area, generally spanning across Wisconsin, Minnesota, and Iowa. These areas are consistent with the high population of farms which are major sources of ammonia (Coe and Reid, 2003; Goebes et al., 2003; Kenski et al., 2004). In addition, nitrate in fine particulate matter displays a seasonal pattern with high concentrations in the wintertime when low temperature and high humidity favors nitrate formation by gas-to-particle conversion. The northerly winds are prevailing winds in the winter in St. Louisa area, which also favors the regional transport of nitrate from its potential source regions to the north. Another region showing high PSCF values for nitrate is in Kansas and Oklahoma where the Flint Hills are burned every spring. The region of high PSCF values for elevated sulfate in St. Louis is over the Ohio River Valley and extends southerly to Georgia. Previous source apportionment analysis has demonstrated that the large number of coal-fired power plants located in the Ohio River Valley is a major source of SO_2 which can form sulfate by various pathways (Lee and Hopke, 2006; Lee et al., 2006). Lee and Hopke (2006) demonstrated that high sulfate concentrations in St. Louis were largely attributed to emissions from these source regions based on CSN data from 2002 to 2004. In this study using sulfate data collected over a 14-year time period similar source regions were observed. However, the

interpretation of the updated analysis should be cautious because the pronounced reduction in ambient sulfate concentration over the past decade may be skewing the PSCF analysis towards the early years because only top 25% the concentration values are included in the PSCF calculation. PM_{10} Se measured at Blair Street displays high PSCF values in the Ohio River Valley which is in good agreement with the source locations for sulfate. This general agreement provides support to Se as a tracer for coal combustion from power plants. However, the same caution applies in that emissions decreases over time will disproportionately weight early time periods in the PSCF analysis.

Figure B-2 shows the summation of PSCF values in each grid cell calculated for multiple sites in the Eastern-Midwest US. The values for sulfate and nitrate are calculated using five sites and the values for Se are based on three sites (Table B-1). The patterns for multisite PSCF analysis are generally consistent to the observation at Blair Street. Higher PSCF values for nitrate are present over a much larger geographical area including entire Central and Upper Midwest. For sulfate, the high PSCF values over the Ohio River Valley – Kentucky – Tennessee area indicate that it is the dominant source region responsible for high sulfate concentrations at the sites included in the analysis. Because Se is not required to be reported by NATTS, only St. Louis, Atlanta and Chesterfield are included in the modeled Se datasets. Multisite PSCF analysis of Se shows the Ohio River Valley as a major source region, and the agreement between potential source region for sulfate and Se provides support to the validity of using Se as a tracer for coal-fired power plant emissions. However, because the ambient Se concentrations have decreased over time, the robustness of Se as a tracer needs to be evaluated by performing PSCF analysis for shorter time periods over the past decade.

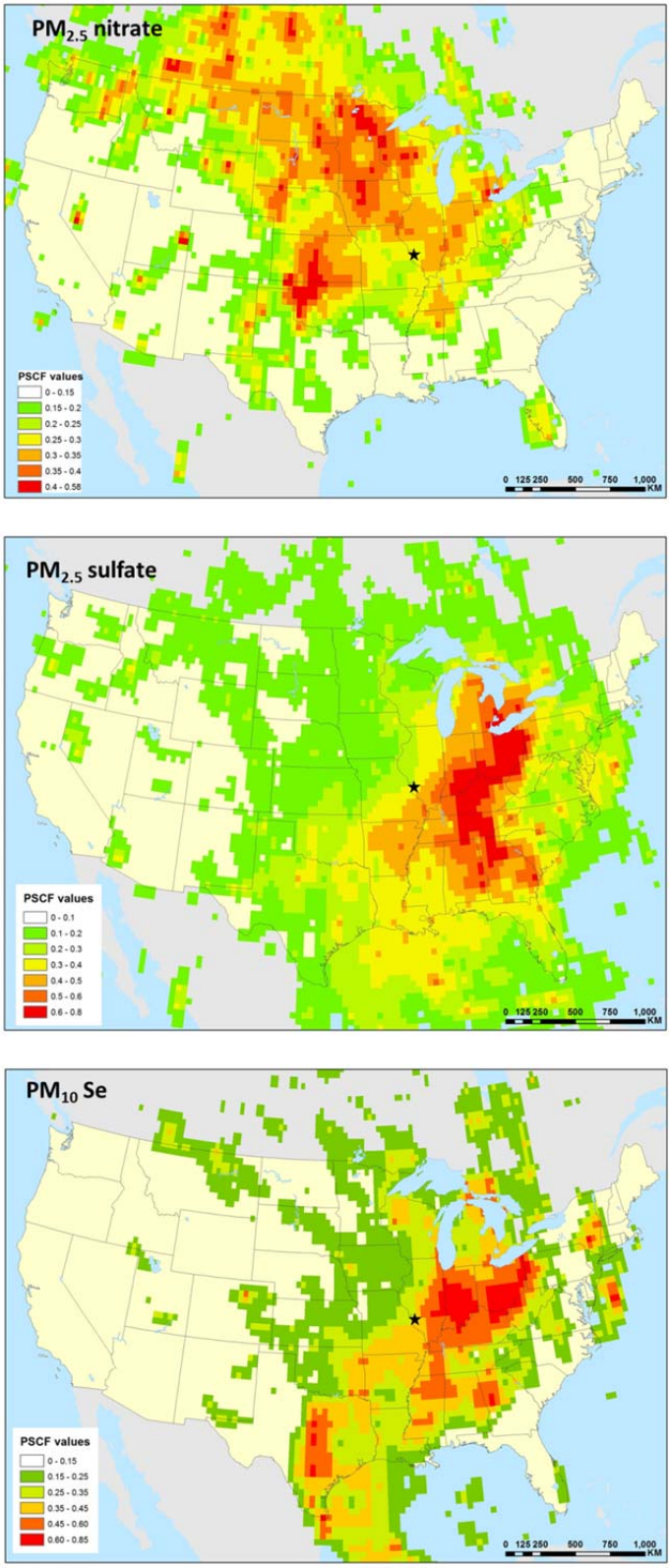

Figure B-1. Potential source regions for elevated $PM_{2.5}$ nitrate, sulfate and PM_{10} Se in St. Louis (star), 2000-2014.

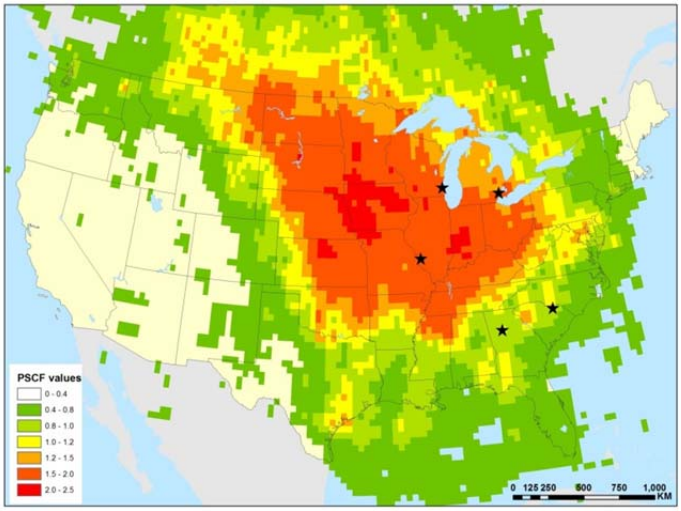

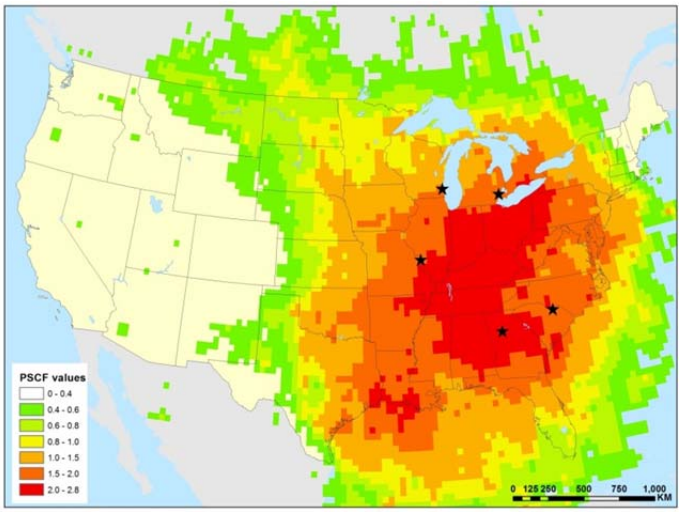

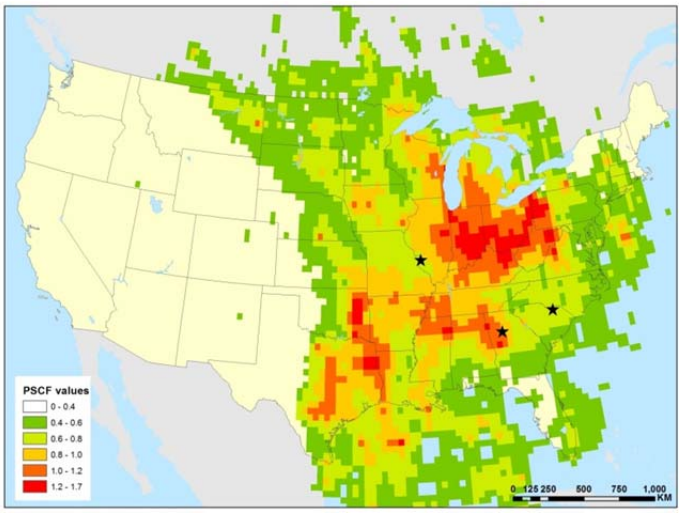

Figure B-2. Potential source regions for elevated $PM_{2.5}$ nitrate, sulfate and PM_{10} Se measured at multiple sites (stars), 2000-2014.

B.4. Ongoing work

1. Perform PSCF analysis at each site for a series of shorter time periods to characterize the temporal variation of the source regions.

2. Retrieve PM_{10} As data and perform PSCF analysis.

3. Identify other sites in the Eastern US which are both CSN sites and NATTS sites to strengthen the multisite PSCF analysis.

B.5. References

Aschner, M., Erikson, K.M., Dorman, D.C., 2005. Manganese dosimetry: Species differences and implications for neurotoxicity. Crit. Rev. Toxicol. 35, 1-32.

Ashbaugh, L.L., Malm, W.C., Sadeh, W.Z., 1985. A residence time probability analysis of sulfur concentrations at grand Canyon National Park. Atmospheric Environment (1967) 19, 1263-1270.

Bollati, V., Marinelli, B., Apostoli, P., Bonzini, M., Nordio, F., Hoxha, M., Pegoraro, V., Motta, V., Tarantini, L., Cantone, L., Schwartz, J., Bertazzi, P.A., Baccarelli, A., 2010. Exposure to Metal-Rich Particulate Matter Modifies the Expression of Candidate MicroRNAs in Peripheral Blood Leukocytes. Environmental Health Perspectives 118, 763-768.

Brown, S.G., Frankel, A., Hafner, H.R., 2007. Source apportionment of VOCs in the Los Angeles area using positive matrix factorization. Atmospheric Environment 41, 227-237.

Burnett, R., Ma, R.J., Jerrett, M., Goldberg, M.S., Cakmak, S., Pope, C.A., Krewski, D., 2001. The spatial association between community air pollution and mortality: A new method of analyzing correlated geographic cohort data. Environmental Health Perspectives 109, 375-380.

Buzcu, B., Fraser, M.P., Kulkarni, P., Chellam, S., 2003. Source identification and apportionment of fine particulate matter in Houston, TX, using positive matrix factorization. Environmental Engineering Science 20, 533-545.

Coe, D.L, Reid, S.B., 2003. Research and development of ammonia emission inventories for the Central States Regional Air planning Association. Final report. STI Report #STI-902501-2241-FR.

Dockery, D.W., Pope III, C.A., Xu, X., Spengler, J.D., Ware, J.H., Fay, M.E., Ferris Jr, B.G., Speizer, F.E., 1993. An association between air pollution and mortality in six U.S. cities. N. Engl. J. Med. 329, 1753-1759.

Goebes, M.D., Strader, R., Davidson, C., 2003. An ammonia emission inventory for fertilizer application in the United States. Atmospheric Environment 37, 2539-2550.

Gu, J., Pitz, M., Schnelle-Kreis, J., Diemer, J., Reller, A., Zimmermann, R., Soentgen, J., Stoelzel, M., Wichmann, H.E., Peters, A., Cyrys, J., 2011. Source apportionment of ambient particles: Comparison of positive matrix factorization analysis applied to particle size distribution and chemical composition data. Atmospheric Environment 45, 1849-1857.

Heo, J., McGinnis, J.E., de Foy, B., Schauer, J.J., 2013. Identification of potential source areas for elevated PM2.5, nitrate and sulfate concentrations. Atmospheric Environment 71, 187-197.

Hsu, Y.K., Holsen, T.M., Hopke, P.K., 2003. Locating and quantifying PCB sources in Chicago: Receptor modeling and field sampling. Environmental Science and Technology 37, 681-690.

Kenski, D.M., Gay, D., Fitzsimmons, S., 2004. Ammonia and its role in midwestern haze, Regional and Global Perspectives on Haze, pp. 163-171.

Kim, E., Hopke, P.K., 2004. Comparison between Conditional Probability Function and Nonparametric Regression for Fine Particle Source Directions. Atmospheric Environment 38, 4667-4673.

Kim, E., Hopke, P.K., Edgerton, E.S., 2003. Source identification of Atlanta aerosol by positive matrix factorization. Journal of the Air & Waste Management Association 53, 731-739.

Lee, J.H., Hopke, P.K., 2006. Apportioning sources of $PM_{2.5}$ in St. Louis, MO using speciation trends network data. Atmospheric Environment 40, Supplement 2, 360-377.

Lee, J.H., Hopke, P.K., Turner, J.R., 2006. Source identification of airborne PM 2.5 at the St. Louis-Midwest Supersite. Journal of Geophysical Research-Part D-Atmospheres 111, 12 pp.-12 pp.

Ondov, J.M., Choquette, C.E., Zoller, W.H., Gordon, G.E., Biermann, A.H., Heft, R.E., 1989. Atmospheric behavior of trace elements on particles emitted from a coal-fired power plant. Atmospheric Environment (1967) 23, 2193-2204.

Pope III, C.A., Burnett, R.T., Thun, M.J., Calle, E.E., Krewski, D., Ito, K., Thurston, G.D., 2002. Lung cancer, cardiopulmonary mortality, and long-term exposure to fine particulate air pollution. Jama-Journal of the American Medical Association 287, 1132-1141.

Pope III, C.A., Ezzati, M., Dockery, D.W., 2013. Fine particulate air pollution and life expectancies in the United States: The role of influential observations. Journal of the Air and Waste Management Association 63, 129-132.

Pope III, C.A., Thun, M.J., Namboodiri, M.M., Dockery, D.W., Evans, J.S., Speizer, F.E., Heath Jr, C.W., 1995. Particulate air pollution as a predictor of mortality in a prospective study of U.S. Adults. American Journal of Respiratory and Critical Care Medicine 151, 669-674.

Solomon, P.A., Crumpler, D., Flanagan, J.B., Jayanty, R.K., Rickman, E.E., McDade, C.E., 2014. U.S. national PM2.5 Chemical Speciation Monitoring Networks-CSN and IMPROVE: description of networks. Journal of the Air & Waste Management Association (1995) 64, 1410-1438.

Thurston, G.D., Ito, K., Lall, R., 2011. A source apportionment of U.S. fine particulate matter air pollution. Atmospheric Environment 45, 3924-3936.

United States Environmental Protection Agency, 2015. National Air Toxics Trends Station work plan template.

Wang, G., Hopke, P.K., Turner, J.R., 2011. Using highly time resolved fine particulate compositions to find particle sources in St. Louis, MO. Atmospheric Pollution Research 2, 12.

Yadav, V., Turner, J., 2014. Gauging intraurban variability of ambient particulate matter arsenic and other air toxic metals from a network of monitoring sites. Atmospheric Environment 89, 318-328.

Curriculum Vita

Li Du

Doctor of Philosophy (Ph.D.) in Energy, Environmental and Chemical Engineering, 2015.
Department of Energy, Environment and Chemical Engineering,
Washington University in St. Louis, St. Louis, MO, USA

Master of Science in Environmental Engineering, 2009.
Department of Environmental Engineering,
University of Science and Technology Beijing, Beijing, China

Bachelor of Science in Environmental Engineering, 2006.
Department of Environmental Engineering,
University of Science and Technology Beijing, Beijing, China

Publications

Du, L., Turner, J., 2015. Using $PM_{2.5}$ lanthanoid elements and nonparametric wind regression to track petroleum refinery FCC emissions. Sci. Total Environ. 529, 65-71.

Du, L., Turner, J.. Measurement of selenium in ambient fine particulate matter by inductively coupled plasma mass spectrometry (ICP-MS) under standard mode.
(In preparation)

Du, L., Turner, J.. Spatial variability of gaseous air toxics in St. Louis area.
(In preparation)

Du, L., Turner, J.. Source apportionment of $PM_{2.5}$ in the St. Louis area using chemical speciation data.
(In preparation)

Wang, S., Wei, W., **Du, L.**, Aunan, K, Hao, J., 2010. Air pollutants in rural homes in Guizhou, China - Concentrations, speciation, and size distribution. Atmospheric Environment 44, 4575 – 4581.

Wang, S., Wei, W., **Du, L.**, Li, G., Hao, J., 2009. Characteristics of gaseous pollutants from biofuel-stoves in rural China. Atmospheric Environment 43, 4148-4154.

Conference Proceedings

Du L., Turner J. (2014) Selenium in Ambient Particulate Matter: Measurement and Analysis. Presented at *33rd Annual American Association for Aerosol Research (AAAR) Conference. Orlando, FL, Oct 24.*

Du L., Haddad K., Turner J. (2014) Intraurban Variability of $PM_{2.5}$ Components across Metropolitan St. Louis. Presented at the *National Ambient Air Monitoring Conference, Atlanta, GA, Aug 13*.

Du L., Turner J. (2013) Measurement of Selenium in Ambient Fine Particulate Matter by Inductively Coupled Plasma/Mass Spectrometry (ICP-MS). Presented at the *Air & Waste Management Association Air Quality Measurement Methods and Technology Conference. Sacramento, CA, Nov 21*.

Du L., Turner J. (2013) Ambient Primary $PM_{2.5}$ from Petroleum Refinery Operations. Presented at the *32nd Annual American Association for Aerosol Research (AAAR) Conference. Portland, OR, Oct 3.*

Du L., Turner J., Pasch A., Brown S. and Rice Joann. (2011) Thermo 1405DF Dichotomous FDMS TEOM Volatile and Non-Volatile Mass Concentrations at Two Contrasting Sites. Poster presented at the *Air & Waste Management Association 104th Annual Conference. Orlando, FL, June 21-24*.

Haddad K., **Du L.**, Turner J. (2014) Assessment of Measurement Error in CSN Data Using Collocated Samples. Presented at the *National Ambient Air Monitoring Conference, Atlanta, GA, Aug 13*.

Williams B., Mitroo D., Martinez R., Zhang Y., Walker M., Oxford C., Zuo X., Hagan D., Dhawan S., **Du L.**, Turner J., McMeeking G., King L., Guo H., Weber R., Baasandorj M., Hu L., Millet D. (2014) Highlights from the St. Louis Air Quality Regional Study (SLAQRS) 2013. Presented at *33rd Annual American Association for Aerosol Research (AAAR) Conference. Orlando, FL, Oct 23.*

Walker M., Williams B., Martinez R., Zhang Y., Mitroo D., Hagan D., Dhawan S., **Du L.**, Turner J., Guo H., King L., Weber R., Hu, L., Baasandorj M., Millet D., McMeeking G. (2014) Instrument Intercomparison of Black Carbon Measurements and Correlations with Gas and Aerosol Composition during an Urban Field Study. Presented at *33rd Annual American Association for Aerosol Research (AAAR) Conference. Orlando, FL, Oct 23.*